A Methodology for Optimal Load Management and Aggregation Strategies in Grid-Interactive Building Clusters

Andrea Petrucci

A Thesis

In the Department
of
Building, Civil, and Environmental Engineering (BCEE)

Presented in the Partial Fulfillment of the Requirements
for the Degree of Doctor of Philosophy (Building Engineering)
at

Concordia University

Montréal, Québec, Canada

March 2025

CONCORDIA UNIVERSITY
SCHOOL OF GRADUATE STUDIES

This is to certify that the thesis prepared

By: *Andrea Petrucci*

Entitled: *A Methodology for Optimal Load Management and Aggregation Strategies in Grid-Interactive Building Clusters*

and submitted in partial fulfillment of the requirements for the degree of

DOCTOR OF PHILOSOPHY (Building Engineering)

complies with the regulations of the University and meets the accepted standards with respect to originality and quality.

Signed by the final examining committee:

Thomas Fevens ______ Chair
Chair's name

James Edward Braun ______ External Examiner
Examiner's name

Chunyan Lai ______ Examiner
Examiner's name

Radu Zmeureanu ______ Examiner
Examiner's name

Mohamed Ouf ______ Examiner
Examiner's name

Adolfo Palombo ______ Examiner
Examiner's name

Andreas Athienitis ______ Thesis Supervisor
Supervisor's name

Annamaria Buonomano ______ Thesis Supervisor
Supervisor's name

Approved by: ______ Po-Han Chen ______
Graduate Program Director

3/13/2025 ______ Mourad Debbabi, ______
Dean, Gina Cody School of Engineering and Computer Science

ABSTRACT

A Methodology for Optimal Load Management and Aggregation Strategies in Grid-Interactive Building Clusters

Andrea Petrucci, Ph.D.

Concordia University, 2025

The decentralization of energy markets, driven by electrification and renewable energy adoption, necessitates a shift from a “follow-the-supply” to a “follow-the-demand” model, requiring grid operators to digitalize and modernize infrastructure to better accommodate distributed energy production and balance demand. In this context, energy aggregators play a crucial role by enabling building clusters to function as unified entities, thereby optimizing interactions with day-ahead coordination and intra-day markets.

This thesis investigates two key aspects of demand-side management: the role of energy aggregators in shaping residential load profiles and the development of optimal aggregation strategies. These aspects have been scarcely investigated, especially by exploiting measured data. To achieve these goals, a hierarchical control methodology is proposed for energy aggregators to coordinate individual homes within clusters. Leveraging data from smart thermostats and power meters, the methodology integrates predictive modelling and control strategies at a building cluster scale. To this aim, buildings are modelled as reduced-order grey-box networks, capturing thermal dynamics in a simplified yet accurate manner. Machine learning techniques are employed to support the creation of these data-driven models, ensuring robustness and adaptability. Advanced control techniques, such as the economic Model Predictive Control, evaluate energy flexibility by comparing performance to reference demand profiles, ensuring adherence to technical constraints while minimizing the economic expense. A Monte Carlo estimation technique is used to account for variability and heterogeneity within portfolios, facilitating probabilistic decision-making to address uncertainties and diverse operational conditions. Clustering techniques are then used to propose a flexibility-informed benchmarking procedure, supporting the creation of control archetypes and diverse strategies.

The proposed methodology is validated through three case studies and measured dataset of varying populations and resolution: (1) the Experimental House for Building Energetics in Shawinigan, Quebec, a fully instrumented, unoccupied research house to test real implementation of demand-side management; (2) a virtual community of 30 houses in Trois-Rivières, Quebec, equipped with smart thermostats and sensors; and (3) a dataset of approximately 100,000 monitored homes provided by a North American thermostat company enables the creation of energy aggregation strategies and prediction of their aggregated impact on the grid. These case studies demonstrate the effectiveness of energy aggregators in optimizing household costs and support transactive power grid management.

By addressing the dual objectives of cost minimization for customers and operational efficiency for grid operators, this research contributes to the design and implementation of energy aggregators as key enablers of the “follow-the-demand” energy paradigm. This thesis provides actionable insights into energy flexibility and portfolio management, paving the way for the scalable deployment of sustainable and efficient energy systems.

Acknowledgements

I want to express my heartfelt gratitude to all those who have played a significant role in the completion of this work. First and foremost, I extend my deepest thanks to my supervisors, Professor Andreas Athienitis and Professor Annamaria Buonomano, for their invaluable guidance, unwavering support, and insightful advice throughout this journey. Their mentorship has been a cornerstone of my academic and personal growth.

I am profoundly grateful to the Strategic Alliance NSERC/Hydro-Québec for their generous support and for providing the resources that made this research possible. Their commitment to advancing sustainable energy solutions is truly inspiring, and I am honoured to have been a part of this endeavour.

I would also like to extend my gratitude to Concordia University and Università degli Studi di Napoli Federico II for fostering a culture of excellence and providing me with the platform to pursue my academic aspirations. Special thanks go to the Sustainable Energy System Lab in Napoli and the Centre for Zero Energy Building Studies in Montreal. These exceptional institutions have provided me with a stimulating environment to explore, learn, and innovate. I am thankful for the opportunities to collaborate with such talented and dedicated teams.

To my colleagues and mentors, your encouragement, suggestions, and insights have enriched my experience beyond measure. The discussions, collaborations, and shared experiences have been both enlightening and enjoyable, and I am deeply appreciative of your contributions to my journey.

To my family and friends, your unwavering belief in me has been my greatest source of strength. Your love, encouragement, and understanding have carried me through the challenges and triumphs alike. To my girlfriend, your constant support, PATIENCE, and love have been my anchor and inspiration throughout this journey.

Finally, to everyone who has contributed, directly or indirectly, to this work—thank you for your support and belief in me. This achievement is as much yours as it is mine.

Table of Contents

List Of Figures

List Of Tables

Nomenclature

Abbreviation and Acronyms

ASHP	Air Source Heat Pump
ADR	Automated Demand Response
AMA	arithmetic moving average
AR	Autoregressive
ARIMA	Autoregressive integrated moving average
ARMA	Autoregressive moving average
ARMAX	Auto Regressive Moving Average with exogenous inputs
BaU	business as usual
BEF	Building Energy Flexibility
BEFC	building energy flexibility curve
BEFI	Building Energy Flexibility Index
BEFI%	Percentage BEFI
BEMS	Building Energy Management System
BESS	Battery Energy Storage System
BH	Baseboard Heater
BIM	building information modeling
BIPVT	Building Integrated Photovoltaic Thermal
CalH	calibration horizon
CBEFI	combined BEFI
CH	Control Horizon
COP	Coefficient Of Performance
CPP	Critical Peak Pricing
CPR	Critical Peak Rebate
CR	Capacity Ratio
CV	Control Volume
CV-RMSE	Coefficient Of Variation Of RMSE
DAC	day-ahead coordination
DAR	dynamic actionable reserve
DER	Distributed Energy Resource
DG	Distributed Generators
DHW	Domestic hot water
DLC	Direct Load Control
DoE	Department Of Energy
DR	Demand Response
DRP	Demand Response Program
DSM	Demand-Side Management

DSO	Distribution System Operator
d-ToU	Dynamic Time of Use
DTW	Dynamic time warping
EA	Energy Aggregator
EE	energy efficiency
EHBE	Experimental House for Building Energetics
EHBE	Experimental House for Building Energetics
eMPC	Economic Model Predictive Control
ES	Energy Storage
EUI	Energy Usage Intensity
EV	Electric Vehicle
EVSE	Electric Vehicle Supply Equipment
EWA	exponentially weighted averages
FF	Flexibility function
FIT	Goodness Of Fit
FSI	Flexibility Savings Index
GEB	Grid-Interactive Efficient Building
GHG	greenhouse gas
GHI	Global Horizontal Irradiance
GSA	General Service Administration
HEMS	Home energy management system
HP	Heat Pump
HQ	Hydro-Québec
HVAC	Heating, Ventilation, And Air Conditioning
ICH	Inverse-Calibration Horizon
ICH	inverse-calibration horizon
ICT	Information And Communication Technologies
IDC	intra-day adjustments
IDM	Intra-day Market
IEA	International Energy Agency
IoT	Internet of Things
ISL	Individual Stress Level
ISO	International Organization for Standardization
KPI	Key Performance Indicator
LF	Load Factor
LHS	Latin Hypercube Sampling
MA	moving average
MAE	Mean Absolute Error
MAPE	Mean Absolute Percentage Error

MBE	Mean Bias Error
MDP	Markov decision process
MOR	Model Order Reduction
MPC	Model Predictive Control
MRI	MPC Relevant Identification
ND	Number Of Datapoint
NRMSE	Normalized Root Mean Square Error
OAT	Outdoor Air Temperature
OLS	ordinary least squares
PH	Prediction Horizon
PTV	Peak To Valley Ratio
PVT	Photovoltaic Thermal
RBC	Rule Based Control
RC	Resistance-Capacitance
RES	renewable energy source
RMPB	Robust Model Predictive Control
RMSE	Root Mean Square Error
ROM	Reduced Order Model
RTP	Real-Time Pricing
SBEMS	Single Building Energy Management System
SDG	Sustainable And Development Goal
SIMEB	Simulation Energetique Des Batiments
SIMEB	Simulation Energetique Des Batiments
sMPC	Stochastic Model Predictive Control
SR	Solar Radiation
SRM	structural risk minimization
s-ToU	Static Time Of Use
SVM	Support Vector Machine
SysR	System Ramping
TES	Thermal Energy Storage
TPES	Total Primary Energy Supply
TSO	Transmission System Operator
V1X	Monodirectional EV charging infrastructure
V2B	vehicle-to-building
V2G	vehicle-to-grid
V2X	bidirectional EV infrastructure

1. *Introduction*

1.1 Problem Statement and Motivation

Throughout history, transformative milestones such as harnessing fire, the Agricultural Revolution driven by water and wind power, the Industrial Revolution powered by steam engines, and ground-breaking discoveries like the photovoltaic effect and nuclear energy have profoundly shaped human civilization. However, a more consistent and defining feature of the past two centuries has been the relentless rise in energy consumption. The trajectory of this growth is striking: per capita total primary energy supply (TPES) has surged by 300% since 1900 and by 166% since 1990 [1].

Evidence of that is the building sector that —accounting for about 35% of the total energy consumption of developed countries, 20% for residential and 15% for commercial buildings — during the last 15 years has registered an increase of 20% of total final-end consumption [2]. The modification of consumption habits and the process of electrification are the predominant factors contributing to this increasing demand in Europe [3], North America [4], Middle East and Asia [5].

Hence, there is a pressing need for transmission system operators (TSOs) to constantly enhance grid capacity by upgrading infrastructure and integrating new plants to accommodate this higher demand. The impact of this phenomenon is acknowledged in a growing degree of complexity in management of electricity grid [6], an increase in the final cost of electricity [7], and a higher carbon footprint [8]. This adjustment strategy is therefore defined as *"follow-the-demand"*.

Conversely, due to the advances in technology, changing customer preferences, and market developments, utilities are looking for new energy-saving opportunities. In both heating [9] and cooling dominated climates [10], many governments worldwide are formulating strategic initiatives to address this concern from a different standpoint, thereby enabling end-users of the energy supply chain to actively participate in the market. These programmes, known as demand-side management (DSM), are based on a *"follow-the-supply"* concept, where demand is related to provision capacity. However, with the integration of additional renewable and distributed resources into the supply and distribution systems, the grid needs to be flexible to effectively and dependably meet customer demand at the most affordable price.

According to market research on smart buildings, it is estimated that over the period of 2017 to 2022, more than five billion new Internet of Things (IoT) devices, such as connected thermostats, smart lighting controls, and smart security systems, will be connected in residential and commercial buildings globally [11-13]. These devices facilitate intelligent energy management by providing occupants with enhanced understanding and authority over their energy usage. This intelligence and connectivity of buildings can potentially contribute to meeting the demand for greater energy savings and enhanced flexibility in energy consumption.

To achieve benefits from the *"follow-the-supply"* concept, the main initiatives in this framework are: *i*) Energy efficiency plans to facilitate the spread of highly efficient technologies and increase the penetration level of DERs [14], and *ii*) demand response (DR) programs, where final users are involved in the strategic management of power demand [15].

The Department of Energy (DoE) of the United States has offered a comprehensive description, investigating barriers and opportunities that building sector will undergo in this transition [11]. With the release of the Grid-Interactive Efficient Buildings (GEBs) program in 2019 [16], for the first time in the digitalization era, energy efficiency and DSM concept have been merged in a new concept of buildings featuring as *energy-efficient*, *grid-connected* that *use DERs* and *optimize energy use for grid services*, as depicted in

Figure 1.1.

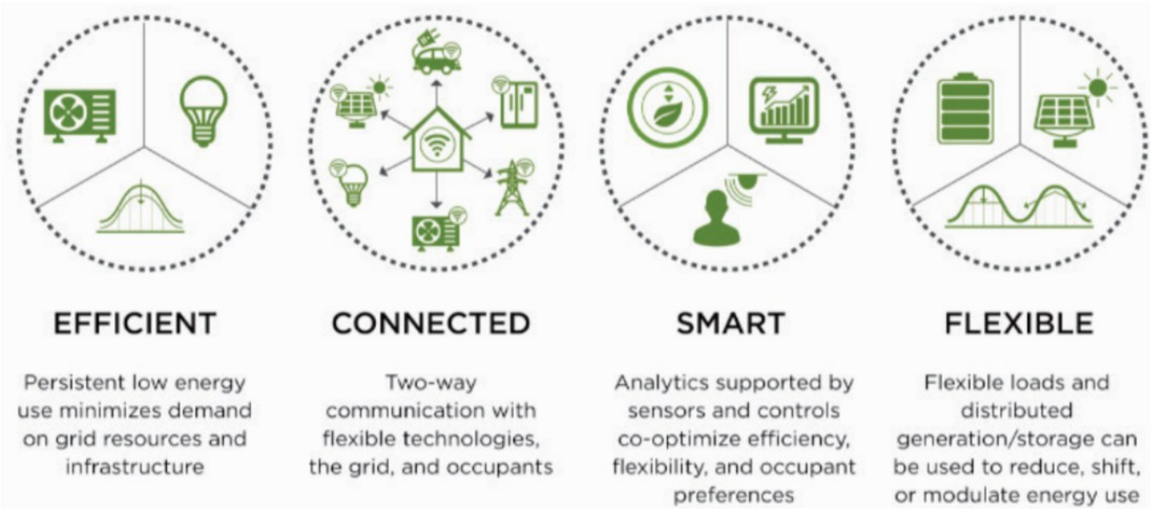

Figure 1.1. The grid-interactive efficient buildings main characteristic [17].

Due to its existing energy efficiency, the building will exhibit a reduced overall energy demand during peak periods compared to similar buildings, making it a valuable asset to the grid. Compared to an efficient smart building, the unique feature of the GEB is its capability to connect and interact with the local grid system. The bidirectional exchange of information between the grid and a GEB allows the building to function as a versatile asset for grid managers. For example, the building can utilize energy storage during times when the grid is experiencing high demand, thus transferring its energy consumption to off-peak periods. Additionally, it has the capability to decrease the demand for resources during periods of high usage, such as by adjusting lighting levels or minimizing energy usage in HVAC systems.

By reviewing the main existing programs or pilots from utilities worldwide, it can be concluded that at the state of the art none of them qualify as full-fledged holistic GEB program. Not considering pure energy efficiency or grid interactivity programs, the remaining who promote both initiatives often clearly prioritize one over the other, limiting opportunities and benefits for customers and grid operators.

Grid-interactivity can be described as evolution from standard DR programs to active participation in the Load Flexibility market (moving upwards), whereas the energy efficiency begins with simple efficiency programs and evolves towards smart energy systems. A visual schematic is presented in Figure 1.2.

Among grid-interactivity programs, most utilities propose DR programs, with either standard or Automated DR (ADR). The participation level can be based on two-level communication, anticipating high-tier periods, or with more sophisticated routines to adjust loads automatically by the help of advanced infrastructures or third-party load aggregators. These programs are often determined by pricing structure. In this framework, a business program is presented by the Duke Energy Carolina's EnergyWise, which provides for free smart thermostats and smart connected switchers for HVAC as well as installation costs, to give the customers the chance to opt in to different participation levels for demand-response events; in return, they receive a commensurate annual bill credit [18]. Other utilities promote ADR programs that also support energy efficiency measures. For example, PG&E's ADR program for commercial and institutional customers [19], or Dominion's Smart Thermostat program for residential and commercials [20] offer additional rebates and/or incentives to whom installed energy efficiency measures.

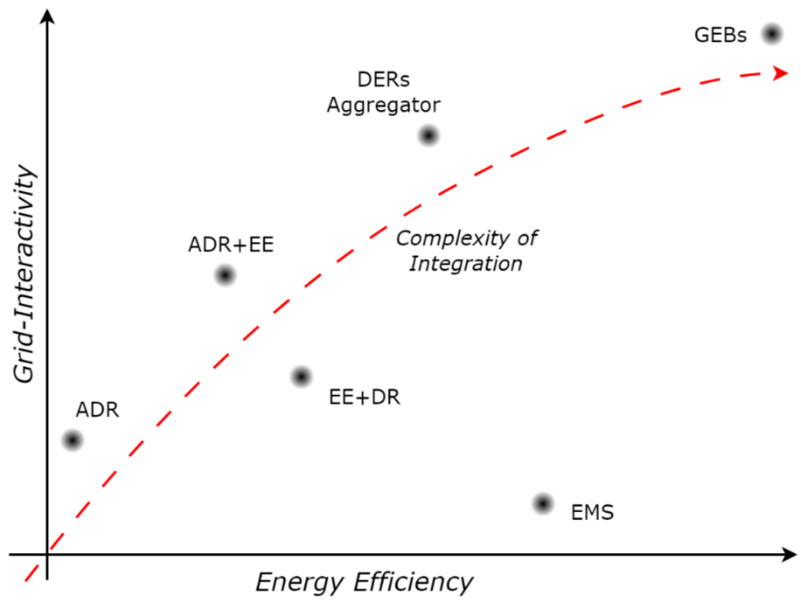

Figure 1.2. Integration level of Grid-interactivity and energy efficiency in the energy market

Another hybrid solution has been investigated by the Southern Company's Smart Neighbourhood pilot where a renewable energy-aggregator integrated multiple producers in a "green fleet", able to provide load flexibility following grid's communication. This approach was able to enhance the self-consumption share of residential producers, and for this reason is presented with a moderate level of energy efficiency benefits.

Most of the energy efficiency initiatives, on the other hand, are mainly promoting Home Energy Management System (HEMS) and Building Energy Management System (BEMS). Fewer recognize incentive or dedicated pricing tariffs for streamlined programs with simultaneous DR.

In 2020, the General Service Administration (GSA) of U.S. and DoE Commercial Buildings Integration program of U.S. selected four GEB technology solutions as test bed in both private sector and GSA facilities [21], to create an high-level energy efficiency (EE) program with participation in load flexibility. The authority concluded that GEBs can reduce energy demand and utility costs and increase customer energy bill savings. They have great potential as a demand resource and as a tool for more-efficient management of the utility grid. They can help mitigate grid stresses, for example by shifting loads to avoid steep ramps and high demand peaks. GEBs can also assist with curtailing renewable energy during times when it is overproduced. From a distribution perspective, GEBs function as a *nonwires* alternative that helps utilities avoid or defer grid upgrades [11]. The outcomes of these relevant demonstration programs have spurred new research investigations to modernize the current state of the electricity industry, generating new frameworks to address the emerging challenges in infrastructure and management [22].

The following sections describe the main problems and barriers, the objectives and the motivation of the presented thesis, whereas the final section identifies the five research questions that this research tries to address.

The problem

In order to fully unlock the advantages of GEBs, it is crucial to establish an initial categorization within the grid-interactivity paradigm: distinguishing between *energy-related* and *power-related* problems.

The *energy-related* issues revolve around the effects of energy efficiency programs, focusing on enhancing system performance to minimize overall energy usage. Much of the literature has concentrated on examining the impact of energy efficiency strategies on thermal comfort [23]. Dedicated rating systems quantify the extent to which total energy consumption is reduced, either in absolute terms or as a percentage, in order to achieve sustainability in buildings. This is accomplished through the development and implementation of policies, utilization of technology, adoption of techniques, and application of strategies. Several articles have examined the LEED green building certification and its impact on energy reduction in buildings [24-26]. Other researchers focused on the formulation and execution of policies aimed at establishing specific objectives and governmental standards [27, 28]. Another intriguing aspect is the application of technologies, specifically active and passive design strategies for energy savings, decrease energy consumption, and optimize energy budgets in building environmental assessment schemes [29-32].

The *power-related* problems encompass load management and analyzes power-related issues. In contrast to the previous class, where the focus was on the magnitude of energy provision for performance metrics, the power-related problems in this class primarily examined the shape of the provision by analyzing daily power trends. Figure 1.3 displays a representative diagram of the 24-hour metering system for residential consumers/prosumers. The top portion illustrates the generation, while the bottom portion shows the demand. The dashed line represents the power generated through net metering.

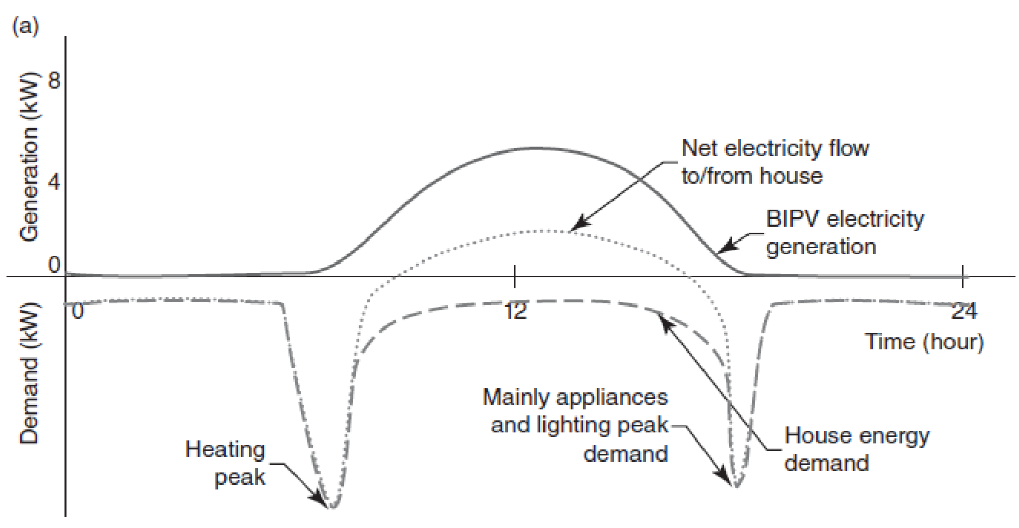

Figure 1.3. Power demand and generation for a representative residential solar building [33].

As evident, although the overall energy consumption might be lower than energy efficiency targets, the power provision is affected by tremendous variations (defined as peaks) throughout the day. In the context of grid-interactivity, such demand from residential buildings might potentially jeopardize the grid stability.

An emblematic example of that is the State of California. In 2009 only the 8.4% of total energy production was from DERs. Because of favorable economics, during the last 15 years, the penetration of solar DERs has reached 64% [34]. Although the drastic drop of primary energy and the reduction of greenhouse gas emissions, the negative effect has been described by the term "canyon curve", to note the extreme variation that happens during the period around noon, as depicted in Figure 1.4. Although the net positive central period, the two cliffs are almost comparable in intensity for all remaining hours.

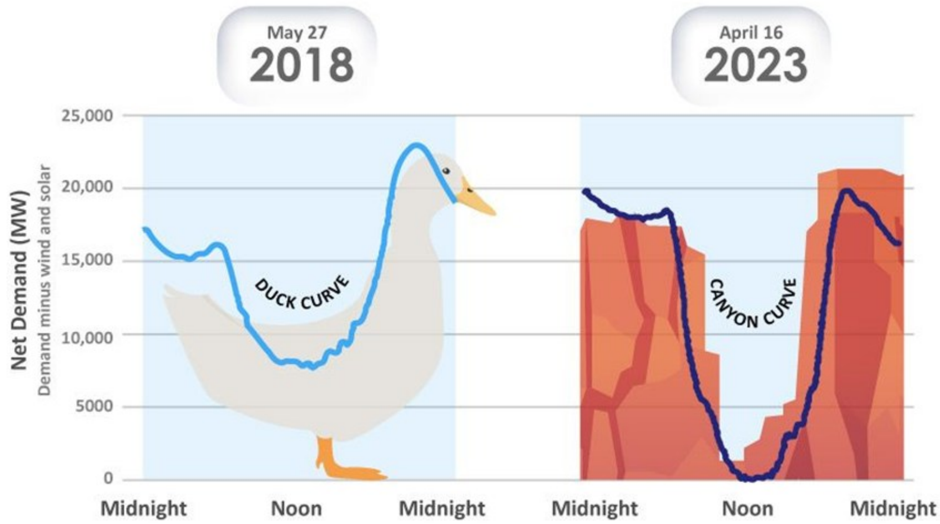

Figure 1.4. From the duck curve to the canyon curve in California [17].

The context of California is highly dependent on DERs, on the other hand the situation of Québec, Canada is different. Québec has 98% of renewable energy production- mainly from hydroelectric plants- and a smaller share of solar-based generation [2]. This energy-mix, along with the fully-electrification program, is resulting in a above-average maximum power demand increase. Around 82% of the overall demand is accounted for space heating. The projections of grid capacity between 2019-2029 was released in 2018 by the utility and recent adjustments, as shown in Figure 1.5.

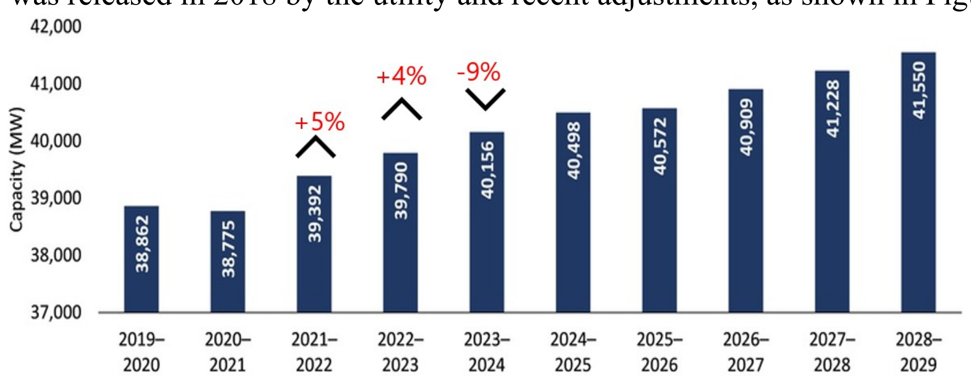

Figure 1.5. Grid capacity projection in Québec, Canada [2] .

Evidence of the dependence of space conditioning as main contributing factor for the increase of aggregated demand is that the weather anomaly with warmer temperature recorded in November

2023-April 2024 has determined a consistent inversion in the projection, with -9%. These market features determine the creation of a *power-related* problem in Québec. As presented by Morovat [35], the aggregated demand for this province is characterized by two peaks, with the highest between 6 a.m. to 9 a.m. and a second lower peak between 5 p.m. to 8 p.m.. This aggregated profile-defined as "beaver curve"- has shown severe increases since 2020 by 15%.

Another interesting market is related to the Canadian province of Ontario. In 2022, this province recorded a maximum peak demand of 22.6 GW whereas the minimum was 10.5 GW (46%). Generators in Ontario are categorized into *baseload generators* (hydroelectric and nuclear) that covers 79.5% of the total annual provision, and *additional generators* (natural gas, wind and solar) that covers the remaining 20.5% [36]. With approximately 90% of Ontario's electricity being emissions-free in 2022, Ontario has the lowest amount of CO_2 emitted for every unit of electricity generated, 22 CO_2e (g/kWh), when compared to neighbouring Great Lakes states: -88% than New York, -131% than Pennsylvania, and up to -3086% lower than Indiana [37]. During demand peaks the daily fluctuations in terms of amount of CO_2 emitted for every unit of electricity generated can vary up to 2000% of the reference annual value, making load management an important asset in energy planning and coordination.

Every energy market, characterized by its unique climates, consumption patterns, and energy sources, presents distinct challenges that necessitate a tailored and comprehensive approach. These variations mean that a one-size-fits-all strategy is impractical and often ineffective. For instance, markets in colder regions may rely heavily on heating during the winter, leading to peak demands that differ significantly from those in warmer climates where air conditioning dominates energy consumption. Additionally, the mix of energy sources - whether predominantly fossil fuels, nuclear, renewable energy, or a hybrid - affects the complexity of managing supply and demand. In renewable-heavy markets, the intermittency of wind and solar power necessitates load management techniques to maintain reliability and efficiency.

Inefficient management practices in these diverse energy markets can lead to significant issues, such as increased operational costs and higher greenhouse gas (GHG) emissions. The use of more polluting power plants, typically kept as backup but activated to meet demand, often results from this inefficiency. These plants usually have higher emissions and operational costs, exacerbating environmental and economic impacts. Moreover, a poorly controlled energy system imposes excessive stress on infrastructure, causing it to operate beyond its ideal conditions. This not only diminishes the longevity of the infrastructure but also heightens the probability of malfunctions and power outages.

The objective

Building energy flexibility (BEF) is a crucial tool within the *"follow-the-supply"* concept, playing a significant role in the achievement of mature load management. BEF is defined as the ability to manage demand and generation according to local climate, user needs, and energy network/grid requirements [38].

Aiming at providing a more reliable and stable network with fewer voltage drops and interruptions, adequate voltage, and maximum power quality, along with improved congestion management due to fluctuations in renewable energy production [39], BEF is a cost-effective concept to support load management at either single and aggregated scales [40]. However, the contribution of a single household is insufficient to improve the grid condition, and its participation in markets can even be disadvantageous because of its limited scale. Therefore, the utilization of energy aggregators (EA) becomes essential to manage and coordinate building portfolios when engaging in power grid, encompassing both wholesale and retail markets, or providing services to system operators [40]. This definition also includes the aggregation of several agents that are not physically connected to each other, hence introducing the notion of virtual communities [41], limiting the eligibility on the location of energy substations.

The main strengths of EAs are versatility and ease of implementation. As evident in the literature, many researchers found convenient solutions with detached houses[42, 43], attached houses [44], multi-family buildings (e.g. tower buildings, condo, etc.) [45-47], and virtual communities [48].

Once identified the residential building portfolio, the final objective of EAs is designing the coordination procedure [49]. Based on the individual features of each household, EAs are effective in generating extra benefits by coordinating the activities of the EAs, rather than the individual building [50], and mitigating the side-effect of market manipulation, such as creation of preheating and rebound effects [51]. Thus, EAs are called to generate diversified control strategies to distribute power peaks over time.

To further enhance the effectiveness of EAs, leveraging data to create an automated methodology is essential. By utilizing advanced data analytics and machine learning algorithms, EAs can develop predictive models that optimize energy consumption and generation patterns. This automated approach facilitates real-time decision-making, ensuring that energy distribution is both efficient and responsive to dynamic market conditions. Additionally, creating a robust methodology to assist the growth of EAs in managing diverse residential building portfolios is crucial. This involves developing standardized frameworks and tools that streamline portfolio management, enhance scalability, and support the integration of emerging technologies, thereby fostering the sustainable expansion of EAs in the energy market.

The motivation

Although it is a recent field of study, EAs and the design of coordination procedures are gaining attention in the research community. The International Energy Agency (IEA) Energy in Buildings and Communities Programme (EBC) Annex 81 – *Data-Driven Smart Buildings*, and Annex 82 – *Energy Flexible Buildings Towards Resilient Low Carbon Energy Systems*, and the previous Annex 67 - *Energy Flexible Buildings*, is concentrating the efforts investigating the aggregated energy flexibility of buildings and the potential effect on energy grids.

The application offers distinct advantages and convenience due to the socio-political context and multidisciplinary nature of energy communities and coordination procedures , and it is well aligned with most of the Sustainable and Development Goals (SDG) of United Nations [52]. According to Eurostat, costs of electricity are increasing worldwide [52], so a *design methodology for optimizing grid interaction of energy aggregators* would ensure access to affordable and clean energy *(SDG7)*; the implementation of such methodology is based on supervisory load management, a not intrusive and cost-effective concept [53], motivating people towards responsible consumption and production *(SDG12)*; the concept of energy communities, as a reliable and safe environment where mutual benefits are generated by energy-sharing mechanisms, would determine a maximization of energy self consumption *(SDG11)*, generating reasonable profits for EAs *(SDG8)*. Finally, a *design methodology for optimizing grid interaction of energy aggregators* defines a win-win condition, where both grid operators and households benefit from lowered expenses and reduced carbon emissions. Therefore, the motivation becomes how to create an appropriate strategy to guide the design of EAs, in order to facilitate mass deployment.

Numerous analyses have been conducted on the recognition of such win-win conditions, demonstrating that EAs are cost-effective [54-56]. Studies show that after an initial transitional period, during which government incentives are necessary, these regimes have significant potential to generate profit [57]. This profitability is attributed to the efficiency gains and cost savings realized through optimized energy distribution and consumption. Furthermore, EAs can easily identify and capitalize on market niches by creating effective price structures. Such structures incentivize participation from residential, commercial, and industrial customers by offering competitive rates and tailored energy solutions. By addressing the specific needs and consumption patterns of different customer segments, EAs can enhance customer engagement and loyalty. This strategic pricing not only supports the growth of EAs but also contributes to the broader adoption of sustainable energy practices. As a result, the market for energy aggregation continues to expand, driven by its inherent economic and environmental benefits.

1.2 Identifying the research questions

A comprehensive literature review has revealed the following five research questions:

1. *What is the level of resolution and the optimal structure for building energy modelling in virtual communities?*

It is essential to identify a trade off between model accuracy and model complexity, since the computational complexity is affected by the combination of the number of households involved and the number of model parameters.

2. *How can we create a generalized control technique for load management in a connected building?*

The creation of a generalized control scheme to manage any configurations of DERs, thermal energy storages (TES), and static and dynamic electrical storages, such as battery energy storage systems (BESS) and electric vehicles (EV).

3. *What is the effect on baseline of consumption of virtual communities when joining energy efficiency programs and demand side management?*

The effect of contemporary energy efficiency and DR programs at the aggregated scale can generate extra profits or adverse reactions and creates convenient trade-off solutions.

4. *How can we design the optimal aggregation strategy in the creation of building portfolios?*

The participation in DR events is influenced by the thermal parameters of buildings, occupant behavior, and diversified strategies are needed to reach optimal performance.

5. *Is there a way to benchmark buildings for a direct aggregation procedure?*

The creation of a benchmarking routine to identify buildings with similar flexibility potential and common strategies in the aggregation procedure.

1.3 Outline of the thesis

In view of the objectives, this thesis is structured as follows:

Chapter *1*. *Introduction* presents an overview of the thesis, illustrating the problems, the objectives and the motivation of the thesis.

Chapter *2*. *Background and Literature Review* is structured into three Sections: *Load Management* with the description of the energy industry, the building energy flexibility of buildings, Demand Response, and the analysis of traditional and advanced control techniques; *Building Energy Modelling* with the dedicated modelling techniques, ensemble setups, and portfolio management. Emphasis is given to reduced order models and supervisory control schemes; *Design and Optimization of energy aggregators,* where load management of aggregators is discussed along with coordination schemes and building benchmarking.

Chapter *3*. *Data-driven methodology for building demand forecasting,* where the design methodology is presented. In this chapter, three subsections address the presented research question for the establishment of modelling procedure for thermal load management, the proposed setup for prediction, and the proposed hierarchical control scheme, designing local and supervisory controls.

Chapter *4*. *The evolution of baseline in demand response* focuses on the mutual relationship between demand-side management and energy efficiency of energy aggregators. In this central chapter, the first section presents the evolution of load profiles from high-performing technologies, the second assess the impact of electricity pricing on load profiles. The third section discusses the integration of electric vehicles in the management of residential buildings, and lastly the thesis identifies supporting pricing structures for prosumers.

Chapter Diversification *strategies for Energy Aggregators* analyses the price-responsiveness of building energy flexibility, elaborating on the relationship between model features and flexibility potential to drive building benchmarking for load management. The final part of the chapter presents the designed aggregation techniques.

Chapter *Conclusions* that concludes the thesis and provides the working assumptions, limitations, as well as recommendations for future works.

Chapter *References*

2. *Background and Literature Review*

A methodology for smart communities and EAs in demand response must take into account the integration of modelling techniques, predictive management, and control schemes.

This chapter examines the current practices in building operation, explaining the concept of load management, and delving into the practices of demand-side management. The present work provides an overview of the primary demand response programs, which include both traditional and advanced control solutions. The thesis discusses the transition from individual to portfolio management in the context of energy aggregators. It highlights the current advancements, as well as the primary limitations and opportunities related to coordination schemes and the utilization of machine learning to streamline the benchmarking process.

2.1 Load management

The research conducted by IEA EBC Annex 67 emphasizes load management and acknowledges that the interactions between buildings and the energy infrastructure in time and scale should be fostered in order to fully benefit from the potential of renewables and mitigate CO_2 emissions on an aggregated level for achieving the intended de-carbonization of energy services until 2050. Consequently, building design and control should also be evaluated beyond that of individual buildings [38]. With markets changing to allow participation of DER and more renewable energy sources coming online as additional loads become electrified, load management is poised to become a critical grid-balancing resource [58].

The "*follow-the-supply*" approach is based on the empowerment of end users via DSM. Load management consists in an arrangement of actions to enhance the energy system on the user side [59], exploiting customers to solve the mismatch between available supply and demand.

To better understand the evolution of the power demand, an examination on the four-stages of *load profiling* is presented.

Load profile of residential buildings is distinctive and unique. In contrast to commercial applications, where profile is mostly influenced by working hours and exhibits a rather stable demand pattern, the load profile of residential buildings is affected by a combination of linear and nonlinear factors including building physics, deployed technologies, weather conditions, and occupant behaviour [60]. Load profile is a time series usually characterised by a repetitive trend with stochastic components and time-based cycle at annual, seasonal, and daily scales [61]. These time series are usually chunked into subsequences through a fixed length window to obtain a time scale-based profile [62]. In most of the energy and buildings applications load profiles are usually well described on a daily scale [63]. While load profiles may exhibit individual variances, the use of data mining techniques facilitates the identification of common patterns and the classification of load profiles into four distinct stages of evolution, as shown in Figure 2.1.

Stage I of Figure 2.1 describes the typical residential building with the two-peaks typical demand profile in winter. This was the reference profile before deployment of DSM strategies. *Stage II* of Figure 2.1 describes the use of energy efficiency as a demand modification tool. Efficient power demand reduces peak-to-valley variations, flattening the load profile and it is characterized by a lower intensity throughout the period. This is realized by the means of highly performance technologies, and improved building envelope. *Stage III* of Figure 2.1 represents an efficient load profile with the exploitation of solar PVs. The net energy consumption registers a significant reduction, but the creation of steep ramping of loads becomes an issue for grid operators. Because of the mismatch between supply and demand, *Stage III* is characterized by bidirectionality. Finally, the last step of evolution of load profile is the *Stage IV* of Figure 2.1. GEBs combines the previous steps with load management and performs a shifting strategy to match generation. It optimizes energy consumption and self consumption [33], minimizes the expense for electricity [11] , ensure energy resiliency [64], and support grid stability.

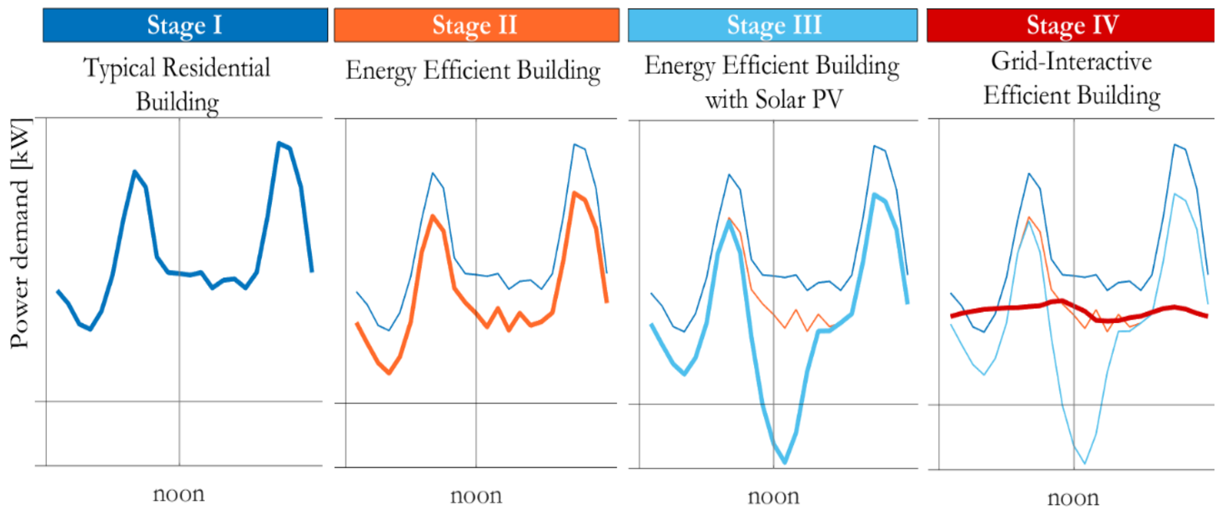

Figure 2.1. The four stages of evolution of Grid-Interactive Efficient Buildings

Currently, the forefront of technological advancements is situated in the transitional phase between *Stage III* and *Stage IV*. In fact, many governments present high penetration levels of solar DERs and mature levels of energy efficiency programs and are now concentrating the effort of the scientific community towards load management programs [65].

Traditionally, the *"follow-the-demand"* model determines the provision of electricity from power plants based on the prediction of the aggregated demand profile. The traditional energy sources, such as coal and natural gas can be modulated according to the need because of their dispatchable nature. The energy market has experienced steady decentralization and growing difficulty in ensuring grid stability as renewable sources have become more common, progressing from *Stage I* to *Stage III*. In fact, supply volatility escalates as the proportion of non-dispatchable technologies, such as wind turbines and solar DERs, grows.

On grid perspective, solar DERs are effective during the middle of the day to fill a portion of the demand, but when the solar radiation begins to drop, the net load curve increases sharply. Thus, these steep ramps become the biggest challenge in the transition from *Stage III* to *Stage IV* [39].

The International Organization for Standardization (ISO) has released in 2018 the ISO50001-*Energy Management System* to define requirements and standards for companies in the field of energy management. The ISO defines the requirements for planning and operation of energy management applications. The planning is divided into *i)* Energy review, *ii)* Energy Performance Indicators , *iii)* Energy baseline, and *iv)* Planning the collection of energy data. A dedicated chapter addresses the support of EMS, defining competences and awareness about the energy policy, and requirements for internal and external communication protocols. Chapter 6 on Operational Planning and Control informs about the requirements for Design and Procurement, whereas

Chapter 7 analyses Performance Evaluation, with Compliance evaluation, Internal audits, and Management Review. The final chapter deals with Improvements, defining Nonconformity and corrective actions, and the trend towards continual improvements [66]. This class of ISO is not limited to requirements, ISO 50001-*Requirement,* ISO 50002-*Energy Audits,* ISO 50004-*Guidance,* ISO 50006-*Measuring Energy Performance*.

These ISOs target different stakeholders of the energy industry and for this reason, the following section describes the whole energy industry, defining responsibilities and opportunities for each player in the new paradigm of *"follow-the-supply"* concept.

2.1.1 The Energy Industry: Identifying stakeholders

The energy and reserve capacity markets are cleared sequentially in Day-Ahead Coordination (DAC) via independent auctions [67]. The reserve capacity market is typically cleared shortly before the energy market, defined as intra-day market (IDM), and the committed reserve capacity needs to be continuously available during the contracting period [67]. In the case of real-time system imbalance, arising from forecast errors and unexpected events [68], the procured reserves are activated according to the merit order; that is, balancing offers are activated in ascending order of activation costs until the system frequency is restored [69]. This continuous operation market is defined as Dynamic Actionable Reserve (DAR). The power system's market operation is addressed in consecutive stages: scheduling of generation units with procurement of reserves (DAC), intra-day adjustments of generation schedules (IDM), and real-time activation of flexibility to compensate for imbalances (DAR). Furthermore, it is essential to accurately measure and quantify energy flexibility, which will be thoroughly examined in the following section. This quantification should encompass both DAC as an additional source of power generation and DAR as a means of addressing imbalances in the energy system. In order to gain a comprehensive understanding of the stakeholders and their specific roles, it is crucial to provide a thorough description of the key participants in the energy supply chain:

- **Regulator**

Electricity industry structures vary significantly across countries, differing in competition levels, integration degrees (vertical and horizontal), ownership (public or private), and development stages. Regardless of these variations, the electricity supply industry performs four fundamental functions: Generation, Transmission, Distribution, and Supply (Retail). These functions can be privately or publicly owned, with multiple functions often contained within a single company. While generation and supply might operate under monopoly or competitive conditions, transmission and distribution are typically provided on a monopoly basis [70].

Regulation is fundamentally designed to address "market failure" and is deemed necessary to safeguard consumers, society, and the environment. The primary motivation for regulating infrastructure sectors such as energy is to ensure fair competition and to prevent the emergence of monopolistic entities. This approach aims to keep prices affordable for consumers. In markets that are not liberalized, the extent of regulation is a direct political decision, closely aligned with policy objectives [71]. In competitive markets, regulation should only be applied when the benefits, such as reduced consumer costs, outweigh the absence of regulation. For instance, regulation may be necessary to prevent market abuse. It is often argued that "competition is the best regulator," suggesting that effective competition naturally leads to the most efficient market operations, as companies are incentivized to meet consumer needs. However, regulation may still be needed to ensure competition remains effective[72].

Regulating markets aims to promote economic efficiency and mitigate market failures to ensure the provision and protection of socially desirable goods and services. The key motivations for regulation in competitive markets include:

- *Economic Efficiency*: Preventing market abuse.
- *Consumer Protection*: Keeping prices low.
- *Environmental Protection*: Reducing harmful emissions like CO_2, SO_2, and NO_x.
- *Social Justice*: Ensuring universal supply.
- *Security of Supply*: Maintaining reliable service.

These objectives can sometimes conflict. For example, keeping prices low might clash with promoting renewable energy technologies, which can be costlier than conventional methods. Policymakers and regulators must balance these conflicts, considering factors such as the intended duration of the regulation. Short-term measures might increase prices due to renewable energy generation or energy efficiency activities, but long-term outcomes could see reduced costs as new technologies become cheaper and fossil fuel prices rise. Ensuring universal supply might also raise prices, but the benefits, such as poverty reduction, improved health, and environmental gains, need to be weighed against these costs.

Balancing these issues is challenging and often falls within the purview of politicians and policymakers. However, implementing these policies is the responsibility of regulators, who must refine the balance of policy aims through specific measures and rules. Regulators also play a crucial role in advising policymakers, leveraging their expertise in economics and practical rulemaking.

For example, Regie de l'Énergie serves as the energy regulator in Québec, overseeing the province's energy sector to ensure regulatory compliance and consumer protection.

- **Policy Maker**

Energy policy is a specialized subset of economic, foreign, and national and international security policies, with a focus on ensuring a reliable, affordable, and environmentally sustainable energy supply. This policy area addresses issues such as energy security, price volatility, resource constraints, and potential threats to energy facilities [73]. Key pillars of energy policies and standards include encouraging energy efficiency, promoting renewable energy, limiting greenhouse gas emissions, and providing information and education [74].

The formulation of energy policy involves six crucial stages [75]:

1. *Awareness Stage*: This initial stage emphasizes gathering information on key issues that necessitate the development of a policy, such as energy access and carbon emissions. Potential barriers and opportunities are identified, collected, and analyzed.
2. *Problem Definition Stage*: At this stage, the implications of identified barriers and problems, such as those related to energy infrastructure provision, are explored.
3. *Identification of Options Stage*: Possible consequences of potential policy options are assessed. For instance, the impact of decentralizing electrical power generation is evaluated at socio-economic, environmental, and technical levels.
4. *Policy Selection Stage*: A preferred policy is chosen based on the understanding gained in previous stages regarding associated problems and their implications. An example

is selecting a decentralization policy for energy generation that addresses energy access issues, enhances energy security, and reduces vulnerability.

5. *Policy Implementation Stage*: This stage involves translating the chosen policy into action, meaning the policy is adopted after thorough deliberation by stakeholders.
6. *Policy Evaluation Stage*: This final stage involves evaluating, monitoring, and tracking the chosen policy to measure progress and awareness. Continuous evaluation and monitoring help determine the number of people with access to energy over time and assess the required infrastructure to address energy access deficits.

For instance, the Government of Quebec's 2030 Energy Policy serves as a reference policy in Québec, outlining strategies to achieve sustainable and secure energy supply.

- **Transmission System Operator**

The TSO operates the transmission system and is responsible for transmitting and balancing power and maintaining and developing the transmission infrastructure. The TSO is involved in the energy transition as the inconsistency and unpredictability of renewable energy, the decentralization of generation, and the increased consumption makes safely operating the transmission system difficult. The Groupe – TransÉnergie et équipement, in its role as transmission provider (the "Transmission Provider"), is tasked with operating the transmission system, marketing system capacity in a non-discriminatory manner, in compliance with applicable regulatory requirements, and managing power flows across Québec. A schematic of the very high and high voltage infrastructure is presented in Figure 2.2.

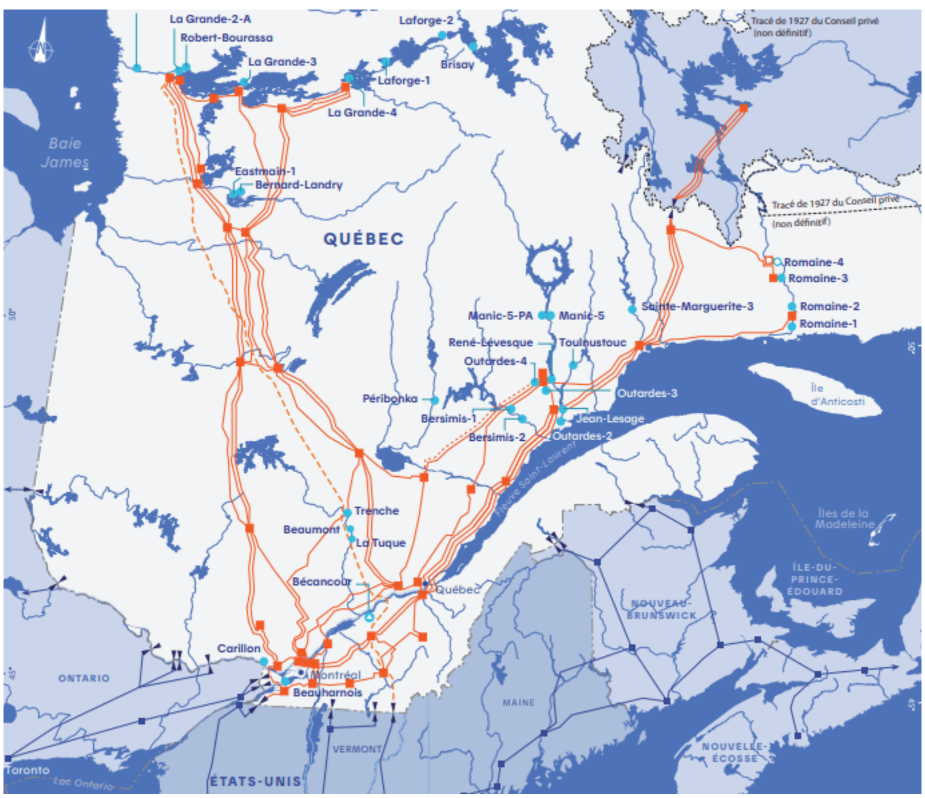

Figure 2.2. High and very high transmission infrastructure for Québec, Canada

34,000 km of transmission lines (in orange), of which a third is operated at very high voltage (735 kV), 533 substations (44 kV to 735 kV), and 15 cross-border interconnections allowing power interchanges with the maritime provinces, Ontario and the U.S. Northeast. Interconnection capacity in 2024 is 6 GW for import, and 8.2 GW for exports.

- **Utilities**

An electric utility is a corporation, person, agency, authority, or other legal entity responsible for the operation and maintenance of distribution facilities for the delivery of electric energy primarily for public use. This category encompasses a variety of entities including investor-owned electric utilities, government and municipal utilities, regional utilities, and electric cooperatives. These organizations are integral to the provision and management of electrical power, ensuring that the energy generated is effectively distributed to meet public demand. Generation of electricity can be managed by utility-owned entities or private (external) entities. Private generators typically enter into individual contracts with utilities to supply the generated power, ensuring a diverse and stable energy supply. The contractual agreements between utilities and private generators are crucial for maintaining reliability and efficiency within the power grid. These contracts often detail the terms of energy provision, including pricing, delivery schedules, and compliance with regulatory standards. By involving both public and private stakeholders, the electric utility sector fosters a competitive, yet regulated environment aimed at enhancing service quality, reducing costs, and promoting innovation. The collaborative efforts of these various entities play a pivotal role in the ongoing development and sustainability of the energy infrastructure, catering to the dynamic needs of the public and industry alike.

- **Distribution System Operator**

The DSO operates the distribution (low and medium voltage) grid and is responsible for maintaining and developing the infrastructure and ensuring that the power quality stays within the physical and regulatory limits of the distribution system. The energy transition brings large-scale generation to the distribution grid and reverses the power flow making it difficult to keep the distribution system within the regulatory operating limits. In Québec, the low and medium voltage infrastructure belongs to the utility, Hydro-Québec.

- **-Aggregators**

Aggregators will become important participants in the operation of future energy systems and electricity market bidding. Aggregators will be vital in bringing together various small-scale distributed energy resources (DERs) and allowing them to participate in the energy market collectively. The hybrid communication control scheme for distributed energy resource (DER) management, which integrates centralized and decentralized coordination approaches, provides significant benefits compared to exclusively centralized or decentralized methods, particularly in relation to the regulatory framework governing energy systems in the European Union and North America for DER and demand response programs (DRP). It is both possible and advantageous to incorporate and execute aggregators in networks and markets. Aggregators offer a platform for individuals to engage in the electricity market in a manner that is advantageous to different parties involved, such as consumers, utilities, and grid operators. Furthermore, aggregators play a crucial role in promoting the attainment of climate objectives by optimizing energy consumption and integrating renewable energy sources. In order to ensure the successful integration and operation of electrical network infrastructures, it is crucial to conduct comprehensive simulations of aggregator concepts, while also taking into account the relevant regulatory provisions. Moreover, the coordination of aggregators can help alleviate the negative effects of distributed energy resources (DERs) on distribution networks, thereby improving the overall stability and efficiency of the grid.

The EU 2019/944 Electricity Directive defines aggregation as a "function performed by a natural or legal person who combines multiple customer loads or generated electricity for sale, purchase or auction in any electricity market" [49]. The stakeholder engaged in aggregation may interact differently with upstream and downstream parties of the electricity market and can be classified accordingly [76, 77]. The two main contributions of energy aggregators are the flexibility activation, and the creation of an "expected demand".

The flexibility activation is an event-driven process where ancillary services and local balancing must be addresses through the flexibility request, in communication with the TSO. The expected demand is the outcome of prediction algorithms to create a reliable forecast for energy consumption. These projections fall in both DAC and IDM. This communication protocol aims at informing the DSO about the expected potential reduction and reserve allocation for either short- or long-term planning. The schematic is shown in Figure 2.3.

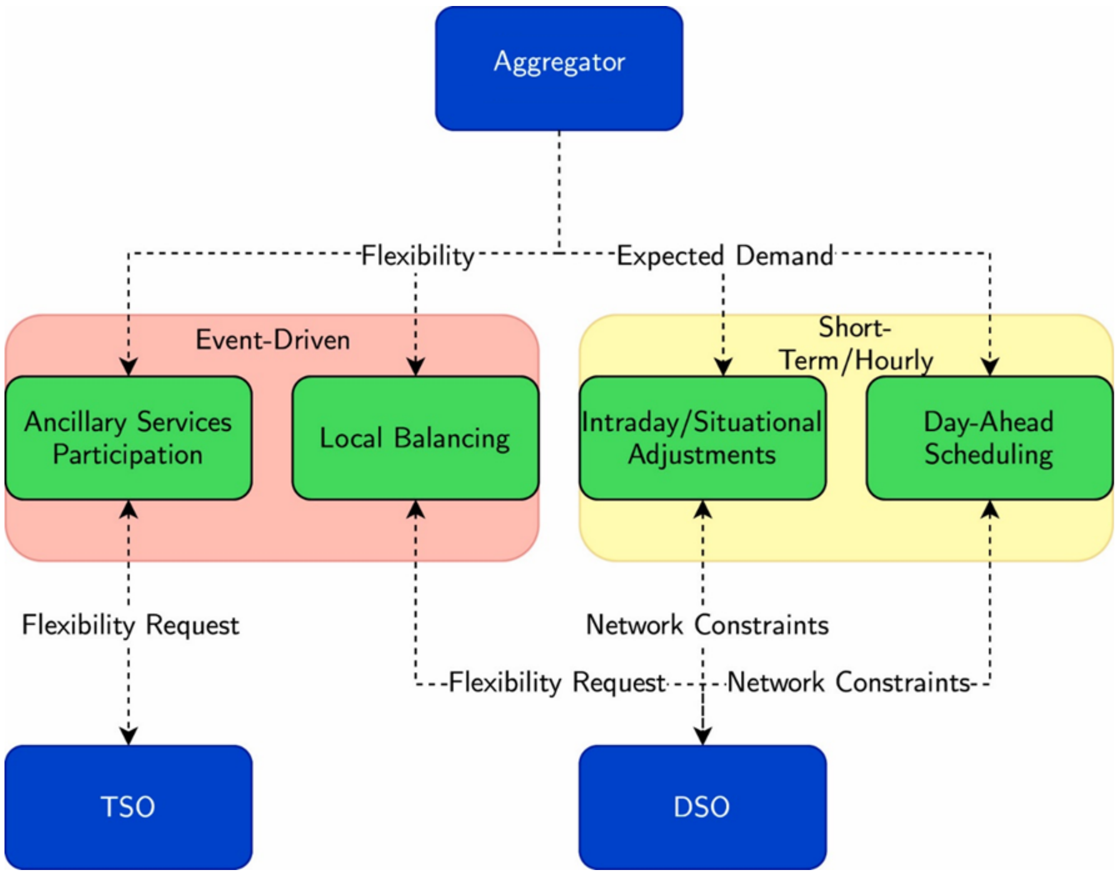

Figure 2.3. The connection process of aggregators among stakeholders

The general classification of EAs, shown in Figure 2.4, is based on the contractual agreement among parties.

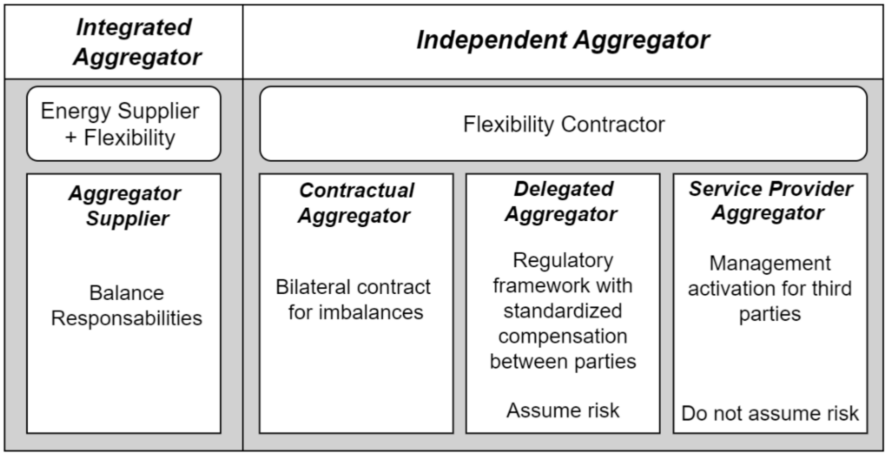

Figure 2.4. Classification of energy aggregators, responsibilities, and risk assumptions.

When the EA acts as either energy supplier or flexibility service for balancing services, the EA is called *Integrated Aggregator*. On the other hand, when the energy supply is separated from the balancing services, the EA is defined as *Independent Aggregator*. Specifically, the recognition of bilateral contract for imbalances defines the *Contractual Aggregator,* where supplier and aggregator share the same connection point. When the aggregator is not responsible for balancing services but deal with the management of energy flexibility the categorization is based on the risk assumption.

An aggregator who owns risk, deal as *delegated aggregator* and has to setup a standardized compensation for the stakeholders, whereas when the aggregator does not assume risk, the only responsibility is in the management of the activation of energy flexibility for third parties. In this case the aggregator is called *service provider.*

2.1.2 Building Energy Flexibility

According to the existing literature, BEF is thought to be the most powerful solution to overcome technical issues for load management in the energy network [78]. Energy flexibility of a building is defined as the ability to manage its demand and generation according to local climate conditions, user needs, and energy network requirements [38].

There are four primary contributions in the building flexibility calculation, as shown in Figure 2.5. The first contribution is energy generation from the building itself, such as solar panels, small wind turbines, etc. The second contribution is building thermal load management, with the slow dynamics of heat absorption and release. The third contribution is energy storages (ES), including TES, BESS, and EVs. The potential in shifting power from peak to valley periods demand can be obtained recurring to strategic management of ES, with charging and discharging scheduling. ESs are the most effective solution to enhance energy resiliency [79]. The last contribution is provided by interruptible loads: the time window of operation of some appliances can be shifted during time (such as cloth washers and dryers), and its management is an additional source of flexibility [80]. Occupant behavior, weather conditions, and energy prices have an influence on these four contributions [81]. The final goal of BEF is to modify power demand according to grid needs. However, the modification strategies are affected by technical limitations (such as maximum output of a heat pump, thermal properties of the envelope, etc.).

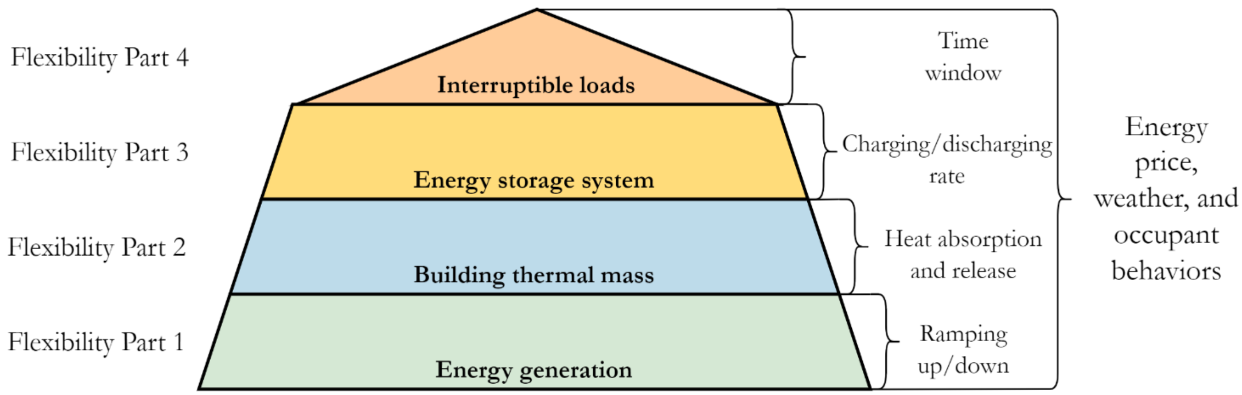

Figure 2.5. The four contributions of building energy flexibility

With a focus on characterization and quantification of BEF, DSM is classified into four levels of application: *system* level, *building* level, *district/community* level, and *building sector* level.

Flexibility services: main and ancillary services

The main flexibility services can be classified into:

i. Efficiency, defined as a persistent power demand reduction regardless of time;
ii. *load shedding*, a short-term power demand reduction during peak demand hours or emergency events [82];
iii. *load shifting*, considered as the evolution of load shedding because the building changes the energy use timing to reduce power demand during peak hours, shifting the energy reduction during off-peak hours of the day [83];
iv. *load modulation*, defined as the process of continuous communication between grid operator and the building that automatically adjusts power demand;
v. *generation*, the process of power generation from DERs from self consumption to the dispatchment [84]. At the state of the art, shifting loads is the dominant flexibility type in 60% of applications, followed by shedding (19%), generation (16%), and modulating (6%) [84].

Quantification of the building energy flexibility and key performance indicators

Quantification is one of the main limitations of the commercialization process of BEF [85]. In fact, the lack of a streamlined and standardized approach for quantification may be attributed to several factors, such as the varying degrees of data resolution, diverse expertise in building modeling and interested stakeholders, and the intrinsic nature of the problem [86].

The dynamic nature of the application, the high number of parameters and disturbances, and the prediction uncertainties make it essential to have a real-time update according to performance goals. With the widespread deployment of sensing and metering in buildings, data-driven approaches have gained importance during the last decade [87]. Therefore, the selection of the appropriate key performance indicators (KPIs) is crucial in the design of methodology for optimizing grid interaction of virtual energy communities [88].

The classification groups evaluation metrics into *baseline-required* and *baseline-free* KPIs, according to the retrospective (based on historical data) and prospective (aimed at the prediction) problem formulation. Baseline-required KPIs are the most diffuse group (80%) and require building modeling. The quantification of BES is evaluated by assessing (in retrospective) or predicting (in prospective) flexible power demand and "business-as-usual" load profile [89]. These KPIs compare the two profiles to quantify variation trends, and the key characteristics comprise low complexity, with the possibility to be applied over single and multiple events, and at building and cluster levels [88].

On the other hand, baseline-free KPIs do not need building modeling expertise and can be calculated in a single scenario, with absolute values. This approach is effective when it is difficult to monitor the performance of a building, or when no data-driven approach can be used to generate the baseline. However, the impact is not consistent, and the proposed methodologies are not scalable for EAs.

Among the baseline-required KPIs, the most relevant for the considered application are: Energy Efficiency of Demand Response Action (η_{ADR}) [90, 91] as :

$$\eta_{ADR} = 1 - \frac{\int_0^{\infty} (Q_{ADR} - Q_{REF})dt}{\int_0^{length(ADR)} (Q_{ADR} - Q_{REF})dt} \tag{2.1}$$

Where, Q_{ADR} is the power supplied during the DR event and Q_{REF} is the power supplied during reference operation. This is a retrospective, baseline-required KPI.

The absolute quantification of the power reduction is defined peak power shedding (ΔP_{SHED}) [92, 93]:

$$\Delta P_{SHED} = P_{baseline,peak} - P_{flexible,peak} \tag{2.2}$$

An economic formulation of the problem is the Flexibility Savings Index (FSI) [78, 94]:

$$FSI = \frac{c_{FLEX,OPERATION}}{c_{BASELINE,OPERATION}} \tag{2.3}$$

Where, c is the cost of flexible and baseline operation respectively. This metric highlights the reduced operational cost during a DR event.

Another reference-required KPI is the Building Energy Flexibility Index (BEFI) [95]:

$$BEFI(t,dt) = \frac{\int_t^{t+dt} P_{REF}dt - \int_t^{t+dt} P_{FLEX}dt}{dt} \tag{2.4}$$

where, P_{REF} is the reference load profile and P_{FLEX} is the flexible profile. It is important to note that based on the selection of *t* and *dt* it is possible to characterize the single-step variation and the overall profile during DR events. This makes possible to classify this KPI as both load shedding (when *dt* describes the entire DR event) and as load shifting (when the *dt* is longer, to also describe the off-peak hours).

This metric can be formulated as a percentage (BEFI%) in Eq. (2.5), and representative of a virtual community defined combined building energy flexibility index (CBEFI) [96] in Eq. (2.6).

$$BEFI\% = \frac{P_{REF} - P_{FLEX}}{P_{REF}} \times 100 \tag{2.5}$$

$$CBEFI(t,dt) = \sum_{j=1:N_{Household}} BEFI_j(t,dt) \tag{2.6}$$

Another KPI is given by Le Dreau et al. [97]. The Flexibility factor is a pure load shifting KPI, as shown in Eq. (2.7)

$$FF = \frac{\left[\int q_{nonpeak} \cdot dt - \int q_{peak} \cdot dt\right]^{REF}}{\left[\int q_{nonpeak} \cdot dt - \int q_{peak} \cdot dt\right]^{FLEX}} \tag{2.7}$$

If the heating use is similar in low and high price periods, the factor is 0. If no heating is used in high price periods, the factor is 1. If no heating is used in low price periods, the factor is −1. One major limitation of this KPI is that is climate sensitive. Therefore, it is not possible to compare FF of different locations. Thus, this metric is useful for building owners, DSO and TSO.

An important contribution is given by Junker et al. [78], where the flexibility activation is described by the Flexibility function (FF). This approach considers that the resulting load when exposed to a penalty signal can be separated into two parts; the load that responds to the penalty, and the non-responsive load. The response is evaluated as in Eq. (2.8).

$$Y_t = \sum_{k=0}^{\infty} h_k \lambda_{t-k} + R_k \tag{2.8}$$

where λ_K is the penalty signal, and R_K is the non-responsive consumption, and h_K the impulse response function.

Baseline-free KPIs are generally full of insight for utilities and grid operators because they focus into the shape of load profiles. These metrics are mainly characterized by single-step variations and describes the operative condition of grid’s elements. Three are presented in this proposal: load factor (LF) in Eq. (2.9), peak-to-valley ratio (PTV) in Eq. (2.10), and system ramping (SysR) in Eq. (2.11).

$$LF = \frac{AVG_L}{\max_L} \tag{2.9}$$

Where, AVG_L is the average demand over a simulation timeframe and $\max_L$ is the peak demand occurred during the same timeframe. PTV is the ratio between the maximum and the minimum power demand during the same timeframe.

$$PTV = \frac{\max_L}{\min_L} \tag{2.10}$$

Finally, SysR is the mean absolute variation recorded from a timestep to the following one.

$$SysR = \sum_{i=0}^{N-1} abs(P_i - P_{i+1}) \frac{1}{N} \tag{2.11}$$

2.1.3 Demand Response

As described in the previous Sections, DSM is based on the engagement of final customers in the process of grid balancing during critical periods [78]. Utilities promote responsive-based market structures defined as DRP, relating the energy demand elasticity to the market's prices [39].

Traditionally, DR has focused on large commercial and industrial customers. But as the technology matures, more and more small commercial and residential customers are getting involved. The idea is to broadcast DR signals continuously from dispatchers to customers with preprogrammed building systems to take actions [98].

The DOE categorizes DR programs into price-based and incentive-based programs [43]:

- Price-based programs are proposed by the utilities, offering participants time-varying rates that reflect the value and cost of electricity over a given period.
- Incentive-based programs consist of rebates or discounts for customers participating in a DR event.

The most deployed pricing structures are shown in Table 2.1, including acronyms, definition, trigger, and participants [99]. The choice of the tariff depends on the local utility, and rates are developed to reflect the technical needs of the considered infrastructure [84].It is important to remark that all the above programs, especially incentive-based, are conceived on prospective baseline-required formulation.

Table 2.1 Main DR programs, definition, trigger, and participants

Program		Definition	Trigger	Participants
Static Time of Use	s-ToU	Prices vary during the day in a fixed and regular way	Price	residential, commercial, industrial
Dynamic Time of Use	d-ToU	Price points are fixed, but the times at which they apply vary from day to day	Price	residential, commercial, industrial
Critical Peak Pricing	CPP	Pricing is mostly flat, but there is occasional high price 'events' of which customers are notified in advance.	Price	residential, commercial, industrial
Real-time Pricing	RTP	Utilities adjust electricity price over short time intervals (e.g., hourly) to invoke customer power demand changes.	Price	residential, commercial, industrial
Critical peak rebates	CPR	Pricing is flat, but at certain times (notifiable in advance) customers are rewarded for reducing their electricity demand compared to some agreed amount.	incentive	residential, commercial, industrial

Direct load control	DLC	Utilities directly control the operation of some customer equipment during peak demand hours, and offer customers some payment incentives	incentive	residential

Demand Response program worldwide

The government efforts towards dynamic tariffs are universal in our world, ten examples of operating utilities are presented [100]: The regulation for Canada is based on the provinces. Ontario's main utility is Hydro One and the three pricing structures offered are used and implemented in the current methodology. In Québec, Hydro Québec diversified the pricing structures since 2018, creating risk-aware and risk-unaware dynamic pricing for residential customers. In Portugal, tariffs can be structured around a fixed, capacity, and volumetric component and the consumption periods are defined by the customer type and voltage levels [101]. In Finland, the electricity structures do not present a capacity component [102], whereas in Spain the pricing structure does not reflect a fixed component. Since the grid features of the system operator (Red Eléctrica de España), the Precio Voluntario para el Pequeño Consumidor (PVPC) consists of volumetric charge and contracted capacity component, which accounts for network, generation capacity, and regulatory costs. Sweden and Norway represent two developed scenarios where the price allocation comprises fixed, capacity, and volumetric components. The high coverage of smart thermostats (in Sweden) and an automated pricing algorithm (in Norway) create the prerequisite for demand side management. In Estonia the monopoly-operated TSO is Elering AS, whereas almost all the DSO belongs to Elektrilevi OÜ [103]. In this framework, three pricing schemes are offered, including fixed, equivalent and exchange packages. The creation of bidding packages can be seen as effort towards dynamicity, even if the lack of regulation creates concerns about the fairness. In Italy the situation is different because there is no separation between DSO and TSO, and everything is led by ENEL Distribuzione. The regulator determines the distribution tariff structures [104], and offers tariff by customer types and voltage levels. The network tariff bill consists of four parts: fixed, volume, capacity, and tax. There is no separation of electricity transmission and distribution tariffs for residential users, and there are no regional differences in tariffs. The pricing is either mono or multi-tier, with a static ToU configuration. The situation of Australia will eventually work as a demonstration case, since proportion of network tariff components is being implemented to gradually reflect the costs of serving their customers. This is the representation of market fairness and transparency since the revenue of the utility is of public domain [105]. However, the creation of pricing algorithms is still to come. The diversity of United States of America delivers a bigger picture about dynamic tariffs, having local utilities promoting several dynamic time-of-use (ToU) or pure dynamic pricing structures. In California, the advance in demand side management has been an example of implementation of incentive strategies to increase the penetration of DERs and EVs to an almost fully electrified market [106]. In Illinois, the Commonwealth Edison's and Ameren Illinois' services promote day-ahead home electricity costs by text, voice mail, email, phone, and internet. The pilot project has shown an overall 15% saving. In France, the Ecowatt project [107] targets consumer behaviour as key lever for the proper functioning of the electricity system and achieving the energy transition targets. Therefore, to encourage the smoothing of the net consumption of the available decarbonized means, the daily spot price signal and the supply curves provide a good indication for experts. The creation of a supplementary indicator to be communicated to a wider audience, based on a forecast of the power generation capacity that does not emit greenhouse gases. This indicator more precisely reflects the ability of French decarbonized electricity production to meet national demand. It therefore does not take into account the possible operation of thermal groups located on the national territory if the power they produce is not indispensable to the satisfaction of French consumption. It is therefore different from the CO2 content indicator already existing in eCO2Mix: it is not a predictive indicator of the "average CO2 contents" of electricity produced in France. This ambition responds to a need expressed by citizens, demand-driven solution providers and public authorities [107, 108]. Finally, the UK support dynamic pricing electricity tariffs Scottish Power, EDF and Octopus Energy, and will use smart meters to monitor the time and amount of energy used. which will offer incentives to use power when the demand is low or the supply is 'green', while charging more at peak times.

Grid Requirements and Performance metrics
From the operational standpoint, the quality and the reliability of power provision is mainly based on the shape and the magnitude of the aggregated provision over a reference period (usually from midnight to midnight). A comprehensive analysis of the most relevant performance metrics – categorized as baseline-free KPIs- was presented by Corbin &Henze [109]. These operative metrics evaluate the aggregated load profiles and the distribution feeder's stress throughout the day for a given building portfolio. The daily fluctuation is assessed by the *Peak to Valley* (PTV) defined as the ratio of the peak demand to the minimum demand calculated over a given simulation time frame (00.00 am to 23:45pm with 15 min intervals for this application). The goal is to produce a load profile as flat as possible. It gives insight about the amount of generation to bring online to satisfy the demand; The average-to-maximum variation is assessed by the *load factor* (LF), where the ratio of the average power to the peak value is calculated to evaluate how well the generation assets are utilized; S*ystem ramping* (SysR), defined as the measure of the absolute daily change in portfolio power demand from one timestep to the next one over a given simulation time frame (00.00 am to 23:45pm with 15 min intervals for the considered application). A fourth metric is presented by Muratori [110], defining the *severity term* (α_x)*(*as the percentage of time during which the demand of the considered portfolio is higher than *x* times the average demand.

2.1.4 Rule-based control and Model Predictive Control

BEF and DSM encompass Building Energy Management Systems (BEMS) or Home Energy Management Systems (HEMS), a collection of control techniques utilized for decision-making at building level. These practices enable customers to effectively attain their objectives as well as align with the goals of utility providers [111].

BEMS and HEMS are terms employed to typify various systems utilized to increase the energy efficiency of operational buildings and ensure indoor comfort for building occupants [112, 113]. BEMS and HEMS are an essential piece of an intelligent grid, enables building administrators to supervise and manage the energy used in their buildings, thus modifying the demand and energy use [114], and promote process automation [115].

The choice or design of an appropriate control strategy can be a challenging task in the design of a methodology for optimizing grid interaction of virtual energy communities. In fact, the most diffuse manipulated variables in BEMS, according to the literature are [116]): *i) Set-point temperature*, with the modulation and creation of set point profiles to control room thermostats [117], *water level* in storage tanks [118], and the *supply* of the systems [119]; *ii) Power of HVAC systems*, with binary routine for switching on and off, or inverter-controlled applications; *iii) Charging/discharging rates and operation scheduling* for modulation or binary control of ESS, such as TES, BESS, and EVs; *iv) Interruptible loads.*

Common control strategies are rule-based controls (RBCs) or model-predictive controls (MPCs). In order to operate energy systems in an efficient way, RBCs typically apply pre-defined decision rules for these variables. Based on the monitoring of state functions, RBCs generate optimized profiles by recognizing the evolving scenario and implement a set of known actions. Conversely, MPC often uses simplified models of the building for predicting future states of the systems and optimizes the schedule over a sliding horizon according to an objective function [120]. RBCs mainly fulfill a certain control objective, such as the maximization of the use of on-site renewable energy but are not designed to achieve optimization of the overall system behavior. On the other hand, MPCs allow the identification of an acceptable trade off between different control objectives [121]. Therefore, a balance between different control objectives, such as a low energy consumption and reduced energy costs, but a high load shifting potential, or provide power reduction while ensuring thermal comfort [122] must be found in MPC [123]. One strategy consists in creating a multiple terms cost function balanced with appropriate weights. The optimal values of the weighting factors are usually computed using Pareto fronts [124].

Another important step in the selection of control strategy to assist EAs towards widespread use is the ability to adapt to time-varying disturbances (e.g. weather variables) or in boundary conditions. Afram et al. [122] concluded that classical control strategies, such as thermostatic on/off control, PI/PID control and are not able to adapt to these time-varying nature, while MPC is seen as one of the most promising developments as it can consider future weather, electricity price variations and uncertainties [125].

The last relevant feature that supports the choice of MPC is given by the potential to deploy BEF. Afram et al. [122] concluded that advanced control systems (OC, fuzzy logic, MPC) in combination with thermal storages show a great opportunity for load management, hence reducing infrastructure and operational costs. Moreover, MPC shows outstanding performance in DR compared to RBC [126].

When the MPC algorithm can account for bounded disturbances, the procedure is called robust MPC (rMPC), whereas when the distribution of the disturbance is known and used in the MPC, the procedure is called stochastic MPC (sMPC) [127].

For the presented research framework and for the dynamic of grid signals by the means of time-dependent pricing tariffs, the application of MPC for cost minimization is defined economic-MPC (eMPC). A general formulation of the problem is presented in Eq. (2.12)

$$J = \omega_{en} \cdot ENERGY \cap \omega_{comfort} \cdot SP_{DEV} \tag{2.12}$$

The first term corresponds to the economic cost of energy. This value is multiplied by its time-dependent cost expressed as a weight (w_{en}) and the corresponding energy consumption. The latter is for deviation from the preferred setpoint. This value set a soft constraint in the identification of a time-dependent lower bound and is multiplied by the corresponding weight ($w_{COMFORT.}$). The objective function has a proper economic unit – usually euro (€), dollar ($), and British pound (£). w_{en} is the cost of electricity [$/kWh], $w_{COMFORT}$ is the cost assigned to the deviation from the preferred setpoint of one degree for an hour [$/°Ch]. The explicit finite difference method is selected for its applicability to control-oriented modelling. For the dynamic optimization, a predictive approach is proposed to identify the optimal control actions according to the selected objective function of the solver. In a DR program, the control aims to minimize the power demand during the peak hours while guaranteeing limited variations from preferred set point. The complexity of the system and the time dependence of state functions make predictive models the most successful for a given optimization problem.

The most relevant elements for the design of such a control are the control horizon, the prediction horizon, the boundary conditions, the constraints, and the cost function. Considering the case-specific communication problem defined between the grid and the energy aggregator, a timestep of 15 minutes is selected. To ensure the best result possible, the control horizon is considered equal to one timestep. Therefore, the optimization is run for each of the timesteps considered.

The minimization problem is performed in a MatLab environment using the *Solver-based Nonlinear Optimization* section of the *Optimization Toolbox.* Specifically, to respect the physical constraints and reduce the computational time, a constrained nonlinear multivariable function has been used.

Due to the nature of the application, the optimization problem is multi-objective. In fact, the optimal heating output must minimize the economic expenditure over the prediction horizon and, in the meantime, guarantee thermal comfort throughout the operation [120]. Thus, because of the existence of conflicting objectives, this class of optimization problems fails to find a single solution [128]. To work around this issue, the proposed approach consists of combining many individual objective functions into a single formulation [129]. The identified solution must be considered as the best trade off among all the possible objectives [130].

The future of control: load shaping theory

A relevant contribution was proposed by Corbin and Henze. In the first paper, the authors addressed the impact on the grid of HVAC and predictive control of residential buildings [131]. They theorized the existence of an ideal aggregated demand to minimize energy feeder's stress. With the companion paper, in 2017 the authors presented a supportive methodology to deploy load shaping concept [109]. Specifically, load shaping is a theory in the DAR market framework who changes the traditional formulation for control-oriented problem and coordination. The idea of load shaping aims at addressing two main points: *i)* assist the optimizer ensuring easier convergency in predictive control; *ii*) support electricity feeder optimization without setting up a coordination framework for the building portfolio.

The methodology can be summarized into the following points:

1) Generate a reference demand curve that represents the desired aggregate feeder demand.
2) Transform the feeder reference demand curve into a reference demand curve for each house.
3) Minimize the difference between the house demand curve and house reference demand curve.

The goal of the optimization is to *shape* the feeder demand curve to have a lower peak and reduced variability. From the idea of shaving peaks and fill-in valleys and limiting the oscillations in demand the authors applied a smoothing algorithm to the base case feeder—of the business as usual (BaU) —to generate the reference demand curve. A smoothing algorithm such as moving average is both eases to automize and effective in recognizing the physical constraints of the systems and buildings. Moreover, such formulation is also useful in assessing the impact of DERs and additional generators at the feeder level. One of the main concerns about using moving average was the selected periods. It is evident that the results of moving average are affected by the simulation period, therefore the authors measured the impact from the 30-minutes interpolation up to 8 hours.

They concluded that for the sake of DAR market, the smoothing period had to be 4 hours to give more insight to variation in the order of 2-3 hours.

The second step of the methodology is about disaggregating the reference demand curve from the aggregator to the single agent level. Limiting the building-to-building coordination, the authors opted to create a new curve to represent the deviation between BaU and reference demand curve (smoothing algorithm) at each home. Therefore, they created a dynamic signal named as *reference signal* to guide the single-home optimization routine. This signal is generated by normalizing the difference between the reference demand and the base case demand. The curves are normalized by dividing the demand at each time step by the sum of demand over the cost horizon. This new signal assumes both positive and negative values. The house base case demand curve is then normalized by the sum of demand over the cost horizon, and then added to the reference signal. The new curve describes the normalized house reference demand.

The third step of the presented methodology is to minimize the difference between the desired curve (the normalized house reference demand) and the candidate curve. The optimization objective can be formulated as a minimization of deviation between candidate and house reference demand curves. Specifically, the objective function to be minimized is the sum of squared error between the house reference and candidate demand curves.

This result is intuitive: given a smooth reference demand curve, the controller will attempt to generate a smooth response. It is somewhat surprising, however, that this emerges from the individual actions of thousands of homes which are not explicitly coordinated but instead directed to a common goal.

2.2 Building Energy Modelling

This section discusses the most diffuse modelling techniques, pointing out the different approaches and the role of measured data, the importance of control-oriented formulation, and the impact of model selection in portfolio management for aggregators, highlighting the most relevant fundings supporting the design of a methodology for optimizing grid interaction.

Energy modelling aims at describing the input-output relationship to produce reliable demand prediction. As shown in Figure 2.3, the creation of reliable and accurate load prediction is essential for the exploitation of BEF. A first classification can be drawn in energy modelling, defining aggregated and single system levels. The aggregated analysis is effective in forecasting the overall demand of the agent, including all the systems and technologies within the customer's environment. The single system prediction, on the other hand, is assessed to model the demand and energy consumption of a single dedicated load type. Figure 2.6 presents the independent energy system within residential buildings. The more digitalized the infrastructure and the more advanced the technologies, the more complex the load prediction. This complexity is underpinned by more detailed datasets, higher number of sensors, and ICT requirements.

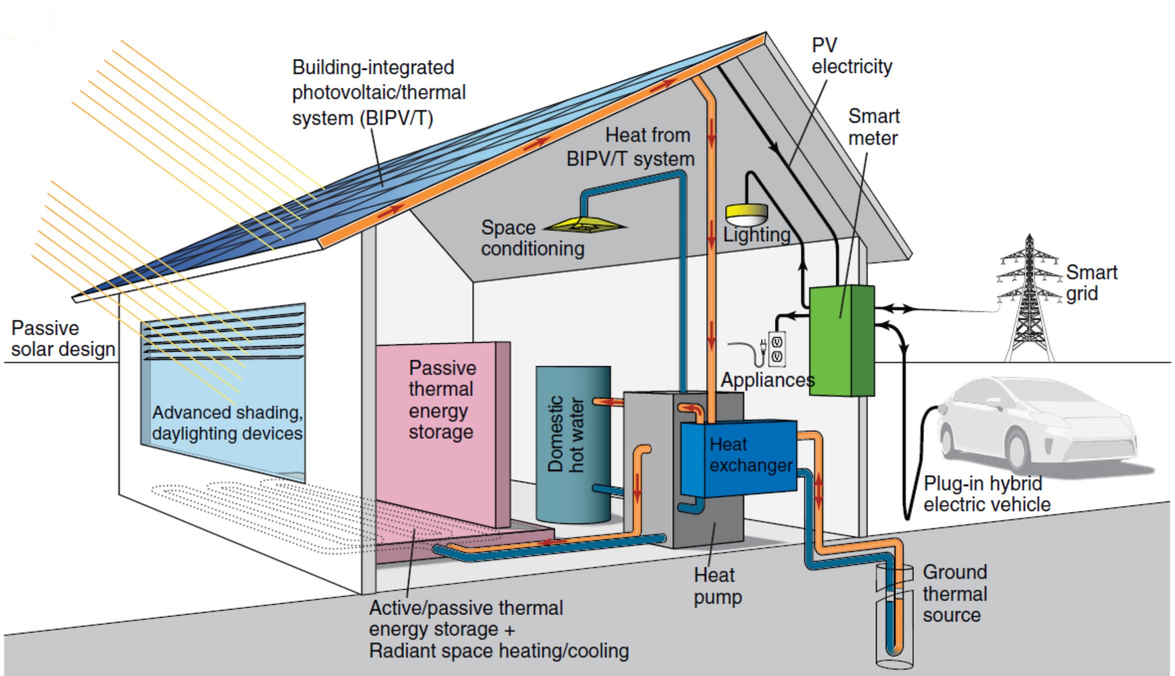

Figure 2.6. Independent energy systems within the building environment [33] .

For the design of a methodology to guide the grid-interactivity of buildings it is essential to create a generalized and *modular* scheme to accommodate different configurations and systems. To simplify the load forecasting, the load within the single home is grouped based on the main energy carrier exploited. Therefore, each building in the portfolio has an electric and a thermal load. In a fully electric domain, as the one of Québec, the final part of the methodology will be designed to convert thermal load into electric demand by mathematical formulation on the coefficient of performance.

In the next sections, the analysis is applied to dedicated models. Once the independence of a sub-model has been identified, it is possible to determine the expected demand by analyzing the individual component rather than the surrounding environment.

2.2.1 Dedicated modelling techniques

An effective prediction model depends on data collected from three primary sources: dynamic measurements from power meters offer valuable information about the technologies and power consumption. Advanced metering systems, like smart meters, deliver the opportunity to enhance dedicated models by incorporating sub-channels and sub-metering data. Statistical analysis and information from sources like building codes, surveys, and census data can compensate for limited datasets and assist in generalizing energy usage across different buildings by generating metadata. Additionally, monitoring infrastructure such as smart devices, switches, intelligent plugs, and cloud-based thermostats enable the collection of precise measurements for each independent energy subsystem. The aforementioned data sources constitute the defined information layer. This information is utilized to construct a dedicated model layer. Once each autonomous prediction model gathers sufficient data, it becomes feasible to provide forecasts of demand and identify recurring patterns in the scheduling. The aggregation technique, which involves superposition, can be created. Figure 2.7 displays the schematic.

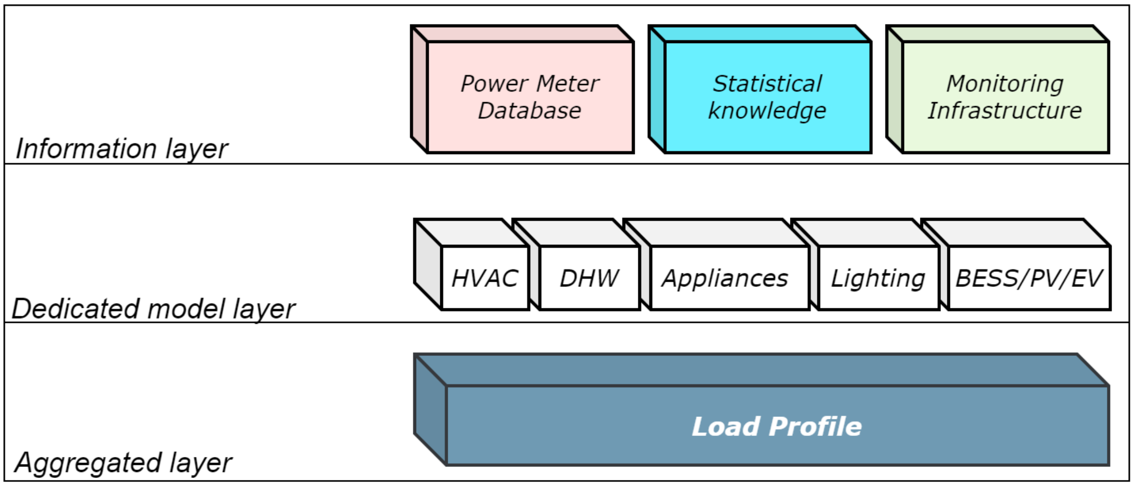

Figure 2.7. The three layers for the creation of aggregated load profile

It is important to note that the building modeler is unable to construct a dedicated model for each individual system. It is crucial to comprehend the influence of an autonomous system and determine if the working hours are sufficient to warrant a greater level of complexity in modeling. This will help prevent any potential interconnections between systems that may appear independent but actually conceal an underlying influence. One example is the use of electric-powered stoves in conjunction with other heating sources. Another example is the transfer of heat from a hot water boiler to its surroundings, or lighting's joule effect. Therefore, it is crucial to group some of them to mitigate the possibility of overestimating their impacts. The primary submodels consist of five categories: HVAC, domestic hot water, main appliances, lighting, and BESS/EV/PV.

Thermal load modelling

The first dedicated model analysed is HVAC and Space conditioning model. According to the heterogeneity of weather conditions and the deployed pricing tariffs, the different occupant behavior patterns, and the resolution of available measured data, different modeling techniques are used to simulate, predict, and control a portfolio of residential buildings [132]. The most common modeling techniques can be classified into white-box, grey-box, and black-box [133], and the choice depends on the purpose of the application.

White-box modeling is based on conservation of mass, energy, and momentum and is designed with a bottom-up approach (or forward approach) to include information about the building envelope, occupant behaviors, electric and heating scheduling, and HVAC systems [33]. Despite ensuring wider applicability at the design stage, it is not preferred for prediction because of its case-specific nature [134]. Conversely, the black-box approach is purely data-driven where the input-output transformation is processed by statistical and machine learning models [135], and the generated parameters do not have a physical meaning.

Grey-box models generally combine physics-based equations for the structure of the model with data-driven parameter calibration. The simultaneous presence of heat equations, physical constraints, and data-driven calibration reaches adequate accuracy in prediction, better interpretability than the black-box, and more computational efficiency and simplicity than the white-box models [136]. One of the most common grey-box modeling approaches is the use of an equivalent resistance-capacitance (RC) thermal network which can also be formulated in state-space format [137], and applicability for control-oriented building frameworks [138]. The scalability of this modeling technique has been shown to be effective for automated model generation [139], in the definition of control-oriented archetypes [140], and for deriving predictive management strategies for the optimal operation of renewables and energy storage technologies [141]. Thereafter, the widespread adoption of smart thermostats and the digitalization of the information and communication technologies (ICT) have boosted the use of grey box technique for large-scale applications.

The definition of data-driven RC models refers to the application of reduced-order model where the model structure is determined by physical knowledge and the parameters are calibrated through a minimization-problem. This technique is also defined as inverse approach and defined as data-driven grey box approach [142]. Berthou et al. [143] identified the three main inputs for the identification problem as order of the model, data length for the training, and timestep of the dataset in a review of data-driven (inverse) grey-box applications.

Control-oriented formulation

Unlike design-oriented optimization that aids at selecting types and sizes of building energy systems [144], control-oriented optimization focuses on optimizing the operational settings of a given system or set of systems to achieve a desired objective function. Control-oriented optimization can involve identification of the best settings of multiple features of a single system and/or several systems through mathematical tools that account for multi-variable interactions between building energy systems [145].

The control system directs the input to another physical system and to regulate its output, helping in determining the system's behavior. The controllability and observability of dynamic systems is therefore presented: *Controllability* is the ability to control the state of the system by applying specific input whereas *observability* is the ability to measure or observe the system's state [146]. These features can be checked using the Kalman Test [147].

Control-oriented optimization can be achieved through a wide range of simulation approaches and methods. Optimizing the controls of a system using a simulation environment often has limitations and requires typically more assumptions than those needed for a design-oriented optimization [133]. Most BEMS tools and frameworks lack the necessary capabilities to readily perform these optimization tasks. Therefore, further investigation is needed to produce practical solutions for their actual implementation.

Building modeling must accommodate an explicit formulation to integrate receding horizons of MPC and be implemented into real controllers [120]. State-Space representations describe systems of linear differential equation in a compact manner [148], as follows:

$$\dot{x} = Ax + Bu + Ew \tag{2.13}$$

$$y = Cx + Du \tag{2.14}$$

Where, x is the state vector, u is the input vector, w is for disturbances, y is the output vector, A is the state matrix, B input-to-state matrix, C is the state-to-output matrix, D is the feedthrough matrix, E is the disturbance distribution matrix.

As discretized form of the Fourier heat diffusion equations, the lumped parameter finite difference method is the most appropriate thermal modeling technique, as discussed in the previous Section 2.2.1.

In the explicit finite difference formulation the current temperature of a given node depends on its temperature and the temperature of the surrounding nodes at a previous time step [149] as well as heat sources. By performing a heat balance on the control volume, the differential equation of a node can then be written in finite difference form as Eq. (2.15), with the variables described in

Table 2.2. Unknown parameters are presented in red.

$$T_i^{t+1} = T^t{}_i + \frac{\Delta t}{C_i}\left[\sum_j U_{ij}{}^t (T_j^t - T_i^t) + \sum_k U_{ik}{}^t (T_k^t - T_i^t) + \dot{Q}_i^t + \alpha_i SR\right] \tag{2.15}$$

Table 2.2. Parameters of the RC formulation

	Description	*Unit*
$U_{ij}{}^t$	Conductance between nodes i and j	W/K
$U_{ik}{}^t$	Conductance between nodes i and k* *(Node k has a defined or known temperature)	W/K
$T^t{}_i$	Temperature at node i	degC
C_i	Thermal Capacitance	J/K
$\dot{Q}_i^t$	Heat flow	W
$\alpha_i SR$	Solar aperture · solar radiation	W
Δt	Timestep	sec

The aim of the thermal model is twofold: *i)* produce reliable single and multi-step ahead predictions; *ii)* create a reference for the baseline-required KPIs to quantify BEF.

Model Calibration techniques

The calibration process for the determination of thermal parameters (such as thermal resistances, capacitances, and solar apertures) is performed with a minimization-problem. This class of optimization problems has three main alternatives: Model Predictive Control (MPC)-Relevant Identification (MRI), traditional least squared, and Kalman filtering.

MRI is designed on a nonlinear least-squares solver evaluated for a calibration horizon (CalH) typically of 24 hours [139]:

$$J_{MRI} = \sum_{i=0}^{Nd-CH} \sum_{t=1}^{CH} (T_{i+t} - \hat{T}_{i+t|i})^2 \tag{2.16}$$

Where *Nd* is the number of datapoints equals to the number of datapoint in a day times the number of days for training, T is the actual measured node temperature and $\hat{T}$ is the predicted temperature.

Least squares method is commonly used in regression analysis for estimating the unknown parameters by minimizing the sum of squared errors between the observed data and the predicted data (residuals).

A simple data set consists of *n* points $\left(x_i, y_i\right)$ for i=1,2,…*n* where x_i is an independent variable and y_i is dependent variable whose value is found by observation. The model function has the form $f(x, \beta)$ where *m* adjustable parameters are held in the vector β . The fit of a model to a data point is measured by its residual, defined as the difference between the observed value of the dependent variable and the value predicted by the model:

$$r_i = y_i - f(x_i, \beta) \tag{2.17}$$

The least-squares method finds the optimal parameter values by minimizing the sum of squared residuals, *S* [150]:

$$J_{LS} = \sum_{i=0}^{n} S_i \tag{2.18}$$

Least square is one of the widely used methods of fitting curves that works by minimizing the sum of squared errors as small as possible. It helps you draw a line of best fit depending on your data points.

Kalman filter is an algorithm that uses a series of measurements observed over time, including statistical noise and other inaccuracies, and produces estimates of unknown variables that tend to be more accurate than those based on a single measurement alone, by estimating a joint probability distribution over the variables for each timeframe [151]. The Kalman filter mechanism is conceptually very simple. In essence it computes new estimates of the state of interest by simply taking a weighted average of a prediction, based on the previous estimate, and a new observation. Despite its essential simplicity the basic algorithm hides an elegance that makes it enormously powerful in a wide range of applications. The recursive nature of the Kalman filter gives the algorithm an essentially cyclic structure in which the same computations are performed at each time-step. The filtering process relies on three cycles; the first describing the evolution of the true state and the observations that are made of this state by the sensors, the second which describes the generation of estimates of the true state on the basis of these observations, and a third cycle which computes covariance information about the estimates and which also computes the gain matrix at each time step [152].

Based on the selected parameter estimation technique, data length is an important factor and is affected by the quality and availability of measured data during calibration. McKinley et al. [153] used 22 hours to calibrate a lumped model of a single room, Gouda et al. [154] used 19 days to calibrate a 3R2C model, Park et al. [155] used nine days to calibrate a 1R1C model. Generally, the available literature suggests a calibration period from three to 14 days [139], to avoid underfitting [156] and overfitting [157].

To evaluate the goodness of fitted models the choice comprises different metrics. Among all the possibilities, the most diffuse and effective are presented in Table 2.3.

Table 2.3. Evaluation metrics for model calibration

Name	Formula

RMSE	Root mean square error	$\sqrt{\frac{\sum_{i=1}^{N}(Y_i-\hat{Y}_i)^2}{N}}$
MBE	Mean bias error	$\frac{1}{N}\cdot\sum_{i=1}^{N}(Y_i-\hat{Y}_i)$
MAE	Mean absolute error	$\frac{1}{N}\cdot\sum_{i=1}^{N}\left\lvert Y_i-\hat{Y}_i\right\rvert$
MAPE	Mean absolute percentage error	$\frac{1}{N}\cdot\sum_{i=1}^{N}\left\lvert\frac{Y_i-\hat{Y}_i}{Y_i}\right\rvert\cdot 100$
CV-RMSE	Coefficient of variation of RMSE	$\frac{1}{\overline{y}}\cdot\sqrt{\frac{\sum_{i=1}^{N}(Y_i-\hat{Y}_i)^2}{N}}$
NRMSE	Normalized root mean square error	$\frac{\sqrt{\frac{1}{N}\sum_{i=1}^{N}(Y_i-\hat{Y}_i)^2}}{\frac{1}{N}\sum_{i=1}^{N}\lvert Y_i\rvert}$
FIT	Goodness of fit	$(1-NRSE)\times 100$

Scale-dependent metrics are more reliable for temperature predictions, whereas scaled-metrics-such as NRME and CV RMSE are intended to power predictions.

According to ASHRAE Guideline 14-Measurement of Energy and Demand Savings [158], the model must have a CV(RMSE) below 30% relative to hourly and sub hourly calibration (measured) data. For reduced order RC models, RMSE below 1°C can be considered acceptable for multi-step ahead predictions [159]. The consideration of thermal comfort of occupants is essential to define methodology and to generate fundings that can be applied to real applications. For the activation of BEF, a good practice is to consider thermal discomfort when the indoor temperature exceeds the setpoint by ± 2 or 3°C [120, 160]. However, the use of reduced-order modelling (ROM) brings the problem of zone-aggregation, where one single node can be potentially representative of many different thermal zones. Consequently, a severe temperature variation from preferred setpoint temperature may go unnoticed as it is averaged with the others. Hence, in order to ensure an adequate level of temperature variation from set point in each thermal zone and avoid overestimating the BEF potential, it is recommended to decrease the range limit to 1 degree Celsius when using ROMs.

Electric load modelling

The modelling domain has acknowledged the ability of statistical analysis to model and produce forecast of power profile with accuracy recurring to time series analysis.

Within the *dedicated model layer* of Figure 2.7, most of the models target electricity as main energy carrier. Except for the thermal load management, with the activation of the building thermal mass, which require a different strategy, the data analysis and the prediction of power demand from domestic hot water production, appliances and lighting, BESS and electric vehicles, and eventually photovoltaic production for prosumers, can be treated as time series.

Time series data are defined as collection of numerical observations arranged in a natural order with each observation associated with a particular instant of time or interval of time which provides the ordering [161].

Like traditional data analysis, there are two general objectives of time series analysis [162]:

- *Descriptive*: which uses graphical and numerical techniques to provide the necessary understanding of underlying long-term or secular[1] behaviour in the presence of trend and seasonal variations. Sometimes, gaining insights into these seasonal or periodic components may itself be the goal. Some of the common techniques are smoothing to better detect an underlying trend and the autocorrelation function to detect serial correlation;
- *inferential* which, by means of a mathematical model, allows future values to be forecast (or predicted) along with a measure of their confidence intervals. Some of the traditional least squares regression methods can be adapted to time series data analysis, but a whole class of versatile models, called ARIMA methods and their extension, namely ARIMAX models have been specifically developed for this purpose.

The smoothing methods can also be used for forecasting, but there are limitations. The lack of understanding of the physics behind the system generating the time series data necessitates the use of curve fitting [163]. However, the subjective nature of selecting an acceptable time series model for a specific dataset is a significant concern. Other practical problems include missing observations, outliers, or interruptions in the series.

Time series data can exhibit different types of behaviour patterns or components, and more commonly, it consists of a mix of these components:

i. *Unpredictable/erratic/irregular variations* around a constant mean value, referred to as a *constant process*. The fluctuations around a mean value may or may not be random, and they can be discerned when trend and cyclical variations are removed.
ii. *Trend or secular* behaviour, i.e., a long-term general direction of change in the mean level which may be linear, or non-linear, A trend can be increasing (upward), decreasing (downward), or horizontal (stationary).
iii. *Seasonal behaviour* exhibits a clear and repetitive periodic pattern with respect to time, direction, and magnitude. "Seasonal" is not restricted to mean the four seasons in a year. Outdoor air temperature and electricity use in buildings exhibit seasonal behaviour:
iv. *Cyclic behaviour* has a similar type of variation, but with much less consistent or set patterns and is usually aperiodic, i.e., does not repeat itself in fixed intervals.
v. *Transient behaviour* is a catch-all type of behaviour, and essentially consists of one or more momentary impulses (step change, ramp up, etc).

After all the above effects have been extracted/removed, what is left over is the white noise or the random fluctuations in the data series. Much of the challenge in time series analysis is distinguishing these basic behaviour components/patterns when they occur in conjunction.

Three types of time series modeling and forecasting techniques are presented. The first general class are *smoothing methods* which include arithmetic moving average (AMA) and exponentially weighted averages (EWA) meant to filter rapid fluctuations in time series so that the underlying long-term or secular and seasonal trends can be seen.

The second class of models are meant to remove the trend and seasonal patterns using ordinary least squares (OLS) regression models with the time variable appearing as a regressor. The main advantage of this model is its capacity to represent the deterministic or structural aspects of the data in a straightforward way, and to generate reasonably precise forecasts together with associated confidence intervals. Fourier series modeling approach and its ability to capture diurnal, weekly, and seasonal patterns in building energy demand is recognized [164, 165].

The third class is the stochastic time series modeling framework which involves the combination of autoregressive (AR), the integrated (I), and the moving average (MA) sub-models: Auto Regressive Moving Average (ARMA), Auto Regressive Integrated Moving Average (ARIMA), Auto Regressive Moving Average with exogenous inputs (ARMAX). The integrated component is meant to detrend the stationary time series data already filtered for the seasonal and cyclic patterns. The MA and AR components capture the stochastic variation using lagged values of the variable and past model errors. The model is linear in its parameters which simplifies the estimation [166, 167].

2.2.2 Ensemble setups: bagging, boosting and stacking techniques

The dedicated models need to be aggregated to produce the overall expected demand. In the field of applied statistics and machine learning, ensemble methods are created on the hypothesis that combining multiple models together can often produce a much more powerful model (*strong learners*) than individual predictions (also referred to as *weak learners*). In machine learning the choice of the model is extremely important to ensure high accuracy[168]. A successful prediction is mainly dependent on the data features themselves (such as quantity, quality, dimensionality of the space, distribution hypothesis). Both a low bias and a low variance are considered to be the most fundamental characteristics that are typically expected from a model, even though they vary in opposite directions. For a problem to be effectively "solved," our model should possess enough degrees of freedom to effectively address the inherent complexity of the data [169]. However, it is also important to avoid excessive degrees of freedom, since this can lead to high variance and compromise the model's robustness. This is the widely recognized bias-variance trade-off and shown in Figure 2.8.

Weak learners often struggle to perform effectively due to either a strong bias or excessive variation, which makes them less robust. The concept of ensemble methods involves mitigating the bias and/or variance of weak learners by combining multiple learners to create a strong learner (or ensemble) that achieves better performances. Based on the application, the choice of training weak learners with the same learning algorithm will generate homogenous base models, but it is also possible to have heterogeneity in weak learners during the aggregation. It is therefore important to understand the problem and make strategic choices in how weak learners are both generated and aggregated into ensemble setups[169].

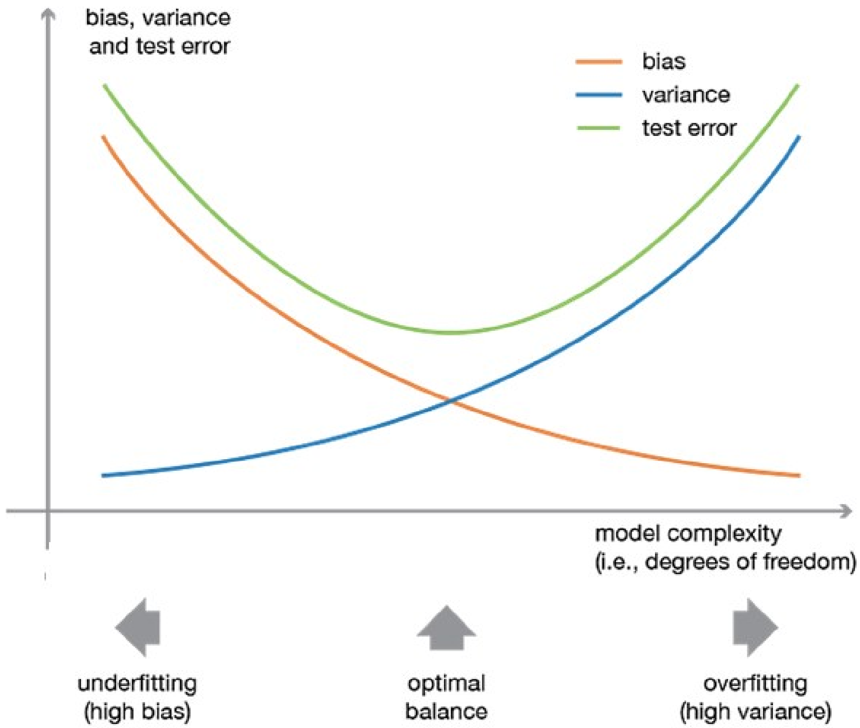

Figure 2.8. Underfitting vs Overfitting: bias-variance trade-off

Three major kinds of meta-algorithms that aims at combining weak learners are [170]:

- Bootstrap aggregating (*bagging*) trains weak learners independently from each other (parallel setup) and combines them following some kind of deterministic averaging process. This technique often considers homogeneous base models and focuses at reducing variance.
- *Boosting* trains weak learners sequentially in a very adaptative way (series setup) and combines them following a deterministic strategy. This technique often considers homogeneous base models and focuses at reducing bias.
- *Stacking* trains weak learners in parallel and combines them by training a meta-model to output a prediction based on the different individual predictions. This technique often considers heterogeneity and focuses at reducing bias.

Bagging

In parallel methods we fit the different considered learners independently from each other and, so, it is possible to train them concurrently, aims at producing an ensemble model that is more robust than the individual models composing it. The scheme relies on bootstrapping, where samples of size B (called bootstrap samples) are generated from an initial dataset of size N by randomly drawing with replacement B observations [171]. These subpopulations are representative and independent of the true data distribution. Two governing assumptions are considered: the size N should be large enough to capture most of the complexity of the underlying distribution so that sampling from the dataset is a good approximation of sampling from the real distribution (*representativity*); the size N of the dataset should be large enough compared to the size B of the bootstrap samples so that samples are not too much correlated (*independence*)[170]. Bagging technique is extremely useful to evaluate variance or confidence intervals of a statistical estimators.

For each subpopulation defined as $\{z_i^j\}$, subject to: $j = 1, 2, ..., L$; $i = 1, 2, ..., B$ a week learner ω_j is trained. By considering the variability of each bootstrap sample, each week learner is trained on a relatively different part of the real data and for this reason differs in the learning process. As the bootstrap samples are approximatively independent and identically distributed (I.I.D.), so are the learned base models. The following step is the aggregation of the output from weak learners. The aggregation procedure is performed through averaging the outputs, defining a resulting output with lower variance than the individual contributions, defined as S_L. Different mathematical formulations might be developed for this purpose, as instance a simple average for regression problem is shown:

$$S_L = \frac{1}{L}\sum_{j=1}^{L}\omega_j \tag{2.19}$$

Another important application of this technique is random forests, where forests are defined as strong learners composed of multiple trees [172].

Boosting

Boosting is the second strategy used in ensemble learning. In this context, the fitting or learning process of weak models is no longer done independently, but rather iteratively. Thus, the learning process of the model is contingent upon the learning process of the weak learner in the preceding stage. Boosting is a widely recognized and highly effective approach for reducing bias. Important to mention that an advantage of this technique lies in the effectiveness of generating weak models as low variance and high bias[173]. The schematic of boosting ensures lower computational complexity in the creation of multiple weak learners, with the disadvantage of creating an iterative procedure to reduce the bias (in contrast to bagging), and therefore very time consuming. In this case, the ensemble model can be presented as:

$$S_L = \sum_{j=1}^{L} c_j \times \omega_j \tag{2.20}$$

Where, c_j are coefficients and ω_j are weak learners. Two important applications are *adaptive* boosting and *gradient* boosting, where the main difference comes from the way both methods try to solve the optimisation problem of finding the best model that can be written as a weighted sum of weak learners. Specifically, adaptive boosting updates the weights attached to each of the training dataset observations whereas gradient boosting updates the value of these observations[174, 175].

In *adaptive* boosting the setup defines a difficult optimization problem. Therefore, the solution is to solve via an iterative optimization process, where instead of finding all the coefficients and weak learners in one iteration, the weak learners are added one by one, finding the i-th coefficient and weak learner as function of the previous iteration[174]. It can be presented as:

$$s_j = s_{j-1} + c_j \times \omega_j \tag{2.21}$$

Where, s_j is the model that fit the best the training data and is the best possible improvement from s_{j-1}. At the beginning, it is possible to assume that each coefficient has the same value $\frac{1}{N}$. Thereafter, the L iterations (as the number of the weak learners) follow the same structure: fit the best possible weak model with the current observation weights, add a weak learner and update weights of observations misclassified; update the strong learner by adding the new weak learner multiplied by its update coefficient.

In *gradient* boosting the optimization is based on a gradient descending problem, where the learning process of a weak learner is trained to the opposite of the gradient of the current fitting error with respect to the current ensemble model.

$$s_j = s_{j-1} - c_j \times \nabla_{s_{j-1}} E(s_{j-1}) \tag{2.22}$$

Where, $E(s_{j-1})$ is the fitting error, and c_j is a coefficient corresponding to the previous training step. The opposite to the gradient of the fitting error is a function that can be evaluated for observations in the training dataset. These evaluations are called pseudo-residuals and are set equal to the observation values at the first model of the sequence. Thereafter, the next step is to fit the best possible weak learner to pseudo-residuals, then update the ensemble model in the direction of the new weak learner, update the ensemble model by adding the new weak learner multiplied by the step size, and finally compute new pseudo-residuals that indicate, for each observation, in which direction we would like to update next the ensemble model predictions.

Stacking

This technique often considers heterogeneous weak learners and learns to combine the base models using a meta-model. Two main features need to be determined: the L learners , and the meta-model. The choice of weak learners is related to the purpose of the investigation. The procedure begins by splitting the training data in two folds, then choosing L weak learners and fit them to data of the first fold, for each of the L weak learners, make predictions for observations in the second fold, and finally fit the meta-model on the second fold, using predictions made by the weak learners as inputs[176].

2.2.3 Level resolution vs computational complexity: the impact of model selection

Despite the advantages of data-driven modelling, the creation of model structure is still critical. The interconnection between the structure of the model and the data used for parameter identification has been widely investigated by researchers worldwide [177-180].

Structural identifiability relates to the suitability of a specific model structure for the current challenge. Model identifiability is determined by its structure and is solely dependent on the model order and parameter configuration [181]. A model with a limited number of parameters and a low order may not possess the capability to precisely depict the physical phenomena that characterize the system. Conversely, a model that has an excessive number of parameters, or is of a very high order, is referred to as an over-parameterized model. This duplication in parameters results in different combinations of parameter values that yield the same model output, thus leading to several "optimal" solutions for parameter sets. This “indeterminacy” of the model brings the calibration of different models with available data into models with accurate predictions, but with different structures with each other, or even structures “incompatible” with reality [182].

Data-dependent identifiability is a concept that links the ability to identify a model to the specific data that it is calibrated with. Only the initial state of the system and the inputs it receives influence this concept [181]. Although a model may be structurally identifiable, the dataset used may be of poor quality and lack sufficient thermal dynamics information for the model's calibration. Ljung [183] suggests stimulating the system with a range of inputs in an open-loop fashion to guarantee that the dataset will have sufficient information for system identification. The sampling duration of the measured data used in the calibration should be determined based on the intended prediction of the model. It should be sufficiently brief to capture adequate thermal dynamics while avoiding excessive measurement errors and noise. For a successful calibration, the dataset must have an adequate amount of dynamic information. This means that there should be a large number of data points spread out over the different dimensions of the model input space (domain)[184].

Regarding the sampling time, Li et al. [84] presented a review of the most diffuse temporal resolution in flexibility quantification problems, highlighting 5 minutes (11%), 15minutes (22%), and one-hour timestep (67%) as the main ones. According to the International Energy Agency (IEA)-Annex 82: Energy Flexible Buildings Towards Resilient Low Carbon Energy Systems [185], the suggested resolution is 15 minutes because it coincides with the grid communication process and given the slow dynamic of building physics, it approximates thermal behaviour adequately [186].Other studies agreed that 15-minute intervals are enough for models that forecast the thermal dynamics of buildings [187]. Both the structural and data-dependent identifiability of a model exist on a continuum, ranging from identifiable to non-identifiable, rather than being a simple binary condition. Furthermore, there is a relationship between structural and data-dependent identifiability. For instance, models with higher complexity typically require larger datasets for training.

For the development of a methodology to support the grid interaction of energy aggregators, it is important to define archetypes for the automated model generation [140] recurring to model order reduction (MOR) techniques to ensure good performance in low simulation times, and limit overparameterization. The creation of these archetypes is affected by measured data available, metadata information, and the deployed sensor infrastructure.

The creation of the building model for the considered detached house- shown in Figure 2.9 can follow different criteria: *i)* maximize performance metrics (such as information criteria, root mean square error (RMSE), coefficient of determination, etc), *ii)* exploit metadata information (such as number of floors, number of climatized zones, year of construction, etc.).

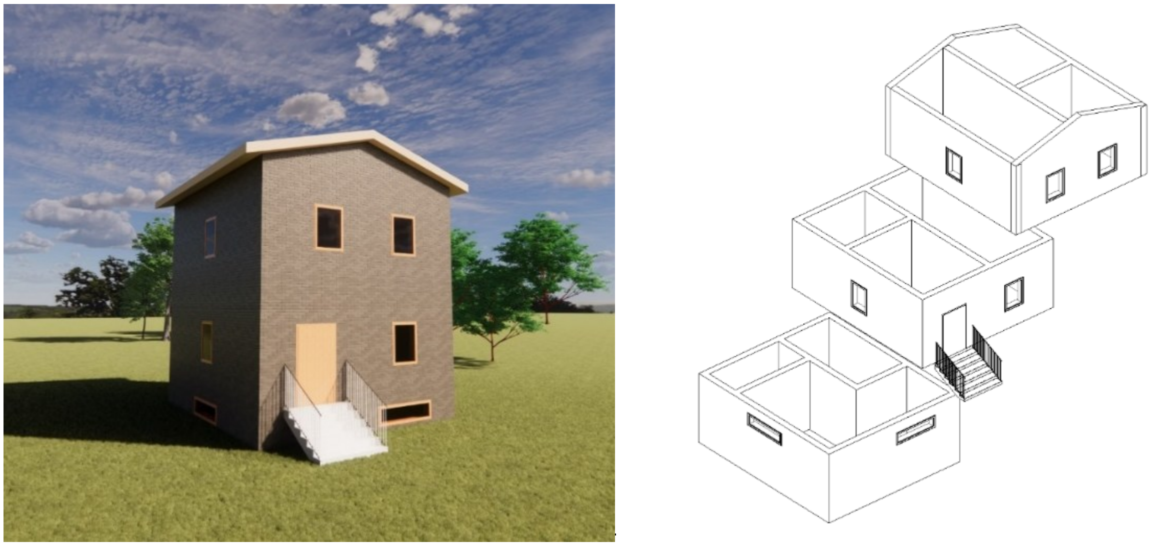

Figure 2.9. Representative detached house (2 story + basement)

Therefore, it is possible to generate infinite numbers of thermal models to represent the same building. From detailed formulation, where a thermal resistance and a capacitance is conceived for each measurement, such as the 16R9C model, to the simplified reduced order such as the 7R3C, 6R3C, and 3R2C shown in Table 2.4, where the number of thermal nodes is smaller than the actual number of thermal zones and the aggregation procedure is carried out by averaging measurements from adjacent or similar zones. The simulation time has been tested on the infrastructure available (Intel Core i7-9750H CPU @2.60GHz, 16.00GB RAM) to produce a visual representation. Figure 2.10. shows the duration of the simulation process with variable number of model parameters (model complexity) on *x* axis, and five different sizes of portfolio (from 10 to 100 households) on the *y* axis.

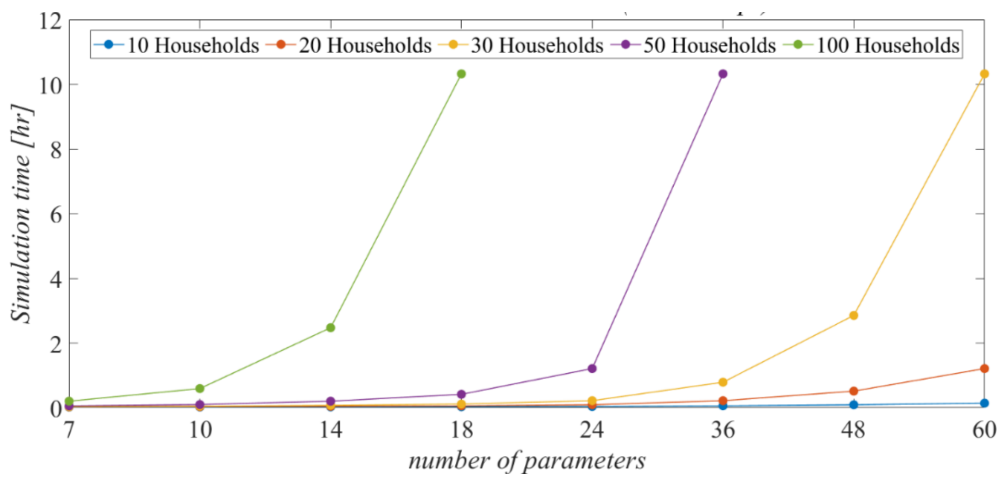

Figure 2.10.Simulation time for data-driven calibration of RC models.

The produced duration curves describe the total calibration time for an MRI procedure with a calibration horizon of 24 hours, and 7 days of 15 minutes measurements.

Table 2.4. Four different approximations for the thermal modeling

Detailed Model (16R9C)

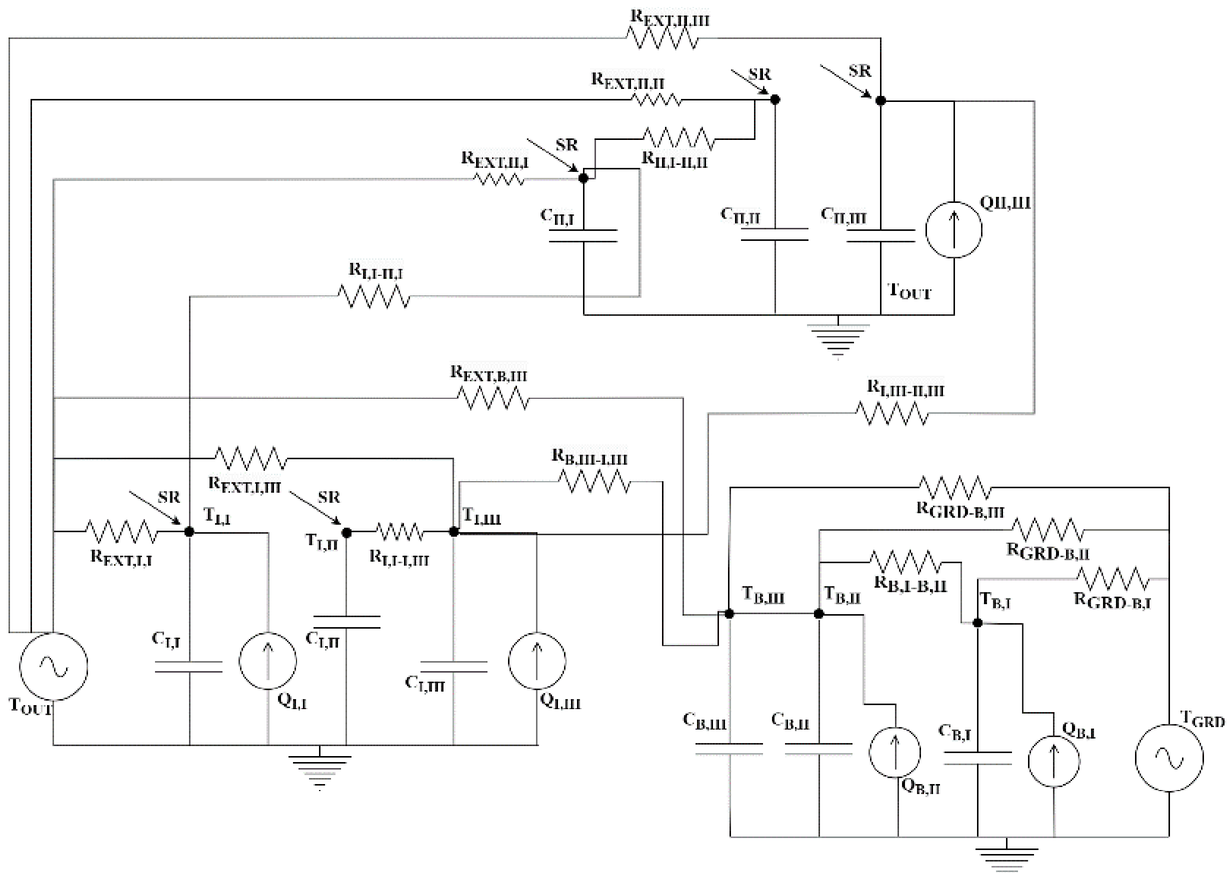

Floor-To-Floor Discretization (6R3C)

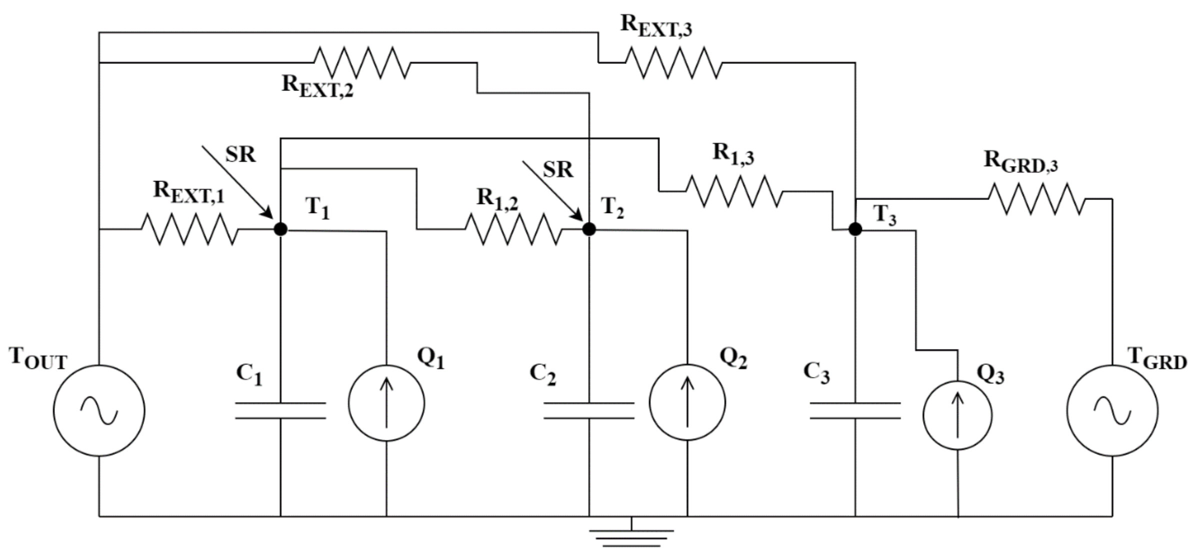

Orientation Discretization(7R3C)

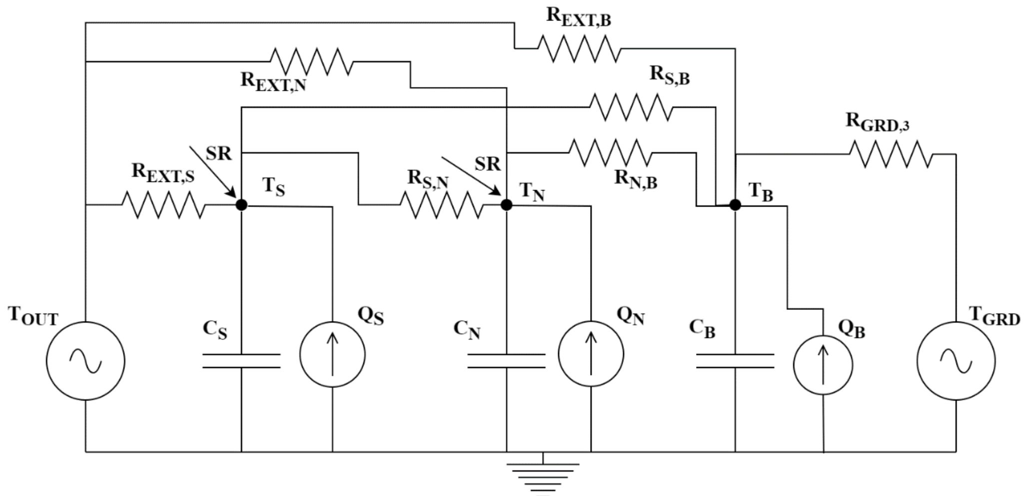

Reduced Order Model (3R2C)

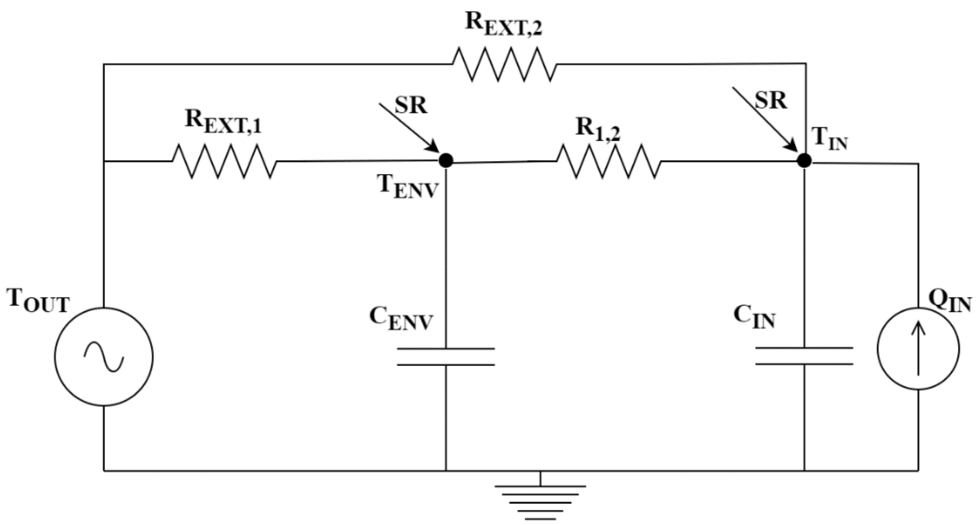

The need for Reduced Order Modelling and uniformity in the portfolio

The load management of energy aggregators depends on the individual agents within the portfolio. Another crucial aspect of utilizing MOR approaches is to attain uniform performance. Implementing a more advanced monitoring system for certain agents would ultimately lead to a greater understanding and influence over supervisory control. Thus, in order to guarantee fairness, it is necessary for the model structure at the higher level of coordination to have a universally implemented archetype.

The creation of archetypes relies on the measured data available, metadata information, and the deployed sensor infrastructure. However, the available datasets differ in these characteristics, and their heterogeneity can be considered the main obstacle to generalizing data-driven procedures. The idea of deriving a lower order model from a high order system while preserving the dominant dynamics of the original high order model is defined as MOR, and numerous research investigations have focused on that. Kim and Braun [188] used the balanced truncation method to create a reduced-order model from a detailed model. TRNSYS was used to create the detailed model, and the Purdue Living Lab was considered to demonstrate the reduced order modeling accuracy and computational requirements as compared with the full order model. De Coninck et al. [189] presented system identification and parameter estimation for a single-family dwelling by exploiting an innovative tool by considering many potential candidates from Modelica and *greybox.py* developed in Python. Deng et al. [190] used a Kullback-Leibler divergence rate to aggregate a regular discrete-time Markov chain applied to a thermal equivalent RC. O'Brien and Athienitis [191] produced a surrogate model for the parametric design tool for net-zero energy buildings. Apart from reducing the model order, a third approach consists of reducing the model complexity using a mix of physics-based and machine learning techniques. Shi and O'Brien [192] proposed a MOR approach using clustering. This approach is based on modeling the thermal characteristics of each individual zone, clustering the resulting parameters, and finally reducing the zones by considering the evaluated centroids and applying a scale factor criterion to represent aggregated zones. Silvestri et al. [193] combined clustering with TRNSYS in the definition of parameter identification

Another important choice is the sampling time. Li et al. [84] presented a review of the most diffuse temporal resolution in flexibility quantification problems, highlighting 5 minutes (11%), 15minutes (22%), and one-hour timestep (67%) as the main ones. According to the International Energy Agency (IEA)-Annex 82: Energy Flexible Buildings Towards Resilient Low Carbon Energy Systems [185], the suggested resolution is 15 minutes because it coincides with the grid communication process and given the slow dynamic of building physics, it approximates thermal behaviour adequately [186].

2.3 Design of energy aggregators

IEA identifies EAs as a valid solution towards a sustainable energy transition [194], because they are designed to address the on-site management of energy flows [195], and for building-to-building coordination which allows a larger share of zero-carbon technologies [40].

Since the early stages of energy aggregators for the coordination of building portfolio, many different investigations are conducted to optimize control architecture for flexibility. A 30-household community in UK was simulated by an emulation software to assess the effects of centralized and decentralized applications of MPC [196], while Hosamo et al. [197] compared 11 machine learning algorithms fed with a simulated-generated dataset produced as a result of the building information modeling (BIM) framework.

Regarding the operation of energy aggregators, the main concerns consist of minimizing uncertainty and limiting economic cost. The first problem addresses demand-side [198, 199], and supply-side [200] strategies to comply with inaccurate predictions of power demand and forecasting errors of DERs [201]. The latter optimizes the operation by considering coordination of grid-connected high-renewable buildings [202], stand-alone communities [203], or creating trading pricing models for energy exchange [96].

The impact of energy aggregators for load management can be appreciated on the supply-side as a valid contribution to mitigate side effects of shared load management strategies. In fact, when many households participate a DR event, the advantages of the power reduction during peak hours might be diminished by the formation of two additional peaks, with the increase of SysR [109].

The effectiveness of control strategies for load management is not limited to the residential sector. Many research works have focused on the definition of energy flexibility for industrial, commercial, and office case studies, like Aelenei et al. [204] which investigated the energy flexibility potential in an office building with a BIPV roof system in Lisbon, or Zhou et al. [205] which proposed a machine-learning approach for a high-rise office in Hong Kong.

The literature review shows that advanced control is both effective and reliable. However, it faces challenges when applied in multi-building setups. The primary obstacles include the absence of a high-resolution measured dataset, the intricacy of characterizing interactions between buildings and the power grid, and the effective management of independent energy systems and renewable energy sources (RESs). Hence, it is crucial to address these challenges by adopting comprehensive control-oriented methodologies for designing and operating energy aggregators. To achieve these targets, the following three sections will focus on coordination methods, pricing manipulation, and building-to-building scalability.

2.3.1 Coordination schemes

In the evolution from the individual management to the cooperation, the control scheme characterized the power exchange and the communication process between appliances, buildings, and EAs [206]. The way of implementing the control levels can be centralized, decentralized, distributed, or in a hierarchical fashion [207], as shown in Figure 2.11.
Centralized structure collects and transmits information to local distributed generators (DGs). The primary controller supervises DGs relying on data communication protocols, whereas decentralized (Figure 2.11.b) and distributed structures (Figure 2.11.c , Figure 2.11.d) do not require a central controller. Decentralized control performs regulation based on local measurements [208] while in comparison, distributed control is based on both local measurement and neighboring communication [209]. The hierarchical control structure distributes the control functions into local controllers and upper-level controllers, so that the complete system operates in a more efficient way [210].

Centralized control, as shown in Figure 2.11.a, requires data collection from all the DR and appliances, such as water boilers, HVAC, EVs [211]. These control architectures are advantageous in terms of observability and controllability, as well as straightforward implementation. However, central controllers are likely to breakdown, depending on a single controller. Other disadvantage is the reduced expandability, with an operational effort in managing complex systems. Therefore, centralized control is usually more suitable for localized and small size applications where the information to be gathered is limited, and centralized optimization can be realized with low communication and computation cost [212].

Decentralized control does not require information from other parts of the system, as shown in Figure 2.11.b. The controller regulates each unit with only local information, lowering the data communication problems by avoiding real-time protocols, and thereafter, the reduced expandability of centralized architectures. The main disadvantage is the lack of coordination between local regulators, limiting the achievement of global coordinated behaviours.

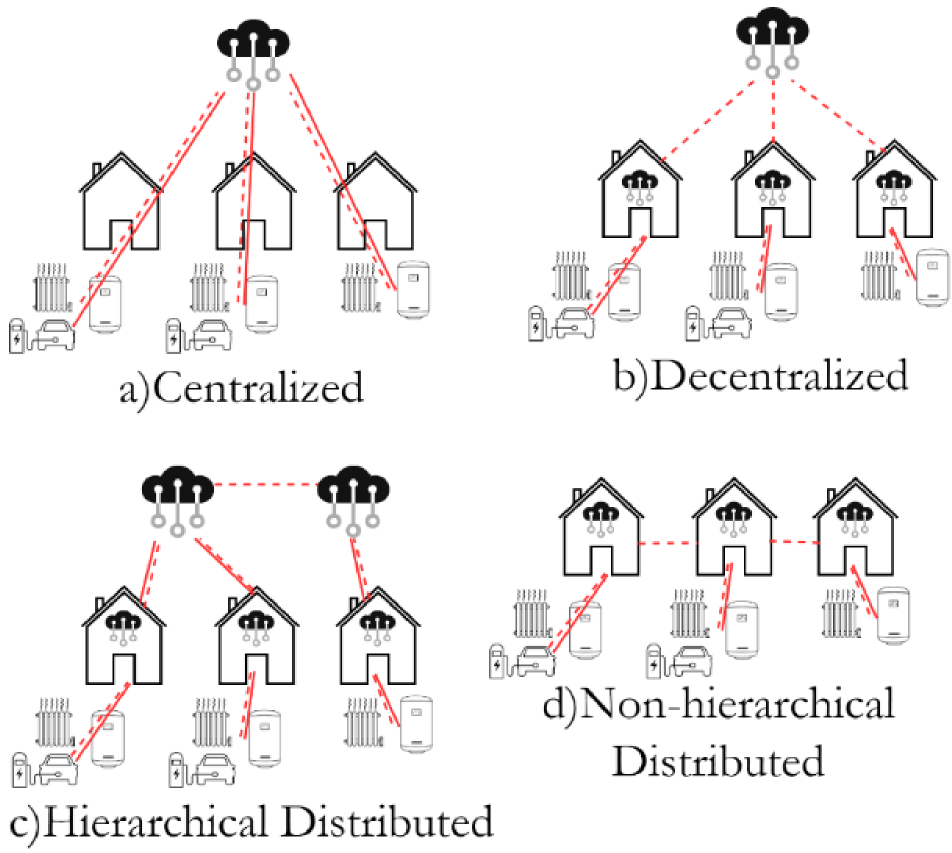

Figure 2.11.The main configuration for supervisory control in energy communities

Recent progresses in ICTs and information-exchange algorithms enable the application of a centralized controller in a distributed way [213], as shown in Figure 2.11.c. The controllers "talk" with each other through communication lines, so that essential information is shared among each local system in order to facilitate a coordinated behavior of all the units [210]. The main disadvantage is the system coordination. Thus, peer-to-peer and consensus algorithms have been used to allow a set of agents to reach an agreement on a quantity of interest by exchanging information through a communication network [214].

To overcome the disadvantages listed above, hierarchical distributed schemes are conceived on the creation of a multi-layer architectures with a local controller used for simple functions (such as voltage/current regulation and power sharing, and a central controller for advanced management functions (those who require global information), as shown in Figure 2.11.c.

As demonstration of hierarchical distributed scheme, Georges et al. [215] investigated the differences of synchronized and desynchronized activation of heat pumps of a building cluster by grouping buildings in two different bins. The results of diversified strategies show around 50% increase in effectiveness from one-strategy-fits all scenarios.

Classification of Load aggregation methods

The effort to incorporate smart grid functions, in particular demand response and peak-load management, has inspired numerous power systems to establish bidirectional communication networks capable of connecting industrial, commercial, and residential loads to utility control centres. The purpose of these communication networks is to transmit data from loads to utility and control signals from the utility to loads, enabling the implementation of smart grid functionalities.

Load aggregation is a crucial necessity for implementing smart grid functions, as it is necessary for processing the data obtained from loads [216]. Specifically, 1) Formulate strategies and create plans for efficient and effective power distribution systems through integrated planning and design; 2) Develop prediction of future electricity demand based on historical data and other relevant factors; 3) Provide detailed information about the patterns and characteristics of electricity consumption; 4) Quantify the fluctuations in electricity consumption that occur on a daily or seasonal basis; 5) Calculate the potential changes in electricity demand due to factors such as time of day or shifting consumer behaviour; 6) Assess the maximum amount of electricity without causing disruptions or failures; 7) Assess the storage capacity of controllable loads [217].

The literature highlighted three main load aggregation techniques:

- **Bottom-Up aggregation**: Simple approach for aggregating commercial and residential loads. This method aggregates loads starting with those connected to low-voltage feeders (residential and small commercial loads fed from distribution transformers) and moving upward toward distribution substations. The BU method produces an equivalent model consisting of loads with their power demands or equivalent impedance (or admittance) matrix.
  As requirement, individual loads need to be categorized into dynamic or static. Static loads do not affect the voltage, whereas dynamic ones must be fed by downstream transformers and/or series impedances that are supplied from upstream circuits.
- **Coordinated aggregation**: Loads are ranked and assigned a given priority based on determined features (e.g., storage capacity, power demands, frequency of ON-OFF, impacts on the feeders and/or transformers, etc.). The ranking of loads is created to avoid using statistical methods to determine load power demands, thus simplifying the load aggregation.
- **Bus-Split Aggregation**: Loads composed of 3-phase induction and synchronous motor. The aggregation is carried out initially to provide an equivalent circuit for a bus, which has one induction machine and one synchronous machine. Each machine is connected to a bus through a transformer. The next stage of the BS aggregation is to lump both equivalent circuits into one equivalent circuit.

2.3.2 Price manipulation

Dynamic pricing gained popularity in the 1980s, thanks to American Airlines' effective use of a pioneering commercial campaign [218]. This represented a crucial turning point, ushering in an era where firms started to acknowledge the influence of dynamically modifying prices to align with market needs in real-time. The exponential expansion of big data and the creation of increasingly precise datasets are driving this evolution. These abundant sources of data offer highly important observations on client behaviour, allowing for a more relevant approach to customization and personalized services, as emphasized by Fisher et al. [219]. Within economic contexts, data is not simply an intangible concept, but rather a powerful form of currency that produces concrete knowledge. This knowledge forms the foundation on which organizations can identify and understand client requirements, capabilities, and competencies. This concept is commonly referred to as data capitalism, as explained by Xia et al. [220]. Companies can use data to effectively navigate the complexities of the market and ultimately increase their profitability.

Utilities find themselves compelled to operate with agility and responsiveness. Constantly shifting market conditions necessitate a swift adaptation setting, prompting organizations to recalibrate strategies, aided by the guidance of automated algorithms [221]. During this rapid adjustment and development process, one factor is particularly crucial: *price*. The concept of incorporating the operational state of the power grid into pricing measures is the result of pricing algorithms [36]. Pricing algorithms utilize input data on markets and actors to examine numerous elements, such as competitors' prices, consumer demand, and individual behaviours and patterns. The algorithms subsequently calculate the output price by considering the largest achievable revenue, which optimizes profits.

Price manipulation is widely acknowledged as a vital and powerful tool for companies, serving as fundamental technique for aligning with market dynamics and competition [100]. From utility and power grid management, a key element to determine is the reservation price defined as the minimum value that the firm (utility or power supplier) would accept. This value comes from inventory management and individual contracts for provision of electricity (different generators, private / government-owned) energy regulators and policy. On the other hand, the customer (or portfolio) management aims at identifying the willingness to pay, that is the maximum price a customer is willing to pay for a given goods or services. Important to mention that both reservation price- for the variability in the energy supply mix at the aggregated scale- and the willingness to pay are highly dynamics [222]. Therefore, these upper and lower bounds evolve throughout the day and the year [223], and are affected by occupants [224]. The last relevant parameter in the creation of a pricing algorithm is the number of competing aggregators. This number defines the pricing options (strategies and structures) in competition. A representative schematic is shown in Figure 2.12.

The iteration aims at defining pricing profiles. These undergo two independent verifications:

1. Ensure that supply and demand meet in a reasonable domain (defined as I. Convergency);
2. Ensure that prices do not generate extra revenue and asymmetric behaviors (defined as II. Fairness).

In recent literature, there has been a focus on utilizing machine learning methods that particularly address behavioural patterns to forecast an individual's willingness to pay [225, 226]. Load profiling is suitable for studying the relationship between occupant behavioural patterns and electricity use due to their strong interdependence [227].

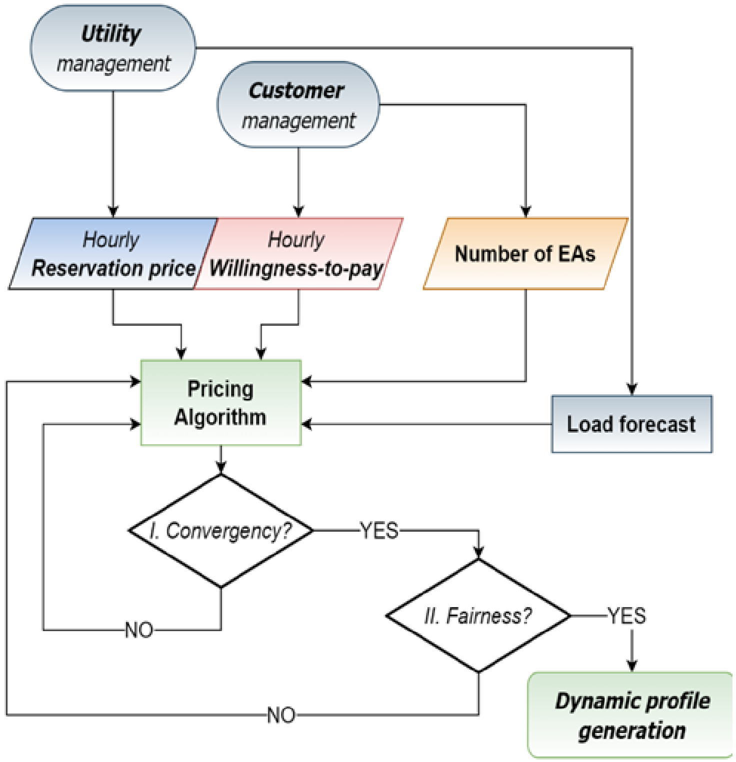

Figure 2.12. Schematic for generation of dynamic pricing profiles.

Dynamic and personalized pricing
Algorithmic pricing, with its extensive applications, is indicated for benefiting supply providers, utilities, and consumers. However, while firms express enthusiasm, consumers harbour concerns over the inherent bias involved in the development of these algorithms [228]. When creating a dynamic pricing profile, it is necessary to establish trust among stakeholders regarding the expected price fluctuations. It should be noted that supervising these prices would be extremely challenging for both regulators and policymakers, as they are subject to frequent change over time.

Dynamic pricing (sometimes also known as real-time pricing) generally refers to the practice of dynamically adjusting prices in order to achieve revenue gains, while responding to a given market situation with uncertain demand [229].

The implementation of dynamic pricing is influenced by the underlying energy policy. Getting information on the financial performance of energy utilities and TSOs is a complex and uncommon task. This frequently occurs as a result of intricate economic structures, involving multiple trade agreements, and the government's intention to withhold confidential information.

Energy aggregators can also be advantageous from this perspective. The local management transfers the problem from the macro to the *meso* level, where revenue and profit may be more easily measured, while also employing various solutions. The premise is that pricing systems should maintain revenue neutrality for utilities, so any additional profits generated by customer involvement are only allocated to electricity cost reduction. This ensures that the utility's profit remains constant while sharing the surplus with DSM participants. This comprehensive approach emphasizes the complex and diverse characteristics of pricing algorithms, which include economic, ethical, and social aspects. As a result, it is essential to establish unified pricing policies to ensure third parties (such as aggregators) to develop and implement dynamic pricing structures.

Another application for pricing algorithms involves the implementation of personalized pricing. First-degree price discrimination, also known as *personalized pricing*, customized pricing, or targeted pricing, is a pricing technique in which firms charge different rates to different consumers based on their willingness to pay [230].

The literature suggests that both first-degree price discrimination and group-specific pricing discrimination provide ethical concerns that warrant additional investigation from academics and authorities. However, identifying specific customer groups within the managed portfolio would yield significantly greater advantages, as it would create pricing strategies that align with their predicted behaviour. Data mining enables organizations to analyze customer behavior data and evaluate specific features and preferences [231]. It is crucial to note that the intended purpose of zones, the type of building (such as residential, industrial, or commercial), and the building structure (such as apartment, attached, or detached) can still be considered as initial factors for discrimination. However, the economic incentive that drives customers to participate in DRP is frequently contingent upon the financial well-being of homeowners.

2.3.3 Building benchmarks for power-related problems

The final aspect examined in developing a methodology for enhancing the grid interaction of energy aggregators is the coordination process. Indeed, a building portfolio can consist of anything from two to hundreds of homes. Despite the potential of hierarchical designs, it is impractical to develop, convey, and implement tailored strategies for each household.

One possible answer is to develop a systematic mechanism for grouping buildings according to their potential for energy efficiency and performance indicators. This would allow for the use of data-driven techniques to efficiently implement a set of optimal strategies across a group of buildings. More precisely, the focus is on the influence of price and the consequences of advanced technologies, such as heat pumps, photovoltaic systems, photovoltaic-thermal systems, energy storage solutions, and electric vehicles.

Although the international community tried to establish a standard system for building benchmarking, the relatively new framework of energy flexibility and load control in demand response has revealed a need in this area. This section summarizes constructing benchmarks and the concept of first-degree discrimination.

Building energy benchmarking is referred to as the comparison of energy performance in buildings with similar characteristics [232]. A qualifying benchmarking process is described by three steps:

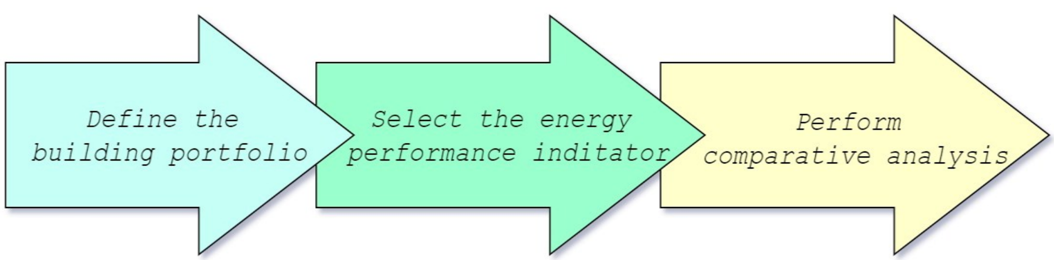

Figure 2.13. The three stages of building benchmarking process.

i. collect a reasonably large database of building samples.
ii. obtain the energy performance information of the candidate buildings.
iii. conduct comparison analysis [233].

The first step defines customer pools, where datasets are gathered and standardized. This process needs to comply with requirements in terms of monitoring infrastructure, minimum level of measurements, and metadata information. For energy aggregators, supplementary information is needed to understand the energy sub-stations a given customer is connected to. The second step defines the energy performance by selecting the investigated variables. These can be extracted straightforward from the dataset or generated/simulated by using building energy modelling. The third and final step of the procedure consists of comparison analysis on the predetermined performance indicators. This is the domain where load management and energy efficiency apply. In fact, the retrofitting, parameter investigations, and activation of BEF is presented.

The choice of the building benchmarks is related to the selected investigation, the problem identified, and the desired outcome for stakeholders. Even in this case, the beforementioned categorization between *energy-related* and *power-related* problems arises.

A typical benchmark for *energy-related* problems is the comparison of the Energy Usage Intensity (EUI) against the corresponding value of the peer group. The recognition of peer groups considers location (climate zone), floor area, and building type (residential, commercial, industrial), year of construction, number of occupants [234]. However, so-called low-dimensional benchmarking methods can be counter intuitive since cannot represent many other factors of influence. A fairer comparison is to create peer groups based on more detailed methods to include more features. In this respect, data mining techniques have the potential to generate load profiles recurring to smart meter data [235].

In *power-related* problems, representative load profiles describe building operations, variations of building energy intensity, and inform about the temporal and absolute trends of power demand. The utilization of unsupervised learning techniques has been acknowledged as a potential strategy for load profiling due to the presence of stochasticity and singularity, which contribute to the distinctiveness of buildings from one another [236].

These methods captured the operational patterns of individual buildings by identifying representative daily profiles, where the variations in building operations are reflected in many differences, such as the number of profiles, the profile shapes, and the corresponding dates of each profile [237]. Many researchers applied unsupervised clustering techniques to benchmark single buildings, such as K-means clustering [238], density-based clustering [239], hierarchical clustering [240], K-shape clustering [241], "follow the leader" clustering [242], and Self-Organizing Map [243].

An interesting application was proposed by Park et al. [244] who considered the iterative use of k-means clustering on daily profiles from hundreds of buildings. The first outcome was the creation of fundamental building types, the last outcome was the characterization of each fundamental type into fundamental profiles. The idea of reflecting time-series analysis into a new benchmarking procedure is evident. Especially in markets where DR programs are already implemented, reflecting potential variation in the load profile seems both impactful for the design of energy aggregators (for the inherent super position effect) and convenient in creating building groups. Among different possibilities, the dynamic time warping techniques is presented [245].

Dynamic time warping (DTW) is an algorithm used to measure the similarity between two temporal time series sequences. The advantage of this technique is that the similarity is not affected by different frequencies. An example to understand this "relativity" comes with two adults walking on a straight line at two different velocities. An immediate indicator for discrimination might be the average speed, resulting in clustering the two walkers into different groups. But if the analysis is considered on the BPM rather than the velocity, the two walkers might be grouped together. Therefore, DTW allows to focus the analysis on hidden properties in the time series analysis.

The objective of time series comparison methods is to produce a distance metric between two input time series. The similarity or dissimilarity of two-time series is typically calculated by converting the data into vectors and calculating the Euclidean distance between those points in vector space [246].

The application of DTW is contingent to the following the rules: 1)Every index from the first sequence must be matched with one or more indices from the other sequence and vice versa; 2)The first index from the first sequence must be matched with the first index from the other sequence (but it does not have to be its only match); 3) The last index from the first sequence must be matched with the last index from the other sequence; 4)The mapping of the indices from the first sequence to indices from the other sequence must be monotonically increasing, and vice versa.

3. *Data-driven methodology for building demand forecasting*

This chapter presents the control-oriented methodology for modelling and produce demand forecasting of residential buildings.

The first Section describes the procedure for thermal modelling. The prediction and thermal load management are performed through grey box modelling, a data-driven calibration (inverse technique), and the main results of parameter estimation. The use of two different case studies is introduced to prove the effectiveness of the presented methodology in either low- or high-resolution measured datasets. The proposed MOR procedure is therefore presented, showing the main results from the supporting unsupervised clustering technique. The accuracy of the model is investigated via KPIs for an overall of seven days of measurements. Lastly, the prediction of electric loads is investigated.

The second Section investigates the creation of the ensemble setup to determine the overall load demand from residential customers, a combination of dedicated models in a streamlined fashion to superpose thermal loads and electrical loads within the agent's environment. A focus on dedicated model is performed, to show the large applicability of the presented methodology to deal with space heating, domestic hot water production, and miscellaneous electricity demand.

The third and last Section of the Chapter investigates the formulation of control schemes for the communication with the grid operator and the focus on the BEMS or HEMS, where the innovative concept of *control volumes* is presented to simplify the schematic of power flows and multi-carrier sources energy management. The layout is designed to be adaptable in adding or removing volumes based on the available technologies to address the issue of generalizability, while also considering the tailoring modeling. The lesson derived from the experimental setup is presented here to emphasize the parallels and enhancements compared to commercially available tools.

3.1 Thermal Load modelling

As explained in the *Background and Literature Review*, the choice of a reduced-order model is suitable for energy aggregators, especially during the design stage of building portfolios. The following analysis consider a low dimensional dataset, with only one measured and controllable temperature. A simplified model is presented in Figure 3.1. The thermal mass of the building is characterized by slow thermodynamics, enabling a consistent time delay between the heating input and the variation in the indoor temperature. In the application of a DRP, this phenomenon allows the definition of a preheating period where the environment can be overheated to reduce power consumption during on-peak hours.

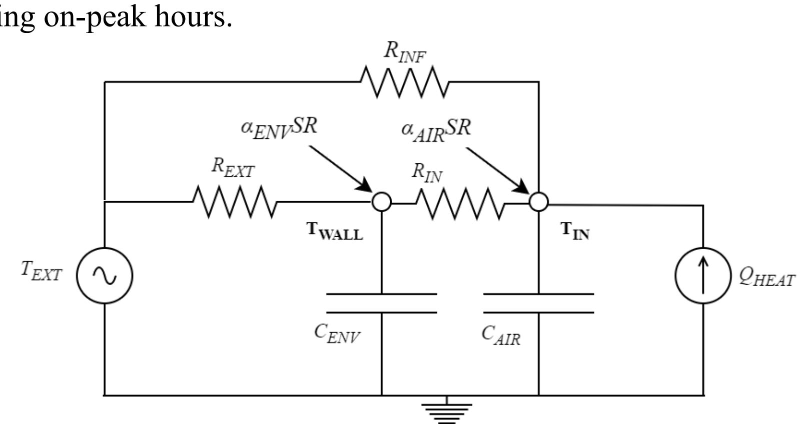

Figure 3.1- Simplified model for thermal modelling of residential houses.

The length and intensity of such preheating is related to the thermal features of the buildings. For this purpose, a second order RC thermal network is exploited, as presented in the Eq. (3.1 and 3.2).

$$C_{AIR}\frac{\partial T_{IN}}{\partial t}=\frac{T_{WALL}-T_{IN}}{R_{IN}}+\frac{T_{EXT}-T_{IN}}{R_{INF}}+Q_{HEAT}+\alpha_{AIR}\cdot SR \tag{3.1}$$

$$C_{ENV}\frac{\partial T_{WALL}}{\partial t}=\frac{T_{EXT}-T_{WALL}}{R_{EXT}}+\frac{T_{IN}-T_{WALL}}{R_{IN}}+\alpha_{ENV}\cdot SR \tag{3.2}$$

where, T_{IN} is the indoor air temperature, T_{WALL} is the wall temperature, T_{EXT} is the ambient temperature, SR is the solar radiation, Q_{HEAT} is the heating power, R_{EXT} is the overall thermal resistance of the building, R_{IN} is the overall thermal resistance between the high inertial and low inertial nodes, R_{INF} is the overall thermal resistance for the infiltration rate, C_{ENV} is the overall high inertial thermal capacitance, C_{AIR} is the overall low inertial thermal capacitance, α_{ENV} is the solar absorption coefficient for the envelope, and α_{AIR} is the solar absorption coefficient for the low capacitance node.

The selection of a second order was dictated by the need for higher resolution. Having one node for the indoor air – assuming a perfect mixture of air and disregarding the vertical gradient – and one node representing the envelopes (hidden state) makes it possible to quantify the actual heat stored into the building mass, streamlining the quantification of BEF.

The estimation of the 7 parameters (C_{ENV}, C_{AIR}, R_{IN}, R_{INF}, R_{EXT}, α_{ENV} and α_{AIR}) is performed through a fitting process designed on a nonlinear least-squares solver evaluated for an inverse-calibration horizon (ICH) up to 24 hours, aiming at minimizing the FIT error. MRI procedure is used to train the model for 7 days, while 2 days are used for the testing. Considering a timestep of 15 minutes, the number of datapoints (*Nd)* corresponds to 7x96, and ICH to 96 points.

Nonlinear constraints are generated to respect the stability of the explicit problem as follows:

$$\begin{cases}\pi_1: dt-\dfrac{C_{AIR}}{\left(\dfrac{1}{R_{IN}}+\dfrac{1}{R_{INF}}\right)}\le 0\\ \pi_2: dt-\dfrac{C_{ENV}}{\left(\dfrac{1}{R_{IN}}+\dfrac{1}{R_{EXT}}\right)}\le 0\\ \pi_3: \dfrac{dt}{(C_{AIR}\cdot R_{IN})}-1\le 0\\ \pi_4: \dfrac{dt}{(C_{ENV}\cdot R_{IN})}-1\le 0\end{cases} \tag{3.3}$$

The calibration considers only positive values of capacitances, resistances, and alpha values. To prevent the risk of local minima, a Latin hypercube sampling (LHS) approach is considered to present 600 different initial conditions. From these 600 initial conditions, around 56% pointed to the following 7 combinations:

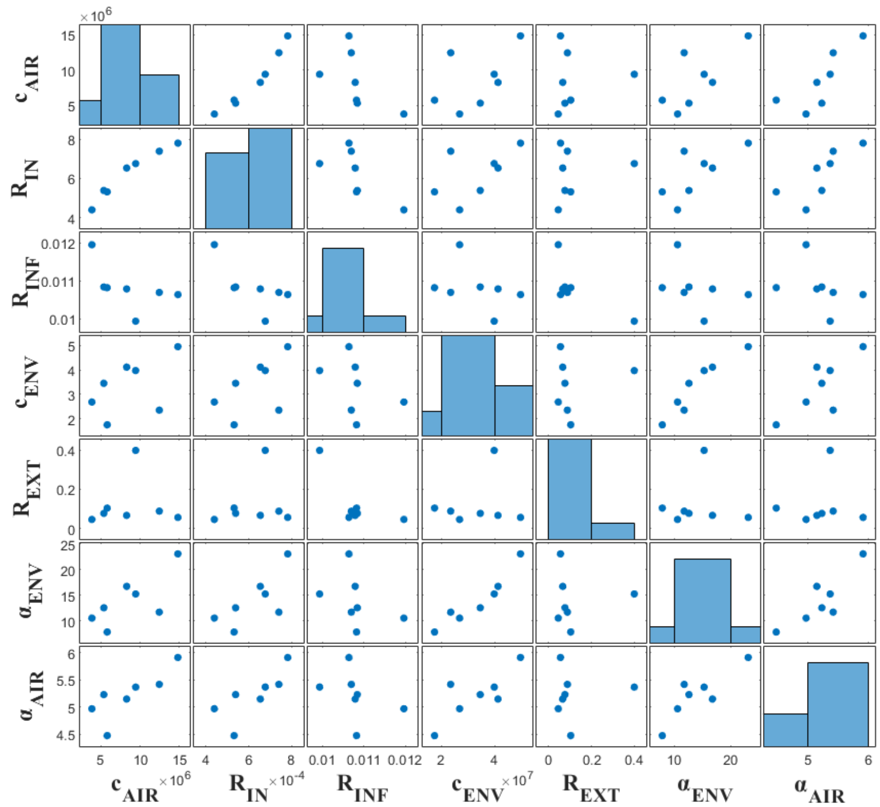

Figure 3.2. Results of LHS for low dimensional dataset

The result of the calibration procedure of the most accurate model for 10 households is presented in Table 3.1

Table 3.1- Results of the MRI calibration for 24hour ahead predictions.

House ID	C_{AIR} [MJ/K]	R_{IN} [K/W]	R_{INF} [K/W]	C_{ENV} [MJ/K]	R_{EXT} [K/W]	α_{ENV} [-]	α_{AIR} [-]
1	12.90	1.03E-3	9.39 E-3	44.19	7.05E-2	49.99	5.52E-4
2	11.92	3.37E-4	7.59E-3	39.89	3.85E-2	49.90	13.72
3	10.51	5.99E-4	8.45E-3	43.92	5.57E-2	41.78	4.86E-6
4	8.78	2.20E-4	2.07E-2	23.25	4.82E-2	9.33	10.70
5	7.93	5.78E-4	7.25E-3	39.59	3.98E-1	20.80	20.49
6	11.63	9.13E-4	9.34E-3	31.79	0.15	32.58	2.61E-3
7	7.86	2.67E-4	7.76E-3	44.02	3.48E-2	50.00	12.94
8	6.58	5.32E-4	7.34E-3	35.40	4.00E-1	11.20	22.11
9	11.63	2.75E-4	1.76E-2	31.80	5.82E-2	10.86	15.61
10	5.35	5.38E-4	1.08E-2	34.55	7.71E-2	12.57	5.23

The results of both training and testing are evaluated by three performance metrics: RMSE, FIT, and coefficient of determination (R^2) and shown in Table 3.2.

Table 3.2. Performance metrics for the considered ten households in the virtual community.

House		1	2	3	4	5	6	7	8	9	10
RMSE	*Train*	**0.36**	0.50	0.47	0.37	0.58	0.42	0.51	0.66	0.38	0.44
	Test	0.39	**0.22**	0.31	0.45	0.42	0.44	0.32	0.35	0.55	0.36
R^2	*Train*	**0.86**	0.81	0.67	0.54	0.83	0.81	0.82	0.59	0.53	0.56
	Test	0.84	**0.93**	0.71	0.54	0.86	0.83	0.89	0.81	0.54	0.62
FIT [%]	*Train*	**61.2**	49.2	37.9	31.0	45.1	54.5	48.3	24.7	31.0	25.7
	Test	56.6	**74.7**	44.8	30.8	48.6	51.5	64.2	49.0	29.8	31.4

The accuracy is acceptable, with a maximum RMSE of 0.66 °C for training and 0.55 °C for testing. The indoor air temperature is shown in Figure 3.3 for the ten houses.

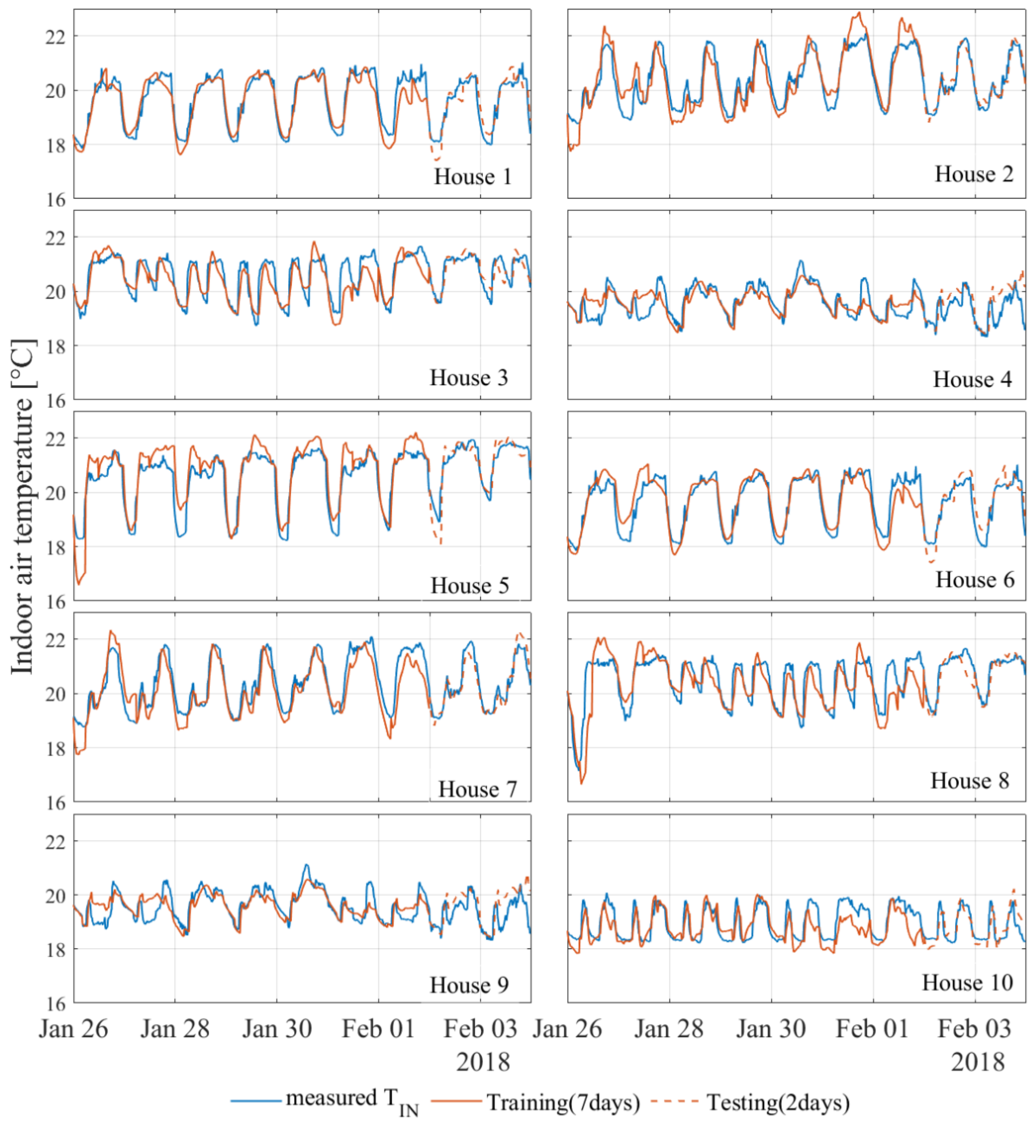

Figure 3.3. Indoor zone air temperature trends. 7 days for training and 2 for testing.

Even with low-resolution datasets, the given methodology is capable of capturing buildings' thermodynamics and generating accurate indoor temperature predictions 24 hours in advance.

This approach allows for standardization of the level of detail within the aggregator while ensuring that the monitoring infrastructure creates no kind of discrimination. However, most of the existing homes with monitoring equipment have several temperature controls and multiple thermostats. The previous chapter recommends against increasing the degree of complexity. Consequently, the following section introduces a novel model-order reduction procedure.

3.1.1 *Model Order Reduction procedure*

This procedure aims at generating a reliable methodology to aggregate individual thermal zones. Unsupervised clustering techniques (Timeseries kMeans) is effective for building-to-building generalization, and pattern recognition when there is abundance of measurements.

The proposed approach exploits a recursive routine of k-means clustering to group thermal zones with similar thermal physics to reduce the number of optimal actions for a given optimization problem.

The detailed procedure is shown in Table 3.3

Table 3.3. Model Selection Algorithm via iterative k-means clustering

1	Preprocess Zone Temperature, Set point temperature, and Power readings
2	Run interpolation for missing values.
3	Replace outlier measurements according to Cook's distance [247]
4	**for** *ir*=1:*NThermalZone*
5	Run Z-Normalization of zone temperature(*ir*)
6	Eliminate normalized daily timeseries containing a single value greater than |2.1|
7	Apply timeseries kmeans with DTW distance algorithm on 300 iterations
8	Start with number of clusters *ki(ir)* =5
9	Consider winter period only (120 timeseries)
10	**if** *min[length(ClusterElements)]<10%*
11	*ki* = *ki* -1
12	Delete timeseries clustered in the smallest cluster
13	**else**
14	Define *ki* cluster trends of zone temperature(*ir*) for the remaining timeseries
15	**end**
16	**end**
17	Apply kmeans clustering algorithm using Euclid distance (*Σ[NThermalZone* ki(ir)]*)cluster trends
18	Apply Bayesian Information Criterion (BIC) to optimize number of clusters i_{FINAL} for model archetype
19	Design a RC reduced order model of order = i_{FINAL}

The presented aggregation algorithm identifies an optimal model structure as:

$$\begin{bmatrix} kC & \frac{k(k-1)}{2}R & k\alpha \end{bmatrix} \tag{3.4}$$

Where k is the number of nodes evaluated as number of final clusters i_{FINAL} plus one node for outdoor air temperature. In fact, each cluster has one capacitance, one resistance and one solar aperture, plus i_{FINAL} resistances to describe zone-to-zone interactions.

To assess the benefit of this MOR technique and evaluate the performance of the evaluated model, an individual house of building portfolio (shown in *Case study*) the virtual community that comprises nine individual thermal zones is analysed. For the considered building, the iterative procedure of k-means-clustering:

i) define the *most representative trends of zone temperature* for the nine thermal zones- shown in Figure 3.4;
and
ii) cluster the most representative trends of zone temperature for the nine thermal zones into *aggregated groups* – shown in Figure 3.5 with the corresponding building schematic and the list of intended uses.

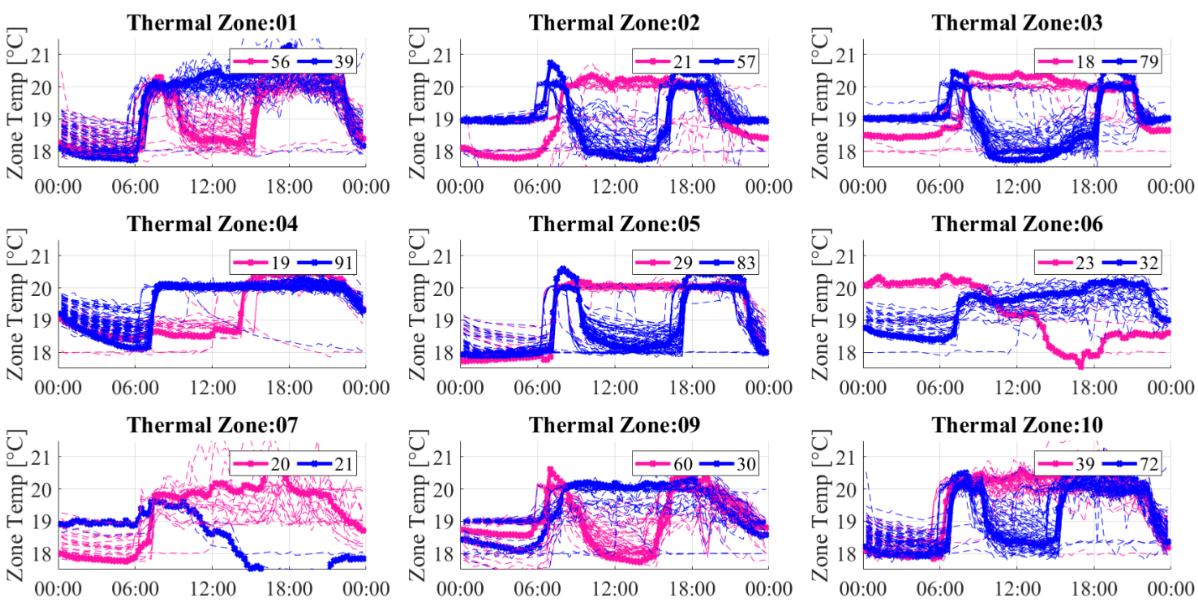

Figure 3.4- The most representative trends of zone temperature for the nine thermal zones

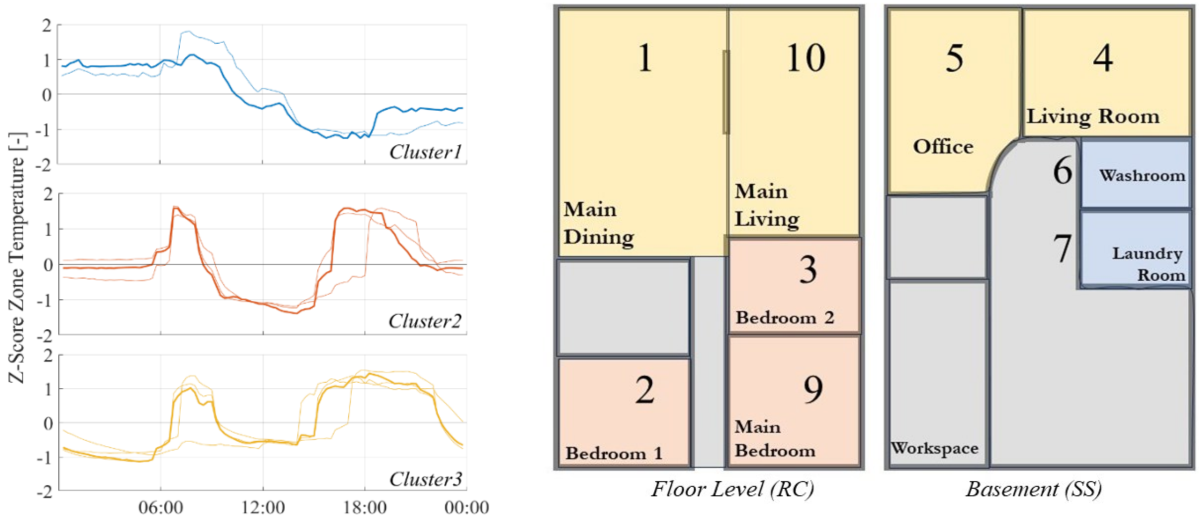

*Figure 3.5.**a**- Aggregated groups: Clusters of the most representative trends of the nine thermal zones; **b** - Building schematic and intended uses*

The proposed MOR methodology has defined three main aggregations. Therefore, the optimal model structure is *6R3C3α*, according to Eq. (3.4).

The network is presented in Figure 3.6.

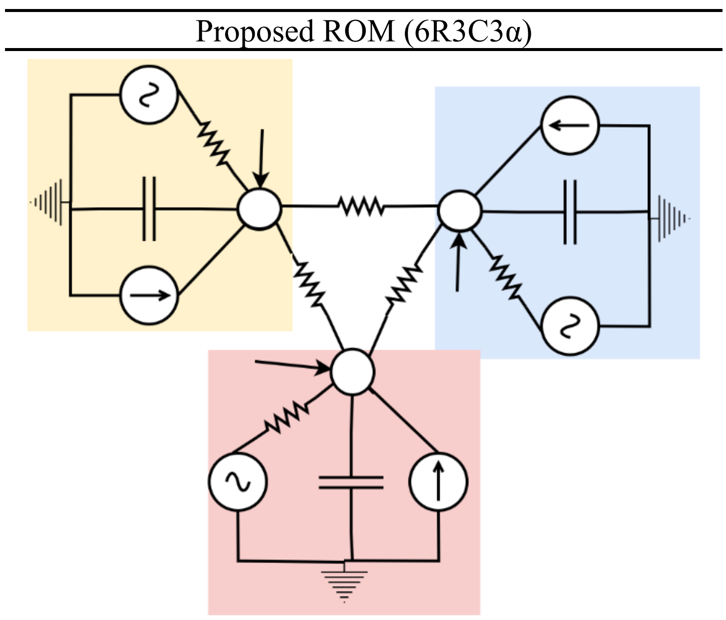

Figure 3.6 - 6R3C3α proposed aggregated model.

The accuracy of the proposed model is evaluated for 7 days of training and 1 day. Figure 3.7 shows the three macrozones Blue –Thermal Zones 06,07,08, Red - Thermal Zones 02,03,09, and Yellow-Thermal Zones 01,04,05,10. The performance metrics – in the form of RMSE- is shown in Table 3.4.

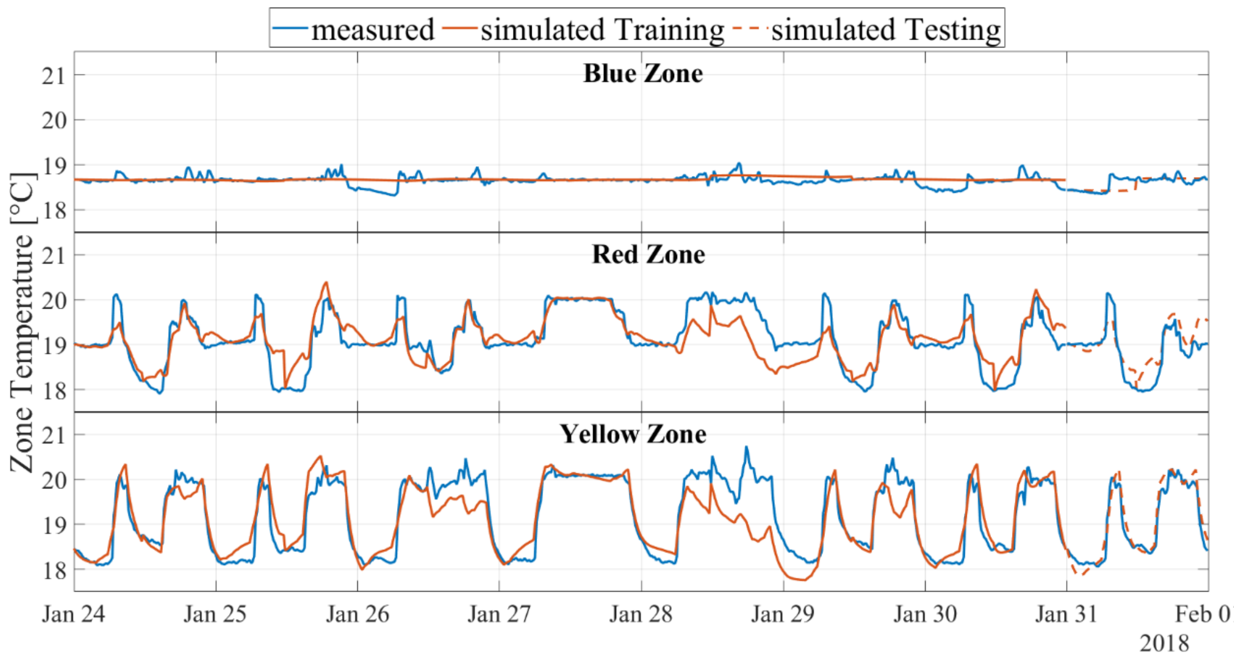

Figure 3.7- Results of the calibration for the proposed model considering seven days for training and one for testing.

Table 3.4-Performance metric (RMSE) for the Reference and Proposed ROMs.

Zone	*Blue*	*Red*	*Yellow*
RMSE Train	0.08	0.17	0.28
RMSE Test	0.13	0.25	0.22

The current methodology offers several advantages. Firstly, it ensures a RMSE below 0.3°C in predicting zone temperatures 24 hours in advance. Secondly, the methodology incorporates a second level clustering technique that identifies important metadata information such as location and intended use of rooms. This additional information aids in better understanding the factors influencing temperature patterns within the building. Lastly, the control-oriented formulation employed in this methodology facilitates the implementation of optimal control by utilizing a lower number of strategies, specifically set-point profiles, to effectively leverage the thermal flexibility of the building and facilitate the modeling of interactions between different zones.

In the design of a methodology for optimizing grid interaction of virtual energy communities, this approach allows EAs to standardize the individual models of a diversified portfolio of buildings.

3.2 Electric Load modelling

The prediction of electric loads requires the definition of predictors for each of sub-models, the analysis investigates the daily energy consumption and hourly energy consumption based on the sub-metering readings. The level of details depends on the monitoring infrastructure, so it is often hard to define a standardized procedure for each sub-load. For the considered building portfolio, sub-measures of domestic hot water, dryer, kitchen and space heating are available. An example for House1 is shown in Figure 3.8.

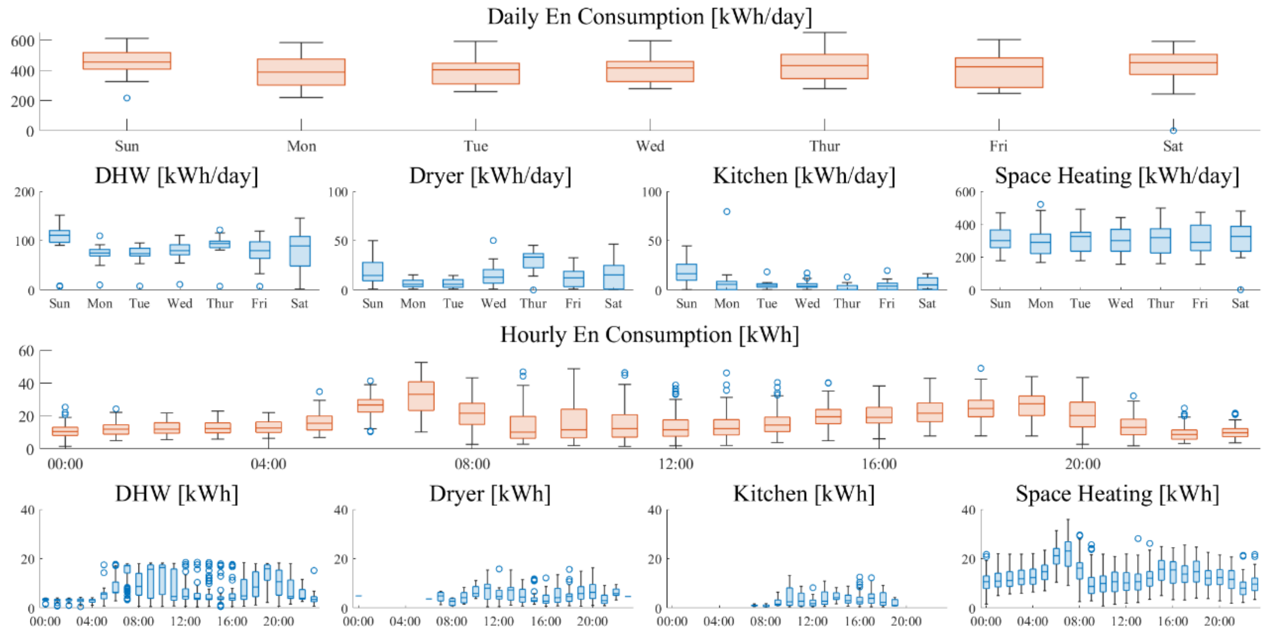

Figure 3.8. Box charts of daily and hourly energy consumption for House1

The daily energy consumption has an almost-constant median point for each day of the week. This is given by the influence of space heating. DHW has its maximum on Sundays and the highest variability on Saturdays. The kitchen presents the lowest values, and it is not considered in the analysis, as well as the dryer, since the demand has occupancy and time of the day as only predictors.

The analysis of the hourly energy consumption shows that the load profile is mainly affected by space heating and DHW, with peak values of around 20kWh. Conversely, the dryer and kitchen are lower in intensity. Note that the dryer is mainly on from 08:00 to 20:00, so it gives no contribution during night hours. The modeling respects these patterns, and the assumptions are conceived to respect the real operation.

Therefore, data analysis is carried out for DHW to give an overall idea of data handling process. In this case, data mining is useful to generate valuable insight and define predictors such as duration of the event, and patterns in demand. As shown in Figure 3.9, time series can be categorized based on distribution of the DHW production event. Where Figure 3.9.*a* shows the duration of the DHW production. The first peak represents the events with a duration shorter than 1 hour. This happens when the systems are on to fill the water tank. The other samples present a duration of around (2.5 ± 1) hours. These events describe the condition of a severe use of hot water, and the DHW production must run for more than 2 hours to compensate the hot water consumption. In Figure 3.9.*b* and Figure 3.9.*c* the power demand for DHW is shown for short and long events respectively. Short events present more variability because the percentage of hot water consumed affects the power consumption, with a mean of 3.7kW. On the other hand, long events present a clear pattern with a mean power demand of 4.3kW, representing the nominal power demand of the water heater.

Finally, in Figure 3.9.*d* and Figure 3.9.*e* the energy consumption per event is shown for short and long events. The mean is of 2.2kWh/event for short ones, and 16kWh for long ones.

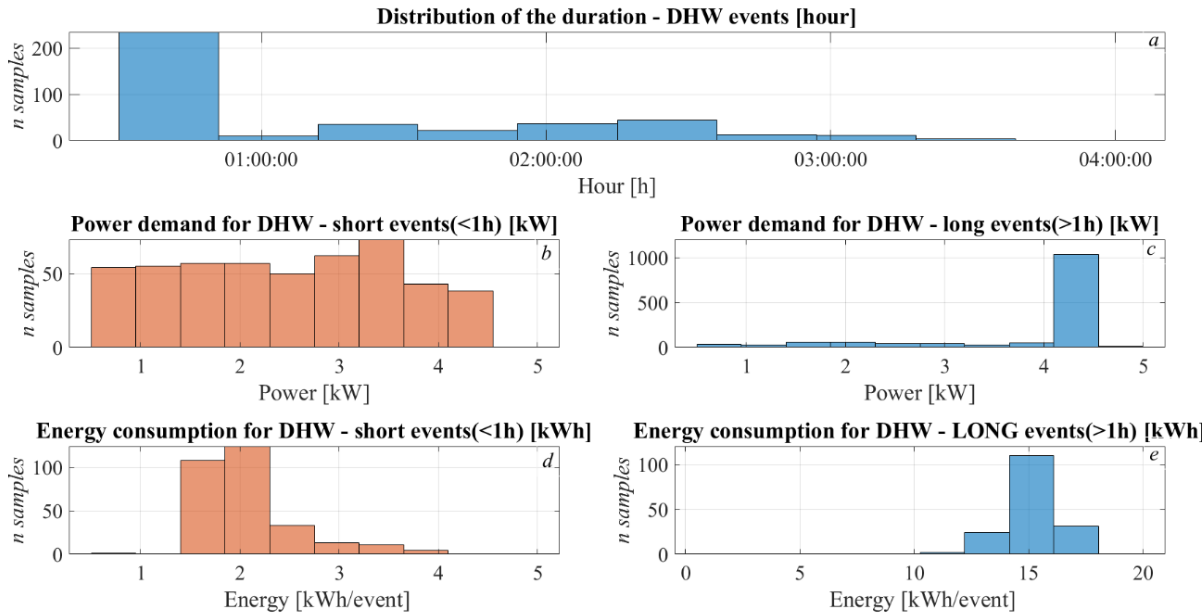

Figure 3.9- Data analysis of DHW for House1

By respecting the energy consumption per event and the typical duration of each household, it is possible to shift in time the load profile for DHW to shape the power demand at the aggregated level as desired.

During the DR events, the predicted consumption for each of the household can differ in intensity. This is due to a different scheduling and human habits, different technologies for the hot water provision, or a different duration of the event (Figure 3.10). Since the data-driven approach, this is an unknown detail.

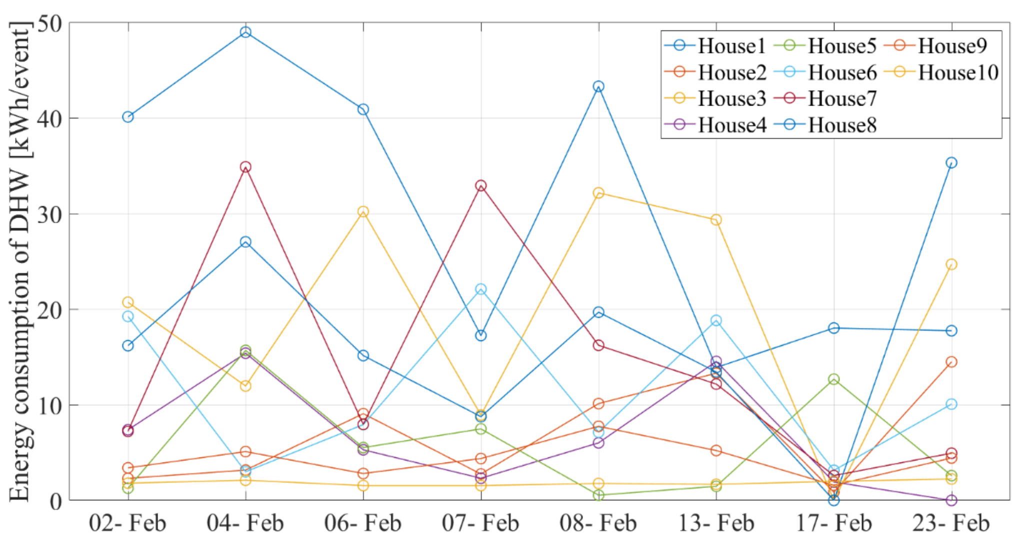

Figure 3.10- Energy consumption of DHW for DR event

Specifically, House1,3,7,8 present an energy consumption that is ten times higher than the others. No evident difference is recorded based on the morning/evening events.

Once identified the predictors, statistical models and machine learning are extremely useful to translate aggregated results into time series.

In the scenario of limited information from the submetering system, the complementary demand is defined as *electric baseload*, which simplifies the methodology by merging heterogeneous sources in one unified measure.

3.2.1 *Support Vector Machine for Electric baseload*

The remaining power demand from the households describes domestic hot water, kitchen, lighting, and main appliances measurements. The sub-metering system gathers power readings and aggregates them as equal to the electric baseload (other than space heating).

Support Vector Machine (SVM) models are created exclusively to predict power demand in the 24-hour communication routine with EAs, showing great potential in this application field [248-250].

The theory of the SVM relies on the structural risk minimization (SRM) principle. The goal of this modelling technique is to minimize an upper bound of the generalization error consisting in the sum of the training error and a confidence interval [251]. Because of the consideration a confidence interval, SVM achieves higher generalization performance than traditional methods [252]. In modelling electric baseloads, a selected data pool is considered to train the prediction models.

$$(x_1, y_1), (x_2, y_2) ... (x_{NDtrain}, y_{NDtrain}) \tag{3.5}$$

Where, x_i is a vector of predictors and y_i is the response, *NDtrain* is the number of datapoints used for the training. Then, SVM approximates the function using the following relationship [253]:

$$f(x) = \omega \cdot \phi(x) + b \tag{3.6}$$

Where, $\phi(x)$ represents the high-dimensional feature spaces and ω and b are coefficients estimated during the minimization of the regularized risk function:

$$\min : \frac{1}{2}\|W\|^2 + C\frac{1}{N}\sum_{i=1}^{N} L_\varepsilon(Y_i, f(x_i)) \tag{3.7}$$

Subject to:

$$L_\varepsilon(Y_i, f(x_i)) = \begin{cases} 0 & |Y_i - f(x_i)| < \varepsilon \\ |Y_i - f(x_i)| - \varepsilon & \textit{others} \end{cases} \tag{3.8}$$

Where, $|Y_i - f(x_i)|$ is the regularized term while the second is the empirical error measured by the ε-insensitive loss function. In this way, the model neglects errors within the ε bound. Hyperparameter identification is essential to ensure high accuracy in prediction. For SVM, the Kernel function can either be presented by gaussian, linear or polynomial curves. Six Kernel functions are investigated: i) *Standard Linear Kernel*, ii) *Quadratic polynomial Kernel*, iii) *Cubic polynomial Kernel*, iv) *Fine Gaussian Kernel*, v) *Medium Gaussian Kernel*, vi) *Coarse Gaussian Kernel.* SVM models are trained by five predictors. The first consists of *previous measurement* from power meter [x_{t-1}], global horizontal irradiance (GHI), and *outdoor air temperature* (OAT).

The last two inputs are chronological, consisting of *Day of The Week*, and *Hour of The Day*. The structure is conceived to present a recursive setup to produce multi-step ahead prediction, therefore $\hat{x}_{t+1} \rightarrow \hat{x}_{t+2} \rightarrow \cdots \rightarrow \hat{x}_{t+PH}$, where $\hat{x}$ is model response, and PH is the prediction horizon of the problem, as shown in Figure 3.11.

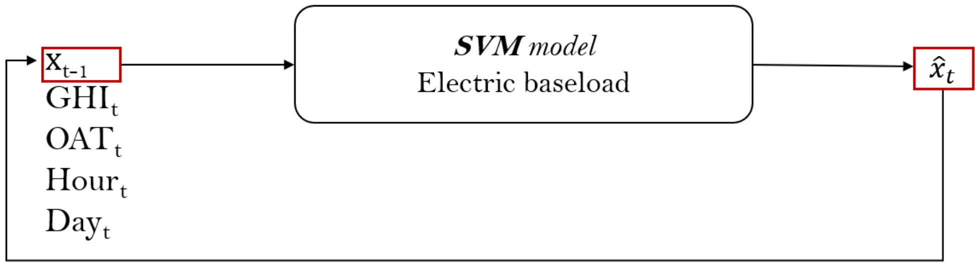

Figure 3.11. Recursive logic for multi-step ahead prediction

It is good practice to produce power load forecasts and control actions from 12 hours to 24 hours in advance for communication setups with the grid operator [254, 255].

The accuracy of SVM in predicting electric baseloads is significantly affected by the choice of kernel function. Performance is measured using the CV-RMSE for the 24 hours ahead predictions, over a week of measurements, as shown in Figure 3.12.

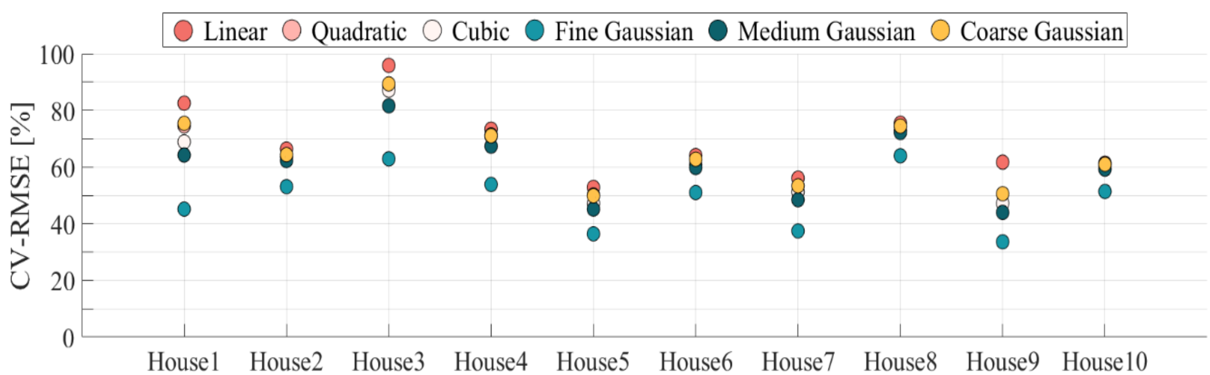

Figure 3.12-Accuracy of SVM in hyperparameter optimization.

The chosen kernel is therefore the Fine Gaussian, able to reduce the CV-RMSE by 19% compared to other kernel configurations across all the considered houses.

The prediction accuracy of the resulting load profiles, depicted in Figure , is evaluated as superposition of the thermal and electric baseload demands and their associated residual errors [256]. Specifically, the errors for the thermal models, referred to as "Heating Residuals" and illustrated in cyan, are compared alongside the errors for the electric baseload model, referred to as "Baseload Residuals" and illustrated in yellow. These residuals are presented individually for each of the considered houses, offering an overall evaluation of model performance across both thermal and electric baseload predictions.

The results show a significant variability in prediction accuracy across the different houses, with CV-RMSE values ranging from 22.1% to 60.2%. Houses 1 and 10 demonstrate relatively lower error rates, indicating better model performance for their load profiles. Conversely, House 5 exhibits the highest CV-RMSE at 60.2%, suggesting considerable challenges in accurately predicting its load profile.

The metrics of load profile models – considering Fine Gaussian as kernel for SVMs- are presented in Table .

Table 3.5. Prediction accuracy Load Profiles.

House	1	2	3	4	5	6	7	8	9	10
CV-RMSE [%]	22.1	34.1	44.5	41.3	60.2	39.0	49.4	45.7	40.9	28.8

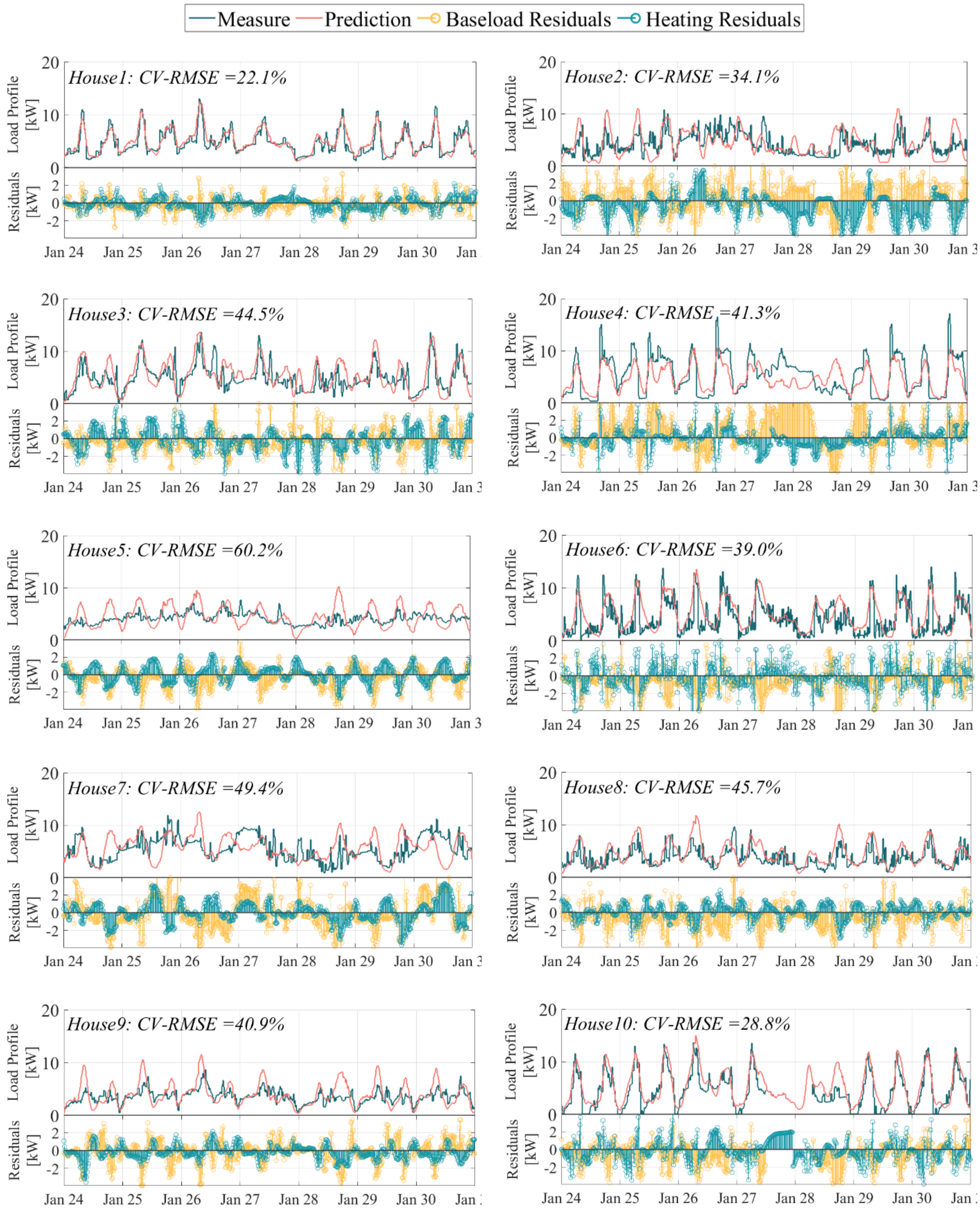

Figure 3.13. Load profiles and residual analysis for the 10 households in the 24 hours ahead prediction framework.

3.2.2 *Long short-term memory for energy prediction*

The prediction of power demand can be also performed via recurrent neural networks (RNN). This model is developed using Deep Learning Toolbox in MATLAB environment to provide a day-ahead forecast. The network scheme comprises a feed-forward connection for information from one cell to the following, with back propagation to adapt weights properly. Other research works exploited this general configuration for the heating load prediction [257], and a cooling load application investigated by Wang et al. [258].

However, RNN presents two main issues when applied in time series forecasting, such as: 1) *overfitting* observed when predictions of data already available in the dataset used for the training stage show a higher accuracy compared to the testing dataset. This could be determined by a wrong learning rate. The general conclusion is that the model is not able to generalize prediction. Overfitting could be avoided by using different strategies (e.g. a proper learning schedule, a lower initial learning rate, an additional dropout layer, or by removing weak data); 2) *local minimum problems* observed when a combination of learning rate and initial allocated weights affects significantly the gradient adjusting process. So, the loss function reaches a minimum value in a local region, resulting in unsatisfactory overall learning. To tackle the vanishing or exploding gradient problem, LSTM overcomes this issue by recurring to an additional gate to control predicted output via hidden state inspection, and the following hidden state.

Figure 3.14 shows the configuration of the LSTM cell.

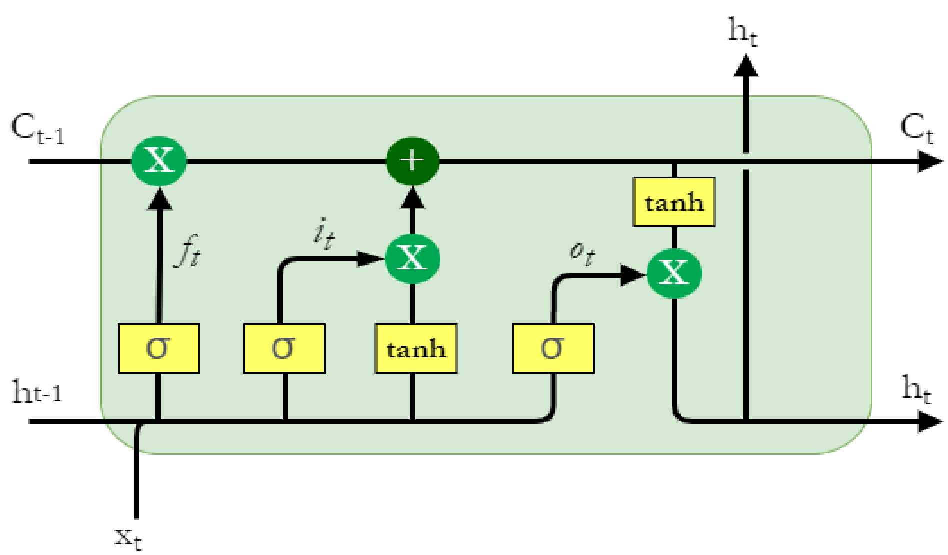

Figure 3.14 Schematic of the LSTM cell

Three multiplicative units are exploited to store temporal sequences: forget gate which selects the cell state at the previous moment (C_{t-1}) and retains part of the information at the current moment adaptively (f_t); input gate which controls the amount of information of the current state to store in the memory cell (i_t); output gate which control the amount of information to send to the following cell (o_t).

The mathematical formulation is described in Eq. (3.9):

$$
\begin{aligned}
f_t &= \sigma(W_f \cdot [h_{t-1}, x_t] + b_f) \\
i_t &= \sigma(W_i \cdot [h_{t-1}, x_t] + b_i) \\
\tilde{C}_t &= \tanh(W_C \cdot [h_{t-1}, x_t] + b_C) \\
C_t &= f_t \cdot C_{t-1} + i_t \cdot \tilde{C}_t \\
o_t &= \sigma(W_o \cdot [h_{t-1}, x_t] + b_o) \\
h_t &= o_t \cdot \tanh(C_t)
\end{aligned}
\tag{3.9}
$$

where, W_f, W_i, and W_o represents weight matrices, b_f, b_i, and b_o are bias vectors, x_t is the current input, and h_t and h_{t-1} are the current and previous output.

To takes any real values in the range [-1,1], hyperbolic tangent (tanh) is considered as state activation function as:

$$
\tanh = \frac{e^x - e^{-x}}{e^x + e^{-x}} \tag{3.10}
$$

To limit the data to the range [0,1] gate activation function is sigmoid, defined as:

$$
\sigma(x) = \frac{1}{1 + e^{-x}} \tag{3.11}
$$

Inputs have been standardized according to mean value and standard deviation, and weights have been initialized using glorot initialization [259]. For this application, the default configuration of Deep Learning Toolbox of mean squared error is chosen as loss function, LSTM layer-by-layer construction for this application is shown in Figure 3.15.

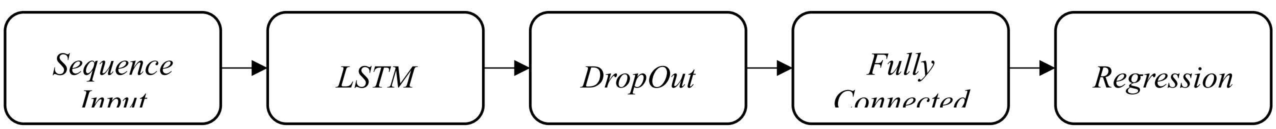

Figure 3.15 Layer by layer construction of LSTM on Deep Learning Toolbox.

So, sequence input layer provides data to LSTM layer. After LSTM a dropout layer is considered to avoid overfitting. A value of 0.2 for dropout is implemented, believed as a good trade off between overfitting and model accuracy.

Hyperparameter tuning is considered to optimize Learning Rate (lr), and number of neurons (numHidNeu). CVPartition function with 0.1 holdout configuration is implemented to define a random partition holding out 10% of data for testing. The parameters to tune are constrained as follows:

$$
\begin{aligned}
&lr \in [0.001, 0.1] \\
&numHidNeu \in [1, 50]
\end{aligned}
\tag{3.12}
$$

The loss function for hyperparameters estimation is root mean square error (RMSE), and Bayesian optimization is exploited to find the global minimum of loss function from Hyperparameter Optimization Package in MatLab. The inputs considered in the sequence input layer are reported in Table 3.6.

Table 3.6 LSTM inputs

	Description	*Unit*	*Category*
Tdb	Dry bulb temperature	[°C]	boundary conditions
GHI	Global Horizontal Irradiance	[W/m^2]	
h	hour of the day	[-]	chronological information
d	day of the week		
flag	holiday/weekend flag		
P (h, d-1)	Load for the same hour of the previous day	[W]	chronological observations
P (h, d-7)	Load for the same hour and day of the previous week		

These inputs are grouped in three main categories: boundary conditions (*Tdb* and *GHI*), chronological information (*h*, *d*, *flag*) and observations (*P(h,d-1)* and *P(h,d-7)*). The choice of utilizing previous measurements of the output is made to consider the occupancy behaviour by considering a daily and weekly periodicity.

3.3 Supervisory and local controller scheme

For the advantages discussed in *2.3.1 Coordination schemes*, the considered control scheme is the distributed-hierarchical. The communication procedure between local controllers and DSO is mitigated by a supervisory controller, as shown in Figure 3.16. The EA Central controller communicates with the DSO and gathers transmitted data from the local controllers. After the supervision of grid's needs, the EA Central controller transmits modification requests to the local controllers for their subsequent implementation.

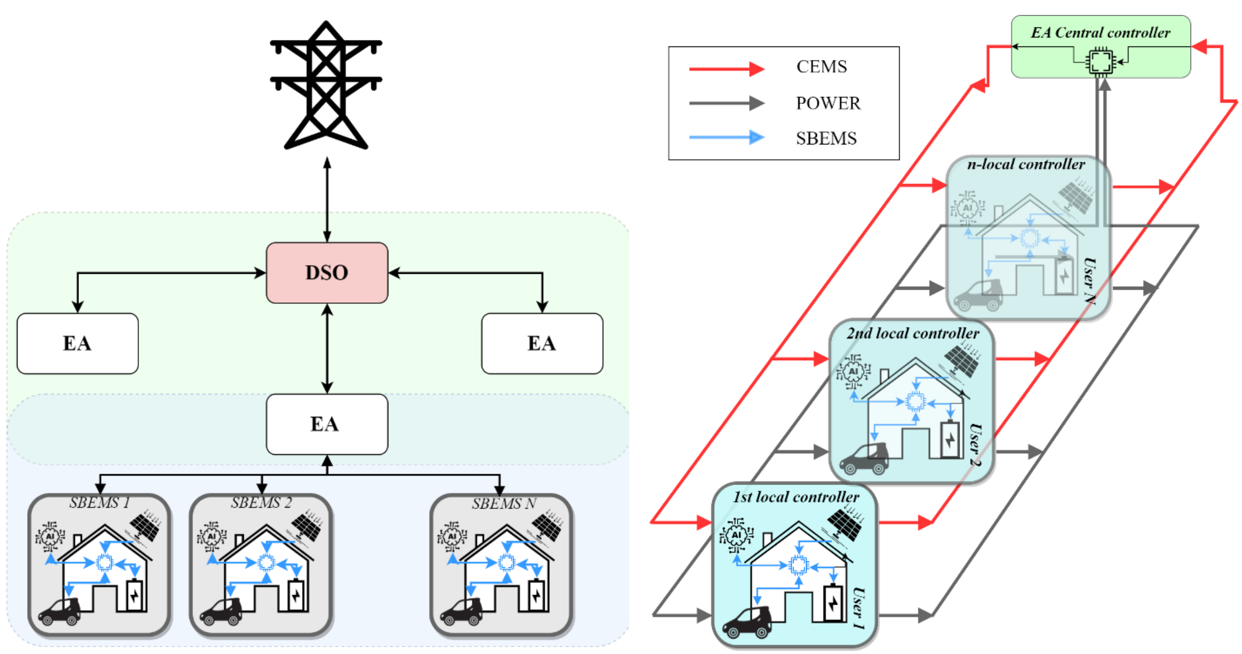

*Figure 3.16.**a** – The schematic of EA for DSO-TSO.**b** – Schematic of local controllers and the supervisory. Hierarchical distributed.*

Figure 3.16.*a* illustrates how EAs act as intermediaries between end users and the DSO. The primary function of the supervisory controller is to convey specific objectives to the local controller, which is referred to as a single-building energy management system (SBEMS). In order

to adhere to the supervisory requirements, the decisions made by the local controller are contingent upon the activation of building energy flexibility, which occurs in four distinct stages, as seen in Figure 2.5. The energy aggregator's bidirectionality is facilitated by information-sharing protocols, represented by the red connectors in Figure 3.16.b

To comprehend the local controller, it is essential to examine the modeling schematic. These schematics measure power flows at key phases to boost the information communicated with the supervisory system and minimize the number of variables involved. When the supervisor communicates power management goals, the local entity attempts to implement the desired changes by activating energy flexibility. The methodology described in this thesis is based on the Control Volume (CV) approach. This approach relies on utilizing five control variables to enhance the performance of DERs, with a primary focus on photovoltaics. The CVs are also utilized to optimize BESS, EV, and the power demand of buildings. P_{DEMAND} is responsible for determining the utilization of thermal load management and electric loads. Subsequently, the EA Central controller merely exchanges the values of P_{NET} and the control variables (*a,b*) in a dynamic manner. The research employs a generalized schematic, which is depicted in Figure 3.17.

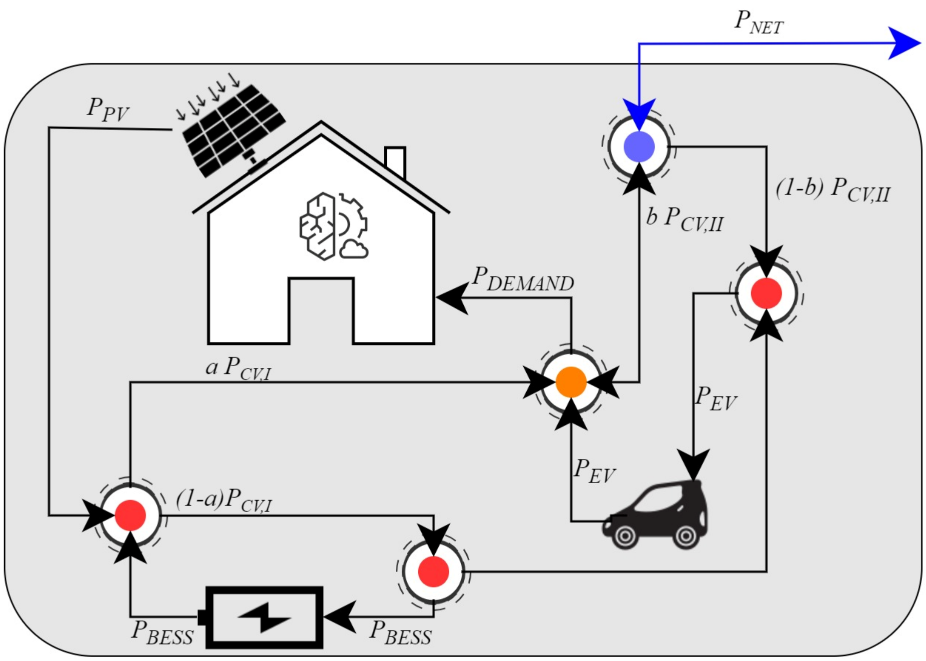

Figure 3.17. The generalized schematic of local controllers based on the control volume approach.

a is a control variable that specifically provides information on the dynamic percentage of electricity supplied by DERs and BESS. The complementary share (1-*a*) represents the portion of renewable energy used specifically for the BESS and/or the electric vehicle. On the other hand, *b* measures the proportion of total power demand from the grid (P_{NET}) that is supplied to the building. The complementary share (1-*b*) represents the electricity consumed for charging the electric vehicle. The subsequent governing equations are employed to simulate local controllers and their modular volumes. Equation (3.13) demonstrates the power equilibrium within the initial control volume.

$$P_{PV} + P_{BESS} = P_{CV,I} \tag{3.13}$$

P_{PV} is a measurable disturbance already known, while P_{BESS} is a control variable as part of the optimization process. After calculating the $P_{CV,I}$ the process then proceeds to the orange control volume.

$$aP_{CV,I} + P_{EV} + bP_{CV,II} = P_{DEMAND} \tag{3.14}$$

In this balance, $aP_{CV,I}$ represents the renewable share, P_{EV} describe the vehicle-to-building (V2B) possibility, and $bP_{CV,II}$ is the target of the minimization problem. Moving forward to the next CV, the method accommodates eventually the bidirectionality: b might be a negative value.

$$P_{NET} = P_{CV,II} \tag{3.15}$$

The last CV measures the different provision to charge EV from a residential station:

$$(1-b)P_{CV,II} + (1-a)P_{CV,I} - P_{BESS} = P_{EV} \tag{3.16}$$

Where, $(1-b)P_{CV,II}$ is the share of electricity from the grid that charges the EV, $(1-a)P_{CV,I} - P_{BESS}$ is the complementary share from the PV and BESS that feeds the EV.

3.4 Conclusions

This chapter detailed a robust, data-driven methodology to model and forecast residential energy demands, addressing critical challenges in efficiency, scalability, and integration. The approach synthesized thermal and electric load modelling, ensemble demand aggregation, and control schemes to optimize energy management in residential and community contexts.

A second-order RC thermal network was employed to capture the thermodynamic properties of buildings, facilitating accurate indoor temperature predictions up to 24 hours ahead. Parameter estimation, validated across low- and high-resolution datasets, confirmed the reliability of this methodology, achieving a maximum RMSE of 0.66 °C. To further streamline system complexity, a Model Order Reduction procedure utilized unsupervised clustering techniques to group thermal zones based on shared characteristics. This approach generated an optimized reduced-order model (6R3C3α), maintaining prediction errors below 0.3 °C.
By standardizing model implementation, this method enabled energy aggregators to efficiently manage diverse building portfolios while leveraging thermal flexibility.

The electric load modelling component analysed detailed sub-metered data to discern daily and hourly consumption trends. Support Vector Machines, particularly with Fine Gaussian kernels, and long short-term memory RNN were employed to enhance the accuracy of baseload predictions. While prediction accuracy varied among households—with CV-RMSE values ranging from 22.1% to 60.2%—the integration of thermal and electric models enabled accurate aggregated demand forecasts. These forecasts effectively bridged communication gaps with grid operators, ensuring more reliable energy distribution.

A distributed-hierarchical control framework was introduced to manage energy flow between local building energy management systems and a supervisory controller. At the heart of this system was the Control Volume approach, which employed dynamic variables to optimize distributed energy resources, such as photovoltaics, battery energy storage systems, and electric vehicles. This modular framework adjusted seamlessly to changing energy demands, enabling efficient bidirectional energy flow. The control schemes prioritized flexibility, scalability, and real-time demand-side management, offering a significant enhancement to grid stability.

The methodology advanced existing energy management strategies by integrating advanced modelling with practical control mechanisms. By leveraging data-driven insights, the approach standardized processes for diverse residential energy systems while accommodating the unique demands of individual households. The combined modelling and control strategies optimized energy efficiency, reduced operational complexity, and improved interaction with grid operators. The MOR and SVM techniques addressed both thermal and electric load forecasting challenges, demonstrating their adaptability to various data resolutions and building configurations.

This integrated methodology sets a new archetype-oriented formulation for residential energy management by addressing scalability, accuracy, and operational efficiency. It provides scalable solutions for virtual energy communities, enhancing energy flexibility and enabling sustainable interactions between end-users and grid operators. The results underscore the feasibility of real-time demand-side management and pave the way for innovations in smart grid technologies and energy strategies. By effectively bridging theoretical modelling with practical applications, this methodology represents a significant step forward in creating sustainable and resilient residential energy systems.

4. The evolution of baseline in demand response

The design of a methodology for optimizing grid interaction of building portfolios aims to determine the expected power demand in the day-ahead market. This expected demand at the aggregator level is influenced by various energy systems, making it essential to understand the impact of high-performing technologies, distributed energy resources, and electric vehicles on both load profile and flexibility potential. Achieving this objective necessitates a data-driven approach, as each new energy system requires a dedicated formulation in the objective function of the considered control routine. The financial benefits of utilizing advanced control routines, such as eMPC, are significant, particularly when evaluating the effects of pricing schemes in demand response programs, and simulation-based scenario investigation.

According to the U.S. DoE through the GEB initiative [260], and the International Energy Agency's Energy in Buildings and Communities program (IEA-EBC) via the final report of Annex 67 [261], there is a pronounced need for detailed methodologies that analyse how the baseline of consumption at the aggregator level is modified. This involves integrating efficiency and flexibility while providing financial results related to the use and scale of high-performing technologies [38]. Such an approach is critical for understanding and leveraging the economic and operational benefits of advanced energy management systems in modern power grids.

In this chapter of the doctoral thesis, two primary studies are included to address these challenges.

First, the effect of high-performing technologies is investigated through a scenario-based approach to quantify the impact of photovoltaic, photovoltaic-thermal systems, and heat pumps on the flexibility potential of building portfolios. By simulating different scenarios, this study aims to elucidate how these technologies can alter the load profile and enhance the overall flexibility of the grid.

Second, the focus shifts to the effect of residential charging infrastructure for electric vehicles. This part of the study examines how private transportation infrastructure impacts the electrical grid, particularly measuring how residential electric vehicle charging, including different infrastructures, mono and bidirectional charging, modifies the baseline power consumption and introduces additional stress at the feeder level.

By exploring these two focal areas, the chapter aims to provide a comprehensive methodology for optimizing the grid interaction of building portfolios, addressing both technological impacts and financial outcomes. This holistic approach will contribute to the development of more resilient, efficient, and economically viable energy systems.

4.1 Evolution of load profile from high-performing technologies

In the residential sector, the main strategies to improve energy efficiency concern retrofitting of building envelopes, the use of high-performing HVAC [262, 263], and solar-based DERs [264]. The effect of these implementations can be appreciated with a drastic reduction in the net provision of primary energy for heating, cooling, and electric needs [265].

Heat pumps (HP) have been widely adopted to reduce operating costs and prevent switching to alternative energy sources in lieu of electricity. The possibility of utilizing a single system for both heating and cooling [266] has resulted in the widespread adoption of this technology within both commercial and residential domains [267]. In addition, technological development has spurred the significant implementation of solar-assisted HPs. This concept involves the utilization of both solar collectors and photovoltaics to improve the energy efficiency and financial viability of the system [268, 269].

Many research works focused on identifying the most convenient system layout for heating provision [270, 271]. Gautam et al. [272] showed that for solar-assisted HPs, photovoltaic-thermal (PVT) systems are more effective than traditional PVs. The idea of combining PV and solar collectors started during the 1970s with the main objective of increasing PV efficiency [273]. One of the most attractive applications of air- or water-based PVT collectors is building-integrated photovoltaic thermal (BIPVT) [274, 275].

BIPVT systems consist of a PV module, an absorber in the form of tubes, a glass cover, and an insulated container [276]. Yu et al. [277] proposed a combination of BIPVT and a centralized heat pump for a façade application, focusing on the different classifications based on the design and coupling of such systems, while Shao et al. [278] conducted an experiment focused on the temperature distribution of a ventilated roof PVT system coupled with a heat pump. They concluded that the system was efficient for residential applications due to its ability to improve stability in indoor thermal environments and reduce energy consumption during summer and winter configurations.

The versatility of the use of BIPVT assisted ASHPs was deepened by You et al. [279]. The authors classified these integrations into direct heating, temperature increase, thermal storage, and multiple energy sources. Yang et al. [280] focused on the potential and constraints of the use of BIPVT systems integrated with ASHPs. However, they concluded that the integration needs to be studied to use the produced thermal energy more efficiently.

On the other side, Demand-side management and DR programs incentivize customers to modify their power demand during critical periods, providing energy flexibility to the grid [78]. The DOE of the United States categorizes DRP into price-based and incentive-based programs [281].

Price-based programs are proposed by the utilities, which offer participants time-varying rates that reflect the value and cost of electricity over a given period. The most deployed pricing structures are ToU, CPP, and RTP. The choice of the tariff depends on the local utility, and rates are developed to reflect the technical needs of the considered infrastructure.

Incentive-based programs consist of rebates or discounts for customers participating in a DR event. These programs rely on the definition of a baseline of consumption to quantify load reductions.

The core concept of demand-side management consists of exploiting customers to solve the mismatch between supply and demand. According to the existing literature, building energy flexibility (BEF) is thought to be the most powerful solution to overcome technical issues in the energy network [78]. <u>Energy Flexibility</u> of a building is defined as the ability to manage its demand and generation according to local climate conditions, user needs, and energy network requirements [132].

The growing interest in BEF is motivating researchers to propose alternative management strategies to modify power demand. Among the advanced building control techniques, MPC has been proven to be effective in real-time applications of DR [282].

MPC frameworks designed for individual buildings are commonly found in the available literature, with the primary objective of minimizing economic costs. Most methodologies are founded on either co-simulation environments or data-driven applications for the estimation of building models [283]. Amato et al. [284] conceived an Energy Plus-MPC formulation for a single-family house located in Denmark, while Lee et al. [285] recurred to TRNSYS for the simulation of a similar case study in the Republic of Korea.

Other applications are conceived from data-driven methodologies such as the ANN-MPC for a residential building test case [286], and large facilities [287], the inverse grey box applied over a large dataset in Ontario [288], or continuous-time stochastic model for a detached house in Denmark [289].

Based on the problem formulation, the resolution can be applied on single, multi-building, and community applications [261].

At the multi-building level, energy aggregators are designed to address the on-site management of energy flows [290], by guaranteeing grid stabilization services to network operators [39], as well as reducing the cost of transmission and distribution systems. Building-to-building coordination allows a larger share of zero-carbon technologies [291], identifying energy aggregators as a valid solution towards a sustainable energy transition [292].

Since the early stages of energy aggregators for the coordination of building portfolios, many different investigations are conducted to optimize control architecture for flexibility. A 30-household community in UK was simulated by an emulation software to assess the effects of centralized and decentralized applications of MPC [196], while Hosamo et al.[293] compared 11 machine learning algorithms fed with a simulated-generated dataset produced as a result of the BIM framework.

Regarding the operation of energy aggregators, the main concerns consist of minimizing uncertainty and limiting economic expenditure. The first problem addresses demand-side [294, 295], and supply-side [296] strategies to comply with inaccurate predictions of power demand and forecasting errors of DERs [297]. The latter optimizes the operation by considering coordination of grid-connected high-renewable buildings [298], stand-alone communities [299], or creating trading pricing models for energy exchange [300, 301].

The effectiveness of control strategies for load management is not limited to the residential sector. Many research works have focused on the definition of energy flexibility for industrial [302], commercial [303], and office case studies, like Aelenei et al. [204] which investigated the energy flexibility potential in an office building with a BIPV roof system in Lisbon, or Zhou et al. [205] which proposed a machine-learning approach for a high rise office in Hong Kong.

As a demonstration of the literature review that was carried out, advanced control is effective and robust, but it is facing many challenges in a multi-building framework, such as the lack of high-resolution measured dataset, the complexity of describing building-grid interactions, and the management of RESs. Therefore, it is essential to overcome these limitations by considering control-oriented approaches for the design and operation of energy aggregators.

There is evidence in support of the effectiveness of considering operation conditions for optimal design aims in multi-building systems, especially when deployed into DR programs.

Saloux et al. [304] proposed a reduced-order grey-box approach to evaluate the effect of storage sizing and rate control of thermal storages for an existing solar district heating system in the Drake Landing Solar Community, Canada.

A parametric analysis for HPs and hot water tanks was investigated over three different electricity tariffs and a predictive control routine by Lyden et al. [305]. The authors used a generic community electrical demand profile synthesized in HOMER and monitored data of thermal need from the West Whitlawburn Housing Co-operative in the UK.

A scenario-based approach for the design stage was proposed by Noorollahi et al. [306], where a stochastic investigation is solved by a genetic algorithm for a multi-carrier energy hub in Iran. The purpose was to investigate the impacts of cooling and heating components like HP, absorption chillers, and thermal storages on optimal operation and energy costs.

Maturo et al. [307] analyzed the impact of operational variables on the design and operation of a solar-assisted HVAC system in Montreal, Canada. The authors considered the impacts of design on the economic expenditure of a home in a static ToU DR program.

As communicated by DOE through the GEBs initiative [260], and the International Energy Agency-Energy in Buildings and Communities program (IEA- EBC) via the final report of Annex67 [261], there is a need for detailed methodologies that analyse how the baseline of consumption at the aggregator level is modified, integrating efficiency and flexibility, and providing financial results related to the use and size of high-performing technologies [308].

To address these research challenges, this section proposes a data-driven method to predict the energy efficiency and flexibility potential of a portfolio of residential buildings within an energy aggregator. A scenario investigation is presented for different configurations of technologies, sizing, and control routines to assess the optimal configuration for the operation and the design of an energy aggregator. Energy and economic results are produced for a constant and critical peak pricing tariff structure to identify the energy efficiency and flexibility nexus, and to enhance the economic feasibility of the aggregator's business models. The algorithm is implemented in an integrated MPC framework purposefully developed in MatLab, and the proof of concept is conducted through a case study analysis.

4.1.1 Method

The method consists of *a)* data-driven RC thermal network for the buildings presented in Figure 3.1, *b)* heat pump and electric baseboard models for the heating sources; *c)* BIPV and BIPVT models for the distributed energy resources, and MPC framework for the load management during DR events. The schematic is presented in Figure 4.1

Specifically, the complete layout is presented in Figure 4.2 to describe the interaction of BIPVT with ASHP. The presented layout includes the option of reducing the heating load of households with the instantaneous heat production from BIPVT. This action is controlled by the Temperature Control I (TCI), which allows for direct heating when the preheated air reaches comfort level for occupants (shown in red). Conversely, when the preheated air is not warm enough for direct heating, integration is provided by an ASHP. The temperature Control II (TCII) guides the mixing of outdoor air (OA) and preheated air for the evaporator of the ASHP. The higher temperature at the evaporator improves the overall efficiency of the ASHP, resulting in energy savings. The definition of the heating load for each of the households is determined by an MPC framework via the formulation of control actions. It is assumed that each household follows these signals slavishly, and that no exergy degradation or heat losses occur in the air channels from the outlet section of BIPVT to the evaporator of the heat pump.

The overall energy consumption and the peak power demand are investigated for a DR event over a representative period of three days. Two design variables are investigated to identify the optimal configuration for the connected virtual community: the aggregated installed PV capacity and the overall size of the ASHP.

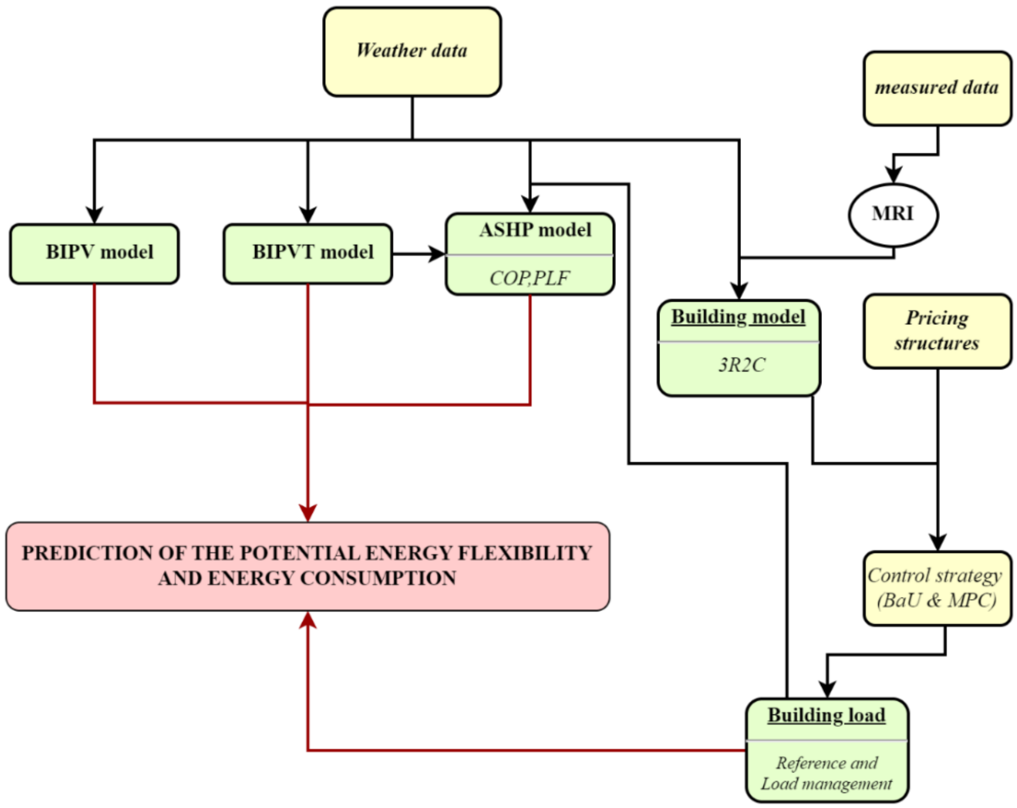

Figure 4.1- Schematic and flow chart of the methodology

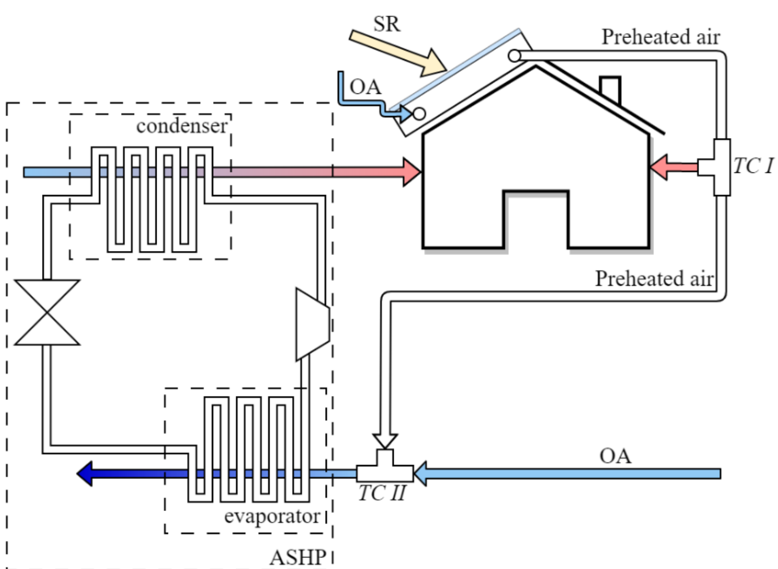

Figure 4.2- The schematic of the BIPVT-ASHP interaction with temperature control.

The model of each of the key components is developed from the mathematical equations presented in this section. The objective is to predict the energy consumption, power demand, and potential savings for the day ahead. This procedure determines the energy flexibility of the virtual communities in preparation for the upcoming DR event.

BIPV/T model

Considering that the integration of BIPV/T for direct heating and as preheating stage of combined systems results effective in cold climate application [309], a one-dimensional model for BIPV/T on roof [310] is used to calculate the electricity production, the heat recovered, and the temperature at the outlet section. The steady state RC network for BIPV/T is shown in Figure 4.3.

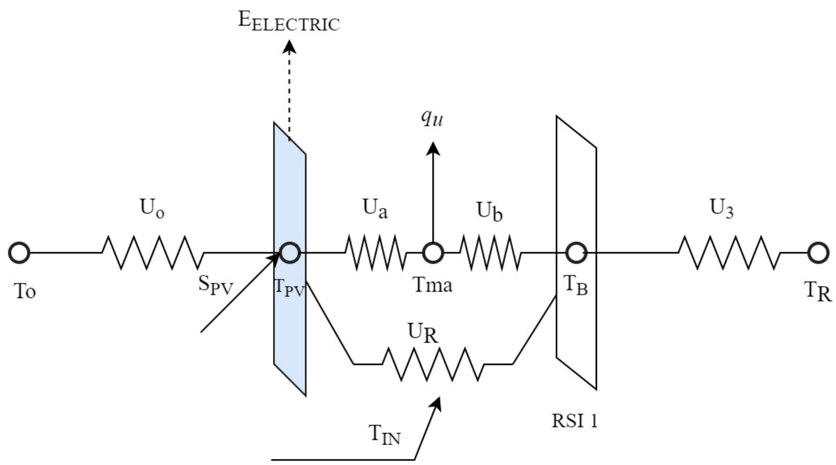

Figure 4.3 -Steady state RC network for BIPV/T

where, T_O is the ambient temperature, T_{PV} is the temperature of the PV layer, Tma is the flawing air mean temperature, T_B is the temperature of the back layer, T_{IN} is the air temperature at the inlet section, and T_R is the attic temperature. It is assumed to be 10°C higher than the external temperature T_0. The transmittance U_3 considers a 1 RSI insulation and a convective conductance for a non climatized attic. The standard efficiency of the electric production is provided by manufacturers as:

$$\eta_{STD} = \frac{P_{PEAK}}{1000W} \tag{4.1}$$

To consider the effect of temperature over the solar production, an effective efficiency is evaluated as:

$$\eta_{EFF} = \eta_{STD} - 0.0004(T_{PV} - 25degC) \tag{4.2}$$

The absorbed solar radiation and the electric production can be calculated as:

$$S_{TOTAL} = \alpha_W A * G \tag{4.3}$$

$$E_{ELECTRIC} = \eta_{EFF} * A_{PV} * G \tag{4.4}$$

Thus, the solar radiation converted into heat can be considered as the difference between the total radiation and the electric production:

$$S_{PV} = S_{TOTAL} - E_{ELECTRIC} \tag{4.5}$$

For the air flow rate, the geometrical properties are considered from the literature, with a thickness of L=0.05m, and a total height (H) of 3m. The width of channel (W)is considered as variable for the sizing process.

Moreover, a PV panel is considered with a peak production of 215W/m^2 and an initial efficiency of 21.6% [311]. The air speed (V) is considered 1 m/s and the air flow rate in channel (M) is evaluated as:

$$M = VLW \tag{4.6}$$

Considering the mentioned geometrical features for the cavity, the convective coefficient in cavity can be evaluated as function of the hydraulic diameter, so defined:

$$Dh = \frac{4(H \cdot W)}{2(H+W)} \tag{4.7}$$

The convective coefficient in cavity (h) is function of the Nusselt number, that is evaluated from the evaluation of Reynolds, Prandtl and Graetz numbers.

$$\mathrm{Re} = \frac{\rho V Dh}{\mu} \tag{4.8}$$

$$\mathrm{Pr} = 0.7 \tag{4.9}$$

$$\mathrm{Gz} = \mathrm{Re} \cdot \mathrm{Pr} \cdot \frac{Dh}{H} \tag{4.10}$$

$$Nu = 3.657 + \frac{0.0668 Gz^{\frac{1}{3}}}{0.04 + Gz^{\frac{-2}{3}}} \tag{4.11}$$

Finally, the coefficient results:

$$h = \frac{Nu \cdot k_{AIR}}{Dh} \tag{4.12}$$

Considering an external film coefficient h_o*=12W/m²degC,* and a radiative coefficient h_R *=6 W/m²degC*:

$$\begin{cases} U_R = A \cdot h_R \\ U_O = h_O A \\ U_a = hA \\ U_b = hA \end{cases} \tag{4.13}$$

Since the steady-state approach, the resolution is conducted through iteration. The temperature of PV and the back are assumed and then replaced. This process is performed in *MatLab* and the average convergence is reach in the first 5 iterations within ±0.5°C.

$$T_{PV} = \frac{U_O T_O + U_a T_{ma} + U_R T_B + S_{TOTAL} - E_{ELECTRIC}}{U_O + U_a + U_R} \tag{4.14}$$

$$T_B = \frac{U_R T_{PV} + U_b T_{ma} + U_3 T_R}{U_3 + U_b + U_R} \tag{4.15}$$

Where the mean flowing air temperature in the air channel is evaluated as:

$$T_i = \frac{T_{PV} + T_B}{2} + \left[T_O - \frac{(T_{PV} + T_B)}{2} \right] e^{\frac{-X_i \cdot 2}{a}} \tag{4.16}$$

For the modelling of the BIPV system, the cavity is not considered, and the previous equations have been modified accordingly to estimate the T_{PV} and the effective efficiency of production.

Air Source Heat Pump model

Space heating and cooling represent a large quota of the overall energy consumption, and the benefit of using electrical compression heat pumps has been widely documented for both residential buildings [307], industrial sites [312], and commercial buildings [313], because of the higher coefficient of performance.

With the spread of electrification these systems have been used to enhance the energy flexibility of the residential sector by avoiding the provision of natural gas. For solar assisted applications in buildings, it is possible to reduce the energy consumption by around 20% by using preheating from renewable sources [314],[315]. For these reasons, many governments are recommending the widespread use of HPs to enhance the energy efficiency of the building sector, which accounts for around a third of the overall energy consumption. Moreover, since their fast response in control, these systems are effective in demand response programs, especially with predictive supervision [316].

To underscore the direct benefit resulting from the implementation of BIPV/T coupled with an air-source heat pump (ASHP), no additional storage technologies are considered apart from the thermal storage of the building itself. For solar assisted ASHP, the coefficient of performance (COP) depends significantly on the evaporator temperature. For that reason, the main benefit of the combination of an ASHP with a BIPV/T system is to provide air warmer than the outdoor ($T_{OUTLET} > T_O$) [317].

$$COP_{T,STD} = 0.065 T_O + 2.625 \tag{4.17}$$

$$COP_{T,EFF} = 0.065 T_{OUTLET} + 2.625 \tag{4.18}$$

The selected cold-climate ASHP presents a cut-off temperature of -25°C. The heated air, especially during the winter period, guarantees a higher COP, so $COP_{T,EFF} > COP_{STD}$ that is translated into a lower power demand for the ASHP and an increased number of hours of operation, being able to exceed the cut off temperature value. For large applications or to evaluate an averaged COP of the HPs within a building portfolio of an energy aggregator, the COP is also dependent on the part load factor (PLF), considered a function of the capacity ratio (CR) [318]:

$$COP_{FINAL} = COP_{T,EFF} \cdot PLF(f(CR)) \tag{4.19}$$

This curve is provided by manufacturers, and it is considered an input for the proposed methods. For this reason, the identification of the optimized size for each of the households is essential to guaranteeing the highest possible COP and avoiding the oversizing of such technologies for both energy and economic reasons. Moreover, because of the scalability of these systems, a constant return to scale is considered, so it is possible to consider all the units within the virtual community aggregated without any reduction in the overall effective COP (Eq. 4.19).

4.1.2 The optimization problem

Due to the nature of the application, the optimization problem is multi-objective. In fact, the optimal heating output must minimize the economic cost over the prediction horizon and, in the meantime, guarantee thermal comfort throughout the operation [120]. Thus, because of the existence of conflicting objectives, this class of optimization problems fails to find a single solution [128]. To work around this issue, the proposed approach consists of combining many individual objective functions into a single formulation to guarantee convergence [129]. The identified solution must be considered as the best trade off among all the possible objectives [130].

The considered building model is presented in Figure 3.1, where the indoor air temperature (T_{IN}) is chosen as state function, and the heating power of baseboard heaters (Q_{BH}) and heat pumps (Q_{HP}) are selected as control variables. Specifically, according to the selected size of the heat pump, the upper bound is updated accordingly. The cost function for this optimization problem is:

$$obj = \sum_{j=1:NumHouse} \left[w_{1,j} \cdot c_{u,EN} \left(\frac{Q_{HP,j}}{COP_{HP}} + Q_{BH,j} \cdot \eta_{BH,j} \right) + w_{2,j} \cdot \left(T_{SET,j} - T_{IN,j} \right) \right] \tag{4.20}$$

Where $w_{1,j}$ and $w_{2,j}$ are the weights of the problem for the j-th household, $c_{u,EN}$ is the price of electricity, COP_{HP} and η_{BH} are the dynamic coefficients of performance of HP and the energy efficiency of BH, and T_{SET} is the preferred set point temperature. This value depends on the activation of the DR event to recognize the preheating/recovery/business as usual configuration.

Hydro Québec - the main utility of Québec [319]- offers time-of-use tariff called *Rate Flex D*, where the price is lower than the static tariff -*Rate D*-but presents up to 100 hours a year "peak hours" with a corresponding disadvantaging tariff. These events are defined as DR and happen in predefined during the high peak demand periods: 6 a.m. -9a.m. and 4 p.m.-8 p.m. The tariffs are presented in Table 4.1.

Table 4.1 - Electricity pricing tariffs (Rate D and Rate Flex D). Update 10/2023

	< 40 kWh/day	> 40kWh/day	peak hours
Rate D [¢/kWh]	6.509	10.041	*na*
Rate Flex D [¢/kWh]	4.582	7.880	53.526

Impact on the grid

To provide a comprehensive analysis, the methodology has been designed to describe different configurations. A reference scenario is used for comparison purposes, representing the actual configuration of the building portfolio. Scenario 1 has the reference heating system, with the addition of PVs. This configuration is interesting to simulate the net power load from the community, and the infamous duck curve. Scenario 2 considers solar-assisted ASHP in addition to baseboard heating (BH) systems, to describe the enhancement of energy efficiency via the heating systems. Scenario 3 presents the ASHP and the BH, as in Scenario 2, for integration with the BIPV/T. This scenario is used to quantify the benefit of the preheating or direct space heating obtained by BIPV/T. Scenario 4 presents the same layout as Scenario 3 but is characterized by the implementation of load management. In fact, the MPC is compared to BaU to define the effectiveness of the optimized load management for different sizes of renewables.

The configurations are summarized in Table 4.2. Moreover, to assess the individual benefit of each of the technologies analyzed, a parametric analysis has been performed for each scenario.

Table 4.2. Description of the case study scenaria

	Heating system	Renewable source	Control routine
Reference Scenario	(BH)		BaU
Scenario 1	(BH)	(BIPV)	BaU
Scenario 2	(ASHP) + (BH)		BaU
Scenario 3	(ASHP) + (BH)	(BIPVT)	BaU
Scenario 4	(ASHP) + (BH)	(BIPVT)	MPC

Note that, as described by metadata, the considered houses - and so the *Reference Scenario* - are equipped with BH systems with an efficiency equal to 1.

In Scenario 1, the algorithm considers the implementation of BIPV on the roof from a minimum installed capacity of 3kW_P to a maximum extension of 12 kW_P for each household. The resulting net power demand is affected during the sun hours, as shown in Figure 4.4.

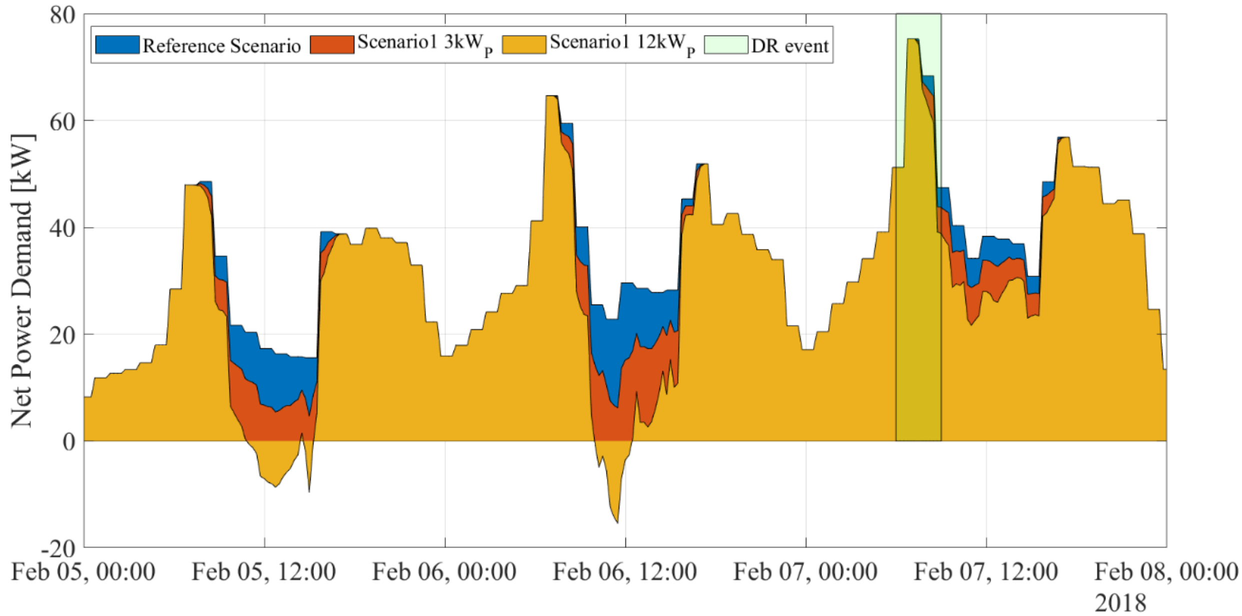

Figure 4.4- Scenario 1. Energy performance for the minimum and maximum sizing.

The baseline is affected by renewable production. However, the maximum number of PVs would determine bidirectionality when the solar radiation is higher, increasing the complexity of the management of the grid. In the case of DR (green area), the reduction is negligible. This result highlights the need to design flexibility tools for DR events, instead of minimizing the overall aggregated monthly or annual performance. In this case, even though the total energy consumption is reduced, the peak power demand during DR remains the same compared to the reference. Moreover, the steep ramps determined by the fluctuation of solar technologies would generate dangerous voltage fluctuations during sunny days, as on February 5th and 6th at 8:00 a.m. and 4:00 p.m. These are responsible for local power outages and severe voltage fluctuations. The energy and economic results are shown in Table 4.3 and Table 4.4.

In Scenario 2, the space heating is provided by BH and ASHP. The parametric analysis over the size of ASHP aims at evaluating the different levels of integration and the relative energy and economic savings. Therefore, by relying on an overall higher COP, the power demand and aggregated energy consumption would decrease significantly. However, considering the extreme low ambient temperatures, the heating from the ASHP is produced with low efficiency. Results for this Scenario are presented by varying the size of the ASHP from 15kW (51k BTU) to 60kW (205k BTU).

In Figure 4.5 the power consumption from ASHP and the integration from BH are presented compared to the reference scenario (blue line) on the left side for each of the ASHP sizes considered in the parametric analysis, while the heating provisions and the effective COP are presented on the right side.

Despite the significant reduction in total energy consumption and a higher overall energy efficiency, the performance during the DR almost coincides with the reference. Specifically, the external temperature is around the cut-off temperature, and the ASHP is not beneficial during the DR event. The corresponding COP varies for each configuration since the PLF affects the performance significantly. The energy and economic results are shown in Table 4.3 and Table 4.4.

Moreover, the lack of a predictive control routine does not make possible the individuation of the preheating stage for flexibility purposes.

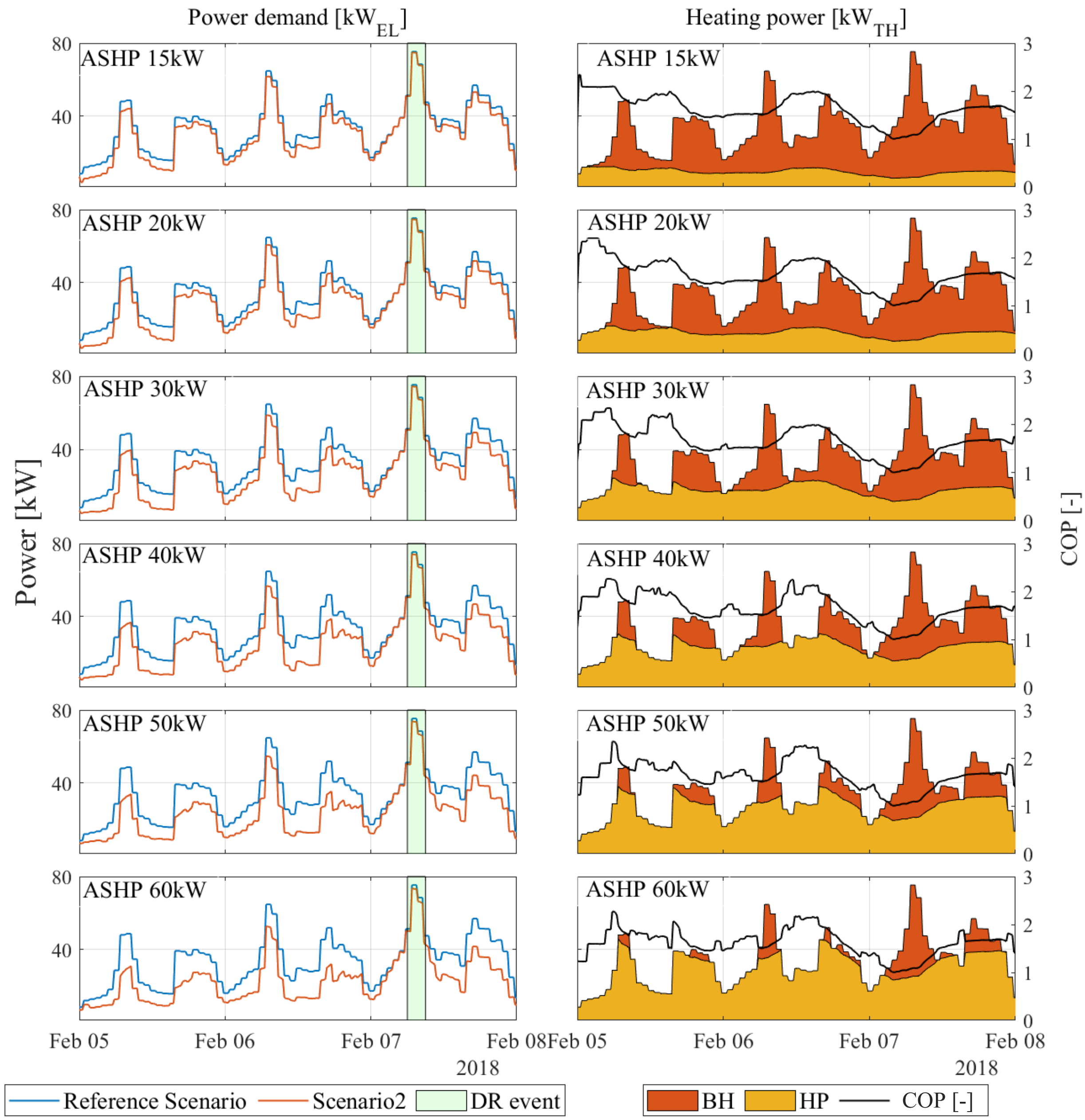

Figure 4.5- Scenario 2. Power demand and heating power divided by ASHP capacity.

To assess the benefit of a preheating stage, Scenario 3 presents the simultaneous application of BIPVT and ASHP with the configuration presented in Figure 4.2. By varying the size of the ASHP and the installed capacity of BIPVT for each of the households, 78 different combinations are presented in the Table of Figure 4.6. As an example, the maximum configuration (60kW ASHP and 12kWp for each roof) is presented in the lower part of Figure 4.6 to identify the maximum possible reduction at the energy aggregator level.

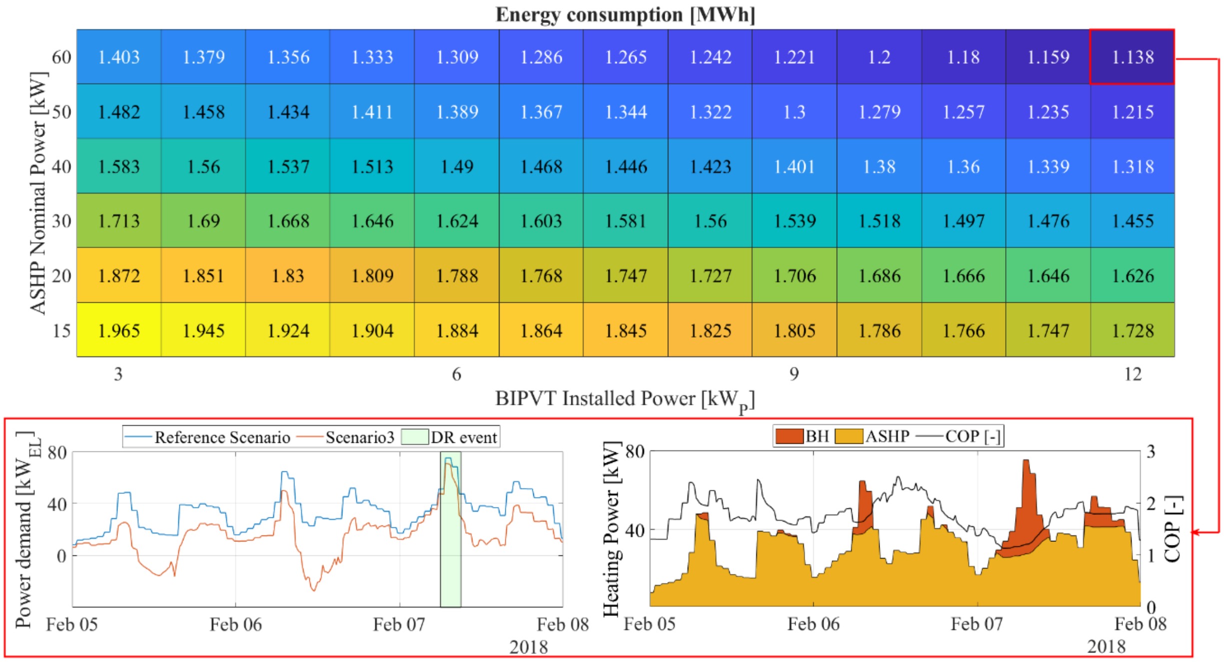

Figure 4.6-Scenario 3. Energy performance of the 78 possible configurations with ASHP total capacity from 15 to 60 kW, and individual BIPVT Installed Power from 3 to 12 kW$_P$; Modification of Power demand and heating provision for the 60kW ASHP and 12kW$_P$ BIPVT configuration.

The size of the ASHP affects the results more than the BIPVT. In fact, while the reduction from 3kWp to 12kWp is around 0.25 MWh, the equivalent reduction from ASHP 15kW to 60kW is almost 0.6MWh. Moreover, for an ASHP smaller than 40kW the reduction is not satisfactory, regardless of the installed capacity of BIPVTs.

Table 4.3 - Energy performance of the three scenarios.

		Energy Consumption		DR PPD*	
		[MWh]	%	[kW]	%
Reference		2.44	-	75.29	-
Scenario1	3kWp	2.26	92.6	75.29	-
	12kWp	2.03	83.2	75.29	-
Scenario2	ASHP 15kW	2.18	89.3	74.87	99.4
	ASHP 20kW	2.10	86.1	74.73	99.2
	ASHP 30kW	1.95	80.3	74.45	98.9
	ASHP 40kW	1.83	75.4	74.17	98.5
	ASHP 50kW	1.73	71.7	73.88	98.1
	ASHP 60kW	1.66	69.3	73.60	97.7
Scenario3	ASHP60kW & 12kWp	1.14	46.7	71.12	94.4

**DR PPD is the peak power demand during a DR event*

The present methodology assesses the modification of power demand and the heating provision at the design stage for any possible configuration. The optimal configuration is affected by the pricing tariffs, location, and incentive initiatives and therefore relies on the financial availability at the time of the initial investment.

Table 4.4 - Expenditure for the three scenarios in the two pricing structures.

		Rate D		Rate Flex D	
		[$]	%	[$]	%
	Reference	154	-	206	-
Scenario1	3kWp	143	92.6	196	95.2
	12kWp	129	83.2	184	89.3
Scenario2	ASHP 15kW	138	89.3	193	93.7
	ASHP 20kW	133	86.1	190	92.2
	ASHP 30kW	124	80.3	183	88.8
	ASHP 40kW	117	75.4	177	85.9
	ASHP 50kW	111	71.7	172	83.5
	ASHP 60kW	107	69.3	168	81.5
Scenario3	ASHP60kW & 12kWp	72	46.7	135	65.5

The implementation of BIPVs is presented in Scenario1. The total reduction in energy consumption is from 7.4% for the 3kWp configuration to 16.8% in the 12kWp. Thus, without a BESS, or the possibility to store the electricity surplus in an electric vehicle, this Scenario seems not to be effective and convenient. Moreover, because of the definition of these pricing structures, the DR events happen far from the peak sun hours, making it not beneficial for BIPVs. This result is also underscored by the reduction in economic expenditure for the Rate Flex D, where a saving of 10.7% is evaluated instead of 16.8% in the Rate D.

To evaluate the potential of ASHP, the Scenario2 varies the size from 15kW to 60kW. The reduction in the energy consumption is between 10.7% to 30.7%. The energy efficiency is improved substantially, but the power demand during the DR event is comparable to the reference, with a reduction of 2.3%. The economic savings for this scenario reflect an improved energy efficiency, with 30.7% in Rate D and 18.5% in Rate Flex D.

In the Scenario3, a higher performance is achieved for the combination of BIPVT and ASHP. A maximum energy reduction of 53.3% is evaluated, with economic savings for 53.3% and 34.5% in Rate D and Rate Flex D respectively. However, the overall reduction in power demand during a DR event is 5.6%. Considering the investment in the purchase of these technologies, these configurations are not cost effective, especially in a DR structure.

Scenario4 is presented as an evolution of Scenario3 for the control routine deployed. Here, the BaU is substituted by the MPC framework.

The performance in terms of BEFI [320] is presented for each household in Figure 4.7 with a period of analysis (*dt*) of 15 minutes to appreciate the energy flexibility from one timestep to the next.

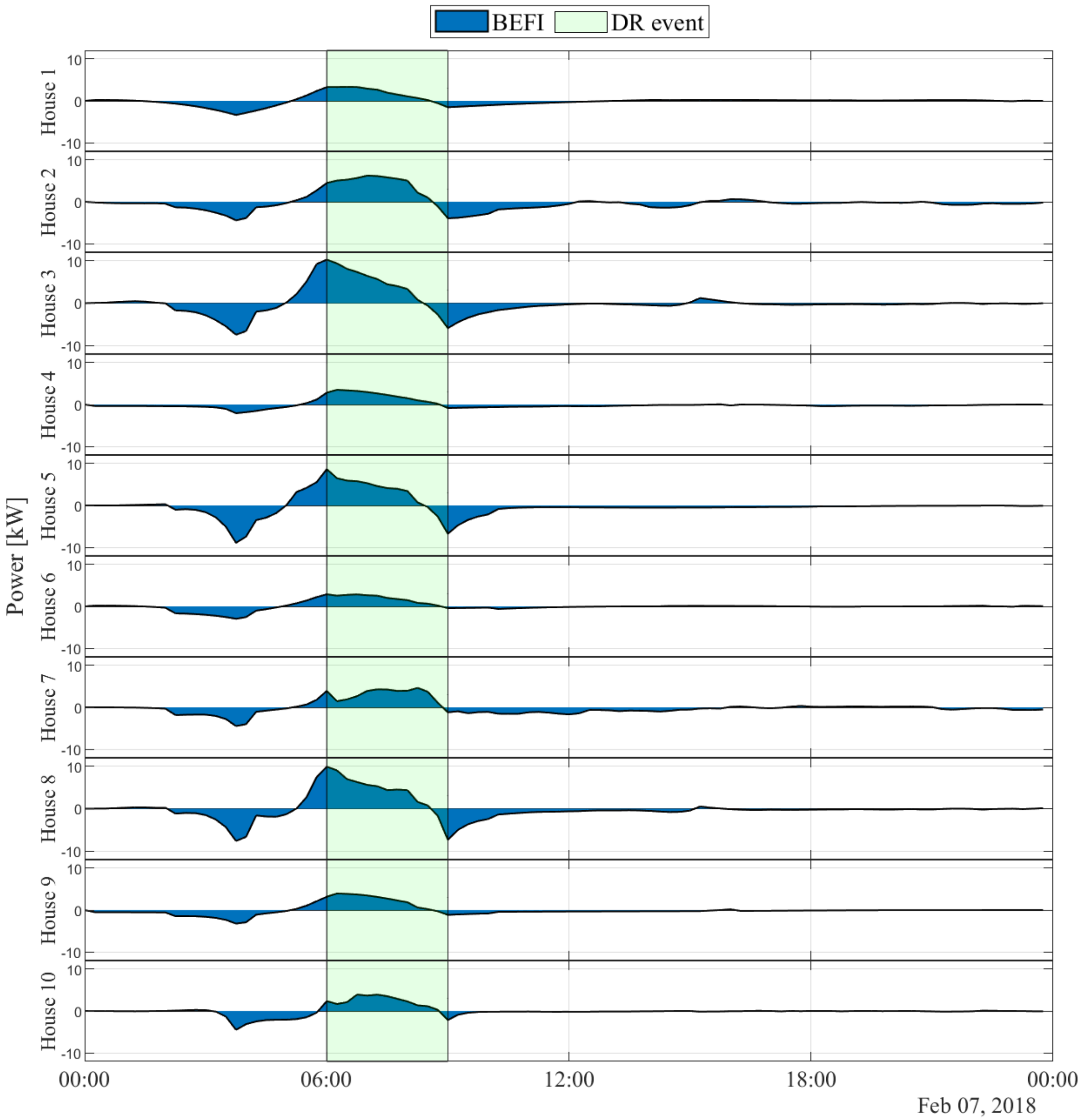

Figure 4.7 -Scenario4, Building Energy Flexibility Index (15min) for each household.

The load reductions for the considered households are affected by the thermodynamics of each building. In particular, House 2,3,5,8 present higher performance compared to House 1,4,6,7,9,10. The plus of the selected metric for flexibility quantification is that the time of analysis (dt) can vary from instantaneous to overall-averaged variation. For the selected DR program, the events have a known duration of 3 hours, and therefore

Figure 4.8.*a* presents the BEFI(3h). This is essential to characterize, by a single metric, the performance of a household during the event. On the other hand, the ability of the energy

aggregator to coordinate the virtual community for a DR event is presented via the CBEFI (15min) in Figure 4.8.*b*.

The choice of a different duration *dt* is determined by the different communication processes. In fact, while the communication with the DSO is useful to predict the modification of the power demand at the aggregator level as the CBEFI (15min), the characterization of a longer *dt* gives better insight about the individual contribution of each household during an entire event (BEFI 3h).

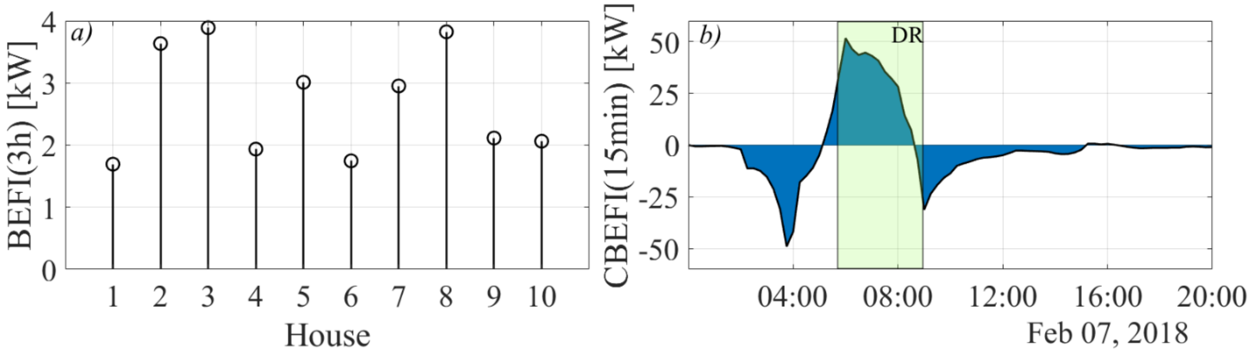

Figure 4.8-Scenario 4: a) BEFI(3h) for the individual household and b) CBEFI (15min) for the grid operator

The overall energy consumption might increase as a result of the predictive control routine [321]. To allay this concern, the variation in energy consumption between Scenario3 and Scenario4 resulted to be negligible (0.48%).

As for the previous scenario, to study the highest penetration of renewable production and its effect on the power demand and heating provision, the 60kW ASHP and 12kWp for roof configuration are presented as a result of the MPC framework in Figure 4.9

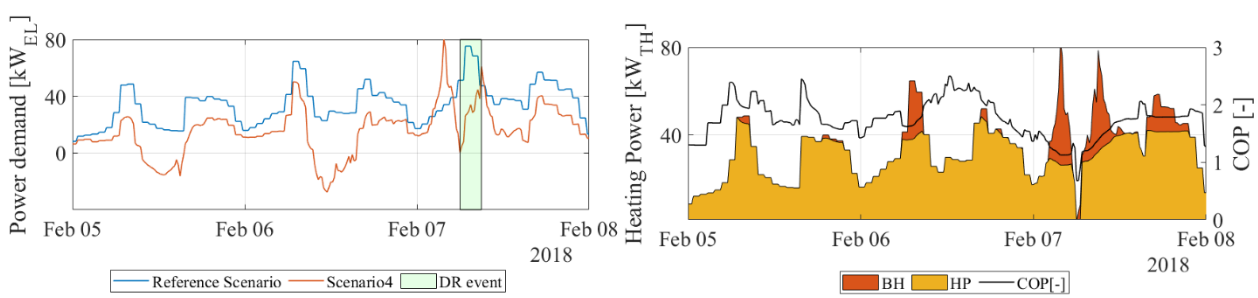

Figure 4.9- Scenario 4. Modification of Power demand and heating provision for the 60kW ASHP and 12kW$_P$ BIPVT configuration with MPC.

Because of the contemporary implementation of high-performing technologies and a load management strategy, the power demand trend in Scenario 4 registers higher variation and two separate peaks. The first peak is due to a variation in the set point temperatures of the house. In fact, the predictive control is aware of a DR event and preheats the space to lower the demand during the event. This period is called the "preheating" stage, and the intensity and length of this period depend on physical aspects such as the thermal capacitance of the building and the level of insulation in the building envelope. Usually, the more inertial, the longer the preheating stage.

Conversely, the second peak in power demand happens at the conclusion of the DR event. The tariff structure influences the magnitude of this peak. In this situation, the controller tries to recover from the event, resulting in the compensation of the thermal imbalance. For this reason, this period is often called the “recovery” stage [322].

The economic results for the static and CPP pricing structures are presented in Table .

Table 4.5 - Economic expenditure of the two pricing structures for Scenario4

			Rate D		Rate Flex D	
			[$]	%	[$]	%
Reference			154	-	206	-
Scenario 4	3kWp	ASHP 15kW	124	81	140	**68**
		ASHP 40kW	101	66	121	**59**
		ASHP 60kW	89	58	111	**54**
	6kWp	ASHP 15kW	119	78	135	**66**
		ASHP 40kW	95	62	116	**57**
		ASHP 60kW	83	54	106	**52**
	9kWp	ASHP 15kW	114	75	131	**64**
		ASHP 40kW	89	58	110	**54**
		ASHP 60kW	77	50	100	**49**
	12kWp	ASHP 15kW	110	72	126	**62**
		ASHP 40kW	83	54	106	**52**
		ASHP 60kW	72	47	95	**47**

The analysis of these two different tariff structures suggests the advantage of implementing Rate Flex D. In fact, regardless of the configuration of the technologies exploited, the percentage economic saving is higher for Rate Flex D in the case of load management.

The absolute values can be interpreted in Figure 4.10, where a swift tool for the assessment of the daily average expense is shown for each of the 78 configurations; the figure outcomes can be considered as general results of the proposed methodology that – as clearly reported in Section 1 – aims at assessing the individual contribution of a household to the overall energy flexibility of an energy aggregator. The figures suggest that the structure of the DR program and the building models determine the convenience of the CPP pricing structure over the static throughout the investigation. In particular, the percentage savings reach a maximum of 17% in the initial configuration of 15kW ASHP and 3kW$_P$ BIPVT, and a minimum of 7.5% in the final configuration of 60kW ASHP and 12kW$_P$ BIPVT. Compared to the Reference Scenario, the daily average expense has been reduced between 20-to-51% in Rate D and between 29-to-56% in Rate Flex D.

The results enable a rapid comprehension of the potential economic savings for households and the energy flexibility potential associated with each configuration.

The comparison with the static tariff gives insight into load management. In fact, with a flat tariff, the MPC follows the the set-point profile blindly. Specifically, the optimal solution is not affected by price fluctuations during the prediction horizon. Therefore, the behaviour of Rate D identifies the benefit of the energy efficiency initiative. Conversely, Rate Flex D identifies the additional benefit provided by load management.

The potential savings resulting from the chosen configuration can be evaluated, along with its impact on the overall energy flexibility of the virtual community. These results are consistent with the energy efficiency-flexibility nexus, where the occurrence of one phenomenon decreases the impact of the other.

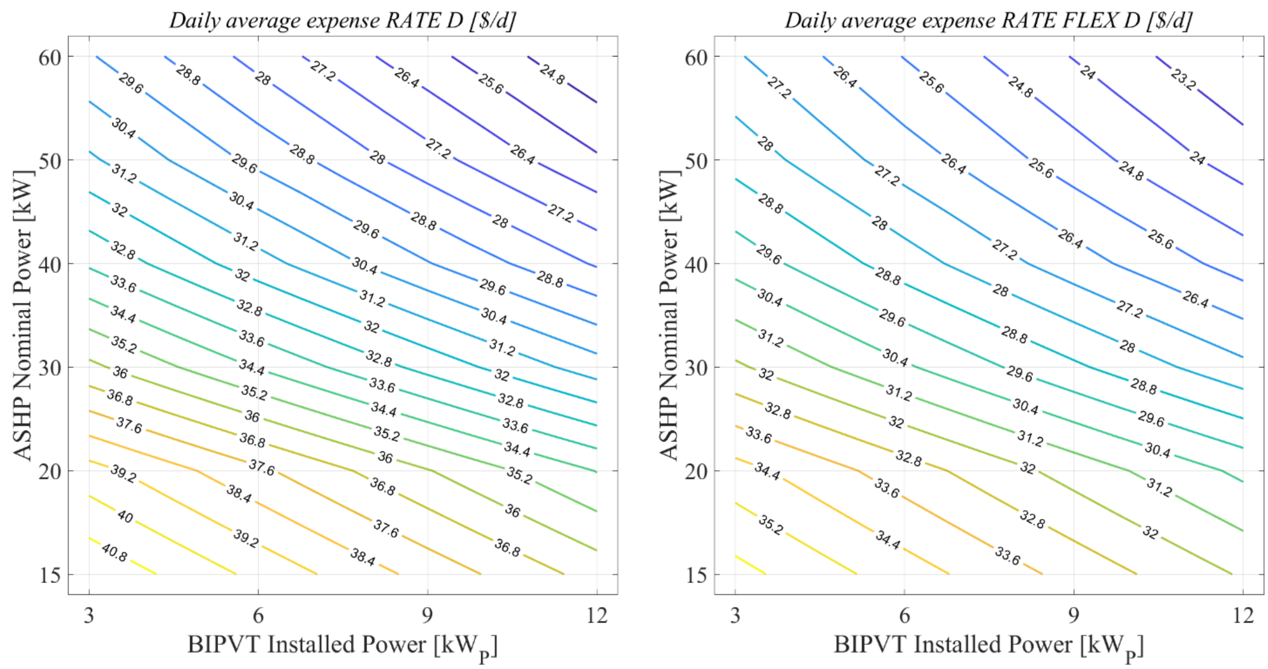

Figure 4.10- Daily average expense [$/day] of every configuration for Rate D and RateFlex D during the winter period.

The figures suggest that the structure of the DR program and the building models determine the convenience of the CPP pricing structure (*Rate Flex D*) over the static one throughout the investigation. In particular, the percentage savings reach a maximum of 17% in the initial configuration of 15kW ASHP and 3kWP BIPVT, and a minimum of 7.5% in the final configuration of 60kW ASHP and 12kWP BIPVT. Compared to the Reference Scenario, the daily average expense has been reduced between 20-to-51% in Rate D and between 29-to-56% in Rate Flex D. The results enable a rapid comprehension of the potential economic savings for households and the energy flexibility potential associated with each configuration.

4.2 Integrating electric vehicle charging and thermal load management

The solutions for in-home charging may differ among several specifications standardized by the Society of Automotive Engineers and by the International Electrotechnical Commission [323]. The main options for residential stations mainly include monodirectional (V1X) – divided into Level 1 and Level 2 - and bidirectional (V2X) charging [324]. Level 1 charging uses a standard 110-120V outlet and provides a slow charging rate. This option is suitable for low-mileage drivers and overnight charging strategies. Level 2 charging, on the other hand, requires a dedicated 240V outlet, offering a significantly faster charging rate, and potentially lead to grid stability issues. While Level 2 charging is becoming increasingly popular due to its efficiency, it does require professional installation and often some upgrades to a home's electrical capacity [325]. V2X offers an innovative solution to enhance flexibility in home energy management. In a bidirectional setup, EVs can act as energy sources for the home- Vehicle-to-Home (V2H)- or the grid -Vehicle-to-Grid (V2G), with the same features of Level 2 infrastructure [326].

There are numerous advantages for both utilities and end-users when successfully incorporating EV charging infrastructure into residential infrastructure [327]. In fact, EVs are effective in both primary and ancillary services [328]. In V1X architectures with load shifting strategies, EVs can alleviate peak load pressures[329, 330], whereas in V2X EVs can actively participate in voltage and frequency regulation, supporting grid reliability [260]. Moreover, by facilitating energy storage and backup capabilities, EVs transform into resilient power sources during grid outages [331], ensuring continuous energy supply to critical systems within homes [332], and facilitate the incorporation of renewable energy at the residential level [333, 334].

One key challenge in the effective application of residential EV charging infrastructure lies in developing a data-driven methodology that accurately predicts both energy consumption and charging demand [335]. Numerous studies have investigated the primary factors influencing EV demand prediction, highlighting key dependencies such as the charging infrastructure, the timing and location of charging events, and driving scenarios [336-338]. To address these complexities, various modeling techniques have been employed, including ensemble machine learning algorithms [339], stochastic methods [340], XGBoost tree regression [341], and cluster-based long short-term memory recurrent neural networks [342] .

The relevance of the available literature extends beyond the model architecture which ranges from statistical methods to advanced deep learning techniques; it also demonstrate strong predictive capabilities using low-dimensional data from real EV stations [343]. This adaptability to simpler data inputs enhances their practical application for the integration of EV management within HEMSs [344].

Integrated load management of electric vehicles and residential buildings

Distribution networks differ significantly in power capacity and ability to support EVs; while some networks can accommodate increased loads with minimal impact, others face more significant limitations [345-347]. To address these challenges, supervisory coordination schemes offer a promising solution by improving load management and fostering BEF [348]. Integrating EVs with residential loads under a DSM framework extends the concept of coordinated charging, enabling a more adaptive and responsive approach to managing energy demand in residential areas.

Coordinated charging, also known as smart or managed charging, involves taking strategic actions within DSM programs to optimize the charging process [349]. These strategies are typically categorized as either active or passive. Active coordination, such as DLM, allows for direct control of EV charging, while passive methods leverage time-based pricing structures to influence charging behavior indirectly [338].

- *Active coordination*: Many studies highlight the potential of active coordination for enhancing load management and economic efficiency. Afentoulis et al. [350] introduced the Electric vehicle aggregator business model, managing EV charging across residential, workplace, and public infrastructures. They found that smart charging strategies reduced operational costs by 10-15%. Barone et al. [351] explored V2X integration within a virtual microgrid, demonstrating that DLM could reduce energy provision by 11.4% and an economic saving of 8.1%. Huang et al. [352] examined a setup integrating EVs with three interconnected buildings, concluding that DLM could reduce daily electricity costs by 36% for the cluster. Zhou et al. [353] presented an investigation to optimize the provision of electricity to buildings and EV stations. The authors introduced a gaussian probability density function for EV arrival times at the charging stations and state of charge (SOC) of EV.
- *Passive coordination*: The adoption of EV charging stations also impacts power tariff structures [354]. In fact, integrating EVs can result in the development of dynamic pricing models, encouraging people to charge their vehicles during times of low demand and promoting efficient energy use [355]. Hernandez Cedillo et al. [356] presented a dynamic pricing scheme to define electricity tariffs for both V1X and V2X in a solar assisted residential application. They concluded that the highest contribution is given by direct current fast charging, level 2 and level 1 respectively. Unlike active coordination, the cost effectiveness of EVs with time-varying tariffs is quite related to the charging infrastructure. Therefore, these investigations are usually applied on broader populations of EVs and buildings. Szinai et al. [357] analysed the impact of EVs on the market and utility revenue in California. The authors concluded that plug-in EVs might save $120-690 million in grid operating costs annually (up to 10% of total costs) and reduce renewable energy curtailment up to 40% relative to unmanaged fleet. The use of passive methods seems to be preferred by utilities, and some pilot project like the Ultra Low Overnight scheme in Ontario, Canada, has been proposed to motivate EVs' residential owners to limit charging specific hours of the night with an extremely low-price tier [358].

The integration of EVs within buildings plays a crucial role in DSM, offering significant potential for optimizing energy usage. Mesaric et al. [359] developed an optimization routine to examine the coordination of home energy management with EV charging in a DSM context. The authors concluded that, given the timescale and power intensity of typical household and EV energy demands, integrating EVs into home energy systems can be achieved with minimal effort and substantial economic benefits, making it an attractive option for residential DSM applications. Mirakhorli et al. [360] investigated through a behavior-driven price-based MPC the effect of ToU, hourly and real time pricing on the energy performance of a 342-node residential distribution network with 15,000 buildings. The authors highlighted real time pricing outperforming other time-dependent pricing structures, with 42% overall saving. In addition to the benefits already discussed, Van Kriekinge et al. [361] analyzed the impact of EV integration on aggregated peak demand using CPP. They investigated charging schedules based on MPC for cost minimization and peak shaving. The study found that V2X charging was effective in reducing morning peaks but noted that all scenarios resulted in higher overall peaks.

4.2.1 Method

Developing the load profile model is crucial for generating and conveying accurate power forecasts. This study proposes an ensemble configuration as shown in Figure 4.11. There are three main components: a grey-box thermal model to represent building thermal dynamics, a SVM model to estimate the electric baseload, and a Monte Carlo simulation for the EV behavior. This configuration is conceived to accommodate a variable number of homes, supporting the need for scalability [132].

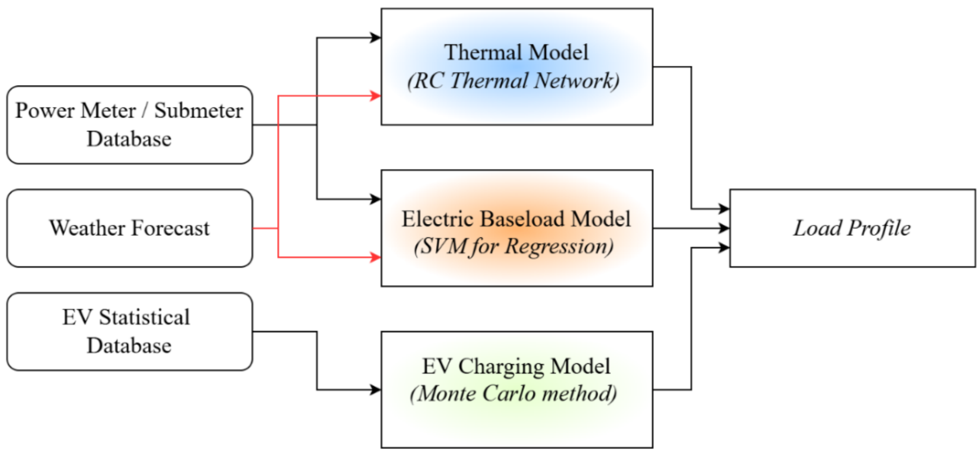

Figure 4.11- Methodology schematic for load profiling of residential buildings.

The primary technical requirements for Buildings, EVs, and DSM are shown as follows:

<u>Buildings</u>*:* Building thermal models necessitate data acquisition from interconnected thermostats and power meters. It is necessary to have at least one measurement of air temperature, coupled with the corresponding heating output. The availability of OAT and incident solar radiation is necessary as measured disturbances. The models of the complementary power demand—defined as *Electric baseloads*—necessitate the collection of power demand data from power meters and submeters. Geographical information about the home, and the energy substation is also required.

<u>EVs</u>*:* EV modelling relies on factors such as the driving conditions and the battery's capacity, as well as historical measures. The EV battery's initial condition is determined by the arrival and departure periods, which significantly impact load management.

<u>Demand-Side Management</u>*:* The grid-interaction, and its optimization routine, necessitate a time-varying demand response program.

Electric vehicles and charging infrastructure

The Electric Vehicle Supply Equipment (EVSE) pilot project by AVISTA launched in 2016 has been used throughout the manuscript to define solid working assumptions. The main objectives of this program were to understand *i)* the light-duty EV load profiles, grid impacts, costs, and benefits, *ii)* how the utility may better serve all customers in the electrification of transportation, and *iii)* begin to support early EV adoption in its service territories. The results were published in October 2019 with a comprehensive overview of EVSE intent and activities, detailed findings about the charging and discharging of EV fleet in North America, and to lay the groundwork for future programs [362].

The average EV capacity of the fleet is considered as a direct representation of the sales statistics by manufacturers and model published by AVISTA in USA, whereas the average daily consumption is estimated around 11.6 kWh and the daily distance travelled 55.05 km, with 70% – 8.08kWh – of electricity from residential charging stations. The characteristics of the two levels of charging, Level 1 and Level 2, represent a site location of North America with charging power up to 1.4 kW and 7.2 kW respectively [363].

EV modeling requires estimating the arrival times of vehicles at residential charging stations. An additional key assumption, based on findings from the AVISTA pilot project, is that the considered EV fleet follows the aggregate distribution of arrival times shown in Figure 4.12.

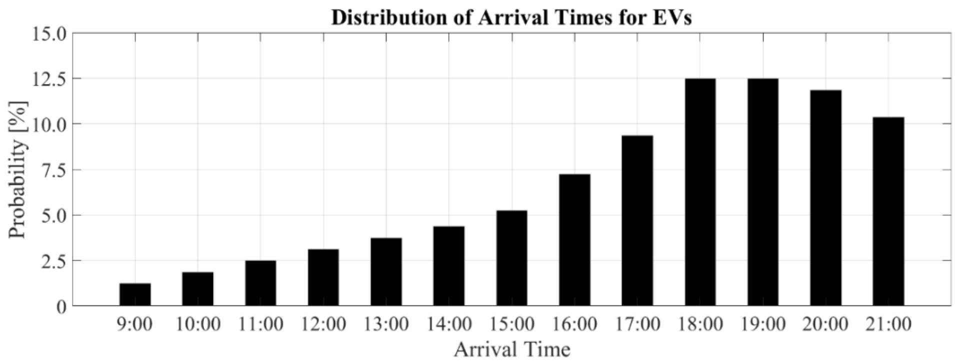

Figure 4.12- Distribution of arrival time of EVs to residential charging stations [364].

Electric baseload model

The remaining power demand from the households describes domestic hot water, kitchen, lighting, and main appliances measurements. The sub-metering system gathers power readings and aggregates them as equal to the electric baseload (other than space heating). However, it is assumed that no energy flexibility is provided by these systems. Thus, this dataset is used via a recursive SVM regression model, showing good results in predicting power demand in the multi timestep ahead framework [248-250].

Hyperparameter identification is then performed to ensure the highest accuracy in 24 hours ahead prediction. For this purpose the kernel function is investigated, reported to be one of the most important parameters in SVM design, helping mapping the original features into a higher-dimensional space [365]. Six different options are considered: i) *Standard Linear Kernel*, ii) *Quadratic polynomial Kernel*, iii) *Cubic polynomial Kernel*, iv) *Fine Gaussian Kernel*, v) *Medium Gaussian Kernel*, vi) *Coarse Gaussian Kernel.* SVM models are then trained by five predictors, consisting in previous measurement from power meter [x_{t-1}], GHI, and OAT. The last two inputs are chronological, consisting of *Day of The Week*, and *Hour of The Day*.

Electric vehicles model

To model and predict EV energy behavior, traditional approaches typically rely on reactive controls, where deterministic conditions—such as the EV's SOC—trigger charging decisions [366]. In this paper, this methodology is advanced by incorporating EVs into an MPC framework. This approach leverages the SOC as the primary decision-making trigger within a predictive, rather than purely reactive, model, allowing for more proactive and optimized load management. An explicit formulation to calculate the SOC can be considered, as shown in Eq. (4.21).

$$SOC_t = SOC_{t-1} \cdot (1-\omega_e) + \frac{\left[P_{in,t}\eta_{Ch} - \dfrac{P_{out,t}}{\eta_{Disch}} \right] \cdot \dfrac{h}{Dt}}{CAP_{EV}} \quad (4.21)$$

where, ω_e [-] is the energy loss rate for a single step variation, η_{Ch} [-] is the charging efficiency, and η_{Disch} [-] is the discharge efficiency. P_{in} [W] is the charging power while P_{out} [W] is the discharging power. The ratio h/Dt is used to standardize measurement on hourly basis considering that the timestep of the current investigation is 15 minutes, and finally CAP_{EV} [Wh] represents the energy capacity of the considered battery. With this formulation, it is possible to describe any charging level and configuration, as V1X and V2X.

The integrated load management of residential buildings and electric private transportation is based on the recognition of periods where EVs are connected or not. This stochasticity cannot be described by deterministic approaches [340, 353]. For this reason, a Monte Carlo numerical estimation method is performed to obtain numerical results, by generating synthetic data using probability sampling [367]. This procedure creates generated data that closely mirrors the distribution of the real data, that in this application consists of the probability distribution of arrival time of EVs. The current investigation opted for a multinomial distribution with random sampling for each one of the 10 customers. At the building level, it is assumed every possible arrival time between 8:00 and 22:00, but as soon as the methodology scales from single to building cluster, the combination of arrival time can be defined as probabilistic problem following AVISTA outcomes [368]. A total of 16,200 combinations are analysed.

Model accuracy

Model selection is performed for each individual submodel, therefore different metrics are considered. Building thermal models rely on RMSE, FIT [369], shown in Table 2.3.

The performance of SVM models for electric baseloads, as well as the resulting load profile model use the coefficient of variation of the RMSE (CVRMSE) defined in Table 2.3.

4.2.2 Control and Optimization

The design of an eMPC in multi-objective optimization frameworks guarantees the identification of optimal strategies through the utilization of carefully selected weights, soft constraints, and penalties [120]. The first part of this section presents the main optimization routine, whereas the second describes the Individual Stress Level.

Economic Model Predictive Control formulation

The objective function is structured to optimize energy management by balancing three primary terms. First, the space heating term ensures acceptable deviations from the set-point temperature. Second, the EV term focuses on optimizing the charging schedule for EVs and incorporates penalties for deviations from desired charging behaviours. Third, the coordination term addresses the synchronization of thermal and EV loads, aiming to minimize conflicts between these demands and ensure overall grid stability.

The minimization problem is performed in a MATLAB environment using the Solver-based Nonlinear Optimization section of the Optimization Toolbox [370]. The detailed formulation of this function within the MPC framework is presented in Eq. (4.22), the power balance is presented in Eq. (4.23), and constraints and penalties are presented in Eq. (4.24).

$$L = \left[c_{en} \cdot \sum_{i=1}^{n} P_{H\,i} + c_{\Delta T} \cdot \sum_{i=1}^{n} DT_i \right] + \left[c_{en} \cdot \sum_{i=1}^{n} PL_{EV\,i} + \beta_{EV_i} \right] + \\ + \left[c_{dc} \sum_{i=1}^{n} (1 + ISL_i) \cdot (P_{LP,i} - NC_i) \right] \tag{4.22}$$

with

$$P_{LP,i} = P_{H\,i} + PL_{EV\,i} + P_{EB,i}$$

so that (4.23)

$$P_{grid} = c_{en} \cdot \sum_{i=1}^{n} P_{LP,i} \cdot \frac{dt}{60}$$

subject to

$$\begin{cases} 0 < P_{H\,i} < \mathrm{hC} \\ lb < PL_{EV\,i} < \mathrm{ub} \\ \mathrm{SP}\ \text{-}\ \rho < DT < \mathrm{SP} + \rho \\ \mathrm{DD} < SOC_{EV} < \mathrm{DC} \\ n_{Pf} < \varepsilon \\ SOC_{EV} \rightarrow SOC_{EV,SP} \end{cases} \tag{4.24}$$

where, c_{en} [$/kWh] is the electricity cost, $c_{\Delta T}$ [$/°Ch] is the equivalent cost of 1°C temperature deviation for one hour, and c_{dc} [$/kW] is the demand charges [371]. DT [°C] is the temperature deviation from reference temperature, and the total demand—defined in this study as load profile P_{LP} [kW] —is considered as sum of power demand for space heating P_H, EV charging PL_{EV}, and the electric baseload P_{EB}. The aggregated demand for the portfolio is defined as P_{GRID} [kW], and NC [kW] is the aggregated normal capacity.

The constraint for P_H limits positive values within the heating capacity (hC). EV charging is constrained between the lower bound (lb) and upper bound (ub), and the considered charging infrastructure for EV, such as Level1/Level2 and V1X/V2X, defines these parameters. Additional penalties are required to ensure safe charging events. Deep discharges (DD) and deep charges (DC) are considered to work within limited ranges of the overall EV capacity to reduce deep charge/discharge cycles, and to limit the control to the section where the applied voltage and the residual capacity of EVs are linear [372]. n_{Pf} is a penalty considered to limit frequent power variations based on the total harmonic distortion levels—ε is a threshold values [373]—and lastly $SOC_{EV,\,SP}$ is a condition to ensure complete charging cycles overnight.

Some assumptions are considered in this work: EVs do not leave charging infrastructure before 8 a.m., and during peak events $c_{\Delta T}$ is considered as 2.5 $/°Ch [374]. The considered electricity tariff is a CPP equal to the one offered by Hydro Québec Rate Flex D, c_{dc} is considered as Hydro Quebec Rate G, that penalise power demand exceeding NC by $20.522/kW. DD and DC are considered between 20% and 95% of capacity, and n_{Pf} lower than 2.5%. ε is considered as 8% for the current harmonic distortion.

Individual Stress Level

To evaluate the impact of load management strategies on the overall stress of a distribution network, this study introduces the Individual Stress Level (ISL), a novel metric that quantifies the contribution of a single agent to the collective stress within a cluster/portfolio. The ISL builds upon existing metrics used to assess distribution feeder performance, including the PTV, which measures daily demand fluctuations, the LF, which evaluates the utilization efficiency of generation assets, and SysR, which quantifies the absolute changes in power demand over time [109]. Additionally, the severity term $\alpha_{1.5}$, introduced by Muratori [110], is incorporated to capture the percentage of time the $P_{LP,i}$ exceeds 150% of its average demand.

The ISL is designed to measure the impact of the i-th agent (e.g., a household) on the overall stress of the grid. It is defined as:

$$ISL_i = \alpha_i \cdot \left(\frac{LF_{grid-i} - LF_{grid}}{LF_{grid}} \right)$$

$$\text{with} \qquad (4.25)$$

$$LF = \frac{\overline{P}}{\max(P)} \qquad \begin{cases} LF_{grid} \rightarrow & P = P_{grid} \\ LF_{grid\text{-}i} \rightarrow & P = P_{grid} - P_{LP,i} \end{cases}$$

Where LF_{grid} represents the portfolio-wide LF, $LF_{grid\text{-}i}$ represents the LF of the portfolio when the i-th agent's load is excluded, calculated by subtracting the i-th agent's power demand $P_{LP,i}$ from P_{grid}.

ISL measures the relative change in the LF caused by removing the i-th agent, amplified by its temporal demand peaks. Higher values of ISL suggest that the agent contributes significantly to instability or inefficiency in the grid. Lower values of ISL (or negative) suggest that the agent contributes flattening the overall demand, and therefore a lower (or negative) demand charge is applied.

4.2.3 Load profile prediction

The prediction of load profile is calculated as superposition of thermal, electric baseload and EV models, as shown in Figure 3.13. Ensuring the accuracy of each individual model is a critical prerequisite for the implementation of eMPC.

To evaluate the accuracy of the 3R2C thermal models used for 24-hour ahead predictions (96 timesteps for the current application), the RMSE and the FIT metrics are used. The performance of the thermal models was assessed over a 7-day training period and a 2-day testing period, with results summarized in Table 4.6.

Table 4.6. Performance metrics for thermal models.

Training		Testing	
RMSE [°C]	FIT [%]	RMSE [°C]	FIT [%]

House1	0.45	75.9	0.52	72.1
House2	0.48	84.7	0.58	81.6
House3	0.55	85.5	0.65	82.9
House4	0.70	81.2	0.77	79.3
House5	0.26	79.9	0.35	73.0
House6	0.57	82.9	0.62	81.4
House7	0.23	79.9	0.28	75.6
House8	0.24	85.0	0.33	79.4
House9	0.72	73.0	0.73	72.6
House10	0.68	82.1	0.70	81.7

The results in Table show consistent performance of the thermal models across the ten houses, with RMSE between 0.23°C to 0.72°C during training and 0.28°C to 0.77°C during testing. Similarly, the FIT ranges from 73.0% to 85.5% during training and from 72.1% to 82.9% during testing, indicating relatively small deviation from the observed temperatures and satisfactory accuracy for 24 hours ahead predictions [159]. Houses with lower RMSE values (e.g., House 7 and House 8) suggest better metrics, possibly due to more stable thermal dynamics or higher-quality input data. On the other hand, houses with higher RMSE values (e.g., House 9) might reflect greater variability in occupant behaviour or less reliable measurements.

Impact of EV charging infrastructure

The aggregated load profile reveals significant differences between the reference profile and the two simulated scenarios with Level 1 and Level 2 charging infrastructures. The analysis is based on 600 subpopulations generated through a Monte Carlo approach. KPIs for these scenarios are summarized in Table 4.7, with the corresponding profiles illustrated in Figure 4.13.

Table 4.7. Performance metrics for Reference case.

		Reference Profile	*Level1$_{MONO}$*	*Level2$_{MONO}$*
Total daily energy consumption	[MWh]	1.19 ±0.02	1.38 ±0.02 (+16.0%)	1.39 ±0.3 (+16.8%)
Energy consumption EVs	[kWh]	-	148.8 ±0.2	151.4 ±0.5
Energy cost Space Heating	[$/day]	81	81	81
Energy cost EV	[$/day]	-	10	10
Average demand	[kW]	49.0 ±0.01	57.6 ±0.9 (+17.6%)	58.1 ±0.2 (+18.6%)
NC *	[kW]	65.3 ±0.2	77.9 ±1.1 (+19.3%)	77.9 ±1.3 (+19.3%)
Maximum demand	[kW]	106.5 ±0.1	113.2 ±2.2 (+6.3%)	125.3 ±0.8 (+17.7%)
Maximum demand Period	[HH:mm]	08:00	06:30	17:30
LF	[%]	46.3	50.8	46.3

PTV	[-]	8.94	9.42	11.31
SysR	[MW]	40.5	42.5	50.8
$\alpha_{150\%}$ [#]	[h]	5.25	9.17	9.45

* NC [kW] as the 67th percentile of power demand historical distribution.

[#] Considered for the 150% of NC in Reference conditions.

The analysis of the aggregated load profiles highlights distinct differences between the reference scenario and the two simulated scenarios involving Level 1 and Level 2 charging infrastructures. Both charging scenarios result in a 16–17% increase in total daily energy consumption compared to the baseline profile, primarily due to the aggregated energy requirements for EV charging, which account for approximately 150 kWh/day.

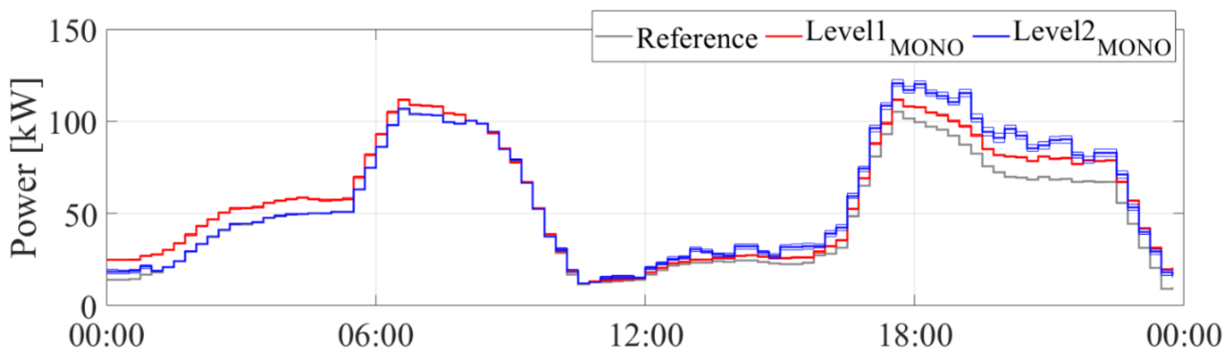

Figure 4.13. Load profile of EA in reference scenario of Space heating and EVs

The similarity in energy consumption between Level 1 and Level 2 scenarios suggests that the faster charging capabilities of Level 2 infrastructure do not significantly alter overall energy requirements. However, average demand rises by roughly 18% across both scenarios, while maximum demand increases by 6.3% and 17.7% for Level 1 and Level 2 charging, respectively. Another important result is that the peak period shifts from morning (06:30) to evening hours (17:30) as the infrastructure evolves from Level1 to Level 2, reflecting differences in how charging infrastructures interact with existing consumption patterns.

The challenges of this integration are highlighted by the grid-related KPIs, revealing improvements of the LF to 50.8% in Level1, indicating better grid utilization, whereas Level 2 charging maintains the LF at the baseline value of 46.3%. Fluctuations in demand are discussed in terms of PTV and *SysR*, showing the highest variability in Level 2 charging configuration. The nearly double increase in $\alpha_{150\%}$ informs about the additional strain on grid infrastructure, and the need for a capacity increase of 19.3% to compensate for the additional EV charging demand.

Load management in Demand Response

The presence of time-dependent tariffs motivates customers to provide BEF during high peak periods. In DSM, predictive optimizations identify strategies to minimize the economic expenditure. Assuming that no flexibility can be provided by the Electric baseload, the two controlled systems are space heating, and EV charging. The control actions are communicated to the corresponding actuator as set point temperatures to thermostats, and as power of charge

/discharge to the battery management system. The quantification of the performance in DSM is presented as BEFI [95] defined as follows:

$$\overline{BEFI}(t, Dt) = \frac{\sum_{t}^{t+Dt} P_{ref} \cdot dt - \sum_{t}^{t+Dt} P_{Flex} \cdot dt}{Dt} \tag{4.26}$$

where, Dt [h] is the duration of the flexibility event, P_{ref} [kW] is the power demand in the reference scenario, and P_{Flex} [kW] is the power demand unlocking BEF. The formulation of this metric at the aggregated level is considered as superposition and measured as CBEFI [375].

The load profiles and the corresponding confidence intervals in DSM are therefore presented, alongside with the CBEFI in Figure 4.14. These profiles underscore the differences in the overall flexibility from Monodirectional Level1, Monodirectional Level2, and Bidirectional Level2 charging infrastructure.

eMPC effectively manages to shift the demand from peak hours to non-peak hours in all configurations, with an average demand reduction between 74-140% for morning events, and 54-98% for evening events compared to the reference. The preheating effect is most pronounced in the monodirectional Level2 configuration, followed by the bidirectional Level2, while the Monodirectional Level1 exhibits milder values. During the first DR event, which is shown by the yellow highlight, the eMPC proved to be successful in improving flexibility in all three configurations. In the case of monodirectionality, the building's thermal mass is responsible for supplying the BEF. However, in the bidirectional arrangement, EVs are also discharging through V2H, adding extra flexibility.

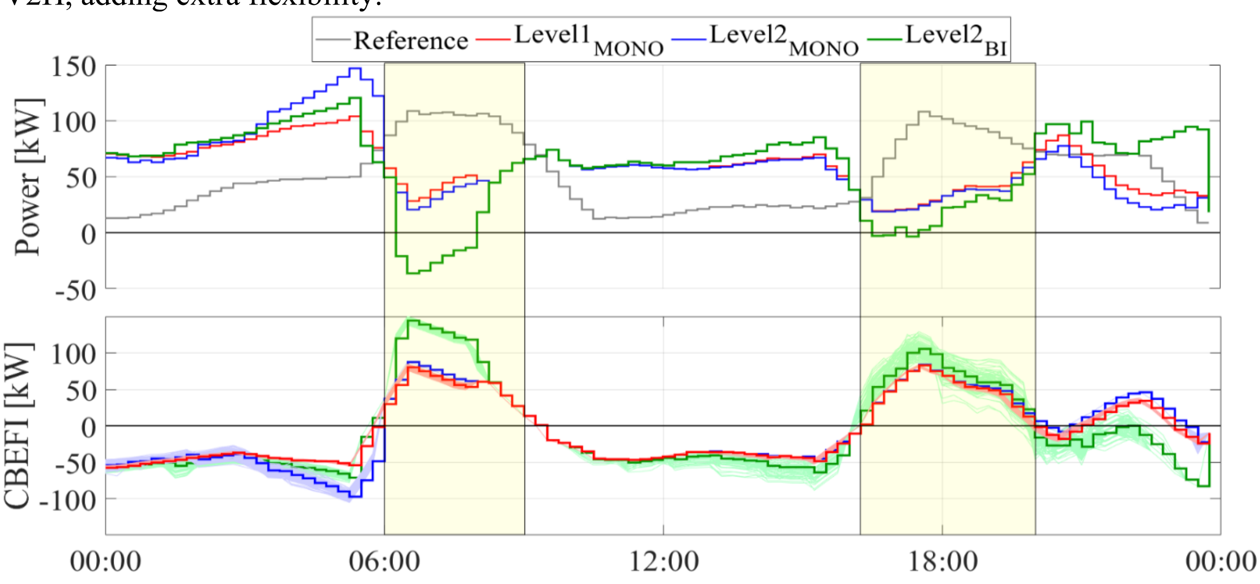

Figure 4.14. Load profile and CBEFI in DSM for Dt=15 min. On-peak events are in yellow.

It is evident that this extra allocation has the potential to result in a net positivity on the aggregated portfolio. In the afternoon, the load profiles of the three configurations are almost identical until the start of the second DR event. At this point, the bidirectional scenario raises the demand in order to achieve a higher SOC at the beginning of the event.

In contrast to the morning event, the probabilistic methodology indicates that the role of EVs is restricted during the evening event. This illustrates the time-dependency of EVs, where their arrival influences the number of EVs accessible for V2H purposes while also resulting in lower SOC levels for those connected. During the night, the eMPC has sufficient time to charge EVs thoughtfully. However, during the evening events, the eMPC cannot control the charging of EVs that are not connected to the infrastructure. The impact of uncertainties in the arrival times of EVs is highlighted by a wider confidence interval observed from noon to midnight. This indicates that the uncertainties can be considered negligible in the morning event, while impact CBEFI by 8% and 25% in the evening for Level2$_{MONO}$ Level2$_{BI}$ respectively. The KPIs for DSM scenario are presented in Table 4.8.

Table 4.8. Performance metrics for DSM

		Reference Profile	*Demand-side Management with CPP*		
			Level1$_{MONO}$	*Level2$_{MONO}$*	*Level2$_{BI}$*
Total energy consumption	[MWh/day]	1.19 ±0.02	1.31 ±0.2 (+10.1%)	1.39 ±0.8 (+16.8%)	1.42 ±0.2 (+19.3%)
Energy cons. EVs	[kWh]	-	146.0 ± 0.1	157.4 ± 0.5	162.2 ± 0.2
Energy cost Space Heating	[$/day]	81	60	60	60
Energy cost EV	[$/day]	-	18	9	-16
Average demand	[kW]	49.0 ±0.01	58.34 ±0.6 (+19.1%)	59.05 ±0.2 (+20.5%)	63.23 ±1.3 (+29%)
NC *	[kW]	65.3 ±0.2	67.0 ±0.4 (+2.6%)	64.75 ±1.3 (-0.85%)	76.75 ±0.2 (+17.5%)
Maximum demand	[kW]	106.5 ±0.1	104.2 ±1.2 (+2.2%)	145.5 ±0.8 (+36.7%)	123.0 ±0.2 (+15.5%)
(On peak)		106.5 ±0.1	58.0±0.4 (-45.5%)	57.0±0.6 (-49.3%)	58.0±0.1 (-45.5%)
Period	[HH:mm]	08:00	05:15	05:15	05:15
LF	[%]	46.3	56.2	40.1	52.29
PTV	[-]	8.94	5.91	7.94	-
SysR	[MW]	40.5	43.0	53.2	82.2
$\alpha_{150\%}$	[h]	5.25	4.1	4.0	8.07

* NC [kW] as the 67th percentile of power demand distribution.

The total daily energy consumption increases in DSM by 10.1, 16.8 and 19.3% respectively for Monodirectional Level1, Monodirectional Level2, and Bidirectional Level2. The increase in energy consumption is an expected consequence of load management [376]. The average demand increases by 19.1%, 20.5%, and 29% from the reference in Level1$_{MONO}$, Level2$_{MONO}$, and Level2$_{BI}$, respectively. The maximum demand registers a +2.2% in the Level1$_{MONO}$, but as soon as the charging infrastructure moves from Level1 to Level2 it reaches +36.7% in Level2$_{MONO}$, and +15.5% in bidirectionality. The presence of DSM also affects the peak-demand period. In fact, while in the reference case the peak corresponds to the ramp-up of most of the heating systems, in the DSM the peak period moves to 05:15, before the beginning of high-priced tariffs at 06:00.

The grid oriented KPIs suggest that Level1$_{MONO}$ and Level2$_{BI}$ produces the highest efficiency, with a LF of 56.2% and 52.3%. These values are higher than reference, proving how residential fleet of EVs might be beneficial for the grid when properly managed. Different results come from the DSM with Level2$_{MONO}$. The high magnitude of charging and the limitation in V2H make the overall metrics for Level2$_{MONO}$ the worst of the considered charging options. The load variability — described by the SysR and the severity factor— is much more affected by the charging infrastructure (e.g. monodirectional, bidirectional) than Levels of charging. In fact, with the possibility of V2H the SysR reaches +54.5% from the corresponding Level2 in Monodirectionality.

The increases in $\alpha_{150\%}$ concern about the NC of the portfolio, suggesting that during two-peak DRs conditions and with high penetration of EVs, the grid capacity should be increased by 53.7% to bring the load stress to the reference value, compared to the +19.3% dictated by static tariffs.

Evolution of LF, NC, and max demand are shown for the six considered configurations in Figure 4.15. The LF is highest for Monodirectional Level1 at 50.8%, indicating that it operates more efficiently than reference and Monodirectional Level2. The additional demand for EVs results on the aggregated scale as balancing effect, increasing consistently the NC, but with limited increase in maximum demand.

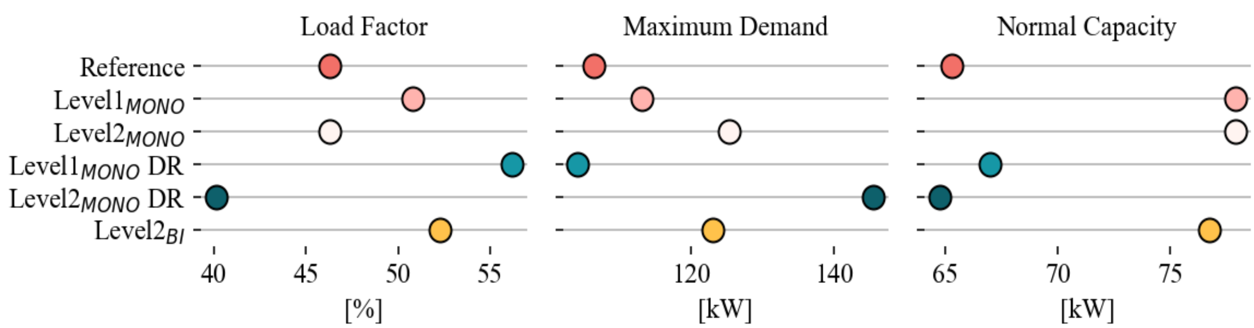

Figure 4.15. Evolution of performance metrics.

Among the DR settings, DR Bidirectional shows the most significant improvement, with a LF of 52.29% and a Maximum demand 15.5% higher than Reference, as product of a successful coordination performed by the ISL formulation. However, the higher NC —76.75 kW and +17.5% from the reference—needs to be accounted for capacity increases from the network operator. The results of monodirectionality in DR shows Level1 outperforming Level2. The elevated intensity in charging, and the influence of time-varying tariffs motivate EV owners to deploy similar strategies (in terms of set point temperature and charging cycles), resulting in the highest demand and lowest LF. This comes from the lack of diversified strategies dictated by equal priorities among customers. However, as result of the ISL formulation, DR Bidirectional mitigates this effect, by shifting the charging from early morning to late night.

A focus on the optimal charging strategies for each arrival times between 08:00 and 22:00 is presented in Figure 4.16 for each configuration.

The lowest magnitude of charging in Level1 presents several limitations. EVs can only participate in DR in 42% of the simulated scenarios, corresponding to arrival times prior to 16:00. If an EV arrives later, it must begin the charging cycle immediately to ensure it is fully charged by the next day, despite of the peak hours tariff. In contrast, Level2$_{MONO}$ infrastructure is more efficient, completing the entire charging cycle in just 3 hours. As a result, EVs are guaranteed to be fully charged without generating additional loads during the upcoming DR event. For bidirectional charging, the success of V2B depends primarily on the initial SOC. The simulations show a 98% success rate, with EVs also able to participate in evening DR events in 78% of cases, when arrival times is before 16:00.

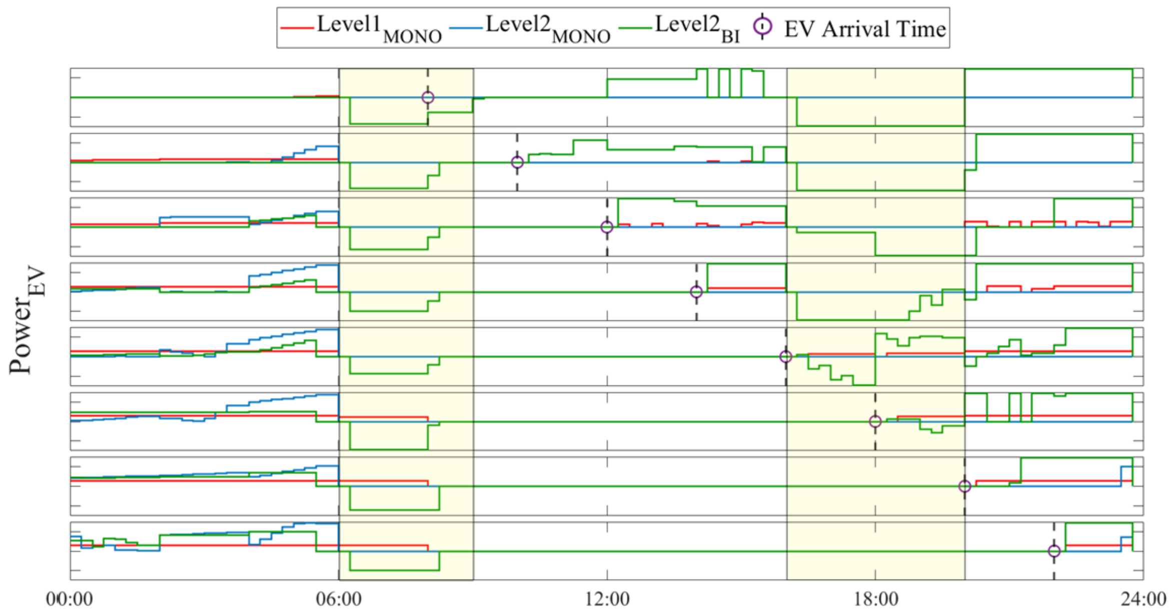

Figure 4.16. Charging strategies for House1 with different arrival times. On-peak events are highlighted in yellow. [Values in ± 7.2kW range]

During DR events, the grid communicates load shifting needs through pricing tariffs, but it might penalize customers with demand exceeding NC. This kind of competitive framework suits the use of eMPC which relies on the set of weights [c_{en}, $c_{\Delta T}$, c_{dc}], as presented in the Eq. (4.17). Thus, a parametric investigation on c_{dc} is shown in Figure 4.17 to describe the price-responsiveness of LF on either individual or aggregated scale.

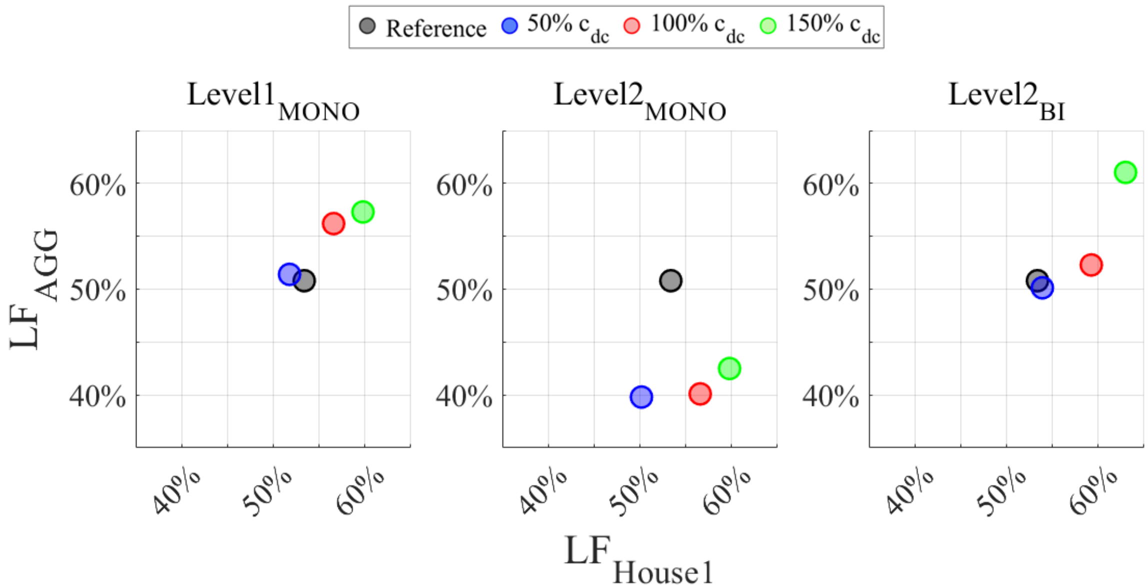

Figure 4.17. Price-responsiveness of ISL for 50%, 100% and 150% of the considered demand charge of \$20.522/kW.

In Level1$_{MONO}$ scenario, the LF registers milder but consistent improvement. In fact, the low intensity of charging adds an almost constant load throughout the night, regardless of the c_{dc}. On the other hand, Level2$_{MONO}$ jeopardizes grid stability for any configuration of c_{dc}. The bidirectionality of Level2$_{BI}$ determines the most convenient improvement, with the highest sensitivity to the c_{dc}.

Incorporating EVs into portfolio management may result in an overall decrease in network stability, leading to a substantial reduction in LF. Nevertheless, the implementation of the ISL in eMPC effectively addresses the issue of EVs' impact on the network and enhances stability through coordination. Using coordination, monodirectional scenarios, both at Level 1 and Level 2, are less beneficial in all the examined scenarios. The latter configuration is especially unfavorable since it leads to the creation of hazardous new peak demands. In contrast, bidirectionality—although the high sensitivity on demand charge—effectively enhances network metrics, making a valuable contribution during DR events through V2X.

The main challenge in implementing managed coordination lies in market policy. In fact, the use of static TOU tariffs or CPP lose effectiveness with high DSM adoption, exacerbating demand peaks, and the absence of demand charges intensify demand volatility. These issues are increasingly problematic given the rapid changes in the energy market. Adopting dynamic pricing, tailored for residential and EVs, could address these challenges. Flexible tariffs and day-ahead pricing communications would align grid stability with customer incentives, enhancing DSM success while benefiting the network, aggregators, and end users.

4.3 Conclusions

This chapter presented a comprehensive methodology for evaluating and optimizing grid interactions in residential energy systems, focusing on the evolution of load profiles influenced by advanced technologies and electric vehicle integration. Through detailed scenario analysis and data-driven approaches, the study addressed critical challenges in demand forecasting, energy flexibility, and economic optimization, offering insights into the potential of high-performing technologies and demand-side management programs.

High-performing technologies such as photovoltaic systems, photovoltaic-thermal systems, and heat pumps were analysed for their impact on residential energy efficiency and flexibility towards a fully-electrified society. Scenarios demonstrated how integrating solar-assisted heat pumps and photovoltaic-thermal systems can significantly reduce net energy consumption and enhance thermal performance, particularly in cold climates. The study highlighted that these technologies could lower energy consumption by up to 53% and reduce economic expenditure by 34% under time-of-use tariffs. However, the findings emphasized the importance of system sizing and operational control to maximize efficiency and avoid creating new grid challenges, such as increased variability in energy demand during peak solar hours.

The integration of electric vehicles into residential energy systems introduced both opportunities and challenges. Monodirectional Level 1 and Level 2 charging, as well as bidirectional Vehicle-to-Home (V2H) and Vehicle-to-Grid (V2G) capabilities, were evaluated for their effects on load profiles. The results revealed that Level 2 charging increased peak demand by 17%, shifting peak periods from morning to evening. In contrast, bidirectional charging demonstrated potential for mitigating grid stress by leveraging electric cars as flexible storage assets. However, the time dependency of electric vehicle charging, particularly during evening demand peaks, underscored the need for predictive control strategies to manage uncertainties in arrival times and residual battery estimations.

The works in this Chapter employed Economic Model Predictive Control frameworks to optimize energy management, balancing variations in set point temperature, electric vehicle charging, and grid interactions. By incorporating building thermal models, Support Vector Machines for electric baseload prediction, and Monte Carlo simulations for electric vehicle behaviour, the methodology provided accurate 24-hour-ahead forecasts. The use of Economic Model Predictive Control demonstrated its effectiveness in reducing peak demand during demand response events, achieving load reductions of up to 49% for morning peaks and 45% for evening peaks in Level 2 monodirectional configurations.

Key performance metrics such as Load Factor, Peak-to-Valley ratio, and Building Energy Flexibility Index) highlighted the advantages of integrating flexibility measures into demand-side management programs. Bidirectional Level 2 configurations showed the highest Load Factor improvements, enhancing grid stability. However, the study acknowledged that the benefits of load management strategies depend on tariff structures, pricing schemes, and the level of adoption among end-users.

By integrating advanced technologies, predictive controls, and demand-side management strategies, this methodology bridges gaps between theoretical research and practical application in residential energy management. The findings underscore the importance of a holistic approach to optimizing energy efficiency and flexibility while minimizing economic and operational costs. This chapter contributes to the development of resilient, sustainable energy systems, supporting grid stability and enabling the adoption of smart energy technologies in virtual energy communities.

5. *Diversification strategies for Energy Aggregators*

The growing complexities of modern energy systems necessitate innovative approaches to demand-side management to balance grid stability and customer satisfaction. Within this framework, energy aggregators have emerged as pivotal actors, bridging the gap between distributed energy resources and grid operators. However, unlocking their full potential requires implementing diversified strategies, as substantiated by the conducted literature review and the investigations outlined in this thesis. Such strategies demand tailored communications and pricing approaches, ensuring individualized engagement with diverse consumer segments.

Central to these efforts is the prioritization of households within virtual communities, guided by the development of dynamic strategies for portfolio management. This chapter introduces two main pillars underlying this diversification: first, approach the generation of differentiated pricing tariffs to desynchronize flexibility activation; and second, the grouping of buildings based on their flexibility performance and thermal properties through a flexibility benchmarking. These methodologies form a cohesive framework for optimizing the role of energy aggregators, addressing challenges associated with demand peaks and operational inefficiencies.

The significance of flexibility benchmarking lies in its ability to systematically group buildings according to their thermal and operational characteristics. As described in previous chapters, data-driven techniques, such as clustering algorithms, facilitate the creation of reduced-order models that capture building-specific dynamics. These models are instrumental in assessing the energy flexibility potential of individual households, enabling aggregators to target specific segments with tailored demand-side management programs. By leveraging these benchmarks, energy aggregators can achieve scalable portfolio management, ensuring equitable and efficient load distribution across diverse building types and locations.

Complementing this grouping mechanism is the development of dynamic pricing strategies that promote flexibility desynchronization, employing techniques such as Fourier series. By incorporating occupancy patterns, critical demand periods, and diversification objectives, these algorithms enable the creation of adaptive pricing profiles that align consumer demand with grid requirements. This strategic desynchronization not only mitigates peak loads but also enhances the overall economic and operational efficiency of energy systems.

The methodologies presented in this chapter represent a significant advancement in demand-side management practices, addressing both technical and economic challenges faced by energy aggregators. By integrating flexibility benchmarking and dynamic pricing, this work establishes a foundation for equitable and efficient demand response strategies, paving the way for the mass deployment of these techniques in diverse energy markets. Furthermore, the findings emphasize the critical role of data-driven decision-making in the transition toward sustainable and resilient energy systems.

In the following sections, the results of these investigations are elaborated, highlighting the implications of these strategies for energy aggregators, utilities, and consumers. Through rigorous analysis and simulation, this chapter demonstrates the feasibility and scalability of these approaches, providing actionable insights for stakeholders aiming to enhance grid stability while meeting the evolving needs of the energy market.

5.1 The impact of electricity pricing on load profiles

Despite the economic savings and reduced grid pressure offered by time-dependent tariffs, these structures face significant criticisms when implemented. Due to the absence of a supervisory system and the predetermined tariffs that do not reflect the actual condition of the grid, the sharp price spikes during events can result in negative profits for participants and increased operational costs for utilities and DSOs [377]. Moreover, if a substantial number of consumers residing in the same geographic region and linked to the same energy sub-station choose to participate in the project, it could have a negative impact on the power grid. This can lead to new peak demands driven by market manipulation, causing an extremely low load factor and high-power fluctuations, potentially resulting in congestion and outages [378]. A pricing algorithm for dynamic pricing can be an effective tool to address these issues by providing communication that reflects the actual grid conditions and allowing for diversified strategies in clusters and building portfolios. This decentralization lowers management costs for utility control centers, delegating this responsibility to energy aggregators[379, 380].

Many researchers are proposing methodologies to generate dynamic profiles to raise the level of DSM from demand response to load management. Cai et al. [381] proposed a dynamic pricing model that integrates the fluctuation characteristics of residential electricity demand with wind and PV output. This model utilizes bi-level optimization to coordinately dispatch flexible loads, generating dynamic profiles that deviate from the utility's rates. Muratori and Rizzoni [349] assessed the impact of demand response programs using different electricity price structures. The authors generated innovative electricity price structures called Multi-ToU and Multi-CPP to cope with the rebound peaks created by the synchronization from time-varying electricity price structures. Lu et al. [379] proposed a successful dynamic pricing DR algorithm for energy management in a hierarchical electricity market that employs reinforcement learning to formulate the dynamic pricing problem as a discrete Markov decision process (MDP). The results showed that this methodology was effective in promoting providers' profit and lowering costs, as well as improving provision efficiency.

Despite these efforts, further investigation is needed into data-driven techniques to generate dynamic profiles that can be interpreted and tailored to the specific conditions and needs of DSOs. In the DAC market, the final price of electricity is determined by various orders of magnitude and frequencies. This section introduces an approach to quantify electricity price impact on building energy flexibility potential as the first effort towards the mass deployment of dynamic pricing algorithms. Space conditioning demand is predicted using the process presented in *3.1.1-Model Order Reduction procedure* for the same Case Study.

The methodology focuses on creating a dynamic electricity price profile using Fourier series, enabling precise manipulation and interpretability. Factors such as the number of peaks and duration of DR events are included.

5.1.1 Method

The methodology encompasses a three-step procedure to assess the impact of dynamic pricing on residential customers. The first section describes the chosen unsupervised clustering technique applied to form the reduced order resistance-capacitance thermal model for a house. The second section outlines the design of the pricing algorithm, including the principal assumptions and the formulation using Fourier series. The third and final section of the methodology elaborates on the control and optimization routine designed to activate building thermal flexibility and manage temperature variation during demand response events.

Clustering techniques - such as Timeseries kMeans- are effective for building-to-building generalization, and pattern recognition when there is adequate measured data. This approach exploits a recursive routine of k-means clustering to group thermal zones with similar thermal physics and operating schedules and setpoints to reduce the number of optimal actions for an optimization problem formulated as dynamic time warping[382]. The detailed ROM is shown in Figure 5.1.

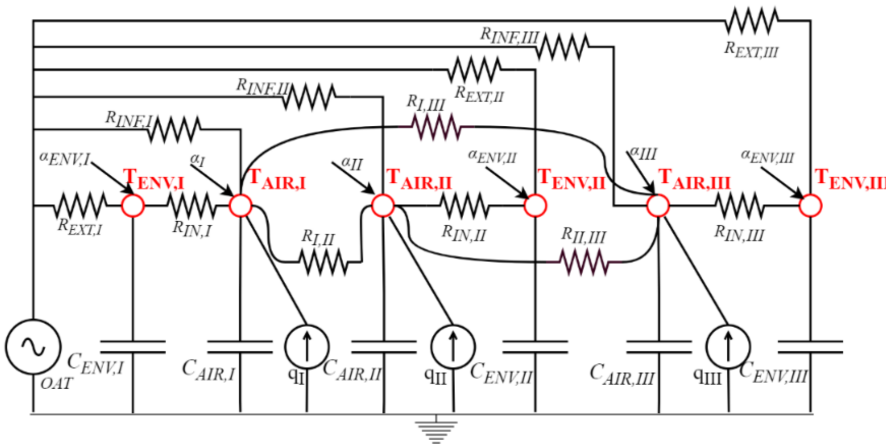

Figure 5.1.-Resulting reduced order model k=3 (6C12R6α)

The presented aggregation algorithm identifies an optimal model structure as:

$$[2k\ C;\ 2k(k\text{-}1)\ R;\ 2k\ \alpha] \tag{5.1}$$

Where, k is the number of nodes evaluated as number of final clusters i_{FINAL} plus one node for outdoor air temperature. In fact, each cluster has one capacitance, one resistance and one solar aperture, plus *k* resistances to describe zone-to-zone interactions. To assess the benefit of this MOR technique and evaluate the performance of the evaluated model, an experimental house is used as test bench (and shown in *6.2-Experimental House for Building Energetics (EHBE)*). The iterative procedure of k-means is structured into[382]:

i. defining the most representative trends of zone temperature for the ten thermal zones,
ii. clustering the representative trends of zone temperature for the nine zones into three aggregated groups.

5.1.2 Pricing algorithm

The design of pricing algorithm is essential to guide the activation of the building energy flexibility by creating dynamic price profile. Pricing rates have been widely acknowledged as the main influencing parameter on advanced control techniques. Electricity prices are influenced by fundamental physical forces from both the demand and supply sides, each operating at different frequencies and independently of one another [383]. The lowest frequency inputs, such as cycles of economic development and generation investment, impact electricity prices over many years. Mid-frequency inputs, including seasonal weather patterns and annual generation maintenance, affect prices for weeks but not beyond a year. The highest frequency inputs, such as intra-day and intra-week variations in electricity load, influence prices for hours, with effects limited to within a week. Consequently, due to these cyclic forces from both demand and supply sides, electricity spot prices exhibit periodic components across various frequencies [384]. Fourier's Theorem states that a continuous time function *f(t)*, t = [0; T], can be reconstructed by a linear combination of sine and cosine functions of different frequencies, providing a useful tool for analyzing electricity spot prices. Thus, the proposed methodology focuses on creating a dynamic price profile using Fourier series, enabling precise manipulation on the three main influencing effects and respective harmonics:

i) the scheduling of occupants,
ii) the presence of a DR event, and
iii) the level of strategy diversification.

The first term (and harmonic) describes the presence of occupants within the building, with the known morning-evening peaks profile. The second term (and harmonic) defines the number of critical periods throughout the day, whereas the third term (and harmonic) is responsible for the customer management towards diversification strategies.

$$p_{spot} = A_0 + \sum_{n=1}^{3} A_n \sin(w_n \cdot t - \varphi_n) \tag{5.2}$$

where, A_n are amplitudes, w_n is the angular frequency, and φ_n relative phases. The angular frequency is defined as:

$$w_n = 2\pi \frac{n_n}{P} \tag{5.3}$$

where, P is the period and n_n is the number of anticipated peaks at a given harmonic. Dynamic simulation and eMPC allow the mapping of price-response of building energy flexibility. Specifically, the impact of pricing on prebound and rebound effect, the maximum power demand, the BEFI [95], the economic feasibility, and the temperature deviations can be assessed. To succeed in this assessment, it is essential to fine constrain the design parameters, as shown in Table 5.1.

Table 5.1. Constraints and mathematical formulation of design parameters for pricing algorithms

Design parameter	Domain	Comment
A_0	*na*	Fixed as the daily mean DR program
A_1, A_2, A_3	$0 \le A_1 + A_2 + A_3 \le A_0 \in \mathbb{N}^+$	Avoid negative tariffs
n_1	[2]	Two-peaks (fundamental harmonic)
φ_1	[-4]	Occupancy scheduling (6-9am)/(5-8pm)
n_2	[1,2]	To describe one/two "*high pressure*" periods
φ_2	[-11h:1h:12h]	Characterize "*high pressure*" periods
n_3	[3 with $n_2 = 1$; 4 with $n_2 = 2$]	Diversification level
φ_3	[-3h:1h:4h with $n_2 = 1$; -2h:1h:3h with $n_2 = 2$]	Characterize the diversification strategy

Building modeling must accommodate an explicit formulation to integrate receding horizons of MPC and be implemented into real controllers [120]. For the presented research framework and for the dynamic of grid signals by time-dependent pricing tariffs, the application of MPC for cost minimization is defined as eMPC. A general formulation of the problem is presented:

$$J = p_{spot} \cdot \left[\sum_{j=1:i_{FINAL}} \frac{P_{HEAT,j}}{COP} \right] + \gamma \cdot \left[\sum_{j=1:i_{FINAL}} \left(T_{SET,j} - T_{IN,j} \right) \right] \tag{5.4}$$

Where *Pspot* is the outcome of the pricing algorithm, γ is the cost for temperature violation, as [2.5 \$/°Ch], $P_{HEAT,J}$ is the power as manipulated variable, COP is the coefficient of performance, T_{IN} is the zone temperature, and T_{SET} is the zone set point temperature. The first term of the objective function *J* represents the energy costs, whereas the second term describes the temperature violation in DR.

The parametric analysis of the seven design parameters in Table 5.1 yielded to 7680 different price profiles and simulations. A representative price profile is selected and presented in Figure 5.2 to show the creation of the dynamic profile as superposition of the three harmonics, and the flexibility activation driven by the eMPC.

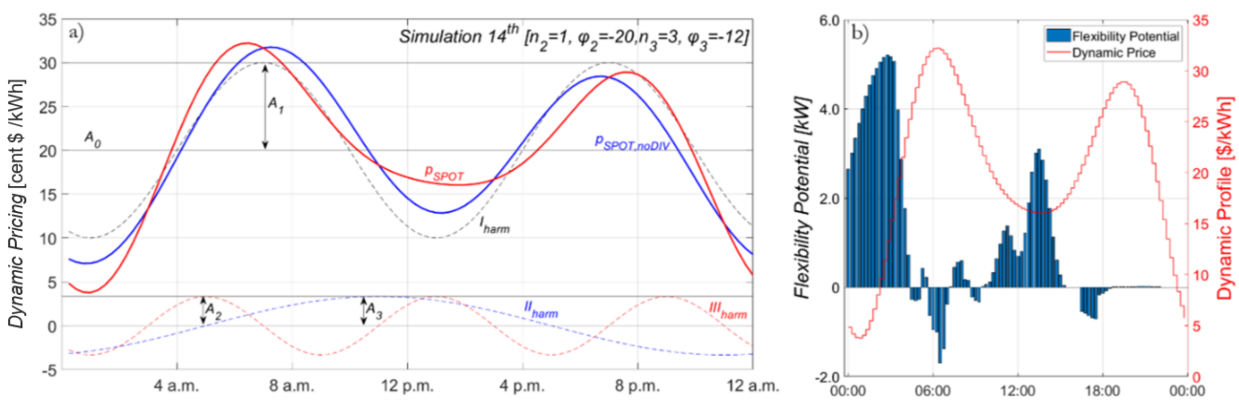

*Figure 5.2.-**a** Price profile and -**b** flexibility activation of EHBE for the 14th Simulation*

The first harmonic -related to the occupancy- as black dotted line. Two clear peaks are created to represent the usual scheduling of residential households. Morning peak happens between 6 a.m. to 9 a.m., whereas the evening peak occurs between 5 p.m. to 8 p.m. The critical periods curve indicates a DR event and is dotted-blue (*II harm*). This harmonic increases *Pspot* between 5 a.m. to 5 p.m., creating lower values during night hours. This harmonic is dictated by DSO according to energy sub-station's needs. Lastly, the diversification signal is shown as a dotted-red line. This harmonic (*III harm*) is conceived to diversify strategies in building cluster management. In the example, *III harm* creates three peaks and as many valleys, and it is regulated by the design variables n_3=3 and φ_3 =-12 hours from Table 5.1. The resulting curves show the dynamic price with diversification strategy *Pspot* in red, and without ($Pspot_{,\ noDIV}$) in blue. The effectiveness of eMPC in thermal load management is shown in Figure 5.2.b. The flexibility provided by the building is presented as a negative value, whereas increases in power demand as positive values. Therefore, the duration of preheating stages can be assessed around 4 hours (before each high-price period). It is important to mention that the flexibility potential is compared to a reference baseline.

The advantage of the presented methodology is the ability to understand the direct impact of pricing structure on flexibility potential (and reduced expense), total energy consumption, and temperature variation from preferred setpoint during the DR events. Therefore, each individual price profile generates different conditions and strategies. Figure 5.3 shows the histogram of the flexibility potential, with some combination of the design variables able to provide a more evident contribution to the DSO, with 70% of the simulations leading to 1.5-2.0 mean kW/event (between 34 and 40% of the reference peak demand). Around 8% of the simulations were not able to provide any flexibility to the grid, with the remaining 22% of simulations yielding a higher flexibility potential, but with 95% increase in energy consumption.

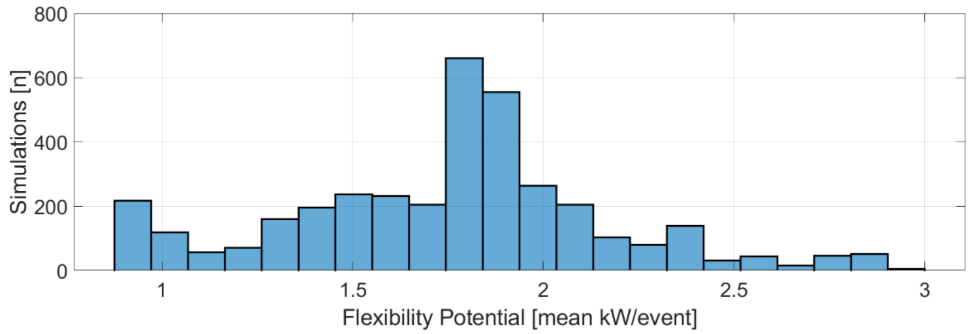

Figure 5.3.- Histogram of Flexibility potential for the 7680 pricing structures analysed

One relevant result is the linear dependance between the energy consumption [kWh/day] and the temperature violations [°Ch/day]. Figure 5.4 shows the relationship between the energy consumption and the flexibility potential. Thus, higher energy consumption causes a more severe temperature variation from preferred setpoint in providing flexibility. In this figure, it is possible to draw a tendency with a second-order polynomial curve to evaluate the flexibility potential (as mean kW/event) as a function of energy consumption. This curve and its fitting process are related to the considered household and assumptions.

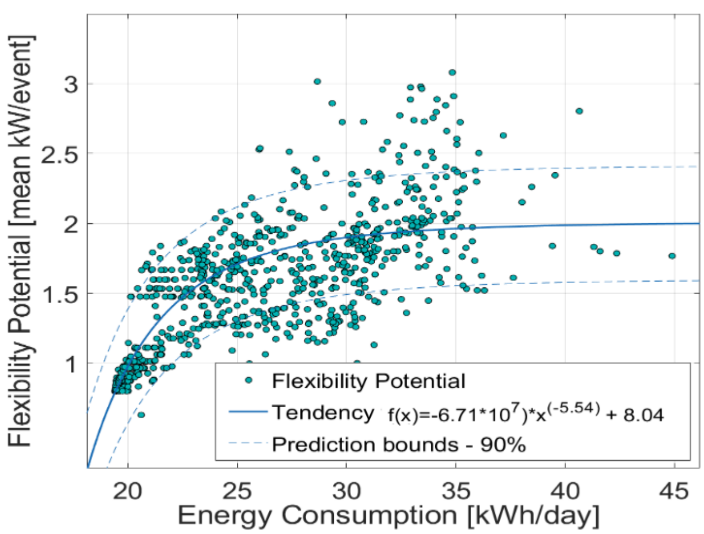

Figure 5.4.- Flexibility Potential and Energy Consumption

This result demonstrates that a higher participation in DSM brings to higher temperature variations from preferred setpoint during the day, demonstrating the energy-intensity of preheating and recovery stages for thermal load management, with an overall increase in the total energy consumption by 100%.

The formulation of the pricing algorithm allows to measure the impact of individual design variables (such as number of peaks a day, magnitude of a single harmonics, etc.) or a combination of those. As instance, Figure 5.5-*a* presents the relationship between the energy consumption and one adimensional groups related to Table 5.1: $(A_1+A_2+A_3)/A_0$. It can be considered an indication of the maximum and minimum fluctuations of *Pspot*. In fact, when the price profile exhibits extremely low and extremely high values (in terms of cent $/kWh) the optimizer is facilitated in determining preheating and recovery stages.

The analysis on the amplitudes ($A_{\#}$) is further analyzed and shown in , Figure 5.5-*b*, recognizing a clear pattern in the adimensional group defined by A3/A0, as the level of diversification strategy. In this case, it is possible to notice that the greatest advantage is recorded when the amplitude of the diversification is around half of the base amplitude (considered as the average cost of the electricity).

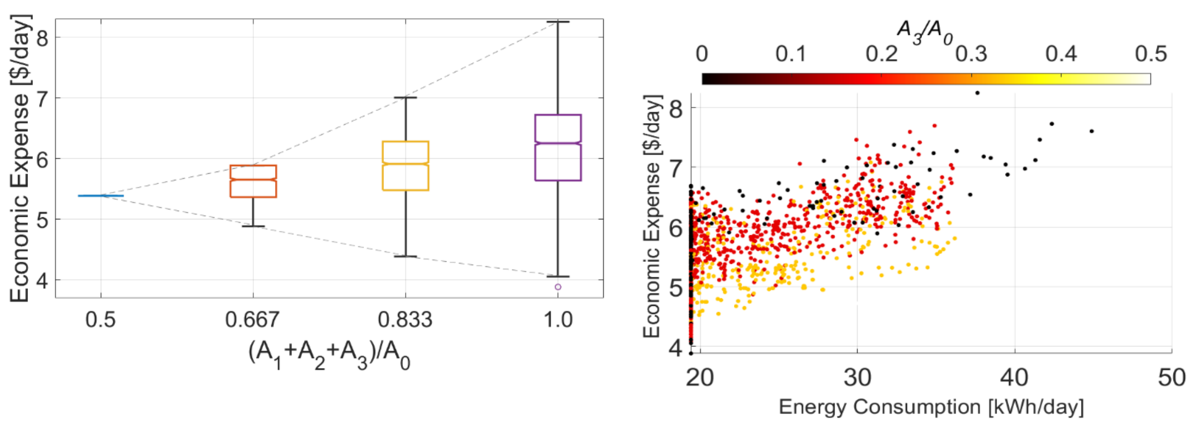

*Figure 5.5.-**a** Economic Expense and the adimensional group (A1+A2+A3)/A0,*
***b**- Economic Expense and the adimensional group A3/A0*

Figure 5.6-***a*** and Figure 5.6-***b*** analyze the relationship between energy consumption and relative phases of the 2nd and 3rd harmonics (respectively φ_2 and φ_3).

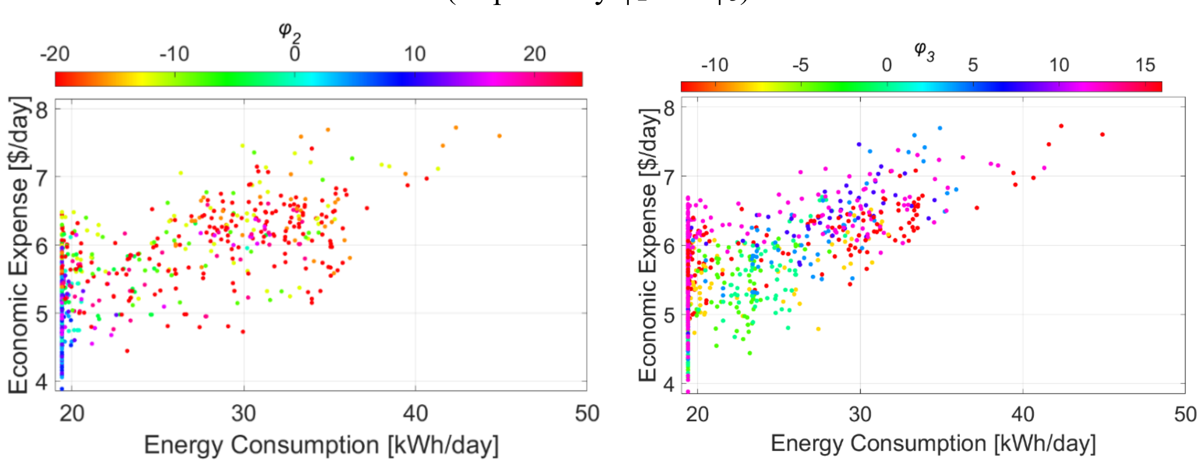

*Figure 5.6.-**a*** analysis of the 2nd harmonic phase, ***b***- analysis of the 3rd harmonic phase.

In the design process of the pricing algorithm, φ_2 values between 5 to 15 hours ensures the lowest energy-intensity, whereas φ_3 exhibits the best performance between -7 to 1 hour. In both configurations, the cause of this behavior can be identified in the level of variation of *Pspot*. By analyzing the phases of the harmonics, all the values outside these two ranges result in leveling *Pspot*, generating eventually local minimum in the cost function of the eMPC.

Moreover, a linear dependance between the energy consumption [kWh/day] and the temperature violations [°Ch/day] is identified. This result demonstrates that a higher participation in DSM brings to higher temperature variations from preferred setpoint during the day, meaning that preheating and recovery stages of thermal load management are energy-intensive, with an overall 100% increase in the total energy consumption.

5.2 Building flexibility-benchmarking potential in demand response

In spite of the potential of hierarchical designs and ICT of energy aggregators and utilities, building portfolios range from two to thousands of homes, making impractical to develop, convey, and implement tailored strategies for each household. One possible answer is to develop a systematic mechanism for grouping buildings according to their flexibility potential. Although the international community tried to establish a standard system for building benchmarking, the relatively new framework of energy flexibility and load management in DR has revealed a need in this area.

Building energy benchmarking is referred to as the comparison of energy performance in buildings with similar characteristics [232]. A qualifying benchmarking process is described by three steps: *i*) collect a reasonably large database of building samples; *ii*) obtain the energy performance information of the candidate buildings; *iii*) conduct comparison analysis [233]. The first step defines customer pools, where datasets are gathered and standardized. This process needs to comply with requirements in terms of monitoring infrastructure, minimum level of measurements, and metadata information. For energy aggregators, supplementary information is needed to understand the energy sub-stations a given customer is connected to. The second step defines the energy performance by selecting the investigated variables. These can be extracted straightforward from the dataset or generated/simulated by using building energy modelling. The third and final step of the procedure consists of comparison analysis on the predetermined performance indicators, context where load management and energy efficiency insist. The choice of the right building benchmarks is related to the considered investigation, the problem identification, and the expected outcome for stakeholders.

Traditional (or low-dimensional) benchmarks such as the EUI, the GHG emissions, and source energy are frequently used to compare the environmental impacts of buildings against the corresponding value of the peer group [385]. The recognition of peer groups considers location (climate zone), floor area, and building type (residential, commercial, industrial), year of construction, number of occupants [234]. Publicly available building energy benchmarking tools exist refer sometimes to these low-dimensional KPIs. The most common in the United States include the Energy Star Portfolio Manager [386], the Building Performance Database, and the Building Energy Quotient [387]. Other benchmarks, such as the Energy Star Score, uses discrepancy between regression models and the actual energy use are used to explain building performance [388].

However, so-called low-dimensional benchmarking methods can be counter intuitive since cannot represent many other factors of influence. Including additional features generates a fairer comparison in the creation of peer groups. Gupta et al. [389] proposed a five-star benchmarking procedure exploring the relationship between Energy Performance Index (EPI) and end-use appliances as additional influencing factor. The authors supported hybrid combinations of benchmarking methodologies to provide a more accurate depiction of the energy performance of buildings. Multi linear regression (MLR), Bayesian approach, and principal component analysis (PCA) were used to generate composite indicators (CI), acknowledging their usefulness in policy analysis [390].

From the publication of the GEB initiative in 2019 [11], many researchers and energy utilities have promoted the use of flexibility-related features to design innovative benchmarking procedures able to characterize the BEF potential of groups and clusters [16]. Liu et al. [391] presented a benchmarking framework focused on load shedding and shifting; to characterize load shed intensity range and variability; influence of event duration and timing. This investigation is applied on two datasets of office and retail buildings. Eight metrics are presented as intensity (normalizing by floor area) and percentage of total building load for comparison. The calculation of these metrics is baseline-required; therefore, the authors assessed a regression model using OAT as single variable. The effect of baseline of consumption for the generation of flexibility-oriented benchmarks is presented in [392]. The authors investigated 203 retail stores in 11 states with most of the DR events and concluded that some particularly useful metrics for flexibility-oriented benchmarking was the shed intensity because the floor area normalized metric allows comparison among buildings. The investigated baseline methods comprises either single and multi variable linear regressions, day-matching, and weather-matching.

A comprehensive review on benchmarking approaches carried out by Ceccolini et al. [393] revealed that 81% of the innovative benchmarks are based on energy cost (16%), consumption (39%) and thermal comfort (26%), whereas the remaining 19% addresses building-grid interaction [394] and load shifting capabilities [395].

Data mining techniques and smart devices are responsible for the evolution of KPIs from low to high-dimensional benchmarking frameworks for their ability in load profiling [235]. Representative load profiles describe building operations, variations of building energy intensity, and inform about the temporal and absolute trends of power demand. The utilization of unsupervised learning techniques has been acknowledged as a potential strategy for load profiling due to the presence of stochasticity and singularity, which contribute to building-to-building distinctiveness [236]. These methods captured the operational patterns of individual buildings by identifying representative daily profiles, where the variations in building operations are reflected in many differences, such as the number and shape of load profiles [237]. Many researchers applied unsupervised clustering techniques to energy dataset, such as K-means clustering [238], density-based clustering [239], hierarchical clustering [240], K-shape clustering [241], “follow the leader” clustering [242], and Self-Organizing Map [243].

In this context, Park et al. [244] considered the iterative use of k-means, bisecting k-Means, and Gaussian mixture model clustering approaches on daily profiles from 3829 buildings. The authors concluded that three fundamental load shape profiles exist for the considered building portfolio. Each profile has a clear peak of energy use, and the resulting benchmarking framework groups homogenously buildings regardless of their type (e.g. residential, industrial, commercial, etc.). The results showed potential implications for portfolio management, building and urban energy simulations, DR, and renewable energy integration.

New metrics of benchmarking to infer the energy performance of a building based on its load shape was proposed by Luo et al. [396]. The methodology analysed 24-h electric load shape with collected smart meter data using over 2000 small- and medium-sized businesses in California. The authors concluded that for small- and medium-sized commercial buildings, the timing and amount of energy use are the most significant indications of the building's operating patterns. Therefore, three dimensionless parameters were introduced to guide the clustering: base load ratio , workday-non workday load ratio, and operating duration.

The idea of reflecting time-series analysis into a new flexibility-oriented benchmarking procedure is evident. Especially in markets where DR programs are already implemented, reflecting potential variation in the load profile seems both impactful for the design of energy aggregators (for the inherent super position effect) and convenient in building portfolio management. Andrews et al. [397] presented a method for embedding demand flexibility into building benchmarking. The data driven methodology uses building characteristics and energy data stream to populate a 306-school building portfolio. The daily profile is clustered using K-medoids using Gower's Distance to produce peer groups. The results show that the method effectively clusters buildings by attributes of demand flexibility and energy efficiency, by including grid-interaction features such as operational duration, load factor, and weekday-to-non weekday variation. The quantification of the BEF – considering fixed operation and preferred set points- is performed using a regression model with hour of the week, hour of the day, and degree-days adjustments.

5.2.1 Method

The proposed benchmarking procedure comprises three separate sections: i) *Building Portfolio Creation* where the main calibration routine is designed to populate the final dataset. In this section, data preprocessing and data cleaning stages are developed, the period selection for the training is identified, and models are filtered based on their performance in the 24 hours ahead prediction; ii) *Flexibility Quantification* where the portfolio—defined in the previous section— is investigated in order to calculate the building energy flexibility contribution by simulating the reference scenario, with pricing tariff from the utility, and the flexibility scenario, where the pricing tariff is customized by the DR Designer. The final comparison between the reference and the flexibility scenario is then used to quantify the flexibility potential of homes; iii) *Flexibility Benchmarking and Clustering* where the flexibility potential is used to define traditional KPIs and the proposed flexibility benchmark by an unsupervised clustering technique for time series. The flowchart is presented in Figure 5.7.

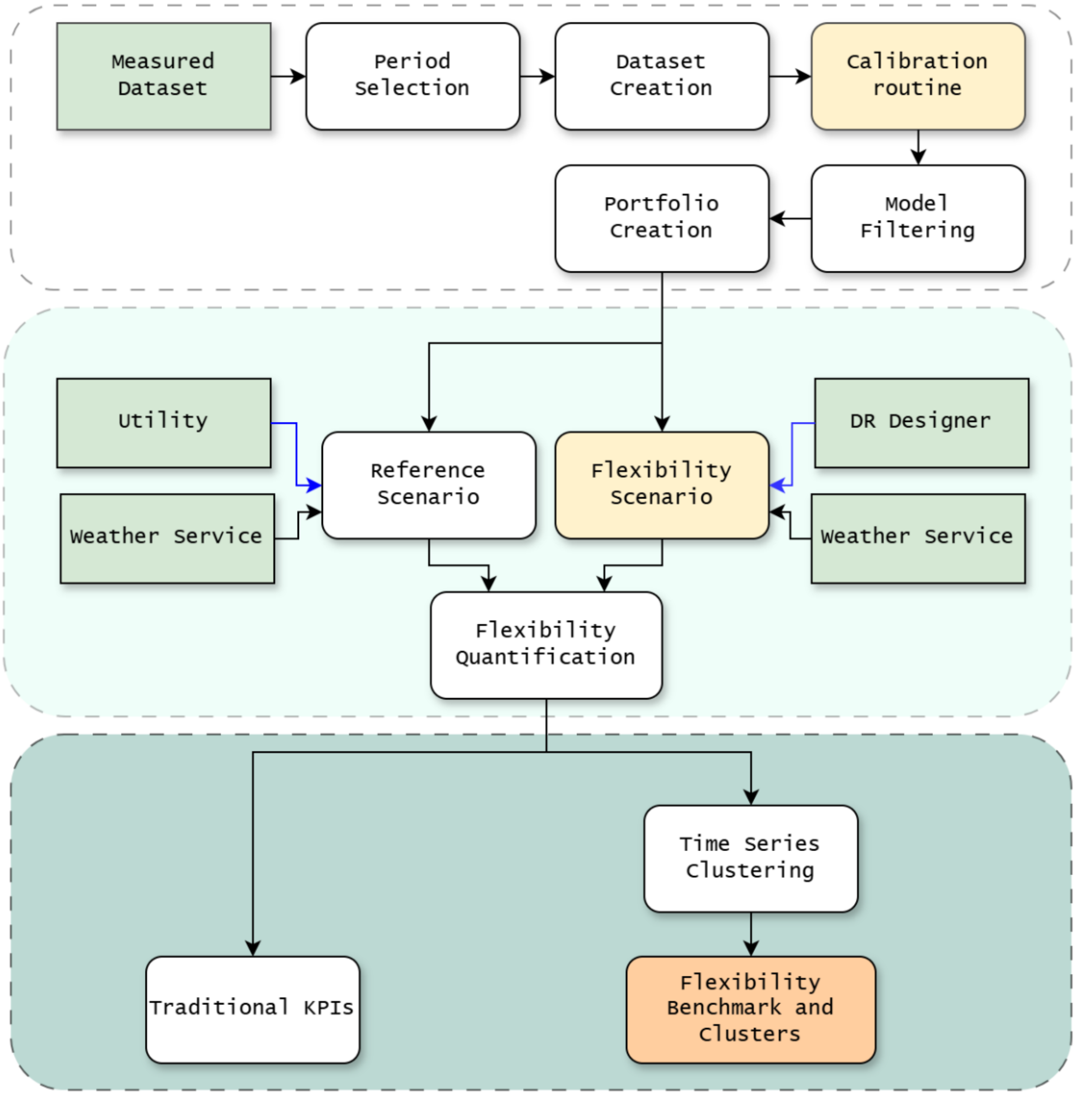

Figure 5.7- Flowchart of the proposed benchmarking technique.

Building Portfolio Creation

This section discusses every step of data processing, data cleaning, data calibration, and model evaluation towards the creation of the flexibility-informed benchmarking procedure proposed in this paper. The structure—conceived to follow the flowchart of Figure 5.7 — is divided into: *Dataset Creation*, *Calibration Routine*, and *Portfolio Creation*. The methodology begins with the collection and preprocessing of smart thermostat data. Subsequently, these processed datasets are used to calibrate reduced-order RC thermal network models for individual buildings. The calibrated models are evaluated for their predictive accuracy and robustness under varying conditions.

The dataset used in this study comprises historical measurements collected by smart thermostats, monitoring several key variables related to indoor climate and energy consumption. A major challenge in dataset creation arises from the complexity of handling large-scale data while ensuring high-quality and consistent measurements across different homes [398]. Each home operates with its unique monitoring system, making it impractical to apply heuristic approaches for period selection.

Thus, the standardization process focuses on extracting one week of consecutive data for calibration purposes. The selection of this period is guided by three main criteria: the availability, the season, and completeness of measurements. The presence of significant fluctuations in indoor air temperature and heating system usage must be ensured [181]. These fluctuations are essential for effectively calibrating the thermal models [183].

The developed routine considers all possible seven-day configurations within the heating season, defined as December 1st to March 21st. Configurations with low energy consumption are excluded to ensure the selected period represents active heating usage. Among the remaining configurations, the week exhibiting the highest variability in indoor air temperature is chosen. Variability is quantified using the standard deviation of the z-score for indoor air temperature over the seven-day period, as calculated in Eq. (5.5).

$$\text{Period Selection} = \max\left[s\left({(T_i - \mu)}/{\sigma} \right) \right] \tag{5.5}$$

Where, s is the sample standard deviation, μ is the mean of the indoor air temperature, and σ is the standard deviation of the population. This approach ensures the calibration dataset is both representative and robust, facilitating accurate model parameterization while minimizing bias due to inconsistent data quality or system operation.

Once ensured an adequate dataset, each house is represented by a second-order RC thermal network, with one effective interior node (T_i) and one effective envelope node (T_e). An explicit formulation is shown in Eq. (5.6).

$$\begin{aligned}
T_i^t &= \left(1 - \frac{\Delta t}{R_{ie}C_i} - \frac{\Delta t}{R_{ia}C_i}\right)\cdot T_i^{t-1} + \frac{\Delta t}{R_{ie}C_i}\cdot T_e^{t-1} + \frac{\Delta t}{R_{ia}C_i}\cdot OAT^{t-1} + \frac{Q_{h,inst}}{C_i}\cdot \delta_h^{t-1} + \frac{\alpha_i \cdot \Delta t}{C_i}\cdot Q_{sol} \\
T_e^t &= \left(1 - \frac{\Delta t}{R_{ie}C_e} - \frac{\Delta t}{R_{ea}C_e}\right)\cdot T_e^{t-1} + \frac{\Delta t}{R_{ie}C_e}\cdot T_i^{t-1} + \frac{\Delta t}{R_{ea}C_e}\cdot OAT^{t-1} + \frac{\alpha_e \cdot \Delta t}{C_e}\cdot Q_{sol}
\end{aligned} \tag{5.6}$$

Where, R_{ie} [K/W] is the overall thermal resistance between the effective interior node and the effective envelope node, R_{ia} [K/W] is the thermal resistance for infiltration rate, R_{ea} [K/W] is the is the overall thermal resistance of the building. C_i [J/K] is the thermal capacitance attached to the effective interior node, C_e [J/K] is the thermal capacitance for the envelope node, α_i [m^2] is the solar aperture for the effective interior node, α_e [m^2] is the solar aperture for the envelope, δ_h [s] is the runtime of the heating system. Q_{sol} [W/m^2] represents the global horizontal irradiance, OAT [°C] is the outdoor air temperature, and $Q_{h,inst}$ [W_{inst}] is the heating installed capacity.

The explicit formulation can be presented as Eq. (5.7), with the state matrix (A) and the input matrix (B) presented in Eq. (5.8).

$$\begin{gathered}
T^{t+1} = AT^t + Bu^t \\
\text{with} \\
T = [T_i\ ,\ T_e],\quad u = [OAT\ ,\ \delta_h\ ,\ Q_{sol}]
\end{gathered} \tag{5.7}$$

$$A = \begin{bmatrix} 1 - \frac{\Delta t}{R_{ie}C_i} - \frac{\Delta t}{R_{ia}C_i} & \frac{\Delta t}{R_{ie}C_i} \\ \frac{\Delta t}{R_{ie}C_e} & 1 - \frac{\Delta t}{R_{ie}C_e} - \frac{\Delta t}{R_{ea}C_e} \end{bmatrix} \qquad B = \begin{bmatrix} \frac{\Delta t}{R_{ia}C_i} & \frac{Q_{h,inst}}{C_i} & \frac{\alpha_i \cdot \Delta t}{C_i} \\ \frac{\Delta t}{R_{ea}C_e} & 0 & \frac{\alpha_e \cdot \Delta t}{C_i} \end{bmatrix} \tag{5.8}$$

Specifically, with a timestep of 5 minutes, the model needs to look forward 288 steps in the calibration process. The calibration variables (x) are shown in Eq. (5.9).

$$x = \left[\frac{1}{R_{ie}C_i} , \frac{1}{R_{ia}C_i} , \frac{Q_{h,inst}}{C_i} , \frac{\alpha_i}{C_i} , \frac{\alpha_e}{C_i} , \frac{1}{R_{ie}C_e} , \frac{1}{R_{ea}C_e} \right] \tag{5.9}$$

These seven parameters are considered as positive values only, and the stability condition is formulated as nonlinear constraint of the curve fitting problem, as shown in Eq. (5.10).

$$\Delta t < \min\left(\frac{1}{x_1 + x_2} , \frac{1}{x_6 + x_7} \right) \tag{5.10}$$

The current methodology considers baseline-required KPIs, assessing the flexibility potential through comparison with a reference scenario [399]. Thus, the presented methodology is conceived to simulate a valid reference of power demand using two representative weather conditions, isolating the effect of solar radiation on power demand. In this context, one cloudy and one sunny day are considered for the same winter season.

Reference Scenario

The reference scenario represents the business-as-usual case, where a traditional proportional-integral (PI) controller regulates space heating based on the deviation between the indoor air temperature and the set point. In this setup, the set point follows a predefined night setback schedule, maintaining an upper temperature limit of 22°C and a lower limit of 20°C between 6:00 AM and 9:00 PM. This scenario assumes static pricing, with a constant energy cost applied uniformly throughout the day.

Flexibility Scenario

The flexibility scenario introduces the proposed approach, where an economic Model Predictive Control (eMPC) algorithm manages space heating. This control system operates based on both a PH and a CH, dynamically adjusting runtime of space heating systems—previously defined as δ_h. The flexibility scenario investigates a rolling horizon of DR events simulating a plurality of grid signals. These signals are translated into constraints and pricing tariff by the means of a DR Designer algorithm. A general formulation of the cost function for this eMPC problem is shown in Eq. (5.11).

$$L = c_{u,EN} \cdot \sum_{j=1:NumHouse} \left(\frac{Q_{h,inst}}{\eta_{HEAT}} \cdot \frac{\delta_h}{3600s} \right) + \lambda_T \cdot \sum_{j=1:NumHouse} \left(T_{SET,j} - T_{i,j} \right) \tag{5.11}$$

where λ_T [$/°Ch] is the equivalent cost of 1°C temperature deviation for one hour, $c_{u,EN}$ [$/kWh] is the electricity cost, and T_{SET} [°C] is the reference set point temperature, and η_{HEAT} [-] is the equivalent Coefficient of Performance (COP) of the considered heating system.

The DR Designer generates five different events—defined as I, II, III, IV, V— between 6 a.m. to 9 p.m. each with a duration of three hours, determining constraints, pricing, and temperature boundaries for each simulation.

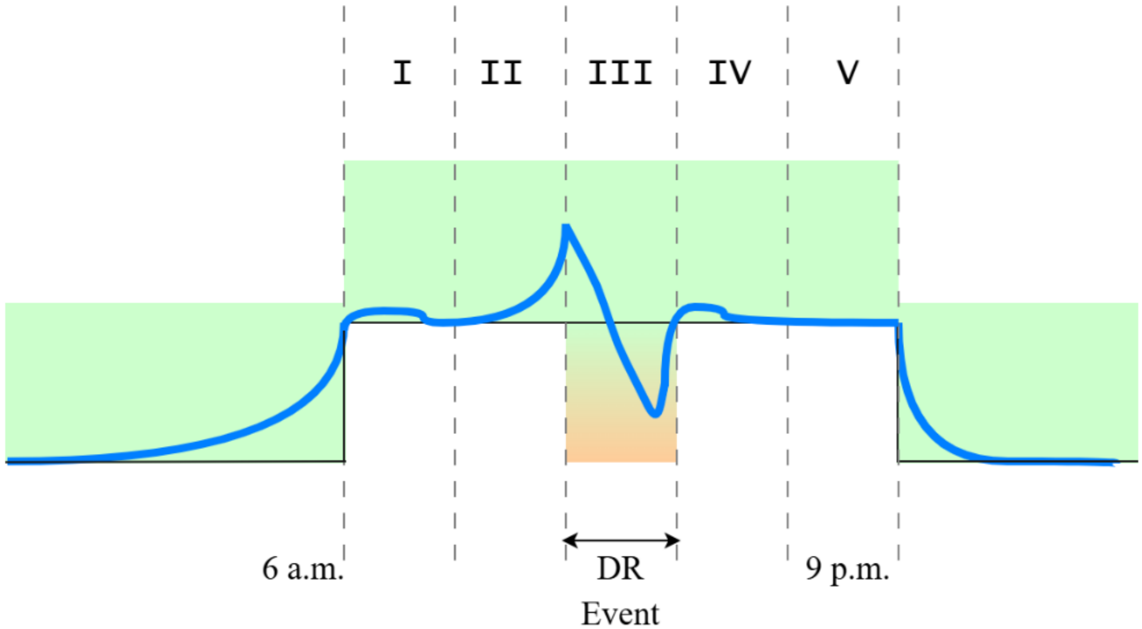

Figure 5.8-.DR Designer for DR Event between 12 a.m. and 3 p.m. Set Point Temperature in black line, and Effective interior node temperature in blue. Green area defines the acceptable temperature violation.

The choice of using such DR Designer is done to analyse any possible strategy in the Day Ahead Coordination (DAC) market, informing the energy aggregator of each possible power reduction during the day. The DR Designer consider two different electricity tariffs, with 0.05 $/kWh for off-peak and 0.50 $/kWh for on-peak hours.

Flexibility Quantification

The quantification of the building energy flexibility is performed using the building energy flexibility index (BEFI) [95], defined to show the potential is either average or percentage, as shown in Eq. (5.12).

$$\overline{BEFI}(t, Dt) = \frac{\sum_{t}^{t+Dt} P_{\text{Ref}} \cdot dt - \sum_{t}^{t+Dt} P_{\text{Flex}} \cdot dt}{Dt}$$

$$BEFI\% = \frac{\overline{P_{\text{Ref}}} - \overline{P_{\text{Flex}}}}{\overline{P_{\text{Ref}}}} \times 100 \tag{5.12}$$

Where, P_{ref} [kW/kW_{inst}] is the power demand in the reference scenario, P_{Flex} [kW/kW_{inst}] is the power demand in flexibility scenario, and Dt [h] is the duration of the flexibility event. By superimposing consecutive DR events, the flexibility performance for each of the five event periods proposed by the DR Designer is characterized during peak hours (Δh_{Peak}) in terms of average reduction, as shown in Eq. (5.13):

$$BEFC_{[6\text{ a.m.- }9\text{ p.m.}]} = \left[\text{BEFI\%}_{I\text{-}DR} \cup BEFI\%_{II\text{-}DR} \cup BEFI\%_{III\text{-}DR} \cup BEFI\%_{IV\text{-}DR} \cup BEFI\%_{V\text{-}DR}\right] \quad (5.13)$$

This approach enables the creation of a comprehensive building energy flexibility curve (BEFC), illustrating the dynamic response of the analyzed day to varying DR signals.

Flexibility Benchmarking and Clustering

This section presents the final step of the proposed benchmarking procedure, considering each BEFC as representation of the flexibility potential of the corresponding home, and define a flexibility-informed benchmark based on this trend

Time Series Clustering for Benchmarking

The proposed methodology leverages smart thermostat data to develop accurate models suitable for predictive load management frameworks. The BEFI is extended into the BEFC, which represents the average anticipated demand reduction during each DR event. The BEFC, expressed as a time series and formulated in Eq. (5.13), quantifies flexibility potential as a percentage of the reference demand, excluding the need for a standardization process.

The benchmarking procedure employs pattern recognition to identify similarities and differences in the BEFC across the population. Time-series data of BEFC trends are analyzed using k-Means clustering, enabling the identification of fundamental load shape profiles that represent flexibility potential [400]. Each cluster reveals a group of homes with highly correlated BEFC trends, characterized by a shared centroid profile, which serves as the expected flexibility pattern for that cluster. Homes within the same cluster exhibit similar flexibility behaviors, while those in different clusters demonstrate distinct trends.

To ensure the clustering approach effectively captures relevant features, it is critical to select an appropriate distance metric, determine the optimal number of clusters, and establish robust measures to evaluate within-cluster similarity and across-cluster dissimilarity [400]. These steps ensure that the clustering results accurately reflect the variability in flexibility potential across the population.

Dynamic Time Warping (DTW) is a distance method for time series that works by minimizing the cumulative distance between the analysed profiles. Given two timeseries Π and P, and their elements π_i and ρ_j, the distance can be formulated as shown in Eq. (5.14).

$$DTW(\Pi, \mathrm{P}) = \min \sum_{i,j} d(\pi_i, \rho_j)^2 \quad (5.14)$$

The clustering design is characterized by the Calinski-Harabasz Score, used to select the most informative number of clusters (k) [396]. Cluster performances are addressed by the Cohesion— shown in Eq. (5.15), and the Separation— shown in Eq. (5.16).

$$\text{Cohesion} = \sum_{i=1}^{k} \sum_{x \in Ci} \left\| x - c_i \right\|^2 \quad (5.15)$$

Where, for a given cluster C_i its cohesion score is considered as the sum of squared distances from each data point (x) to the corresponding centroid (c_i).

$$\text{Separation} = \sum_{i=1}^{k} n_{C_i} \left\| c_i - c \right\|^2 \quad (5.16)$$

Where, for a given cluster C_i its Separation score is considered as the sum of squared distances from each centroid (c_i) to the overall centroid adjusted by the number of datapoints (n_{C_i}).

5.2.2 *Flexibility-Informed Benchmarking procedure*

The number of eligible homes with adequate dataset for model calibration is assessed to be equal to 4760 in both Montreal and Toronto area. The first relevant outcome is that only the 42.7% of these presents satisfactory accuracy metrics in prediction.

The RMSE for training and testing, and the FIT function are presented in Figure 5.9.

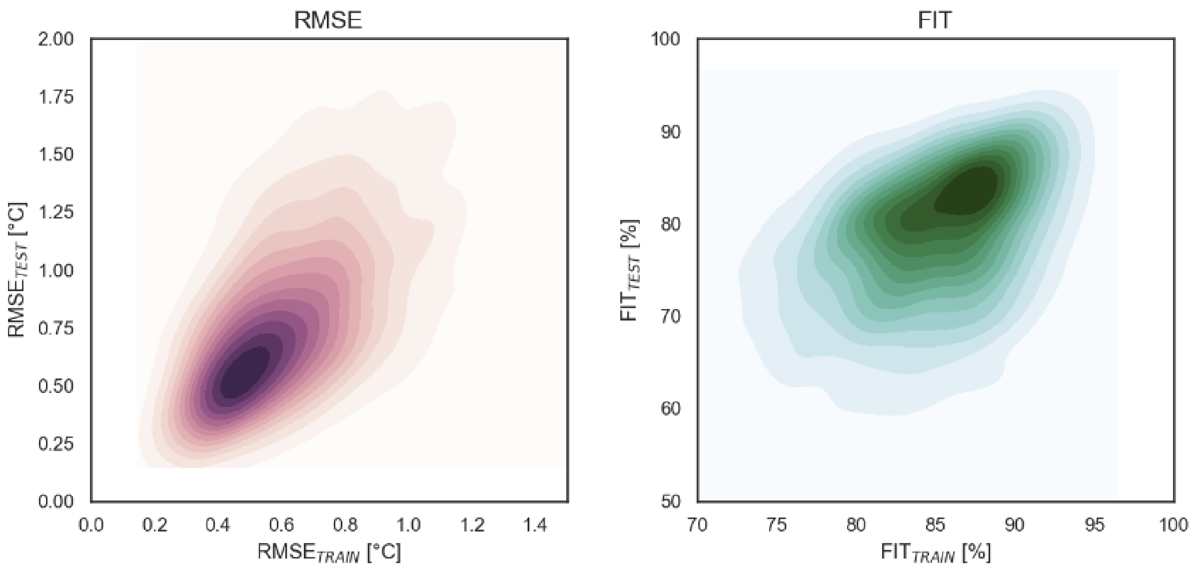

Figure 5.9- Model Evaluation metrics for the 2031 acceptable models

The model accuracy exhibits variability, with the majority of homes showing a $RMSE_{TRAIN}$ between 0.35°C and 0.70°C for 24-hour-ahead predictions. A smaller fraction of the dataset demonstrates $RMSE_{TRAIN}$ values exceeding 0.70°C. The accompanying figure, illustrating the FIT function, reveals a similar distribution: approximately 70% of homes achieve a FIT_{TRAIN} above 77% and a FIT_{TEST} above 67%. Notably, 40% of homes attain FIT_{TRAIN} values exceeding 85% and FIT_{TEST} values exceeding 80%.

The activation of the BEF expressed as BEFC, highlights the distinct impacts of the scenarios proposed by the DR Designer. The intrinsic characteristics of BEFI%—a key performance indicator grounded in baseline requirements [399]—quantifies flexibility potential as a percentage of the reference profile. This metric provides valuable insights but is inherently complex due to uncertainties associated with load forecasting.

As detailed in Section *5.2.1-Method*, the clustering algorithm was designed to balance the Separation and Cohesion metrics. This approach revealed that six clusters effectively capture the patterns within both the single-city subpopulations and the overall dataset, ensuring robust pattern recognition. The resulting clusters are presented in Figure 5.10.

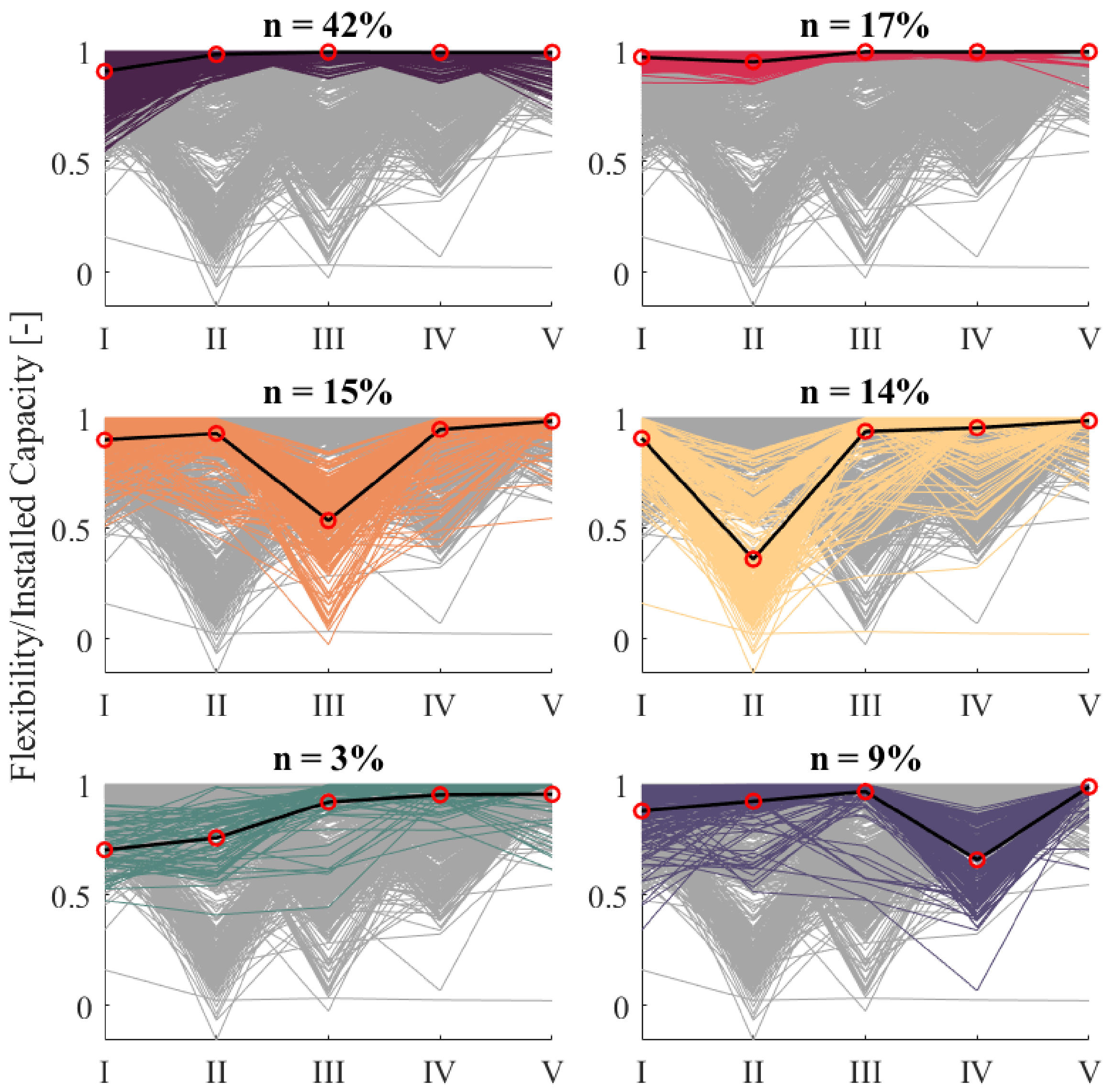

Figure 5.10-The resulting clusters of the flexibility-informed benchmarking procedure for the 2031 homes

Most of the residential buildings—42% of the population— exhibits an almost constant BEFC, with potential flexibility almost equals to the installed capacity during the day, and slightly lower values for the I event (6 a.m. to 9 a.m.). This means that these homes can provide almost 100% BEFI% for any three hours critical peak events but the first. The second group is populated by the 17% of the eligible dataset, and it shows the best performance and the least time dependence. Customers in this group can be considered as the most valuable.

The third, the fourth and the sixth group account for 15, 14, and 9% respectively. These groups exhibit decent BEFC values during the day, with the only difference of a severe valley in the central events III, II and IV. This result can be considered as an indication of when not to trigger these clients, limiting their ability to provide BEFI% above 80% in the remaining events of the day.

The fifth group is characterized by an increasing BEFI%, the limited number of homes in this group — only 3%—might suggest that outliers but coherent curves are grouped together. In fact, this group presents the lowest Separation index, especially compared to the first and second, but a relatively satisfactory cohesion metric.

The influence of weather and solar radiation on the resulting BEFC is a critical factor, particularly in the context of the DAC market. Quantifying flexibility potential under varying weather conditions—characterized by clear-sunny and cloudy-overcast days—provides valuable insights for designing effective DR strategies.

Four representative customers are shown in Figure 5.11, each exhibiting distinct characteristics in their flexibility response to solar radiation:

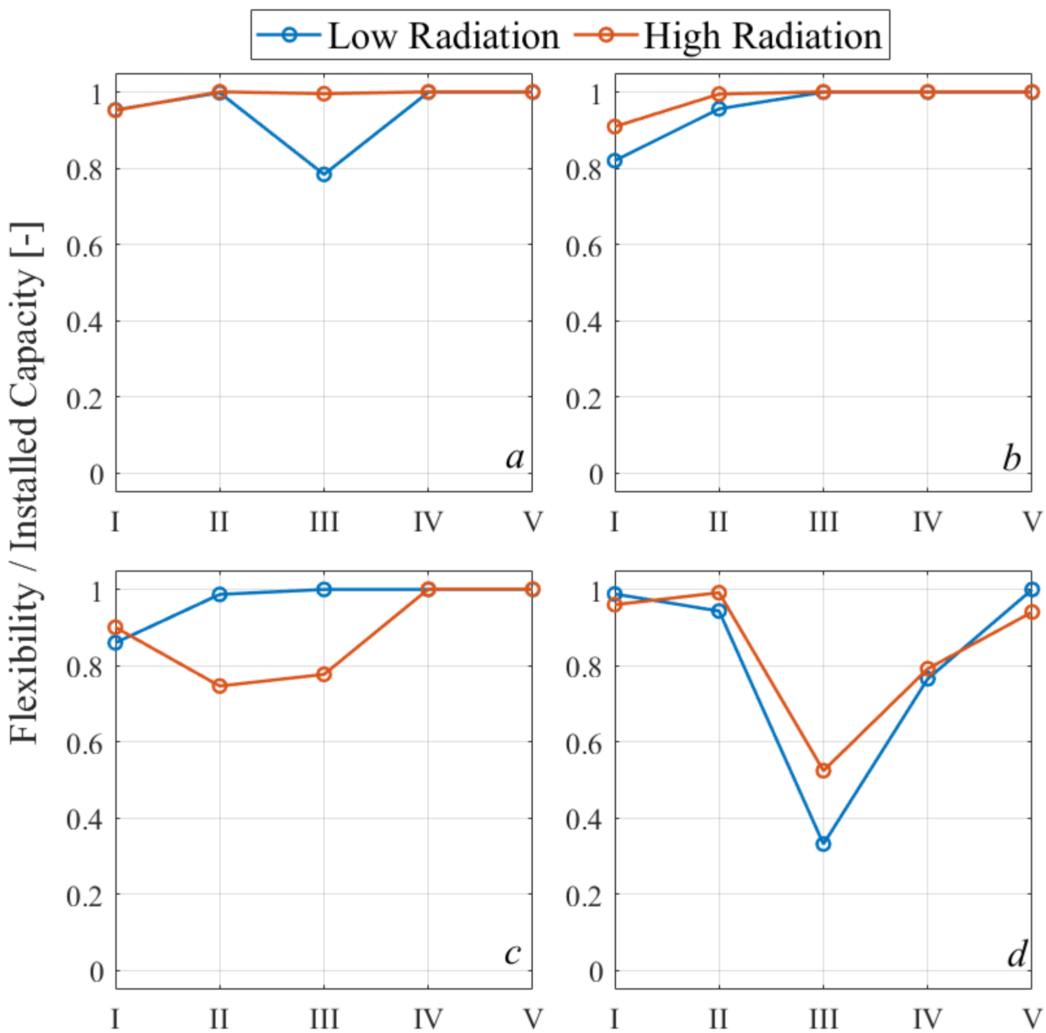

Figure 5.11- Four representative homes showing the impact of solar radiation on the flexibility potential.

Figure 5.11.*a* represents the BEFC for a customer in the Third Group, which demonstrates a BEFC content near unity throughout the day, except during the III event (12 p.m.–3 p.m.). On sunny days, the higher solar radiation reduces baseline consumption, thereby increasing the BEFC potential

significantly. This behavior highlights the role of solar radiation in amplifying flexibility potential during midday periods when solar gains peak. A similar behaviour is shown in Figure 5.11.*b* with a customer in the First Group, with a BEFC content close to one throughout the day except during the I event (6 a.m.–9 a.m.). Customers in this group are less sensitive to changes in solar radiation, with only marginal improvements (<10%) observed during the I and II events. This stability suggests that their flexibility potential is less influenced by solar-driven variations in the reference load profile. Figure 5.11.*c* shows a customer which experiences a significant reduction in BEFC under higher solar radiation conditions. In this case, the reference load profile, already influenced by solar radiation, is substantially diminished, limiting the flexibility improvement. This scenario underscores the need to consider weather dependencies in flexibility assessments, as high solar gains may not uniformly benefit all customers. Figure 5.11.*d* shows another customer from the Third Group with a more variable BEFC content, with the flexibility curve shifted upward under higher solar radiation. This indicates that increased solar radiation consistently enhances percentage flexibility potential, emphasizing the importance of accurate solar forecasting for optimal DR program design.

5.3 Conclusions

This study establishes a robust framework for benchmarking building energy flexibility through a systematic methodology encompassing data preprocessing, flexibility quantification, and clustering-based benchmarking. By integrating advanced modelling techniques, weather-dependent scenarios, and flexibility-informed key performance indicators, the research delivers actionable insights into the dynamic behaviour of building portfolios under demand response programs.

The findings highlight the potential of high-dimensional benchmarking approaches to complement traditional metrics like Energy Usage Intensity, enabling more nuanced assessments of energy performance and flexibility potential. The proposed clustering framework identified six distinct groups of buildings with unique flexibility patterns. These ranged from highly consistent performers, such as Group 1 (42% of the population) with nearly constant flexibility potential, to specialized cases like Group 5, which exhibited increasing flexibility trends under specific conditions. Other groups displayed variability during central DR events or under certain weather conditions, underscoring the need for targeted and adaptive DR strategies tailored to the operational characteristics of each cluster.

These results demonstrate the value of segmentation in optimizing demand-side interventions.

The benchmarking system offers a practical and scalable tool for utilities and policymakers to design and implement demand-side management strategies. By capturing the variability of energy use across building portfolios and quantifying flexibility potential under different scenarios, this methodology equips stakeholders with actionable insights for load management, grid stability, and energy efficiency improvements. Additionally, the system’s ability to integrate weather dependencies and time-series analysis enhances its utility for dynamic DR program design and tariff structuring, ensuring greater alignment with real-world conditions.

In conclusion, the proposed benchmarking procedure advances the state of the art in assessing building energy flexibility. By empowering energy aggregators, utilities, and policymakers to develop adaptive, equitable, and efficient DSM strategies, this research contributes significantly to the transition toward sustainable and resilient energy systems. Future research should explore scalability across different climatic regions, integrate additional influencing factors such as occupant behaviour, and investigate the long-term impacts of flexibility-driven energy policies.

6. *Case study*

6.1 Building Portfolio – The 30 Houses

As part of the 30 Houses ESA Project under the NSERC Hydro Quebec Industrial Chair, a measured dataset is used in the present investigation. The case study investigated is in Trois-Rivieres, Quebec, Canada, as shown in Figure 6.1.

Figure 6.1. The virtual neighborhood of ten 2storey houses in Trois-Rivieres, Quebec, Canada

Each house is equipped with smart thermostats. Information for indoor temperature, setpoint temperature, and heating output is provided for each thermal zone. The heating output is reported every hour, while the sampling time of internal and ambient temperatures varies. For that purpose, linear interpolation has been considered for resampling. Measurements from power meters are collected for space heating, kitchen and main appliances, and domestic hot water production. The average winter profiles are depicted in Figure 6.2. The top figures are showing the load profile from smart meters, identifying most representative trends and outliers. The bottom figures show the impact of space heating and DHW. For some of the presented houses- such as House 68, House 73, House 82, etc- the contemporary use of space heating and DHW is generating steep ramps in the daily profiles, whereas in other configurations – such as House 83, House 91, and House 92- the profile is quite flat throughout the day.

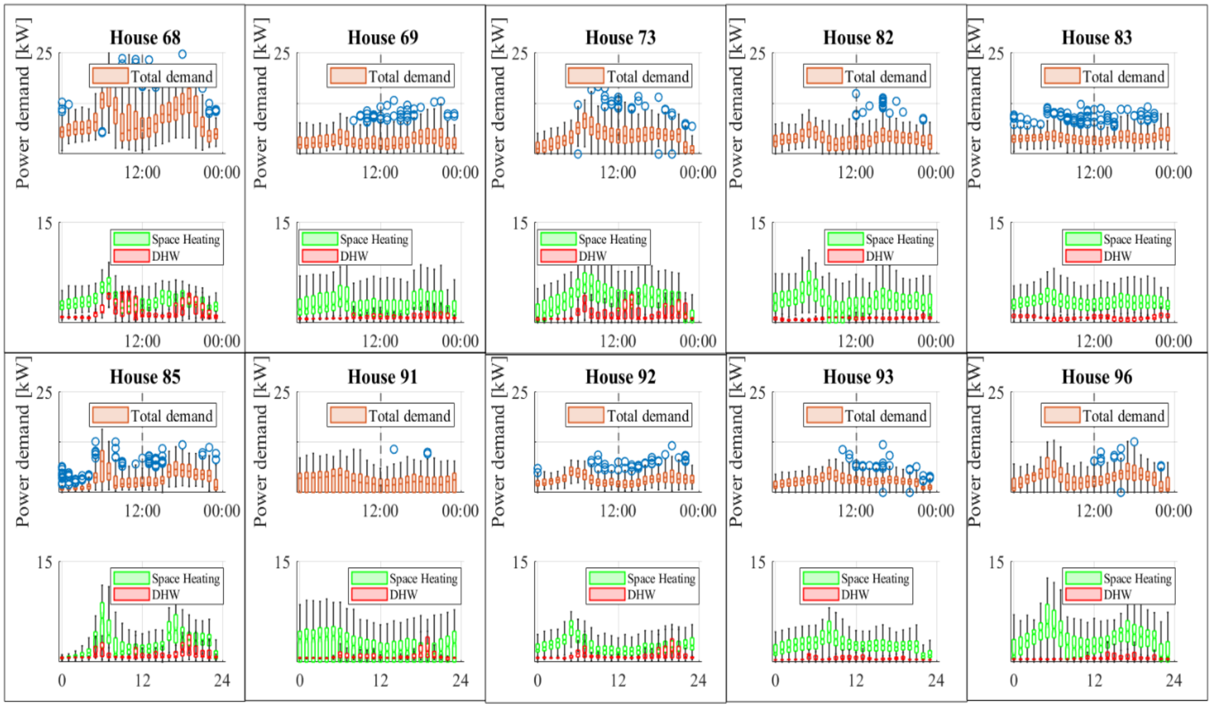

Figure 6.2- Measured data from power meters of the ten houses considered: On top the overall power demand, at the bottom space heating and DHW.

The metadata provides information about the floor area, the number of thermostats for each household, the number of occupants, as well as information about construction and renovation. Moreover, each thermal zone is equipped with a baseboard heater and a dedicated thermostat. The Simulation Energetique Des Batiments (SIMEB) weather data service provided measurements of OAT, relative humidity, wind speed and direction, and GHI for the selected location.

Additional details on the monitoring infrastructure of this case study are presented in *9.1-Details and Description of the 30 Houses dataset.*

6.2 Experimental House for Building Energetics (EHBE)

The Experimental House for Building Energetics is an unoccupied fully instrumented research house of Hydro-Québec located in Shawinigan, Québec. It is a 60 m^2-footprint two-storey house with an excavated basement and an attached garage. The dimensions of the home are 7.6 meters by 7.9 meters, and it has a basement that is not insulated. The first floor comprises the living room, dining room, kitchen, and a compact powder room, whereas the second floor encompasses 3 bedrooms and a full bathroom. The property in question is a conventional Québec dwelling, with R-20 insulation for the walls, R-30 insulation for the roof, and a total of 19 m^2 of fenestration made of double-glass windows with an air gap. The building walls exemplify the characteristic lightweight wood-framed houses commonly found in Québec, yet the basement is more thermally massive and features an exposed concrete floor. The house is positioned at a 35° angle west of south and is heated using an electric baseboard in each room, with each baseboard having its own thermostat for control. Figure 6.3 displays the arrangement of the house, while Table 6.1 provides information on the position and heating capacity of each electric baseboard.

Table 6.1. Installed heating capacity of electric baseboards

Abbreviation	*Room*	*Location*	*Orientation*	*Heating capacity (kW)*
SS	Basement 1	Basement	-	2
SS2	Basement 2	Basement	-	2
CU	Kitchen	First Floor	North	1.5
SM	Dining Room	First Floor	North	1.25
SA	Living Room	First Floor	South	1.5
SE	Powder Room	First Floor	South	–
C1	Bedroom 1	Second Floor	North	1.25
C2	Bedroom 2	Second Floor	South	1.25
C3	Bedroom 3	Second Floor	South	1.25
SB	Bathroom	Second Floor	North	1
Total				**13**

Figure 6.3. Layout of Experimental House for Building Energetics

This facility provides the opportunity to control set point temperature of smart thermostats and charging cycles of a 5kWh BESS. 16 PV modules are connected to a MPPT and an inverter. Two electrical panels (main and secondary) regulate power provision through a smart switch. The home is grid-connected, but bidirectionality is discouraged. The power schematic is shown in Figure 6.4

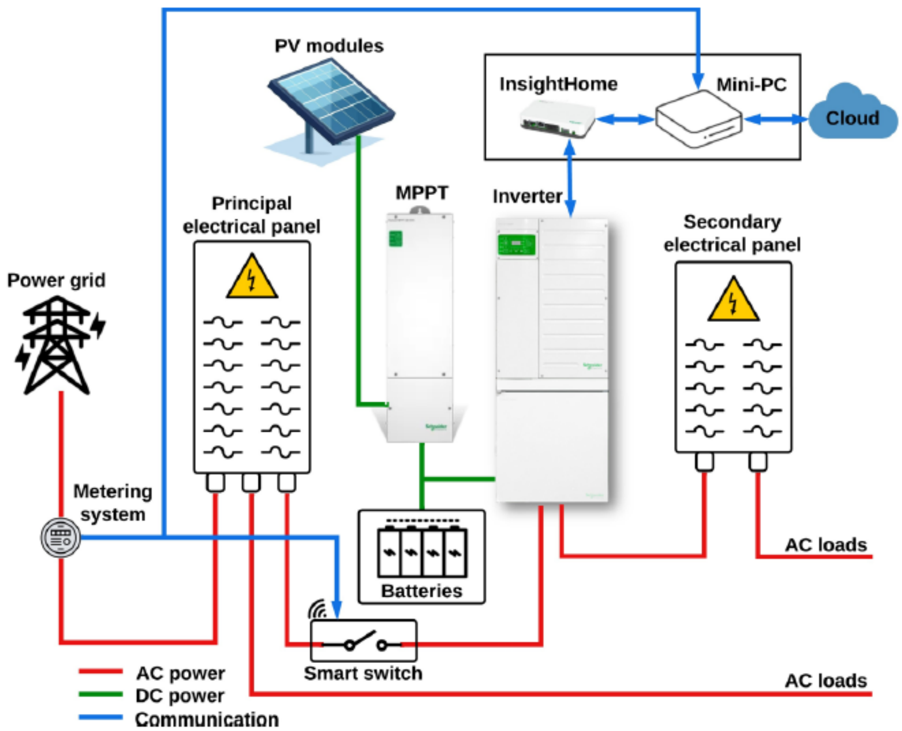

Figure 6.4. AC/DC Power schematic of EHBE

The communication layer needs to be further explained because different protocols and systems governates the information-sharing process between devices, actuators, and the cloud.

Thermostats and charging/discharging power from BESS are control variables, it is possible in fact to control set point temperature in each room, as well as power rate every 15 minutes. The state functions are therefore the indoor temperature and the state of charge.

MQTT (Message Queuing Telemetry Transport) protocol is used to bridge the gap between Zigbee devices and the home automation system, along with a Raspberry Pi4.

Two representational state transfer (REST) APIs are used:

1) Schneider *InsightHome* (for BESS/PV/inverter) [401]
2) *Home Assistant* [402].

Influxdb is used as time series database [403]. The weather service used in this experiment is *Solcast* forecast API [404], triggered each up to 6 times a day.

As per *Table 6.1. Installed heating capacity of electric baseboards* , the ten thermal zones of the experimental house are equipped with indoor temperature, set point temperature, and heating source readings.

An example of the dataset is presented for the investigation conducted by the Industrial Chair between February 24th and February 28th, 2024.

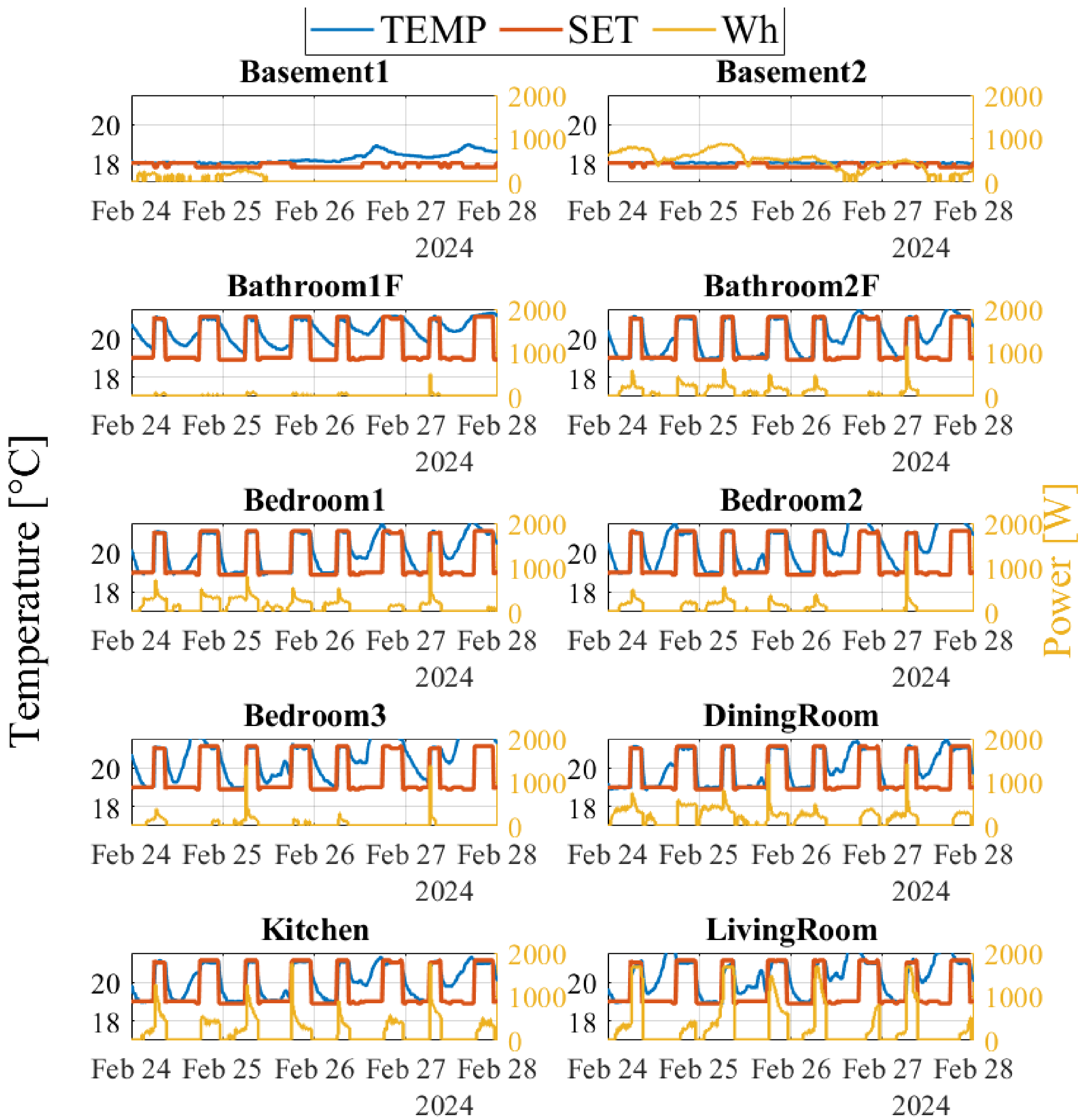

Figure 6.5. Temperature and Heating trends of each controllable room.

6.3 North American Smart Thermostat large dataset

Ecobee, one of the main smart thermostat companies in North America, offers researchers with user-provided metadata from 104,693 homes located in 51 countries, including a distinct identifier for each residence, the country, province/state, and city where the residence is situated, the floor area and age of the residence, the number of occupants and floors, the architectural style of the residence, whether it has a heat pump or not, and the type of auxiliary fuel used, via the *Donate Your Data* program [405]. The Ecobee thermostats collect 5-minute interval measurements for each house, which include data on the indoor temperature, cooling, and heating setpoints, outdoor temperature, relative humidity, upper and lower setpoints, and the runtime of the heating and cooling systems in seconds [288]. Figure 6.6 provides a visual overview on the homes, with a focus on the considered area. Choosing a diameter of 1°LAT/LONG around the city center of Toronto and Montreal, there are 5270 residential customers—4509 for Toronto, ON and 529 for Montreal, QB—equipped with connected thermostats.

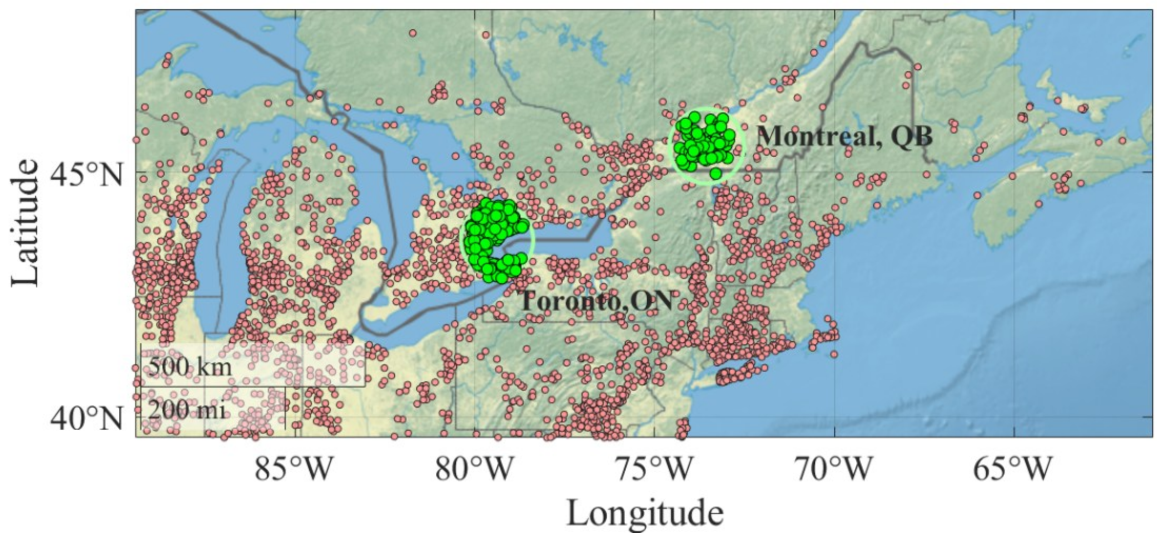

Figure 6.6. Eligible customers of Ecobee in North America

This dataset has been used by researchers and energy experts to have a better understanding of the energy trajectory for space heating in North America. Some of the available literature exploited Ecobee's large dataset to investigate load coordination. Chen et al. [406] conceptualize and develop a methodology for coordinating thermostatically controlled loads towards an open-source simulation environment [407]. Other works have proposed multi-layer hierarchical controller [408], or peer-to-peer market frameworks [409] with the same aim.

Other researchers investigated occupant and users' preferences. Jung et al. [410] created a residential occupancy schedule simulator using homes in US, Sarran et al. [411] analysed almost 7000 houses to study overrides during demand response events. The benefit of using Ecobee's dataset for urban planning is also evident, with investigation on mapping GHG emissions in municipalities [412], understand the effects of climate, seasonal and prices [413], and to prioritize retrofitting interventions [414].

The quality of this dataset motivated some researchers to investigate model generation at the aggregated scale, recurring to a Bayesian neural network to support parameter estimation in grey box modelling for around 9000 homes [415], or leveraging deep transfer learning to enhance accuracy in building modelling [416]. A comprehensive analysis of the flexibility potential of a building cluster was proposed by Martinez et al. [417] where 337 dwelling units from Ecobee populated the building portfolio with the goal of understanding the most influencing factors and the correlated uncertainty.

Lastly, Vallianos et al. [288] proposed a method to calibrate and control through an MPC framework almost 8000 homes in the Canadian provinces of Ontario and Quebec. The authors studied the effect of training data length, interval, and calibration horizon and concluded that 15-minute data intervals, 7 days of data and calibration horizon of one day showed the best results. Another important result was given by the MPC, able to reduce the median high-price peak power by 60 and 70% compared to traditional controllers. In a second work [179], the authors analysed the effect of model structure and the inner correlation between parameter estimation and metadata information, concluding that 61% of the models were classified as good fits, and 80% were of 5^{th} order.

7. Conclusions

The evolution from the “follow-the-demand” to the “follow-the-supply” paradigm has fundamentally reshaped load management practices, unlocking transformative opportunities for all stakeholders in the energy sector. This shift aligns with global efforts to transition towards a cleaner, more efficient, and resilient energy system, where the electrification and digitalization of residential buildings play pivotal roles. These processes are not merely technological advancements but are heralded as key enablers of the broader energy transition, bridging the gap between renewable energy supply and demand. Within this evolving framework, energy aggregators are emerging as essential mediators between the grid and end-users, leveraging the energy flexibility potential of participants in DSM programs. This intermediary role highlights the need for innovative solutions to manage energy systems within the built environment under increasingly dynamic conditions.

The thesis addresses this critical need by proposing a comprehensive methodology for optimal load management and aggregation strategies in grid-interactive building clusters. Organized into three interlinked chapters, this work provides a systematic approach to overcome scalability, generalizability, and operational challenges faced by energy aggregators in order to assess the most suitable control-oriented formulation, an exploratory framework to analyse the dynamic consumption baseline, and the creation of a flexibility-oriented benchmarking procedure in grid-aware demand response programs.

The **first chapter** introduces a control-oriented framework for modelling and forecasting energy demand in residential buildings. This chapter emphasizes the balance between model accuracy and complexity, recognizing that the practical application at the energy aggregator level requires scalable solutions. The methodology also proposes a generalized control technique capable of managing diverse configurations of DERs, TESs, and static and dynamic electrical storages, such as BESS and EVs. This lays the foundation for a distributed-hierarchical control scheme that addresses generalizability issues, making it applicable to various energy scenarios.

The **second chapter** delves into the evolution of baseline predictions in DR programs. It investigates the influence of advanced technologies, DERs, and EVs on load profiles and flexibility potential within day-ahead coordination markets. By examining how these factors interact with energy efficiency and DSM programs, the research identifies critical trade-offs and opportunities for optimizing both profitability and operational performance. The results provide energy aggregators with actionable insights to balance enhanced flexibility against potential adverse reactions, ensuring sustainable participation in energy markets.

The **third chapter** focuses on diversification strategies in portfolio management for energy aggregators. It presents a novel flexibility-informed benchmarking procedure that simplifies the identification and management of customer groups based on their flexibility potential. By integrating dynamic pricing mechanisms, this chapter also examines the impact of price variations on load behaviour in day-ahead markets, revealing opportunities to enhance both efficiency and profitability. These findings underscore the importance of personalized approaches to portfolio diversification, empowering aggregators to maximize the value of their managed resources.

The outcomes of the presented methodology have demonstrated the applicability of a supervisory-to-local control routine via dynamic optimization through an economic Model Predictive Control, and the possibility of generating personalized pricing structures by identifying macro groups of consumers within the portfolio management. The proposed methodology has been validated through three distinct case studies, each involving varying numbers of households, resolution levels, and data granularity. These practical scenarios ensure that the findings are grounded in real-world applicability, aligning with the goals of the Industrial Chair to which this research contributes. However, more research is needed on the comfort-related aspect of the optimization, developing methodologies that account for the whole thermal comfort assessment, rather than addressing acceptable temperature variations from setpoint. Future fully electric and digitalized residential houses will provide valuable data aiming at this objective.

The research has been rigorously disseminated and discussed with leading institutions and professionals worldwide, including the International Energy Agency (IEA)- Annex 82: Energy Flexible Buildings Towards Resilient Low Carbon Energy Systems and ASHRAE communities. Their feedback and interest have enriched the work, ensuring its relevance and contribution to the global energy community.

7.1 Contributions

The major contributions of this thesis are listed below:

- *Development of a Robust Methodology for Building Energy Aggregation*

Introduced a reliable procedure for aggregating individual thermal zones using unsupervised clustering techniques designing an iterative routine to group thermal zones based on similar thermal properties, reducing the computational complexity of optimization problems while maintaining accuracy. The methodology is validated on a virtual community comprising nine individual thermal zones, demonstrating its ability to generalize across different buildings and conditions.

- *Ensemble Model for Load Prediction*

Created a 24-hour-ahead predictive model using a stacking approach to integrate thermal and electrical loads, enabling the generation of accurate load profiles by leveraging the superposition of diverse energy system dynamics, improving the prediction of aggregated consumption patterns.

- *Design of a Hierarchical-Distributed Control Framework*

Developed a hierarchical energy management system combining supervisory and local controllers, utilizing a Control Volume approach, focusing on five key control variables to control building power demand. This scheme enhances communication between supervisory systems and local controllers and streamline power management goals while minimizing the complexity of involved variables.

- *Quantification of the Impact of Advanced Technologies on Baseline Consumption*

Investigated the impact of high-performing technologies, including photovoltaics, photovoltaic-thermal systems, and heat pumps, on the flexibility potential of building portfolios. Simulated scenario-based analyses to demonstrate how these technologies reshape load profiles and improve grid flexibility. Evaluated the influence of residential EV charging infrastructure, examining both mono- and bi-directional charging modes and their effects on feeder-level power consumption and grid stress.

- *Dynamic Portfolio Management for Virtual Communities*

Developed dynamic strategies to optimize household prioritization within virtual communities, introducing personalized pricing tariffs to desynchronize flexibility activation and minimize grid congestion during demand response events. Implemented flexibility benchmarking to group buildings based on performance and thermal properties, creating scalable solutions for energy aggregators, and addressing challenges of demand peaks and operational inefficiencies in virtual energy systems.

- *Github repository for more relevant codes*

The three most important codes for: thermal model calibration using MRI, clustering approach with kMeans for Timeseries using DTW, and the optimization routine of eMPC can be found at : github_link

7.2 Scientific Publications

The contributions will be in the form of a thesis, journal, and conference papers.

Parts of the work have already been published or submitted to be published in scientific journals and international conferences:

Published Journal Papers

1. Petrucci, A., Kloutse, F.A., Buonomano, Athienitis, A., Development of energy aggregators for virtual communities: The energy efficiency-flexibility nexus for demand response (2023), Renewable Energy. 215: p.118975 . https://doi.org/10.1016/j.renene.2023.118975
2. Petrucci, G. Barone, A. Buonomano, A. Athienitis, Modelling of a multi-stage energy management control routine for energy demand forecasting, flexibility, and optimization of smart communities using a Recurrent Neural Network. *Energy Conversion and Management*. 268 (2022), https://doi.org/10.1016/j.enconman.2022.115995
3. Maturo, A., Petrucci, A., Forzano, C., Giuzio, G.F., Buonomano, A., Athienitis A. Design, and environmental sustainability assessment of energy-independent communities: The case study of a livestock farm in the North of Italy, Accepted July 8, 2021. Energy Reports. Volume 7, Pages 8091- 8107 (2021) https://doi.org/10.1016/j.egyr.2021.05.080

Under Review

4. Petrucci, A., Vallianos C., Candanedo JA., Delcroix B., Buonomano, A., Athienitis, A., *Coordinated Load Management of Building Clusters and EV Charging: an economic Model Predictive Control investigation in Demand Response,* Submitted to Energy Conversion and Management, December 2024

Submission Stage

5. IEA Annex 82. Contribution in Polly B., Henze G.,…, Petrucci et al., "*An international common exercise to evaluate the energy flexibility potential of building portfolios*", TBD (Applied Energy/ Journal of Building Simulation)
6. Petrucci, A., Vallianos C., Candanedo JA., Buonomano, A., Athienitis, A., *Data-Driven Benchmarking of Residential Energy Flexibility with Aggregated Demand Analysis for Enhanced Grid Stability*

Conference Proceedings

7. Petrucci, A., Vallianos, C., Candanedo, JA., Delcroix B., Buonomano, A., Athienitis, A., Towards dynamic pricing algorithm for residential buildings: A Model Predictive Control framework for load aggregation. In: 2024 3rd International Conference on Energy Transition in the Mediterranean Area (SyNERGY MED). IEEE, 2024. p. 1-5. (BEST Student Paper AWARD).https://doi.org/10.1109/SyNERGYMED62435.2024.10799262
8. Petrucci, A., Athienitis, A., Kloutse, F.A., *Baseline Estimation of Heating Consumption for Different House Archetypes Through a Data-Driven Clustering Methodology*, In *International Conference on Building Energy and Environment* (pp. 949-957). Singapore: Springer Nature Singapore. 10.1007/978-981-19-9822-5_101

Accepted

9. Petrucci, A., Vallianos, C., Candanedo, JA., Buonomano, A., Athienitis, A., *Leveraging the potential of load aggregators in residential clusters: A Model Predictive Control (MPC) framework for the Toronto metropolitan area*, Proceeding of the 19th Conference on Sustainable Development of Energy, Water and Environmental Systems (SDEWES), Rome, 10.09.2024.
10. Petrucci, A., Buonomano, A., Athienitis, A., Delcroix B., *Model order reduction based on clustering approach for Energy Aggregators in Demand Response,* ASHRAE Winter Conference 2024, Chicago, IL.
11. Petrucci, A., Kloutse, F.A., Buonomano, Athienitis, A. A data-driven methodology to optimize the integrated energy management of Electric Vehicles and a cluster of residential buildings in a Demand Response Program., Proceeding of the 18th Conference on Sustainable Development of Energy, Water and Environmental Systems (SDEWES), Dubrovnik, 23.09.2023.
12. Petrucci, A., Kloutse, F.A., Buonomano, Athienitis, A. Implementation of different renewable technologies in a Canadian virtual community, Proceeding of the 17th Conference on Sustainable Development of Energy, Water and Environmental Systems (SDEWES), Paphos, 07.11.2022.
13. Petrucci, A., Buonomano, A., Barone, G., Athienitis, A. Application of Artificial Neural Network for energy management of a smart community, Proceeding of the 16th Conference on Sustainable Development of Energy, Water and Environmental Systems (SDEWES), Dubrovnik,10-15.10.2021.
14. Petrucci, A., Maturo A., Buonomano, A., Barone, G., Athienitis, A. Thermal and electrical modelling of a double-skin façades integrating bifacial photovoltaics: energy and economic performance assessment, Proceeding of the 16th Conference on Sustainable Development of Energy, Water and Environmental Systems (SDEWES), Dubrovnik,10-15.10.2021.
15. Petrucci, A. Barone G., Buonomano, A., Giuzio, G.F., Forzano, C., Maturo, A., Palombo, A. Dynamic Simulation for Highly Energy-Independent Communities Design: The Case Study of a Livestock Farm in the North of Italy. Proceeding of the 15th Conference on Sustainable Development of Energy, Water and Environmental Systems (SDEWES), Cologne,1-5.9.(2020).

In Press

16. Petrucci, A., LFR Vasquez, A., Delcroix B., Athienitis, A., The Effect of Dynamic Pricing on Residential Buildings: An Experimental Investigation to Evaluate Energy Flexibility Potential and Temperature Variation in Demand Response, ASHRAE Winter Conference 2025, Orlando, FL.

7.3 Recommendation for future work

The transition from simulated to experimental results remains a critical area of uncertainty. Real-world implementation and deployment of the proposed methodology may reveal unforeseen challenges and complexities that theoretical models cannot fully anticipate. Key among these challenges is the integration of the methodology within the constraints of existing infrastructure, including computing power, device interoperability, and household behavioural dynamics. Future research should prioritize experimental validation, conducting feasibility studies in real virtual communities to provide detailed quantitative insights. These studies could serve to refine the methodology further while contributing valuable data to the literature and inspiring subsequent investigations.

One promising direction is diversifying calibration techniques for thermal models. While the current approach provides a solid foundation, exploring more advanced online weight-tuning techniques—such as Kalman filtering or adaptive parameter estimation—could enhance model precision. Similarly, the ensemble model for load profiling could benefit from integrating state-of-the-art machine learning and artificial intelligence (AI) approaches. With the surge in AI-driven modelling techniques, the opportunity to leverage broader, more robust modelling alternatives could lead to significant performance improvements in prediction accuracy, computational efficiency, and adaptability to dynamic conditions. Specifically, an interesting area of application is the analysis of nonlinearities due to different seasons of operation, and the concept of transfer learning.

Another critical issue lies in the costs associated with installing and maintaining the monitoring and control infrastructure necessary for deploying these methodologies. While the financial benefits of increased energy flexibility ultimately accrue to the investor, the grid itself is the primary beneficiary, raising important questions about the role of energy providers in incentivizing such investments. At present, energy aggregators and demand response consultants often shy away from residential applications due to the challenges they pose—such as complex modelling requirements, privacy concerns, and high initial capital costs. This highlights the need for strategic policy interventions and incentive structures that make residential demand response more viable and attractive for stakeholders.

In this context, applications at the scale of condominiums or multi-unit residential buildings might be promising. These settings offer distinct advantages: repetitive housing units with uniform geometric characteristics, centralized or adjustable supply systems equipped with metering and sub-metering capabilities, and the presence of a building manager who can act as an intermediary. Such environments provide a mature platform for deploying supervisory controllers capable of managing advanced mechanisms like peer-to-peer energy trading and aggregated self-consumption.

Finally, a comprehensive investigation into the social and economic dynamics of residential demand response programs would be beneficial. Understanding homeowner motivations, privacy concerns, and willingness to participate in flexibility programs can inform the design of strategic commercial campaigns. These campaigns could emphasize the benefits of energy security, economic savings, and the potential for residential units to generate income through energy trading. By aligning the interests of energy aggregators, utilities, and end-users, such efforts could foster greater adoption and success in the residential sector.

8. *References*

1. Bithas, K., et al., *A brief history of energy use in human societies.* Revisiting the Energy-Development Link: Evidence from the 20th Century for Knowledge-based Developing Economies, 2016: p. 5-10.
2. Hydro-Quebec, *Consommation de différentes formes d'énergie par secteur d'activité au Québec*. 2019.
3. Hainsch, K., et al., *Energy transition scenarios: What policies, societal attitudes, and technology developments will realize the EU Green Deal?* 2022. **239**: p. 122067.
4. Conlon, T., et al., *Assessing trade-offs among electrification and grid decarbonization in a clean energy transition: Application to New York State.* 2022. **249**: p. 123787.
5. Bayomi, N. and J.E. Fernandez, *Trends of energy demand in the Middle East: A sectoral level analysis.* International journal of energy research, 2018. **42**(2): p. 731-753.
6. Vanzetta, J. and C. Schneiders. *Current and imminent challenges for the transmission system operator in Germany*. in *2011 2nd IEEE PES International Conference and Exhibition on Innovative Smart Grid Technologies*. 2011. IEEE.
7. Rossi, M., et al., *TSO-DSO coordination to acquire services from distribution grids: Simulations, cost-benefit analysis and regulatory conclusions from the SmartNet project.* 2020. **189**: p. 106700.
8. Fleten, S.-E., et al., *Structural estimation of switching costs for peaking power plants.* European Journal of Operational Research, 2020. **285**(1): p. 23-33.
9. HydroQuebec, *Forecasting Plan for Energy Infrastructure*. (2023).
10. Naderi, S., et al., *Demand response via pre-cooling and solar pre-cooling: a review.* 2022: p. 112340.
11. Perry, C., H. Bastian, and D. York, *Grid-interactive efficient building utility programs: State of the market.* American Council for an Energy-Efficient Economy, Washington, DC, Tech. Rep, 2019.
12. Choi, W., et al., *Smart home and internet of things: A bibliometric study.* Journal of Cleaner Production, 2021. **301**: p. 126908.
13. Yan, W., et al., *Survey on recent smart gateways for smart home: Systems, technologies, and challenges.* 2022. **33**(6): p. e4067.
14. Buonomano, A., G. Barone, and C. Forzano, *Advanced energy technologies, methods, and policies to support the sustainable development of energy, water and environment systems.* Energy Reports, 2022. **8**: p. 4844-4853.
15. Herc, L., A. Pfeifer, and N. Duić, *Optimization of the possible pathways for gradual energy system decarbonization.* Renewable Energy, 2022. **193**: p. 617-633.
16. Neukomm, M., V. Nubbe, and R. Fares, *Grid-interactive efficient buildings*. 2019, US Dept. of Energy (USDOE), Washington DC (United States); Navigant ….
17. ACEEE, *Grid-Interactive Efficient Building, Utility Programs: State of the Market*. 2019.
18. *EnergyWise Business*. Duke Carolinas, Duke Progress]. Available from: www.duke-energy.com/business/products/energywisebusiness.
19. PG&E. *Automated Demand Response program*. Available from: www.pge.com/en_US/large-business/save-energy-andmoney/.
20. DominionEnergy. *Smart Thermostat Program*. 2024; Available from: www.scc.virginia.gov/docketsearch/DOCS/3l3501!.PDF.
21. Satchwell, A., et al., *A national roadmap for grid-interactive efficient buildings*. 2021, Lawrence Berkeley National Lab.(LBNL), Berkeley, CA (United States).

22. Aguero, J.R., et al., *Modernizing the grid: Challenges and opportunities for a sustainable future.* IEEE Power Energy Magazine, 2017. **15**(3): p. 74-83.
23. Arowoiya, V.A., R.C. Moehler, and Y. Fang, *Digital twin technology for thermal comfort and energy efficiency in buildings: A state-of-the-art and future directions.* Energy and Built Environment, 2024. **5**(5): p. 641-656.
24. Amiri, A., J. Ottelin, and J. Sorvari, *Are LEED-certified buildings energy-efficient in practice?* Sustainability, 2019. **11**(6): p. 1672.
25. Vosoughkhosravi, S., L. Dixon-Grasso, and A. Jafari, *The impact of LEED certification on energy performance and occupant satisfaction: A case study of residential college buildings.* Journal of Building Engineering, 2022. **59**: p. 105097.
26. Ferreira, A., et al., *A critical analysis of LEED, BREEAM and DGNB as sustainability assessment methods for retail buildings.* Journal of Building Engineering, 2023. **66**: p. 105825.
27. Hu, S., et al., *A systematic review of building energy sufficiency towards energy and climate targets.* Renewable Sustainable Energy Reviews, 2023. **181**: p. 113316.
28. Goubran, S., T. Walker, and C. Cucuzzella, *Green building standards and the united nations' sustainable development goals.* Journal of Environmental Management, 2023. **326**: p. 116552.
29. Papadakis, N. and D.A. Katsaprakakis, *A review of energy efficiency interventions in public buildings.* Energies, 2023. **16**(17): p. 6329.
30. Díaz-López, C., et al., *Passive action strategies in schools: A scientific mapping towards eco-efficiency in educational buildings.* Building Engineering, 2022. **45**: p. 103598.
31. Athienitis, A.K. and M. Santamouris, *Thermal analysis and design of passive solar buildings*. 2013: Routledge.
32. Athienitis, A. and W. O'Brien, *Net ZEB case studies: Modeling, Design, Optimization of Net-Zero Energy Buildings.* 2015: p. 241-350.
33. Athienitis, A.K. and W. O'Brien, *Modeling, design, and optimization of net-zero energy buildings*. 2015: Wiley Online Library.
34. Zhang, N., et al., *Regional comprehensive environmental impact assessment of renewable energy system in California.* 2022. **376**: p. 134349.
35. Morovat, N., *Model-Based Predictive Control Strategies and Renewable Energy Integration for Energy Flexibility Enhancement in School Buildings*. 2024, Concordia University.
36. Young, G., *Independent Electricity System Operator, Ontario, Spokesperson.* Get set for darker November mornings, The Toronto Star, 2005. **21**: p. A1.
37. Ontario, G.o. https://www.ontario.ca/page/ontario-energy-snapshot. 2024.
38. Jensen, S.Ø., et al., *Annex 67: Energy Flexible Buildings-Energy Flexibility as a key asset in a smart building future*. 2017.
39. Lawrence, T.M., et al., *Ten questions concerning integrating smart buildings into the smart grid.* 2016. **108**: p. 273-283.
40. WorldMeteorologicalOrganization, *Mitigation of climate change.* Assessment Report: Intergovernmental Panel on Climate Change (IPCC), 2014. **1454**: p. 147.
41. Wu, Y., et al., *Towards collective energy Community: Potential roles of microgrid and blockchain to go beyond P2P energy trading.* Applied Energy, 2022. **314**: p. 119003.
42. Good, N. and P. Mancarella, *Flexibility in multi-energy communities with electrical and thermal storage: A stochastic, robust approach for multi-service demand response.* IEEE Transactions on Smart Grid, 2017. **10**(1): p. 503-513.

43. Marique, A.-F. and S. Reiter, *A simplified framework to assess the feasibility of zero-energy at the neighbourhood/community scale.* Energy and Buildings, 2014. **82**: p. 114-122.
44. Thiers, S. and B. Peuportier, *Energy and environmental assessment of two high energy performance residential buildings.* Building and Environment, 2012. **51**: p. 276-284.
45. Braeuer, F., et al., *Optimal system design for energy communities in multi-family buildings: the case of the German Tenant Electricity Law.* 2022. **305**: p. 117884.
46. Gjorgievski, V.Z., S. Cundeva, and G.E. Georghiou, *Social arrangements, technical designs and impacts of energy communities: A review.* Renewable Energy, 2021. **169**: p. 1138-1156.
47. Casalicchio, V., et al., *Renewable energy communities: business models of multi-family housing buildings.* 2021: p. 261-276.
48. Park, D.-H., et al., *A bidding-based peer-to-peer energy transaction model considering the green energy preference in virtual energy community.* 2021. **9**: p. 87410-87419.
49. Kerscher, S. and P. Arboleya, *The key role of aggregators in the energy transition under the latest European regulatory framework.* International Journal of Electrical Power & Energy Systems, 2022. **134**: p. 107361.
50. Koirala, B.P., et al., *Energetic communities for community energy: A review of key issues and trends shaping integrated community energy systems.* 2016. **56**: p. 722-744.
51. Kazmi, H., et al., *Towards data-driven energy communities: A review of open-source datasets, models and tools.* 2021. **148**: p. 111290.
52. European-Union. *Eurostat-Electricity Price statistics*. 2024; Available from: https://ec.europa.eu/eurostat/statistics-explained/index.php?title=Electricity_price_statistics.
53. Gopinath, R., et al., *Energy management using non-intrusive load monitoring techniques–State-of-the-art and future research directions.* 2020. **62**: p. 102411.
54. Zhang, R., et al., *Stochastic optimal energy management and pricing for load serving entity with aggregated TCLs of smart buildings: A Stackelberg game approach.* IEEE Transactions on industrial informatics, 2020. **17**(3): p. 1821-1830.
55. Yin, S., et al., *Energy management for aggregate prosumers in a virtual power plant: A robust Stackelberg game approach.* International Journal of Electrical Power & Energy Systems, 2020. **117**: p. 105605.
56. De Vizia, C., et al., *A win-win algorithm for learning the flexibility of aggregated residential appliances.* IEEE Access, 2021. **9**: p. 150495-150507.
57. Chen, J., et al., *Optimal operation between electric power aggregator and electric vehicle based on Stackelberg game model.* Energy Reports, 2023. **9**: p. 699-706.
58. Li, J., et al., *Grid-side flexibility of power systems in integrating large-scale renewable generations: A critical review on concepts, formulations and solution approaches.* Renewable Sustainable Energy Reviews, 2018. **93**: p. 272-284.
59. Mariano-Hernández, D., et al., *A review of strategies for building energy management system: Model predictive control, demand side management, optimization, and fault detect & diagnosis.* 2021. **33**: p. 101692.
60. Clevenger, C.M., J.R. Haymaker, and M.J.J.o.c.i.c.e. Jalili, *Demonstrating the impact of the occupant on building performance.* 2014. **28**(1): p. 99-102.
61. Dudek, G.J.N., *Neural networks for pattern-based short-term load forecasting: A comparative study.* 2016. **205**: p. 64-74.
62. Capozzoli, A., M.S. Piscitelli, and S.J.E.P. Brandi, *Mining typical load profiles in buildings to support energy management in the smart city context.* 2017. **134**: p. 865-874.

63. Fu, T.-c., *A review on time series data mining.* Engineering Applications of Artificial Intelligence, 2011. **24**(1): p. 164-181.
64. Zhou, Y.J.E. and Buildings, *Climate change adaptation with energy resilience in energy districts—A state-of-the-art review.* 2022: p. 112649.
65. Faruqui, A. and N. Lessem, *Managing the benefits and costs of dynamic pricing in Australia.* Prepared for the Australian Energy Market Commission (AEMC), 2012.
66. Fiedler, T. and P.-M. Mircea. *Energy management systems according to the ISO 50001 standard—Challenges and benefits*. in *2012 International conference on applied and theoretical electricity (ICATE)*. 2012. IEEE.
67. Hermans, M., et al., *On the temporal granularity of joint energy-reserve markets in a high-RES system.* Applied Energy, 2021. **297**: p. 117172.
68. Exizidis, L., et al., *Impact of public aggregate wind forecasts on electricity market outcomes.* IEEE Transactions on Sustainable Energy, 2017. **8**(4): p. 1394-1405.
69. Bottieau, J., et al., *Very-short-term probabilistic forecasting for a risk-aware participation in the single price imbalance settlement.* IEEE Transactions on Power Systems, 2019. **35**(2): p. 1218-1230.
70. Falchetta, G., et al., *The role of regulatory, market and governance risk for electricity access investment in sub-Saharan Africa.* Energy for Sustainable Development, 2021. **62**: p. 136-150.
71. Stiglitz, J.E., *Government failure vs. market failure: Principles of regulation.* Government markets: toward a new theory of regulation, 2010: p. 13-51.
72. Cook, P., et al., *Competition, regulation and regulatory governance: an overview.* Leading issues in competition, regulation development, 2004: p. 3-35.
73. Kohl, W.L., *National Security and Energy*, in *Encyclopedia of Energy*, C.J. Cleveland, Editor. 2004, Elsevier: New York. p. 193-206.
74. Lu, Y., et al., *A critical review of sustainable energy policies for the promotion of renewable energy sources.* Sustainability, 2020. **12**(12): p. 5078.
75. Jann, W. and K. Wegrich, *Theories of the policy cycle*, in *Handbook of public policy analysis*. 2017, Routledge. p. 69-88.
76. Pontes L, Guilherme A., and S. R., *Modeling energy communities with collective photovoltaic self-consumption: Synergies between a small city and a winery in Portugal.* Energies, 2021. **14**(2): p. 323.
77. Horstink, L., et al., *Collective renewable energy prosumers and the promises of the energy union: Taking stock.* Energies, 2020. **13**(2): p. 421.
78. Junker, R.G., et al., *Characterizing the energy flexibility of buildings and districts.* 2018. **225**: p. 175-182.
79. Sharifi, A., Y.J.R. Yamagata, and S.E. Reviews, *Principles and criteria for assessing urban energy resilience: A literature review.* 2016. **60**: p. 1654-1677.
80. Chen, Y., et al., *Measures to improve energy demand flexibility in buildings for demand response (DR): A review.* Energy and Buildings, 2018. **177**: p. 125-139.
81. Hu, S., et al., *A systematic review of occupant behavior in building energy policy.* Building and Environment, 2020. **175**: p. 106807.
82. Laghari, J., et al., *Application of computational intelligence techniques for load shedding in power systems: A review.* 2013. **75**: p. 130-140.
83. Sharda, S., et al., *Demand side management through load shifting in IoT based HEMS: Overview, challenges and opportunities.* 2021. **65**: p. 102517.

84. Li, H., et al., *Energy flexibility of residential buildings: A systematic review of characterization and quantification methods and applications.* 2021. **3**: p. 100054.
85. Reynders, G., et al., *Energy flexible buildings: An evaluation of definitions and quantification methodologies applied to thermal storage.* 2018. **166**: p. 372-390.
86. Li, R., et al., *Ten questions concerning energy flexibility in buildings.* 2022. **223**: p. 109461.
87. Deb, C. and A. Schlueter, *Review of data-driven energy modelling techniques for building retrofit.* Renewable Sustainable Energy Reviews, 2021. **144**: p. 110990.
88. Li, H., et al., *Data-driven key performance indicators and datasets for building energy flexibility: A review and perspectives.* 2023. **343**: p. 121217.
89. Li, H., T.J.E. Hong, and Buildings, *On data-driven energy flexibility quantification: A framework and case study.* 2023. **296**: p. 113381.
90. Bampoulas, A., et al., *A fundamental unified framework to quantify and characterise energy flexibility of residential buildings with multiple electrical and thermal energy systems.* Applied Energy, 2021. **282**: p. 116096.
91. Zhang, L., N. Good, and P. Mancarella, *Building-to-grid flexibility: Modelling and assessment metrics for residential demand response from heat pump aggregations.* Applied Energy, 2019. **233**: p. 709-723.
92. Reynders, G., J. Diriken, and D.J.A.e. Saelens, *Generic characterization method for energy flexibility: Applied to structural thermal storage in residential buildings.* 2017. **198**: p. 192-202.
93. Yin, R., et al., *Quantifying flexibility of commercial and residential loads for demand response using setpoint changes.* 2016. **177**: p. 149-164.
94. Majdalani, N., et al., *The potential of energy flexibility of space heating and cooling in Portugal.* 2020. **66**: p. 101086.
95. Athienitis, A.K., et al., *Development of a dynamic energy flexibility index for buildings and their interaction with smart grids.* Proceedings of the Summer Study on Energy Efficiency in Buildings, Virtual, 2020: p. 17-21.
96. Petrucci, A., et al., *Modelling of a multi-stage energy management control routine for energy demand forecasting, flexibility, and optimization of smart communities using a Recurrent Neural Network.* Energy Conversion Management, 2022. **268**: p. 115995.
97. Le Dréau, J. and P.J.E. Heiselberg, *Energy flexibility of residential buildings using short term heat storage in the thermal mass.* Energy, 2016. **111**: p. 991-1002.
98. Patsonakis, C., et al., *Optimal, dynamic and reliable demand-response via openadr-compliant multi-agent virtual nodes: Design, implementation & evaluation.* 2021. **314**: p. 127844.
99. Nicolson, M.L., M.J. Fell, and G.M. Huebner, *Consumer demand for time of use electricity tariffs: A systematized review of the empirical evidence.* Renewable Sustainable Energy Reviews, 2018. **97**: p. 276-289.
100. Wang, K., et al., *Dynamic network tariffs: Current practices, key issues and challenges.* Energy Conversion Economics, 2023. **4**(1): p. 23-35.
101. Wang, K., et al., *Dynamic network tariffs: Current practices, key issues and challenges.* 2023. **4**(1): p. 23-35.
102. Honkapuro, S., et al. *Development options for distribution tariff structures in Finland*. in *2017 14th International Conference on the European Energy Market (EEM)*. 2017. IEEE.
103. Riigikogu. *Electricity Market Act* 2022; Available from: https://www.riigiteataja.ee/en/eli/528082014005/consolide.

104. Lu, L. and C. Waddams Price, *Designing distribution network tariffs that are fair for different consumer groups*. 2018.
105. Market, E., *Australian Energy Market Commission*. 2022.
106. Skantze, P. and J. Chapman. *Price dynamics in the deregulated California energy market*. in *IEEE Power Engineering Society. 1999 Winter Meeting (Cat. No. 99CH36233)*. 1999. IEEE.
107. France, E. *The EcoWatt Low carbon hours indicator forecasts*. 2024; Available from: https://analysesetdonnees.rte-france.com/en/ecowatt.
108. Shahid, M.S., et al., *An Assessment of Energy Flexibility Solutions from the Perspective of Low-Tech.* 2023. **16**(7): p. 3298.
109. Corbin, C.D. and G.P. Henze, *Predictive control of residential HVAC and its impact on the grid. Part II: simulation studies of residential HVAC as a supply following resource.* Journal of Building Performance Simulation, 2017. **10**(4): p. 365-377.
110. Muratori, M.J.N.E., *Impact of uncoordinated plug-in electric vehicle charging on residential power demand.* 2018. **3**(3): p. 193-201.
111. Di Piazza, M., et al., *A two-stage Energy Management System for smart buildings reducing the impact of demand uncertainty.* Energy and Buildings, 2017. **139**: p. 1-9.
112. McGlinn, K., et al., *Usability evaluation of a web-based tool for supporting holistic building energy management.* 2017. **84**: p. 154-165.
113. Javed, A., et al., *Experimental testing of a random neural network smart controller using a single zone test chamber.* IET Networks, 2015. **4**(6): p. 350-358.
114. Sivaneasan, B., et al., *Preemptive demand response management for buildings.* 2014. **6**(2): p. 346-356.
115. Parisio, A., et al. *Control of HVAC systems via scenario-based explicit MPC*. in *53rd IEEE conference on decision and control*. 2014. IEEE.
116. Péan, T.Q., J. Salom, and R. Costa-Castelló, *Review of control strategies for improving the energy flexibility provided by heat pump systems in buildings.* Journal of Process Control, 2019. **74**: p. 35-49.
117. Hong, J., et al., *Discrete demand side control performance under dynamic building simulation: A heat pump application.* Renewable energy, 2012. **39**(1): p. 85-95.
118. Miara, M., et al., *Simulation of an Air-to-Water Heat Pump System to Evaluate the Impact of Demand-Side-Management Measures on Efficiency and Load-Shifting Potential.* 2014. **2**(1): p. 90-99.
119. Madani, H., et al., *A descriptive and comparative analysis of three common control techniques for an on/off controlled Ground Source Heat Pump (GSHP) system.* 2013. **65**: p. 1-9.
120. Drgoňa, J., et al., *All you need to know about model predictive control for buildings.* Annual Reviews in Control, 2020. **50**: p. 190-232.
121. Tamashiro, K., et al., *Optimal components capacity based multi-objective optimization and optimal scheduling based MPC-optimization algorithm in smart apartment buildings.* 2023. **278**: p. 112616.
122. Afram, A., F.J.B. Janabi-Sharifi, and Environment, *Theory and applications of HVAC control systems–A review of model predictive control (MPC).* Building and Environment, 2014. **72**: p. 343-355.
123. Clauß, J., et al. *Control strategies for building energy systems to unlock demand side flexibility: a review*. in *15th IBPSA Conference: Building Simulation 2017*. 2017. IBPSA.

124. Kim, I.Y. and O.L. De Weck, *Adaptive weighted-sum method for bi-objective optimization: Pareto front generation.* Structural multidisciplinary optimization, 2005. **29**: p. 149-158.
125. De Coninck, R. and L. Helsen, *Quantification of flexibility in buildings by cost curves–Methodology and application.* Applied Energy, 2016. **162**: p. 653-665.
126. Zhang, K. and M. Kummert. *Evaluating the impact of thermostat control strategies on the energy flexibility of residential buildings for space heating*. in *Building Simulation*. 2021. Springer.
127. Mayne, D., *Robust and stochastic model predictive control: Are we going in the right direction?* Annual Reviews in Control, 2016. **41**: p. 184-192.
128. Sergeyev, Y.D. and R. De Leone, *Numerical infinities and infinitesimals in optimization*. 2022: Springer.
129. Gouda, M.M., S. Danaher, and C.P. Underwood, *Building thermal model reduction using nonlinear constrained optimization.* Building and Environment, 2002. **37**(12): p. 1255-1265.
130. Serale, G., et al., *Model predictive control (MPC) for enhancing building and HVAC system energy efficiency: Problem formulation, applications and opportunities.* Energies, 2018. **11**(3): p. 631.
131. Corbin, C. and G. Henze, *Predictive control of residential HVAC and its impact on the grid. Part I: simulation framework and models.* Journal of Building Performance Simulation, 2017. **10**(3): p. 294-312.
132. Jensen, S.Ø., et al., *Annex 67: Energy Flexible Buildings-Energy Flexibility as a key asset in a smart building future.* 2017.
133. Buonomano, A., *Code-to-code validation and application of a dynamic simulation tool for the building energy performance analysis.* Energies, 2016. **9**(4): p. 301.
134. Runge, J. and R.J.E. Zmeureanu, *Forecasting energy use in buildings using artificial neural networks: A review.* 2019. **12**(17): p. 3254.
135. Gassar, A.A.A. and S.H. Cha, *Energy prediction techniques for large-scale buildings towards a sustainable built environment: A review.* Energy and Buildings, 2020. **224**: p. 110238.
136. Arendt, K., et al. *Comparative analysis of white-, gray-and black-box models for thermal simulation of indoor environment: Teaching building case study*. in *Proceedings of the 2018 Building Performance Modeling Conference and SimBuild co-organized by ASHRAE and IBPSA-USA, Chicago, IL, USA*. 2018.
137. Buonomano, A. and A. Palombo, *Building energy performance analysis by an in-house developed dynamic simulation code: An investigation for different case studies.* Applied Energy, 2014. **113**: p. 788-807.
138. Tang, H. and S. Wang, *Multi-level optimal dispatch strategy and profit-sharing mechanism for unlocking energy flexibilities of non-residential building clusters in electricity markets of multiple flexibility services.* Renewable Energy, 2022. **201**: p. 35-45.
139. Vallianos, C., et al., *Automatic generation of multi-zone RC models using smart thermostat data from homes.* 2022. **277**: p. 112571.
140. Candanedo, J.A., et al., *Control-oriented archetypes: a pathway for the systematic application of advanced controls in buildings.* Journal of Building Performance Simulation, 2022. **15**(4): p. 433-444.
141. Maturo, A., et al., *A novel multi-level predictive management strategy to optimize phase-change energy storage and building-integrated renewable technologies operation under dynamic tariffs.* Energy Conversion Management, 2023. **291**: p. 117220.

142. Li, Y., et al., *Grey-box modeling and application for building energy simulations-A critical review.* 2021. **146**: p. 111174.
143. Berthou, T., et al., *Development and validation of a gray box model to predict thermal behavior of occupied office buildings.* Energy and Buildings, 2014. **74**: p. 91-100.
144. Zou, Y., Q. Zhan, and K. Xiang, *A comprehensive method for optimizing the design of a regular architectural space to improve building performance.* Energy Reports, 2021. **7**: p. 981-996.
145. Barber, K.A. and M. Krarti, *A review of optimization based tools for design and control of building energy systems.* Renewable Sustainable Energy Reviews, 2022. **160**: p. 112359.
146. Gilbert, E.G., *Controllability and observability in multivariable control systems.* Journal of the Society for Industrial Applied Mathematics, 1963. **1**(2): p. 128-151.
147. Southallzy, B., B. Buxtony, and J. Marchant. *Controllability and observability: Tools for Kalman filter design*. in *British Machine Vision Conference*. 1998.
148. Ghiaus, C. and N. Ahmad, *Thermal circuits assembling and state-space extraction for modelling heat transfer in buildings.* Energy, 2020. **195**: p. 117019.
149. Athienitis, A.K., *Thermal analysis and design of passive solar buildings*. 2013: Routledge.
150. Belloto, J. and T. Sokolovski, *Residual analysis in regression.* American Journal of Pharmaceutical Education, 1985. **49**(3): p. 295-303.
151. Thacker, N. and A. Lacey, *Tutorial: The likelihood interpretation of the kalman filter.* Advanced Applied Statistics, 1996. **2**(1): p. 1-11.
152. Durrant-Whyte, H., *Introduction to estimation and the Kalman filter.* Australian Centre for Field Robotics, 2001. **28**(3): p. 65-94.
153. McKinley, T.L. and A.G. Alleyne, *Identification of building model parameters and loads using on-site data logs.* Proceedings of SimBuild, 2008. **3**(1): p. 9-16.
154. Gouda, M., S. Danaher, and C. Underwood, *Building thermal model reduction using nonlinear constrained optimization.* Building and Environment, 2002. **37**(12): p. 1255-1265.
155. Park, H., et al. *Thermal parameter identification of simplified building model with electric appliance*. in *11th International Conference on Electrical Power Quality and Utilisation*. 2011. IEEE.
156. Bernstein, G.M., *Shape measurement biases from underfitting and ellipticity gradients.* Monthly Notices of the Royal Astronomical Society, 2010. **406**(4): p. 2793-2804.
157. Hawkins, D.M., *The problem of overfitting.* Journal of chemical information computer sciences, 2004. **44**(1): p. 1-12.
158. Garrett, A. and J.R. New, *Suitability of ASHRAE guideline 14 metrics for calibration*. 2016, Oak Ridge National Lab.(ORNL), Oak Ridge, TN (United States).
159. Sperber, E., et al., *Reduced-order models for assessing demand response with heat pumps–Insights from the German energy system.* 2020. **223**: p. 110144.
160. Candanedo, J.A., et al., *Control-oriented archetypes: a pathway for the systematic application of advanced controls in buildings.* Journal of Building Performance Simulation, 2022. **15**(4): p. 433-444.
161. Bloomfield, P., *Fourier analysis of time series: an introduction*. 2004: John Wiley & Sons.
162. Reddy, T.A. and G.P. Henze, *Applied data analysis and modeling for energy engineers and scientists*. Vol. 1. 2011: Springer.
163. Arlinghaus, S., *Practical handbook of curve fitting*. 2023: CRC press.

164. González-Romera, E., M.A. Jaramillo-Morán, and D. Carmona-Fernández, *Monthly electric energy demand forecasting with neural networks and Fourier series.* Energy Conversion and Management, 2008. **49**(11): p. 3135-3142.
165. Tsai, C.-L., W.T. Chen, and C.-S. Chang, *Polynomial-Fourier series model for analyzing and predicting electricity consumption in buildings.* Energy and Buildings, 2016. **127**: p. 301-312.
166. Pappas, S.S., et al., *Electricity demand loads modeling using AutoRegressive Moving Average (ARMA) models.* Energy, 2008. **33**(9): p. 1353-1360.
167. Li, Y., Y. Su, and L. Shu, *An ARMAX model for forecasting the power output of a grid connected photovoltaic system.* Renewable Energy, 2014. **66**: p. 78-89.
168. Chen, W., et al., *Evaluation of different boosting ensemble machine learning models and novel deep learning and boosting framework for head-cut gully erosion susceptibility.* Journal of Environmental Management, 2021. **284**: p. 112015.
169. Zhang, C. and Y. Ma, *Ensemble machine learning*. Vol. 144. 2012: Springer.
170. Drucker, H., et al., *Boosting and other ensemble methods.* Neural computation, 1994. **6**(6): p. 1289-1301.
171. Didona, D. and P. Romano, *On bootstrapping machine learning performance predictors via analytical models.* arXiv preprint, 2014.
172. Cutler, A., D.R. Cutler, and J.R. Stevens, *Random forests.* Ensemble machine learning: Methods applications, 2012: p. 157-175.
173. Schapire, R.E., *The boosting approach to machine learning: An overview.* Nonlinear estimation classification, 2003: p. 149-171.
174. Bentéjac, C., A. Csörgő, and G. Martínez-Muñoz, *A comparative analysis of gradient boosting algorithms.* Artificial Intelligence Review, 2021. **54**: p. 1937-1967.
175. Nie, P., et al., *Prediction of home energy consumption based on gradient boosting regression tree.* Energy Reports, 2021. **7**: p. 1246-1255.
176. Reddy, S., et al., *Stacking Deep learning and Machine learning models for short-term energy consumption forecasting.* Advanced Engineering Informatics, 2022. **52**: p. 101542.
177. Peherstorfer, B. and K. Willcox, *Dynamic data-driven reduced-order models.* Computer Methods in Applied Mechanics Engineering, 2015. **291**: p. 21-41.
178. Guo, M. and J.S. Hesthaven, *Data-driven reduced order modeling for time-dependent problems.* Computer methods in applied mechanics engineering, 2019. **345**: p. 75-99.
179. Vallianos, C., J. Candanedo, and A. Athienitis, *Thermal modeling for control applications of 60,000 homes in North America using smart thermostat data.* Energy and Buildings, 2024. **303**: p. 113811.
180. De Coninck, R., et al. *Grey-box building models for model order reduction and control*. in *10th International Modelica Conference*. 2014. Linköping University Electronic Press.
181. Agbi, C., Z. Song, and B. Krogh. *Parameter identifiability for multi-zone building models*. in *2012 IEEE 51st IEEE conference on decision and control (CDC)*. 2012. IEEE.
182. Coakley, D., P. Raftery, and M. Keane, *A review of methods to match building energy simulation models to measured data.* Renewable sustainable energy reviews, 2014. **37**: p. 123-141.
183. Ljung, L., *System identification*, in *Signal analysis and prediction*. 1998, Springer. p. 163-173.
184. Bacher, P. and H. Madsen, *Identifying suitable models for the heat dynamics of buildings.* Energy and Buildings, 2011. **43**(7): p. 1511-1522.

185. InternationalEnergyAgency-(IEA), *IEA EBC - Annex 82 - Energy Flexible Buildings Towards Resilient Low Carbon Energy Systems*.
186. Pallonetto, F., et al., *Demand response algorithms for smart-grid ready residential buildings using machine learning models.* 2019. **239**: p. 1265-1282.
187. Lauster, M., et al., *Low order thermal network models for dynamic simulations of buildings on city district scale.* Building Environment, 2014. **73**: p. 223-231.
188. Kim, D. and J. Braun, *Reduced-order building modeling for application to model-based predictive control 2.* 2012. **1**: p. 2.
189. De Coninck, R., et al. *Grey-box building models for model order reduction and control*. in *10th international Modelica conference*. 2014. Modelica Association and Linköping University Electronic Press.
190. Deng, K., et al. *Building thermal model reduction via aggregation of states*. in *Proceedings of the 2010 American Control Conference*. 2010.
191. O'Brien, W., A. Athienitis, and T. Kesik, *Parametric Analysis to support the integrated design and performance modeling of net-zero energy houses.* ASHRAE Transactions, 2011. **117**(1): p. 945-960.
192. Shi, Z. and W. O'Brien, *Building energy model reduction using model-cluster-reduce pipeline.* Journal of Building Performance Simulation, 2018. **11**(5): p. 553-567.
193. Silvestri, A., et al. *Data-driven reduced order modelling using clusters of thermal dynamics*. in *Proceedings of the 18th IBPSA Conference*. 2023.
194. Kılkış, Ş., et al., *Effective mitigation of climate change with sustainable development of energy, water and environment systems.* Energy conversion management, 2022. **269**: p. 116146.
195. Gržanić, M., et al., *Prosumers as active market participants: A systematic review of evolution of opportunities, models and challenges.* Renewable Sustainable Energy Reviews, 2022. **154**: p. 111859.
196. El Geneidy, R. and B. Howard, *Contracted energy flexibility characteristics of communities: Analysis of a control strategy for demand response.* Applied Energy, 2020. **263**: p. 114600.
197. Hosamo, H.H., et al., *Multiobjective optimization of building energy consumption and thermal comfort based on integrated BIM framework with machine learning-NSGA II.* Energy and Buildings, 2022. **277**: p. 112479.
198. Li, B., et al., *Distributionally robust offering strategy of the aggregator integrating renewable energy generator and energy storage considering uncertainty and connections between the mid-to-long-term and spot electricity markets.* 2022. **201**: p. 400-417.
199. Yan, C., et al., *A multi-timescale cold storage system within energy flexible buildings for power balance management of smart grids.* 2020. **161**: p. 626-634.
200. Tomin, N., et al., *Design and optimal energy management of community microgrids with flexible renewable energy sources.* 2022. **183**: p. 903-921.
201. Yang, X., et al., *Optimal energy flow control strategy for a residential energy local network combined with demand-side management and real-time pricing.* 2017. **150**: p. 177-188.
202. Xu, D., et al., *Real-time multi-energy demand response for high-renewable buildings.* 2023. **281**: p. 112764.
203. Tostado-Véliz, M., et al., *Day-ahead scheduling of 100% isolated communities under uncertainties through a novel stochastic-robust model.* 2022. **328**: p. 120257.
204. Aelenei, D., et al., *Investigating the potential for energy flexibility in an office building with a vertical BIPV and a PV roof system.* Renewable Energy, 2019. **137**: p. 189-197.

205. Zhou, Y. and S. Zheng, *Machine-learning based hybrid demand-side controller for high-rise office buildings with high energy flexibilities.* Applied Energy, 2020. **262**: p. 114416.
206. Dragičević, T., et al., *DC microgrids—Part I: A review of control strategies and stabilization techniques.* IEEE Transactions on power electronics, 2015. **31**(7): p. 4876-4891.
207. Dragičević, T., et al., *DC microgrids—Part II: A review of power architectures, applications, and standardization issues.* IEEE transactions on power electronics, 2015. **31**(5): p. 3528-3549.
208. Wang, P., H. Su, and R. Wang, *Asynchronously intermittent decentralized control of large-scale systems.* IEEE Control Systems Letters, 2022. **6**: p. 2737-2742.
209. Scattolini, R., *Architectures for distributed and hierarchical model predictive control–a review.* Journal of process control, 2009. **19**(5): p. 723-731.
210. Meng, L., et al., *Review on control of DC microgrids and multiple microgrid clusters.* 2017. **5**(3): p. 928-948.
211. Tsikalakis, A.G. and N.D. Hatziargyriou. *Centralized control for optimizing microgrids operation*. in *2011 IEEE power and energy society general meeting*. 2011. IEEE.
212. Vaccaro, A., et al., *An integrated framework for smart microgrids modeling, monitoring, control, communication, and verification.* Proceedings of the IEEE, 2010. **99**(1): p. 119-132.
213. Gungor, V.C., et al., *Smart grid technologies: Communication technologies and standards.* IEEE transactions on Industrial informatics, 2011. **7**(4): p. 529-539.
214. Olfati-Saber, R. *Ultrafast consensus in small-world networks*. in *Proceedings of the 2005, American Control Conference, 2005.* 2005. IEEE.
215. Georges, E., et al., *Residential heat pump as flexible load for direct control service with parametrized duration and rebound effect.* Applied Energy, 2017. **187**: p. 140-153.
216. Mozina, C.J., *Impact of smart grids and green power generation on distribution systems.* IEEE Transactions on Industry Applications, 2013. **49**(3): p. 1079-1090.
217. Saleh, S., P. Pijnenburg, and E. Castillo-Guerra, *Load aggregation from generation-follows-load to load-follows-generation: Residential loads.* IEEE Transactions on Industry Applications, 2016. **53**(2): p. 833-842.
218. Škare, V. and D. Gospić, *Dynamic pricing and customers' perceptions of price fairness in the airline industry.* Tourism: an international interdisciplinary journal, 2015. **63**(4): p. 515-528.
219. Fisher, M., S. Gallino, and J. Li, *Competition-based dynamic pricing in online retailing: A methodology validated with field experiments.* Management science, 2018. **64**(6): p. 2496-2514.
220. Xia, L., K.B. Monroe, and J.L. Cox, *The price is unfair! A conceptual framework of price fairness perceptions.* Journal of marketing, 2004. **68**(4): p. 1-15.
221. Cohen, M.C., *Big Data and Service Operations.* 2018. **27**(9): p. 1709-1723.
222. Gerpott, T.J. and M. Paukert, *Determinants of willingness to pay for smart meters: An empirical analysis of household customers in Germany.* Energy Policy, 2013. **61**: p. 483-495.
223. Hensher, D.A., N. Shore, and K. Train, *Willingness to pay for residential electricity supply quality and reliability.* Applied Energy, 2014. **115**: p. 280-292.
224. Abdullah, S. and P. Mariel, *Choice experiment study on the willingness to pay to improve electricity services.* Energy Policy, 2010. **38**(8): p. 4570-4581.

225. Harsha, P., S. Subramanian, and M. Ettl, *A practical price optimization approach for omnichannel retailing.* INFORMS Journal on Optimization, 2019. **1**(3): p. 241-264.
226. Miklós-Thal, J. and C. Tucker, *Collusion by algorithm: Does better demand prediction facilitate coordination between sellers?* Management Science, 2019. **65**(4): p. 1552-1561.
227. Causone, F., et al., *A data-driven procedure to model occupancy and occupant-related electric load profiles in residential buildings for energy simulation.* Energy and Buildings, 2019. **202**: p. 109342.
228. Martin, K., *Designing ethical algorithms.* MIS Quarterly Executive June, 2019.
229. Aviv, Y. and G. Vulcano, *Dynamic list pricing.* Oxford Academic, 2012.
230. Ghose, A. and K.W. Huang, *Personalized pricing and quality customization.* Journal of Economics Management Strategy, 2009. **18**(4): p. 1095-1135.
231. Steppe, R., *Online price discrimination and personal data: A General Data Protection Regulation perspective.* Computer Law Security Review, 2017. **33**(6): p. 768-785.
232. Pérez-Lombard, L., et al., *A review of benchmarking, rating and labelling concepts within the framework of building energy certification schemes.* 2009. **41**(3): p. 272-278.
233. Casals, X.G., *Analysis of building energy regulation and certification in Europe: Their role, limitations and differences.* Energy and Buildings, 2006. **38**(5): p. 381-392.
234. Scofield, J.H. *Energy star building benchmarking scores: good idea, bad science*. in *ACEEE Summer Study on Energy Efficiency in Buildings*. 2014.
235. Wei, Y., et al., *A review of data-driven approaches for prediction and classification of building energy consumption.* 2018. **82**: p. 1027-1047.
236. Miller, C., et al., *A review of unsupervised statistical learning and visual analytics techniques applied to performance analysis of non-residential buildings.* 2018. **81**: p. 1365-1377.
237. Zhan, S., et al., *Building categorization revisited: A clustering-based approach to using smart meter data for building energy benchmarking.* 2020. **269**: p. 114920.
238. Lavin, A. and D.J.E.e. Klabjan, *Clustering time-series energy data from smart meters.* 2015. **8**: p. 681-689.
239. Jalori, S. and T.A. Reddy, *A New Clustering Method to Identify Outliers and Diurnal Schedules from Building Energy Interval Data.* ASHRAE Transactions, 2015. **121**(2).
240. Fan, C., F. Xiao, and C. Yan, *A framework for knowledge discovery in massive building automation data and its application in building diagnostics.* Automation in Construction, 2015. **50**: p. 81-90.
241. Yang, J., et al., *k-Shape clustering algorithm for building energy usage patterns analysis and forecasting model accuracy improvement.* 2017. **146**: p. 27-37.
242. Piscitelli, M.S., S. Brandi, and A. Capozzoli, *Recognition and classification of typical load profiles in buildings with non-intrusive learning approach.* Applied Energy, 2019. **255**: p. 113727.
243. Verdú, S.V., et al., *Classification, filtering, and identification of electrical customer load patterns through the use of self-organizing maps.* 2006. **21**(4): p. 1672-1682.
244. Park, J.Y., et al., *Apples or oranges? Identification of fundamental load shape profiles for benchmarking buildings using a large and diverse dataset.* 2019. **236**: p. 1280-1295.
245. Müller, M., *Dynamic time warping.* Information retrieval for music motion, 2007: p. 69-84.
246. Niennattrakul, V. and C.A. Ratanamahatana. *On clustering multimedia time series data using k-means and dynamic time warping*. in *2007 International Conference on Multimedia and Ubiquitous Engineering (MUE'07)*. 2007. IEEE.

247. Neter, J., et al., *Applied linear statistical models*. 1996.
248. Duan, M., et al., *A novel hybrid prediction model for aggregated loads of buildings by considering the electric vehicles.* Sustainable Cities and Society, 2018. **41**: p. 205-219.
249. Li, Q., et al., *Applying support vector machine to predict hourly cooling load in the building.* Applied Energy, 2009. **86**(10): p. 2249-2256.
250. Fu, Y., et al., *Using Support Vector Machine to Predict Next Day Electricity Load of Public Buildings with Sub-metering Devices.* Procedia Engineering, 2015. **121**: p. 1016-1022.
251. Samui, P., *Vector machine techniques for modeling of seismic liquefaction data.* Ain Shams Engineering Journal, 2014. **5**(2): p. 355-360.
252. Dong, B., et al., *Applying support vector machines to predict building energy consumption in tropical region.* 2005. **37**(5): p. 545-553.
253. Cao, L.J. and F.E.H. Tay, *Support vector machine with adaptive parameters in financial time series forecasting.* IEEE Transactions on Neural Networks, 2003. **14**(6): p. 1506-1518.
254. Albogamy, F.R., et al., *Efficient energy optimization day-ahead energy forecasting in smart grid considering demand response and microgrids.* 2021. **13**(20): p. 11429.
255. Thilker, C.A., H. Madsen, and J.B. Jørgensen, *Advanced forecasting and disturbance modelling for model predictive control of smart energy systems.* Applied Energy, 2021. **292**: p. 116889.
256. Ma, Z., G. Jiang, and J. Chen, *Physics-informed ensemble learning with residual modeling for enhanced building energy prediction.* Energy and Buildings, 2024. **323**: p. 114853.
257. Panyafong, A., N. Neamsorn, and C. Chaichana, *Heat load estimation using Artificial Neural Network.* Energy Reports, 2020. **6**: p. 742-747.
258. Wang, L., E.W.M. Lee, and R.K.K. Yuen, *Novel dynamic forecasting model for building cooling loads combining an artificial neural network and an ensemble approach.* Applied Energy, 2018. **228**: p. 1740-1753.
259. Glorot, X. and Y. Bengio. *Understanding the difficulty of training deep feedforward neural networks*. in *Proceedings of the thirteenth international conference on artificial intelligence and statistics*. 2010. JMLR Workshop and Conference Proceedings.
260. Neukomm, M., V. Nubbe, and R. Fares, *Grid-interactive efficient buildings technical report series: Overview of research challenges and gaps.* 2019.
261. Li, R., et al., *Ten questions concerning energy flexibility in buildings.* Building and Environment, 2022. **223**: p. 109461.
262. Egea, A., et al., *Experimental performance of a novel scraped surface heat exchanger for latent energy storage for domestic hot water generation.* Renewable Energy, 2022. **193**: p. 870-878.
263. Forzano, C., et al., *Building integrating phase change materials: A dynamic hygrothermal simulation model for system analysis.* 2019. **7**(2): p. 325-342.
264. Chung, M., et al., *Economic evaluation of renewable energy systems for the optimal planning and design in Korea–a case study.* 2018. **6**(4): p. 725-741.
265. Bilardo, M., M. Ferrara, and E. Fabrizio, *The role of solar cooling for nearly zero energy multifamily buildings: Performance analysis across different climates.* Renewable Energy, 2022. **194**: p. 1343-1353.
266. Garcia-Saez, I., et al., *Energy and economic assessment of solar Organic Rankine Cycle for combined heat and power generation in residential applications.* Renewable Energy, 2019. **140**: p. 461-476.
267. Carroll, P., M. Chesser, and P. Lyons, *Air Source Heat Pumps field studies: A systematic literature review.* Renewable and Sustainable Energy Reviews, 2020. **134**: p. 110275.

268. Athienitis, A.K., et al., *Assessing active and passive effects of façade building integrated photovoltaics/thermal systems: Dynamic modelling and simulation.* 2018. **209**: p. 355-382.
269. Sigounis, A.-M., C. Vallianos, and A. Athienitis, *Model predictive control of air-based building integrated PV/T systems for optimal HVAC integration.* Renewable Energy, 2023.
270. Herrando, M., et al., *Solar combined cooling, heating and power systems based on hybrid PVT, PV or solar-thermal collectors for building applications.* 2019. **143**: p. 637-647.
271. Razmjoo, A., et al., *A Technical analysis investigating energy sustainability utilizing reliable renewable energy sources to reduce CO2 emissions in a high potential area.* 2021. **164**: p. 46-57.
272. Gautam, K.R. and G.B. Andresen, *Performance comparison of building-integrated combined photovoltaic thermal solar collectors (BiPVT) with other building-integrated solar technologies.* Solar Energy, 2017. **155**: p. 93-102.
273. Mbewe, D., H. Card, and D. Card, *A model of silicon solar cells for concentrator photovoltaic and photovoltaic/thermal system design.* Solar energy, 1985. **35**(3): p. 247-258.
274. Ibrahim, A., et al., *Efficiencies and improvement potential of building integrated photovoltaic thermal (BIPVT) system.* 2014. **77**: p. 527-534.
275. Novelli, N., et al., *Experimental investigation of a building-integrated, transparent, concentrating photovoltaic and thermal collector.* 2021. **176**: p. 617-634.
276. Maghrabie, H.M., et al., *Building-integrated photovoltaic/thermal (BIPVT) systems: Applications and challenges.* 2021. **45**: p. 101151.
277. Yu, G., et al., *A review of designs and performance of façade-based building integrated photovoltaic-thermal (BIPVT) systems.* 2021. **182**: p. 116081.
278. Shao, N., et al., *Experimental study on the heat transfer performance of the PVT ventilated roof as heat exchanger for heat pump system.* 2022. **187**: p. 995-1008.
279. You, T., et al., *Hybrid photovoltaic/thermal and ground source heat pump: Review and perspective.* 2021. **151**: p. 111569.
280. Yang, T., A.K.J.R. Athienitis, and S.E. Reviews, *A review of research and developments of building-integrated photovoltaic/thermal (BIPV/T) systems.* 2016. **66**: p. 886-912.
281. Qdr, Q.J.U.D.E., Washington, DC, USA, Tech. Rep, *Benefits of demand response in electricity markets and recommendations for achieving them.* 2006. **2006**.
282. Kwak, Y., J.-H. Huh, and C. Jang, *Development of a model predictive control framework through real-time building energy management system data.* Applied Energy, 2015. **155**: p. 1-13.
283. Drgoňa, J., et al., *All you need to know about model predictive control for buildings.* 2020. **50**: p. 190-232.
284. Amato, V., M.D. Knudsen, and S. Petersen, *Dual-zone economic model predictive control of residential space heating for demand response using a single heat meter.* Energy and Buildings, 2023. **281**: p. 112759.
285. Lee, H. and Y. Heo, *Simplified data-driven models for model predictive control of residential buildings.* Energy and Buildings, 2022. **265**: p. 112067.
286. Finck, C., R. Li, and W. Zeiler, *Economic model predictive control for demand flexibility of a residential building.* Energy, 2019. **176**: p. 365-379.
287. Elnour, M., et al., *Neural network-based model predictive control system for optimizing building automation and management systems of sports facilities.* Applied Energy, 2022. **318**: p. 119153.

288. Vallianos, C., J. Candanedo, and A. Athienitis, *Application of a large smart thermostat dataset for model calibration and Model Predictive Control implementation in the residential sector.* Energy, 2023. **278**: p. 127839.
289. Cibin, N., et al., *Machine learning-based algorithms to estimate thermal dynamics of residential buildings with energy flexibility.* Journal of Building Engineering, 2023. **65**: p. 105683.
290. Gržanić, M., et al., *Prosumers as active market participants: A systematic review of evolution of opportunities, models and challenges.* 2022. **154**: p. 111859.
291. Change, I.C.J.C.o.w.g.I.t.t.f.a.r.o.t.i.p.o.c.c., *Mitigation of climate change.* 2014. **1454**: p. 147.
292. Kılkış, Ş., et al., *Accelerating mitigation of climate change with sustainable development of energy, water and environment systems.* Energy Conversion and Management, 2021. **245**: p. 114606.
293. Hosamo, H.H., et al., *Multiobjective optimization of building energy consumption and thermal comfort based on integrated BIM framework with machine learning-NSGA II.* Energy and Buildings, 2022. **277**: p. 112479.
294. Li, B., et al., *Distributionally robust offering strategy of the aggregator integrating renewable energy generator and energy storage considering uncertainty and connections between the mid-to-long-term and spot electricity markets.* Renewable Energy, 2022. **201**: p. 400-417.
295. Yan, C., et al., *A multi-timescale cold storage system within energy flexible buildings for power balance management of smart grids.* Renewable Energy, 2020. **161**: p. 626-634.
296. Tomin, N., et al., *Design and optimal energy management of community microgrids with flexible renewable energy sources.* Renewable Energy, 2022. **183**: p. 903-921.
297. Yang, X., et al., *Optimal energy flow control strategy for a residential energy local network combined with demand-side management and real-time pricing.* Energy and Buildings, 2017. **150**: p. 177-188.
298. Xu, D., et al., *Real-time multi-energy demand response for high-renewable buildings.* Energy and Buildings, 2023. **281**: p. 112764.
299. Tostado-Véliz, M., et al., *Day-ahead scheduling of 100% isolated communities under uncertainties through a novel stochastic-robust model.* Applied Energy, 2022. **328**: p. 120257.
300. Petrucci, A., et al., *Modelling of a multi-stage energy management control routine for energy demand forecasting, flexibility, and optimization of smart communities using a Recurrent Neural Network.* Energy Conversion and Management, 2022. **268**: p. 115995.
301. Zhou, Y. and P.D. Lund, *Peer-to-peer energy sharing and trading of renewable energy in smart communities ─ trading pricing models, decision-making and agent-based collaboration.* Renewable Energy, 2023. **207**: p. 177-193.
302. Maturo, A., et al., *Design and environmental sustainability assessment of energy-independent communities: The case study of a livestock farm in the North of Italy.* Energy Reports, 2021. **7**: p. 8091-8107.
303. Meschede, H.J.R.E., *Analysis on the demand response potential in hotels with varying probabilistic influencing time-series for the Canary Islands.* 2020. **160**: p. 1480-1491.
304. Saloux, E. and J.A. Candanedo, *Sizing and control optimization of thermal energy storage in a solar district heating system.* Energy Reports, 2021. **7**: p. 389-400.

305. Lyden, A. and P.G. Tuohy, *Planning level sizing of heat pumps and hot water tanks incorporating model predictive control and future electricity tariffs.* Energy, 2022. **238**: p. 121731.
306. Noorollahi, Y., A. Golshanfard, and H. Hashemi-Dezaki, *A scenario-based approach for optimal operation of energy hub under different schemes and structures.* Energy, 2022. **251**: p. 123740.
307. Maturo, A., A. Buonomano, and A. Athienitis, *Design for energy flexibility in smart buildings through solar based and thermal storage systems: Modelling, simulation and control for the system optimization.* Energy, 2022. **260**: p. 125024.
308. Okur, Ö., P. Heijnen, and Z. Lukszo, *Aggregator's business models in residential and service sectors: A review of operational and financial aspects.* Renewable and Sustainable Energy Reviews, 2021. **139**: p. 110702.
309. Rounis, E.D., A. Athienitis, and T.J.R.E. Stathopoulos, *Review of air-based PV/T and BIPV/T systems-Performance and modelling.* 2021. **163**: p. 1729-1753.
310. Charron, R. and A.K.J.S.E. Athienitis, *Optimization of the performance of double-facades with integrated photovoltaic panels and motorized blinds.* 2006. **80**(5): p. 482-491.
311. Solar, C. *Hiku 7*.
312. Sadjjadi, B.S., J.-N. Gerdes, and A. Sauer, *Energy flexible heat pumps in industrial energy systems: A review.* Energy Reports, 2023. **9**: p. 386-394.
313. Chen, Y., et al., *Integrated performance analysis of a space heating system assisted by photovoltaic/thermal collectors and ground source heat pump for hotel and office building types.* Renewable Energy, 2021. **169**: p. 925-934.
314. Gaucher-Loksts, E., A. Athienitis, and M. Ouf, *Design and energy flexibility analysis for building integrated photovoltaics-heat pump combinations in a house.* Renewable Energy, 2022. **195**: p. 872-884.
315. Barone, G., et al., *Chapter 6 - Solar thermal collectors*, in *Solar Hydrogen Production*, F. Calise, et al., Editors. 2019, Academic Press. p. 151-178.
316. Bechtel, S., et al., *Influence of thermal energy storage and heat pump parametrization for demand-side-management in a nearly-zero-energy-building using model predictive control.* Energy and Buildings, 2020. **226**: p. 110364.
317. Huan, C., et al., *Performance analysis of a combined solar-assisted heat pump heating system in Xi'an, China.* 2019. **12**(13): p. 2515.
318. Schibuola, L., M.J.E. Scarpa, and Buildings, *Experimental analysis of the performances of a surface water source heat pump.* 2016. **113**: p. 182-188.
319. Pelletier, F. and A.J.T.E.J. Faruqui, *Does dynamic pricing work in a winter-peaking climate? a case study of hydro quebec.* 2022. **35**(2): p. 107080.
320. Athienitis, A.K., et al. *Development of a dynamic energy flexibility index for buildings and their interaction with smart grids*. in *Proceedings of the ACEEE*. 2020.
321. O'Brien, W. and A. Athienitis, *Modeling, design, and optimization of net-zero energy buildings*. 2015: John Wiley & Sons.
322. Dominković, D.F., et al., *Utilizing thermal building mass for storage in district heating systems: Combined building level simulations and system level optimization.* Energy, 2018. **153**: p. 949-966.
323. Khan, S., et al., *A comprehensive review on solar powered electric vehicle charging system.* 2018. **6**(1): p. 54-79.

324. Sears, J., D. Roberts, and K. Glitman. *A comparison of electric vehicle Level 1 and Level 2 charging efficiency*. in *2014 IEEE Conference on Technologies for Sustainability (SusTech)*. 2014. IEEE.
325. Das, H.S., et al., *Electric vehicles standards, charging infrastructure, and impact on grid integration: A technological review.* Renewable Sustainable Energy Reviews, 2020. **120**: p. 109618.
326. Elma, O., U. Cali, and M. Kuzlu, *An overview of bidirectional electric vehicles charging system as a Vehicle to Anything (V2X) under Cyber–Physical Power System (CPPS).* Energy Reports, 2022. **8**: p. 25-32.
327. Crozier, C., T. Morstyn, and M. McCulloch, *The opportunity for smart charging to mitigate the impact of electric vehicles on transmission and distribution systems.* Applied Energy, 2020. **268**: p. 114973.
328. Denholm, P.L., Y. Sun, and T.T. Mai, *An introduction to grid services: Concepts, technical requirements, and provision from wind*. 2019, National Renewable Energy Lab.(NREL), Golden, CO (United States).
329. Almutairi, A. and M.M. Salama, *Assessment and enhancement frameworks for system reliability performance using different PEV charging models.* IEEE Transactions on Sustainable Energy, 2018. **9**(4): p. 1969-1984.
330. Rahman, S., et al., *Comprehensive review & impact analysis of integrating projected electric vehicle charging load to the existing low voltage distribution system.* Renewable and Sustainable Energy Reviews, 2022. **153**: p. 111756.
331. Lee, J., G. Razeghi, and S. Samuelsen, *Utilization of Battery Electric Buses for the Resiliency of Islanded Microgrids.* Applied Energy, 2023. **347**: p. 121295.
332. Colmenar-Santos, A., et al., *Estimating the benefits of vehicle-to-home in islands: The case of the Canary Islands.* Energy, 2017. **134**: p. 311-322.
333. Lyu, C., Y. Jia, and Z. Xu, *Fully decentralized peer-to-peer energy sharing framework for smart buildings with local battery system and aggregated electric vehicles.* Applied Energy, 2021. **299**: p. 117243.
334. Fachrizal, R. and J. Munkhammar, *Improved Photovoltaic Self-Consumption in Residential Buildings with Distributed and Centralized Smart Charging of Electric Vehicles.* 2020. **13**(5): p. 1153.
335. Monteiro, V., et al., *Vehicle electrification: New challenges and opportunities for smart grids.* Energies, 2018. **12**(1): p. 118.
336. Pillai, J.R., B. Bak-Jensen, and P. Thøgersen. *Electric vehicles to support large wind power penetration in future danish power systems*. in *2012 IEEE Vehicle Power and Propulsion Conference*. 2012. IEEE.
337. Anastasiadis, A.G., et al., *Effects of increased electric vehicles into a distribution network.* 2019. **157**: p. 586-593.
338. Anwar, M.B., et al., *Assessing the value of electric vehicle managed charging: a review of methodologies and results.* 2022. **15**(2): p. 466-498.
339. Chung, Y.-W., et al., *Ensemble machine learning-based algorithm for electric vehicle user behavior prediction.* Applied Energy, 2019. **254**: p. 113732.
340. Thomas, D., O. Deblecker, and C.S. Ioakimidis, *Optimal operation of an energy management system for a grid-connected smart building considering photovoltaics' uncertainty and stochastic electric vehicles' driving schedule.* Applied Energy, 2018. **210**: p. 1188-1206.

341. dmlc. *XGBoost Documentation*. 2024; Available from: https://xgboost.readthedocs.io/en/stable/.
342. Jahangir, H., et al., *Plug-in electric vehicle behavior modeling in energy market: A novel deep learning-based approach with clustering technique.* IEEE Transactions on Smart Grid, 2020. **11**(6): p. 4738-4748.
343. Kuang, Y., et al., *Influence analysis of driver behavior and building category on economic performance of electric vehicle to grid and building integration.* Applied Energy, 2017. **207**: p. 427-437.
344. Barone, G., et al., *Energy virtual networks based on electric vehicles for sustainable buildings: System modelling for comparative energy and economic analyses.* Energy, 2022. **242**: p. 122931.
345. Neaimeh, M., et al., *A probabilistic approach to combining smart meter and electric vehicle charging data to investigate distribution network impacts.* Applied Energy, 2015. **157**: p. 688-698.
346. Arias, N.B., et al., *Distribution system services provided by electric vehicles: Recent status, challenges, and future prospects.* 2019. **20**(12): p. 4277-4296.
347. Das, H.S., et al., *Electric vehicles standards, charging infrastructure, and impact on grid integration: A technological review.* 2020. **120**: p. 109618.
348. Fachrizal, R., et al., *Smart charging of electric vehicles considering photovoltaic power production and electricity consumption: A review.* ETransportation, 2020. **4**: p. 100056.
349. Muratori, M. and G. Rizzoni, *Residential Demand Response: Dynamic Energy Management and Time-Varying Electricity Pricing.* IEEE Transactions on Power Systems, 2016. **31**(2): p. 1108-1117.
350. Afentoulis, K.D., et al., *Smart charging business model framework for electric vehicle aggregators.* Applied Energy, 2022. **328**: p. 120179.
351. Barone, G., et al., *Increasing self-consumption of renewable energy through the Building to Vehicle to Building approach applied to multiple users connected in a virtual micro-grid.* Renewable Energy, 2020. **159**: p. 1165-1176.
352. Huang, P., et al., *A coordinated control to improve performance for a building cluster with energy storage, electric vehicles, and energy sharing considered.* Applied energy, 2020. **268**: p. 114983.
353. Zhou, F., et al., *Integrated energy management of a smart community with electric vehicle charging using scenario based stochastic model predictive control.* Energy and Buildings, 2022. **260**: p. 111916.
354. Wang, W.H., V. Moreno-Casas, and J.J.E. Huerta de Soto, *A free-market environmentalist transition toward renewable energy: The cases of Germany, Denmark, and the United Kingdom.* 2021. **14**(15): p. 4659.
355. EIA-861, *Annual Electric Power Industry Report, Form*. 2022.
356. Cedillo, M.H., et al., *Dynamic pricing and control for EV charging stations with solar generation.* Applied Energy, 2022. **326**: p. 119920.
357. Szinai, J.K., et al., *Reduced grid operating costs and renewable energy curtailment with electric vehicle charge management.* Energy Policy, 2020. **136**: p. 111051.
358. Ontario, G.o. 2023; Available from: https://news.ontario.ca/en/release/1002916/ontario-launches-new-ultra-low-overnight-electricity-price-plan.
359. Mesarić, P. and S. Krajcar, *Home demand side management integrated with electric vehicles and renewable energy sources.* Energy and Buildings, 2015. **108**: p. 1-9.

360. Mirakhorli, A. and B. Dong, *Market and behavior driven predictive energy management for residential buildings.* Sustainable Cities and Society, 2018. **38**: p. 723-735.
361. Van Kriekinge, G., et al., *Peak shaving and cost minimization using model predictive control for uni- and bi-directional charging of electric vehicles.* Energy Reports, 2021. **7**: p. 8760-8771.
362. Banwell, P., *Driving Energy Efficiency into North American Electric Vehicle Charging Infrastructure*. 2020.
363. HydroQuebec. *Electric Vehicle Charging Times and Locations*. 2024; Available from: https://www.hydroquebec.com/transportation-electrification/electric-vehicles/charging.html.
364. Farley, R., M. Vervair, and J. Czerniak, *Electric vehicle supply equipment pilot final report.* Washington Utilities Transp. Commission , Tech. Rep, 2019.
365. Wu, C.-H., G.-H. Tzeng, and R.-H. Lin, *A Novel hybrid genetic algorithm for kernel function and parameter optimization in support vector regression.* Expert Systems with Applications, 2009. **36**(3, Part 1): p. 4725-4735.
366. Khezri, R., D. Steen, and L.A. Tuan. *Vehicle to Everything (V2X) - A Survey on Standards and Operational Strategies*. in *2022 IEEE International Conference on Environment and Electrical Engineering and 2022 IEEE Industrial and Commercial Power Systems Europe (EEEIC / I&CPS Europe)*. 2022.
367. Ucer, E., et al., *Modeling and analysis of a fast charging station and evaluation of service quality for electric vehicles.* IEEE Transactions on Transportation Electrification, 2019. **5**(1): p. 215-225.
368. Farley, R., M. Vervair, and J.J.A.C. Czerniak, Oct, *Electric vehicle supply equipment pilot final report.* 2019.
369. Vallianos, C., A. Athienitis, and B. Delcroix, *Automatic generation of multi-zone RC models using smart thermostat data from homes.* Energy and Buildings, 2022. **277**: p. 112571.
370. MATLAB. *Optimization Toolbox*. 2024; Available from: https://it.mathworks.com/products/optimization.html.
371. Lee, Z.J., J.Z.F. Pang, and S.H. Low, *Pricing EV charging service with demand charge.* Electric Power Systems Research, 2020. **189**: p. 106694.
372. Han, X., et al., *A review on the key issues of the lithium ion battery degradation among the whole life cycle.* ETransportation, 2019. **1**: p. 100005.
373. Hu, Z., et al., *Harmonic sources modeling and characterization in modern power systems: A comprehensive overview.* Electric Power Systems Research, 2023. **218**: p. 109234.
374. Vallianos, C., et al., *Online model-based predictive control with smart thermostats: application to an experimental house in Québec.* Journal of Building Performance Simulation, 2024. **17**(1): p. 94-110.
375. Petrucci, A., et al., *Development of energy aggregators for virtual communities: The energy efficiency-flexibility nexus for demand response.* Renewable Energy, 2023. **215**: p. 118975.
376. Li, R., et al., *Ten questions concerning energy flexibility in buildings.* Building and Environment, 2022. **223**: p. 109461.
377. Yang, Y., et al., *Peak-off-peak load shifting: Are public willing to accept the peak and off-peak time of use electricity price?* 2018. **199**: p. 1066-1071.
378. Faruqui, A. and J.R. Malko, *The residential demand for electricity by time-of-use: A survey of twelve experiments with peak load pricing.* Energy, 1983. **8**(10): p. 781-795.

379. Lu, R., S.H. Hong, and X. Zhang, *A Dynamic pricing demand response algorithm for smart grid: Reinforcement learning approach.* Applied Energy, 2018. **220**: p. 220-230.
380. Panda, S., et al., *A comprehensive review on demand side management and market design for renewable energy support and integration.* Energy Reports, 2023. **10**: p. 2228-2250.
381. Cai, Q., et al., *Promoting wind and photovoltaics renewable energy integration through demand response: Dynamic pricing mechanism design and economic analysis for smart residential communities.* Energy, 2022. **261**: p. 125293.
382. Petrucci, A., et al., *Model Order Reduction Based on Clustering Approach for Energy Aggregators in Demand Response.* ASHRAE Conference Proceedings, 2024. **(CH-24-C069)**(Machine Learning and Other Control Systems).
383. Ding, J.Y., et al., *Parallel Machine Scheduling Under Time-of-Use Electricity Prices: New Models and Optimization Approaches.* IEEE Transactions on Automation Science and Engineering, 2016. **13**(2): p. 1138-1154.
384. Yang, H., *Modeling Electricity Prices for Generation Investment and Scheduling Analysis*. 2010, Citeseer.
385. Guillén, E.E., H.W. Samuelson, and J.G.C. Laurent, *Comparing energy and comfort metrics for building benchmarking.* Energy and Buildings, 2019. **205**: p. 109539.
386. EnergyStar, *Energy Star Portfolio Manager.* Environmental Protection Agency, USA., 2018.
387. Luo, N., M. Pritoni, and T. Hong, *An overview of data tools for representing and managing building information and performance data.* Renewable Sustainable Energy Reviews, 2021. **147**: p. 111224.
388. Estrella Guillén, E., H.W. Samuelson, and J.G. Cedeño Laurent, *Comparing energy and comfort metrics for building benchmarking.* Energy and Buildings, 2019. **205**: p. 109539.
389. Gupta, G., et al., *Comparison of energy-efficiency benchmarking methodologies for residential buildings.* Energy and Buildings, 2023. **285**: p. 112920.
390. El Gibari, S., T. Gómez, and F. Ruiz, *Building composite indicators using multicriteria methods: a review.* Business Economics, 2019. **89**(1): p. 1-24.
391. Liu, J., et al., *Defining and applying an electricity demand flexibility benchmarking metrics framework for grid-interactive efficient commercial buildings.* Advances in Applied Energy, 2022. **8**: p. 100107.
392. Liu, J., et al., *Benchmarking demand flexibility in commercial buildings and flattening the duck–addressing baseline and commissioning challenges.* 2022.
393. Ceccolini, C. and R. Sangi, *Benchmarking approaches for assessing the performance of building control strategies: A review.* Energies, 2022. **15**(4): p. 1270.
394. Miller, A. and K. Carbonnier. *New Metrics for Evaluating Building-Grid Integration*. in *2020 ACEEE Summer Study on Energy Efficiency in Buildings (Virtual Conference)*. 2020.
395. Clauß, J., et al., *Control strategies for building energy systems to unlock demand side flexibility–A review.* IBPSA Building Simulation, 2017.
396. Luo, X., et al., *Electric load shape benchmarking for small- and medium-sized commercial buildings.* Applied Energy, 2017. **204**: p. 715-725.
397. Andrews, A. and R.K. Jain, *Beyond Energy Efficiency: A clustering approach to embed demand flexibility into building energy benchmarking.* Applied Energy, 2022. **327**: p. 119989.
398. Wang, J., et al., *Industrial big data analytics: challenges, methodologies, and applications.* arXiv, 2018.

399. Li, H., et al., *Data-driven key performance indicators and datasets for building energy flexibility: A review and perspectives.* Applied Energy, 2023. **343**: p. 121217.
400. Park, J.Y., et al., *Apples or oranges? Identification of fundamental load shape profiles for benchmarking buildings using a large and diverse dataset.* Applied Energy, 2019. **236**: p. 1280-1295.
401. InsightHome, S. *InsightHome and InsightFacility Edge Devices*. 2023; Available from: https://solar.se.com/eu/en/product/insighthome-and-insightfacility-edge-devices/.
402. HomeAssistant. *HomeAssistant RESTAPI*. 2024; Available from: https://www.home-assistant.io/.
403. influxdb. *influxdata 4 TimeSeries*. 2024; Available from: https://www.influxdata.com/.
404. Solcast. *Solar API and Weather Forecasting Tool*. 2024; Available from: https://solcast.com/.
405. Huchuk, B., W. O'Brien, and S. Sanner, *A longitudinal study of thermostat behaviors based on climate, seasonal, and energy price considerations using connected thermostat data.* Building and Environment, 2018. **139**: p. 199-210.
406. Chen, B., et al. *Cohort: Coordination of heterogeneous thermostatically controlled loads for demand flexibility*. in *Proceedings of the 7th ACM International Conference on Systems for Energy-Efficient Buildings, Cities, and Transportation*. 2020.
407. Wang, Z., et al., *AlphaBuilding ResCommunity: A multi-agent virtual testbed for community-level load coordination.* Advances in Applied Energy, 2021. **4**: p. 100061.
408. Amadeh, A., Z.E. Lee, and K. Max Zhang, *Building cluster demand flexibility: An innovative characterization framework and applications at the planning and operational levels.* Energy Conversion and Management, 2023. **283**: p. 116884.
409. Lee, Z.E. and K.M. Zhang, *Regulated peer-to-peer energy markets for harnessing decentralized demand flexibility.* Applied Energy, 2023. **336**: p. 120672.
410. Jung, W., et al., *Smart thermostat data-driven U.S. residential occupancy schedules and development of a U.S. residential occupancy schedule simulator.* Building and Environment, 2023. **243**: p. 110628.
411. Sarran, L., et al., *A data-driven study of thermostat overrides during demand response events.* Energy Policy, 2021. **153**: p. 112290.
412. Hosseinihaghighi, S., et al., *Discovering, processing and consolidating housing stock and smart thermostat data in support of energy end-use mapping and housing retrofit program planning.* Sustainable cities and society, 2022. **78**: p. 103640.
413. Huchuk, B., W. O'Brien, and S. Sanner, *A longitudinal study of thermostat behaviors based on climate, seasonal, and energy price considerations using connected thermostat data.* Building Environment, 2018. **139**: p. 199-210.
414. Doma, A. and M. Ouf, *Data-driven approach to prioritize residential buildings' retrofits in cold climates using smart thermostat data.* Architectural Science Review, 2023. **66**(3): p. 172-186.
415. Hossain, M.M., T. Zhang, and O. Ardakanian, *Identifying grey-box thermal models with Bayesian neural networks.* Energy & Buildings, 2021. **238**: p. 110836.
416. Li, H., et al., *Building thermal dynamics modeling with deep transfer learning using a large residential smart thermostat dataset.* Engineering Applications of Artificial Intelligence, 2024. **130**: p. 107701.
417. Martinez, S., M. Vellei, and J. Le Dréau, *Demand-side flexibility in a residential district: What are the main sources of uncertainty?* Energy and Buildings, 2022. **255**: p. 111595.

9. *Appendix*

9.1 Details and Description of the 30 Houses dataset

The case study of the Building Portfolio is part of the ESA pilot project exploring remote thermostat control for demand management events. 30 single-family homes heated with electric baseboards were equipped with advanced monitoring systems. In each home, standard high-voltage thermostats were replaced with smart, connected devices capable of recording setpoint temperatures, actual room temperatures, and energy consumption.

Additionally, for 10 of these homes that included a wall-mounted heat pump, an Egauge monitoring system was installed at the electrical panel to track the energy usage of key circuits. Finally, total household electricity consumption was also recorded using data from the main utility meter.

Profile of the 30 Homes: Variables and Data Collection
A detailed profile of the 30 homes was created based on various factors. Some data were gathered through a survey completed by the primary resident, while other information was recorded by a technician during the installation of monitoring equipment. The key variables included:

- *Home ID:* A unique identifier for each residence.
- *City:* Location data used to match the home with historical weather conditions.
- *Smart Thermostats:* Number of connected thermostats installed.
- *Occupancy:* Number of residents categorized by age group.
- *Existing Equipment:* Presence of devices such as wall-mounted heat pumps, heat recovery ventilators (HRVs), pools, air conditioners, etc.
- *Home Characteristics:* Number of floors, number of rooms, total area, year of construction, and other structural details.
- *Additional Heating Systems:* Any heating equipment other than electric baseboards.
- *Doors:* Monitoring of door openings and closings.

By compiling these data points, the project aimed to gain deeper insights into energy usage patterns and the impact of smart thermostat integration in different residential settings.

Variables Associated with Smart Thermostats and Other Heating Equipment
Each installed smart thermostat and additional heating system in the homes was documented with the following variables:

- *House ID:* Unique identifier for the home.
- *Device Key:* Unique key for each device. Thermostat identifiers start with "TXX," while other heating equipment identifiers begin with "OXX."
- *Device Type:* Specifies the type of equipment. If labeled as "thermostat," it refers to a smart thermostat with recorded measurement data.
- *Device Location:* The general room or area within the home where the equipment is installed.
- *Device ID / Device ID2:* Internal equipment identifiers (not relevant for analysis).
- *Heat Channel:* The electrical circuit linked to the Egauge sub-metering system (CH1, CH2, CH3, CH4, or CH5) if applicable.
- *Area (sq. feet):* The size of the room (in square feet) where the equipment is installed.
- *Installation Level:* The floor where the equipment is located:

    - *RC*: Ground floor
    - *SS*: Basement
    - *ET*: Upper floor
- *Power (Watts):* The estimated capacity of the connected baseboard heater, calculated by measuring the instantaneous current (A) during thermostat installation and multiplying it by 240V (P = VI for a resistive load).

This structured dataset enables a detailed analysis of heating equipment performance and energy consumption patterns within each home.

An example for a random house of the dataset is therefore shown:

Table Appendix A. 1. Example of Variables Associated with Smart Thermostats

House ID	Device Key	Device Type	Device Location	Heat Channel	Area (feet^2)	Location	Power (kW)
#1	T01	therm	Main Dinning	4	299	RC	1.6
#1	T02	therm	Bedroom 1	5	123	RC	1.5
#1	T03	therm	Master Bedroom	1	144	RC	1.9
#1	T04	therm	Basement Living	1	168	SS	1.5
#1	T05	therm	Basement Office	2	159	SS	1.4
#1	T06	therm	Basement washroom	2	60	SS	0.3
#1	T07	therm	Basement laundry room	5	84	SS	0.5
#1	T08	therm	Basement Workspace	3	164	SS	1.5
#1	T09	therm	Bedroom 2	3	104	RC	1.5
#1	T10	therm	Main Living	4	299	RC	1.9

Electricity Consumption Data File

A text file contains the total electricity consumption, recorded every 15 minutes, for 30 homes based on data from Hydro-Québec's smart meters. The dataset covers the period between *201X-XX-XX* and *201Y-YY-YY* and includes the following variables:

- *Standard Time (UTC-5):* Timestamp in Eastern Standard Time (UTC-5).
- *Column XX:* Unique identifier for each home.

Each recorded value represents the average power consumption (in kW) over the previous 15 minutes. Due to occasional communication losses, data gaps of up to 5% per home may be present.

An example for a random house of the dataset is therefore shown:

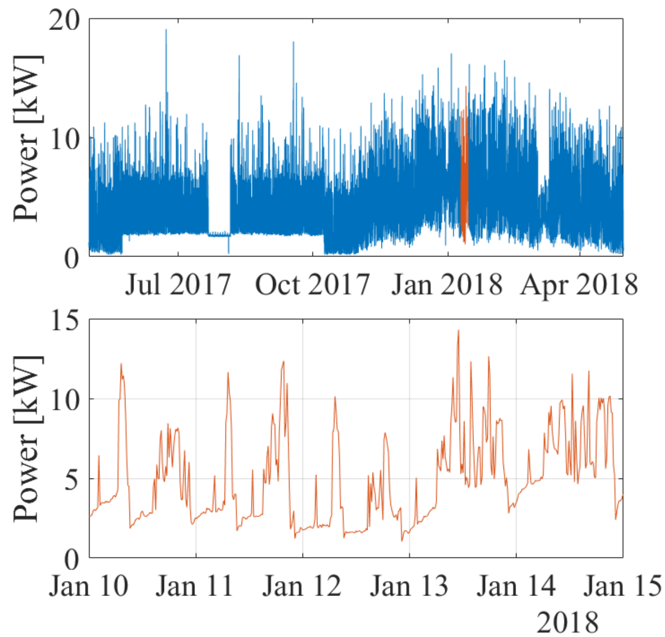

Figure 9.1. Electricity Consumption Data File

Electricity Consumption Data File – Circuit-Level Monitoring
A text file contains minute-by-minute electricity consumption data for the main electrical circuits of home ZZ, recorded between 201X-XX-XX and 201Y-YY-YY. This dataset is available for 10 homes equipped with an Egauge monitoring system.

Data Structure:

- *Standard Time (UTC-5):* Timestamp in Eastern Standard Time (UTC-5).
- *Columns:* Each column represents a sub-metered electrical circuit, linked to a specific load.

Monitored Circuits:

- *CH1 – CH5:* Heating circuits 1 through 5.
- *CHT:* Total calculated heating consumption *(CH1 + CH2 + CH3 + CH4 + CH5 + THP).*
- *CUI:* Stove.
- *ECS:* Water heater.
- *GAR:* Garage.
- *MAIN:* Main power supply.
- *PISC:* Pool.
- *PRECH:* Preheating system.
- *REF:* Refrigerator.
- *SEC:* Dryer.
- *SPA:* Spa.
- *THP:* Heat pump.
- *UONDE:* Microwave.
- *VRC:* Air exchanger.

An example for a random house of the dataset is therefore shown for the main channels:

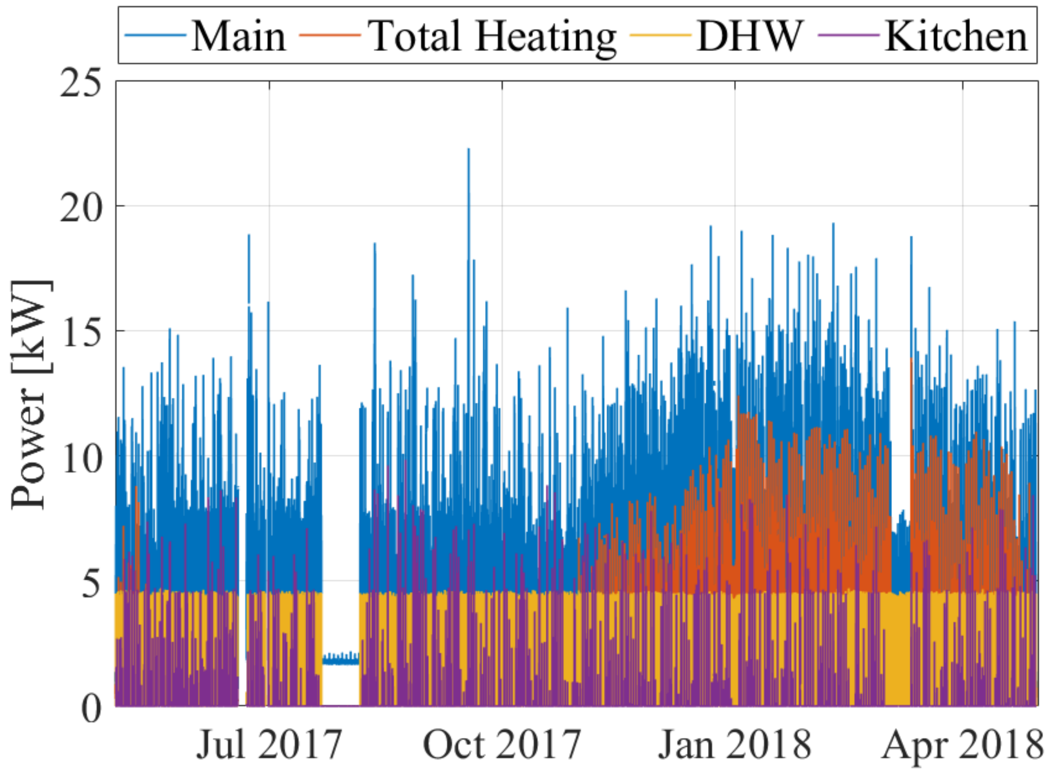

Figure 9.2. Electricity Consumption Data File – Circuit-Level Monitoring

Thermostat Data File – Temperature and Energy Consumption

A text file contains temperature and energy consumption data recorded for each thermostat in home ZZ between 201X-XX-XX and 201Y-YY-YY. This dataset is available for 30 homes equipped with smart thermostats.

Data Structure:

- *Standard Time (UTC-5):* Timestamp in Eastern Standard Time (UTC-5).
- *Device Key:* Unique identifier for each thermostat, as referenced in *baseboardThermostat_attributes.csv*.
- *Value:* Recorded measurement.
- *Variable:* Type of data recorded.

Recorded Variables:

- *TEMP:* Measured room temperature (°C).
  - Instantaneous value at the recorded timestamp.
  - Data frequency is irregular.
- *SET:* Setpoint temperature (°C).
  - Instantaneous value at the recorded timestamp.
  - Recorded when the setpoint changes and at other random intervals.
- *Wh:* Hourly energy consumption recorded by the thermostat (Wh).
  - Represents consumption in the previous hour.

An example for a random house of the dataset is therefore shown for the ten thermal zones:

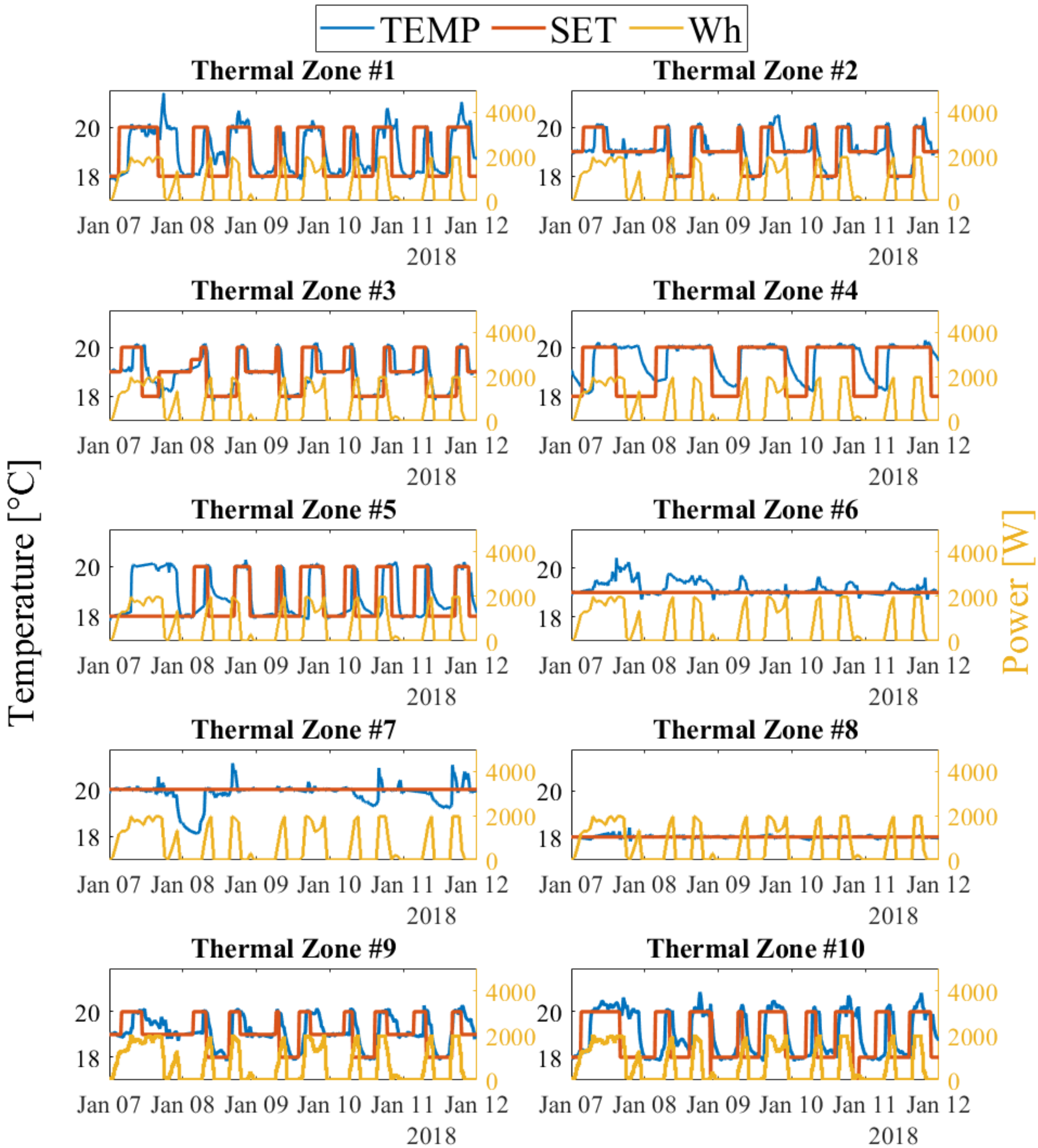

Figure 9.3. Thermostat Data File for the ten Thermal Zones of the considered home